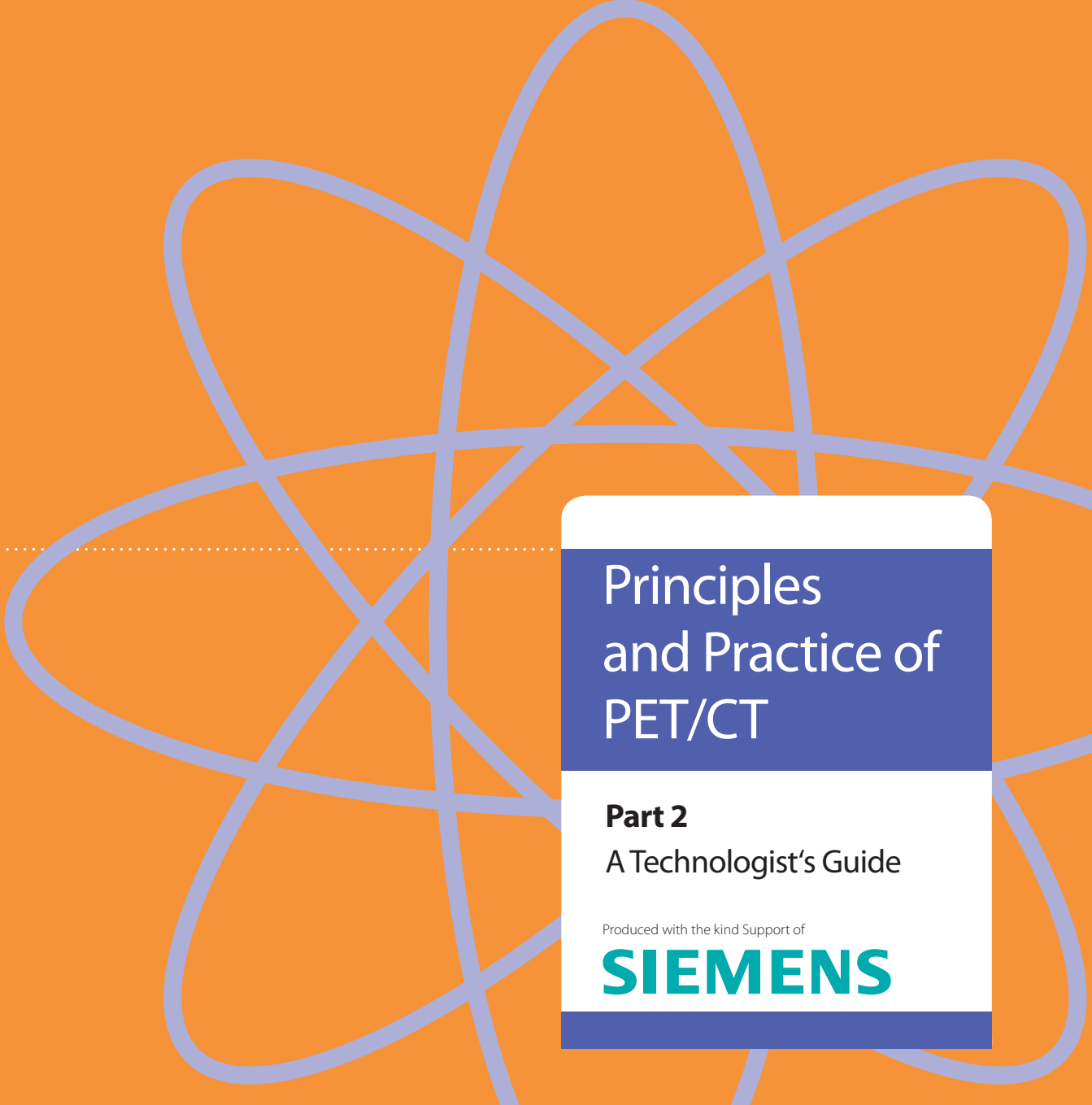


Publications · Brochures

A large, stylized graphic of an atomic symbol, composed of several overlapping, light blue elliptical orbits, is centered on the page. It is partially overlaid by a white rectangular box containing the title and other text.

# Principles and Practice of PET/CT

**Part 2**  
A Technologist's Guide

Produced with the kind Support of

**SIEMENS**



---

## Editors

**Giorgio Testanera**  
Rozzano (MI), Italy

**Wim J.M. van den Broek**  
Nijmegen, The Netherlands

## Contributors

**Ambrosini, Valentina** (Italy)

**Beijer, Emiel** (The Netherlands)

**Bomanji, Jamshed B.** (UK)

**Booij, Jan** (The Netherlands)

**Bozkurt, Murat Fani** (Turkey)

**Carreras Delgado, José L.** (Spain)

**Chiti, Arturo** (Italy)

**Darcourt, Jacques** (France)

**Decristoforo, Clemens** (Austria)

**Delgado-Bolton, Roberto C.** (Spain)

**Dennan, Suzanne** (Ireland)

**Elsinga, Philip H.** (The Netherlands)

**Fanti, Stefano** (Italy)

**Gaemperli, Oliver** (Switzerland)

**Giammarile, Francesco** (France)

**Giurgola, Francesca** (Italy)

**Grugni, Stefano** (Italy)

**Halders, Servé** (The Netherlands)

**Hanin, François-Xavier** (Belgium)

**Houizard, Claire** (France)

**Jamar, François** (Belgium)

**Kaufmann, Philipp A.** (Switzerland)

**Krause, Bernd J.** (Germany)

**Królicki, Leszek** (Poland)

**Kunikowska, Jolanta** (Poland)

**Mottaghy, Felix Manuel** (Germany)

**Nobili, Flavio** (Italy)

**Oyen, Wim J.G.** (The Netherlands)

**Pagani, Marco** (Italy)

**Papathanasiou, Nikolaos D.** (Greece)

**Petyt, Gregory** (France)

**Poepperl, Gabriele** (Germany)

**Prompers, Leonne** (The Netherlands)

**Schwarzenboeck, Sarah** (Germany)

**Semah, Franck** (France)

**Souvatoglou, Michael** (Germany)

**Tarullo, Gianluca** (Italy)

**Tatsch, Klaus** (Germany)

**Testanera, Giorgio** (Italy)

**Urbach, Christian** (The Netherlands)

**Vaccaro, Ilaria** (Italy)

# Contents

<b>Foreword</b>	5
Suzanne Dennan	
<b>Introduction</b>	6
Wim van den Broek and Giorgio Testanera	
<b>Chapter 1 – Principles of PET radiochemistry</b>	8
<b>1.1 Introduction to PET radiochemistry</b>	8
Clemens Decristoforo	
<b>1.2 Common practice in PET tracer quality control</b>	10
Gianluca Tarullo and Stefano Grugni	
<b>1.3 Basics of <math>^{18}\text{F}</math> and <math>^{11}\text{C}</math> radiopharmaceutical chemistry</b>	18
Philip H. Elsinga	
<b>1.4 [<math>^{18}\text{F}</math>]FDG synthesis</b>	26
Francesca Giurgola, Ilaria Vaccaro and Giorgio Testanera	
<b>1.5 <math>^{68}\text{Ga}</math>-peptide tracers</b>	32
Jamshed B. Bomanji and Nikolaos D. Papatnasiou	
<b>Chapter 2 – Clinical applications of PET/CT in oncology</b>	43
<b>2.1 Introduction</b>	43
Wim J.G. Oyen and Arturo Chiti	
<b>2.2 Head and neck cancer</b>	44
Murat Fani Bozkurt	
<b>2.3 Lung cancer</b>	50
Francesco Giammarile and Claire Houzard	
<b>2.4 Breast cancer</b>	60
Leonne Prompers, Emiel Beijer, Christian Urbach, Servé Halders and Felix Manuel Mottaghy	
<b>2.5 Prostate cancer</b>	67
Sarah Schwarzenboeck, Michael Souvatzoglou and Bernd J. Krause	
<b>2.6 Lymphomas</b>	80
Roberto C. Delgado-Bolton and José L. Carreras Delgado	
<b>2.7 Digestive tract tumours</b>	89
Jolanta Kunikowska and Leszek Królicki	
<b>2.8 Neuroendocrine tumour</b>	102
Valentina Ambrosini and Stefano Fanti	



# Contents

---

<b>Chapter 3 – Clinical applications of PET/CT in infection and inflammation</b>	<b>110</b>
François-Xavier Hanin and François Jamar	
<b>Chapter 4 – Clinical applications of PET/CT in cardiology</b>	<b>121</b>
Oliver Gaemperli and Philipp A. Kaufmann	
<b>Chapter 5 – Clinical applications of PET/CT in neurology</b>	<b>139</b>
<b>5.1 Introduction to brain PET</b>	<b>139</b>
Jacques Darcourt	
<b>5.2 Dementia and related disorders</b>	<b>141</b>
Flavio Nobili	
<b>5.3 Psychiatry</b>	<b>146</b>
Marco Pagani	
<b>5.4 Movement disorders</b>	<b>150</b>
Jan Booij	
<b>5.5 Brain tumours</b>	<b>153</b>
Klaus Tatsch and Gabriele Poepperl	
<b>5.6 Epilepsy</b>	<b>159</b>
Franck Semah and Gregory Petyt	
<b>Imprint</b>	<b>163</b>

# Foreword

Suzanne Dennan

The **EANM Technologist** Committee has produced a highly successful “Technologist’s Guide” on an annual basis since 2004. The “Technologist’s Guide” aims to develop expertise in key and developing areas of nuclear medicine and to promote high standards of professional practice. In recent years, the rapid advancement of PET/CT techniques has increased the requirement for involvement of competent and reflective personnel in the management and care of patients undergoing PET/CT examinations.

In 2010, the Technologist Committee decided that the next three guides would be dedicated to the topic of hybrid PET/CT imaging. Part 1 of the PET/CT series focussed on the principles and practice of PET/CT and included topics ranging from practical radiation protection, quality assurance and quality control to patient care. It is a great privilege to introduce part 2 of the PET/CT series, devoted to PET radiochemistry and to the clinical applications of PET/CT in oncology, cardiology, infection, inflammation and neurology.

I am grateful for the efforts and hard work of the authors, who have ensured the outstanding quality of this PET/CT book. I am very much indebted to the editors, Giorgio Testanera and Wim van den Broek, for their enthusiasm and dedication in preparing and editing this guide within a record short time for our annual series. Special thanks are due to Siemens Medical for their support and generous sponsorship of the three-part PET/CT series.

I am confident that this PET/CT book will be of immense help to all professionals working in PET/CT departments and also to those who would like to develop their understanding of PET/CT. It is hoped that this eighth “Technologist’s Guide” will prove to be a useful and comprehensive tool that will contribute to the quality of the PET/CT patient service. I look forward to the next PET/CT book in 2012.

*Suzanne Dennan*  
*Chair, EANM Technologist Committee*



# Introduction

Wim van den Broek and Giorgio Testanera

Owing primarily to the wide availability of  $^{18}\text{F}$ -FDG, PET/CT has established its place in the diagnosis and management of several prominent diseases, especially in the field of oncology. In recent years, an increasing number of alternative new PET radiopharmaceuticals have become commercially available, opening the way to new applications of PET/CT imaging. Since a greater variety of biological functions can be visualised by PET/CT with these new positron radiopharmaceuticals, the number of PET/CT applications will increase in cardiology and neurology as well as in oncology.

This second PET/CT Technologist's Guide will be of value not only for nuclear medicine technologists but also for other professionals working with PET/CT. As the first book covered instrumentation, protocol optimisation, radiation protection and patient care issues, this book provides the reader with information on the principles of PET radiochemistry and the current state of clinical applications of PET/CT in the fields of oncology, cardiology, infection and inflammation and neurology.

- The first chapter covers the principles of PET radiochemistry. In addition to presenting the basic knowledge on PET chemistry, it also discusses the regulatory rules which require increasing awareness of the challenges involved in the production and quality assurance of PET radiopharmaceuticals. This chapter offers the reader an excellent overview of all the issues and aspects related to the preparation of PET tracers.
- Chapter 2 presents the clinical applications of PET/CT in oncology, with a review of the strengths, weaknesses, current evidence and future directions of this imaging technique over a wide range of tumours.
- PET/CT applications in the detection and follow-up of infection and inflammatory disease are rather new and still unrecognised by some. Chapter 3 reviews the main indications for  $^{18}\text{F}$ -FDG PET/CT in this field and discusses the advantages and pitfalls compared with imaging using labelled white blood cells.
- The introduction of new PET tracers such as  $^{82}\text{Rb}$  and the increasing availability of PET devices in combination with high-end CT scanners is opening the way for increasing use of PET/CT in cardiology. Chapter 4 discusses the clinical applications in the field and covers patient preparation and PET/CT protocols.
- Imaging of the brain with PET/CT is still an open field with many possibilities. Thanks to the large number of PET tracers for brain imaging that are either already available or expected to become available. This final chapter offers an overview of the current applications of PET/CT imaging in different brain diseases.

## Introduction

---

After the broad view offered by the first two volumes on technology, radiation protection, patient care and clinical applications of PET/CT, the third book in this series, to be published in 2012, will address the great challenge posed by multimodality approaches involving PET/CT. In particular, it will consider the radiotherapy applications of PET/CT imaging.

The ultimate quality of PET/CT imaging depends on the expert input of a number of professionals, including physicians, physicists, chemists, pharmacists and technologists. Only good teamwork between the professionals

working in the area of PET/CT imaging will ultimately ensure high-quality diagnosis of disease. The importance of such collaboration also applies to this booklet, in which the good quality reflects the excellent teamwork between the EANM Radiopharmacy, Oncology, Cardiovascular and Neurology Committees and Task Group on Infection and Inflammation and the EANM Technologist Committee.

We hope that you enjoy reading this book and that it will prove a valuable resource for all professionals who work in the area of PET/CT or are interested in this topic.



# Chapter 1 – Principles of PET radiochemistry

## 1.1 Introduction to PET radiochemistry

Clemens Decristoforo

PET/CT has seen tremendous growth over recent years, mainly driven by the wide use and availability of  $^{18}\text{F}$ -FDG. Imaging with  $^{18}\text{F}$ -FDG has now become the clinical standard for a number of indications, especially in oncology. However, a major potential of molecular imaging with PET lies in the great variety of biological functions that can be visualised, including other transporters, receptors and enzymes.

Even though an increasing number of alternative PET radiopharmaceuticals are becoming widely commercially available based on supply from commercial producers – a trend expected to increase in the future –, the local production of PET radiopharmaceuticals will remain a central pillar in the years to come. Especially the use of ultra-short-lived radionuclides such as  $^{11}\text{C}$ , but also the increased use of PET radionuclides from generators such as  $^{68}\text{Ga}$  and the wide interest in PET radionuclides with longer half-lives such as  $^{124}\text{I}$ ,  $^{64}\text{Cu}$  and  $^{89}\text{Zr}$ , requires the in-house production of PET radiopharmaceuticals based on individual patient needs or for use in clinical trials.

Regulatory demands concerning the preparation of radiopharmaceuticals in Europe have become a major hurdle in the establishment of PET radiopharmaceutical production, particularly in hospitals and academic institutions. The Radiopharmacy Committee of EANM has addressed these problems re-

cently by drafting Guidelines and Guidance documents on Good Radiopharmacy Practice for the Small-Scale Preparation of Radiopharmaceuticals.

The role of the technologist in such an environment requires increasing awareness especially regarding challenges in the production and quality assurance of such highly specific pharmaceuticals. Basic knowledge on the chemical processes involved and the technical challenges encountered in everyday practice and an understanding of the necessity to work in an environment with high demands on quality assurance are of the utmost importance in ensuring compliance with the highest standards, as patients rightfully demand.

This technologists' booklet provides an excellent overview of major principles of PET chemistry. Section 1.2 gives an overview of quality control procedures for PET radiopharmaceuticals, providing an understanding of the daily procedures necessary to ensure the efficacy and safety of PET radiopharmaceuticals. The following section on basic principles of  $^{18}\text{F}$  and  $^{11}\text{C}$  provides information on how major PET radiopharmaceuticals are prepared and which challenges need to be overcome in these procedures. Section 1.4 then describes the synthesis of FDG, giving details on the principles of preparation of the work-horse of PET. In the final section relat-



ing to PET radiochemistry, specific aspects of  $^{68}\text{Ga}$  are addressed, in particular peptide radiopharmaceuticals.

We believe that this booklet will help not only technologists but also other nuclear medicine professionals not directly involved in PET radiopharmaceutical production to understand the challenges and prospects of PET chemistry and radiopharmaceutical preparation, thereby improving their professionalism to the benefit of patients.



# Chapter 1 – Principles of PET radiochemistry

## 1.2 Common practice in PET tracer quality control

Gianluca Tarullo and Stefano Grugni

### Introduction

The use of radiopharmaceuticals in humans requires a system of quality control tests that ensure the purity, safety and efficacy of the products. Some of these tests are normally carried out for conventional drugs while others are specific for radiolabelled compounds. Quality control tests of these compounds, which are short-lived products, should be very fast and simple. It is possible to distinguish two categories of test: physicochemical tests and biological tests [1].

### Physicochemical tests

Physicochemical tests are used to ensure the purity and the integrity of radiopharmaceuticals and are based on the chemical identities of the substances and their physical properties.

### *Appearance and pH*

In normal conditions, a solution of radiopharmaceutical should not contain particulate. The measure of pH is very important because both the stability of the product and its compatibility with human administration are dependent on the pH value. In order to investigate the pH value, different methods are available, but measurement with a pH meter is certainly more accurate than the colorimetric test with pH paper.

### *Radiochemical and chemical purities*

Physicochemical tests also include those for the determination of radiochemical and chemical purities.

The radiochemical purity is the fraction of the total activity of the product in the desired chemical form. Radiochemical impurities may originate from:

- radionuclide production;
- chemical synthesis of the product;
- incomplete purification;
- chemical changes after synthesis.

For example in the case of the most common PET tracer, [ $^{18}\text{F}$ ]FDG, different impurities may be created during the synthesis process. [ $^{18}\text{F}$ ]FDM and [ $^{18}\text{F}$ ]TAG are two collateral products of different synthesis methods. Partially hydrolysed labelled precursors are an example of incomplete purification, as are  $^{18}\text{F}^-$  free ions.

Other by-products may originate during storage of the radioactive product for radiolysis [2,3] owing to:

- high pH values;
- high temperature;
- high concentration of activity.

Usually the minimum level of radiochemical purity required for the administration of radiopharmaceuticals is 95% of the total activity, but the exact limit for each product is reported in the specific Ph. Eur monographs.

These tests require methods based on the separation of the various chemical radioac-

tive compounds present in the product. The most common method is chromatographic analysis. Chromatography is a technique for separation of different elements in a mixture of substances based on the different eluotropic strengths of the mobile phase [4]. The most simple chromatographic method useful for determination of radiochemical purity is thin-layer chromatography (TLC; Fig. 1). In TLC a small amount of the product is spotted on one side of a paper or a strip made of several substances such as silica gel or aluminium oxide and this side is then immersed in a mobile phase that may include physiological solution, organic solvents and buffers. The mobile phase runs on the strip and the different compounds distribute themselves and migrate separately according to the different affinity with the mobile and the stationary phase.

The value that serves to identify compounds in both TLC and other chromatographic techniques is the  $R_f$ , the ratio of the distance travelled by the compound to the distance from the original point to the solvent front. To obtain the results of the analysis when the solvent arrives at the required distance, the strip should be removed from the chamber with the mobile phase; it is then possible to evaluate the radiochemical purity in two ways. The first method is to divide the strip into small segments and measure the activity of each segment. Radiochemical purity is the ratio between the activity of the segment where the product should be expected to run and the total activity, which is the sum of the activities due to the desired compound, the free isotope and any other impurities. The alternative method employs a radiochromatographic scanner that measures the activity at each point of the strip (Fig. 2).

W  
N  
A  
E

Courtesy of Department of Nuclear Medicine,  
IRCCS Istituto Clinico Humanitas, Rozzano (Milan)

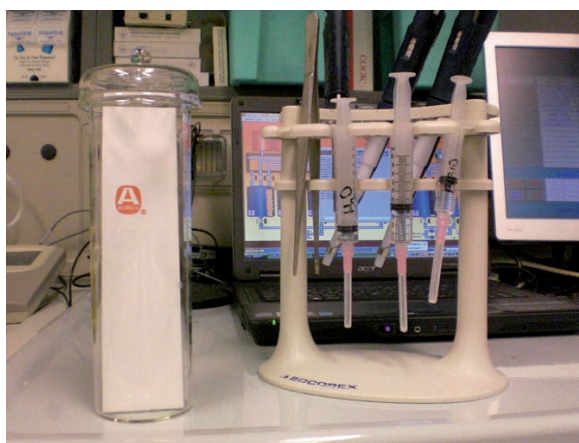


Figure 1: Thin-layer chromatography

Courtesy of Department of Nuclear Medicine,  
IRCCS Istituto Clinico Humanitas, Rozzano (Milan)



Figure 2: Radiochromatographic scanner

Figure 3 shows an example of an [<sup>18</sup>F]FDG TLC report.

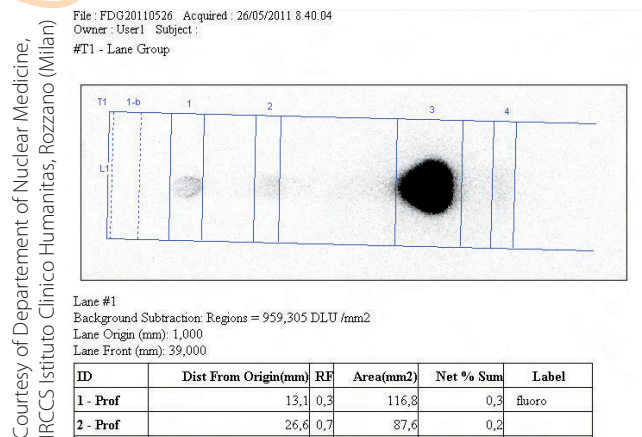


Figure 3: [<sup>18</sup>F]FDG TLC report

An alternative method for determination of the radiochemical purity is high-performance/pressure liquid chromatography (HPLC, Fig. 4). These two techniques are based on the typical principles of liquid chromatography. In HPLC, mobile phases are pushed into the columns by electrical pumps, and the stationary phase is packed in a column. Working under a high pressure condition, it is possible to separate different compounds with high resolution.

Generally, HPLC columns are stainless steel tubes packed with appropriate packing materials. Depending on the composition of the stationary phase, it is possible to distinguish two types of chromatographic method:

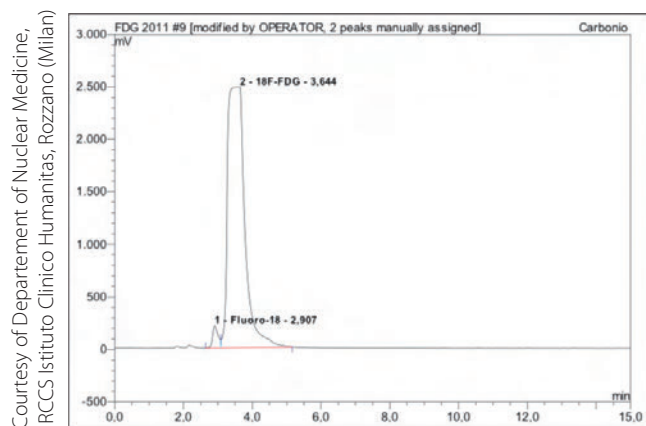
- normal phase;
- reverse phase.

Normal-phase methods are based on the use of polar materials as the stationary phase and of non-polar solvents, usually mixed with a small amount of polar solvents. These methods are useful for the separation of polar compounds.

In reverse-phase methods, non-polar materials are used as the stationary phase. Usually this kind of stationary phase is made up of hydrophobic alkyl chains with different lengths, named C4, C8 or C18 depending on their length. Longer chains are useful for small molecular analysis and shorter ones for proteins and peptides.



Figure 4: HPLC system



Courtesy of Department of Nuclear Medicine, IRCCS Istituto Clinico Humanitas, Rozzano (Milan)

Figure 5: [<sup>18</sup>F]FDG HPLC report

In HPLC methods, a small amount of the sample is manually injected into an injection valve. After the injection, the substances present on the sample are separated, eluted from the column depending on their affinity with the stationary and the mobile phase and analysed using a detector. Various detectors are used in the analysis of radiopharmaceuticals for the determination of chemical and radiochemical purities, as shown in Table 1.

Figure 5 shows an example of an [<sup>18</sup>F]FDG HPLC report.

Radiopharmaceutical	Chemical purity	Radiochemical purity
[ <sup>18</sup> F]Fluorodeoxyglucose	UV, amperometric detector	Radiochemical detector
[ <sup>11</sup> C]Methionine	UV detector	Radiochemical detector
[ <sup>11</sup> C]Choline	Conductivity, UV detector	Radiochemical detector

Table 1: Detectors commonly used for PET tracer quality control

Systems like those shown in Table 1, with a radiometric and a non-radiometric detector [5,6], allow determination within the same analysis of both the radiochemical and the chemical purity of the product.

Several radiochemical synthesis processes need solvents to obtain the required product. In these cases the possible presence of a small amount of residual solvents must be evaluated. A common technique for this purpose is gas chromatography (GC; Figs. 6, 7).





Figure 6: A GC system

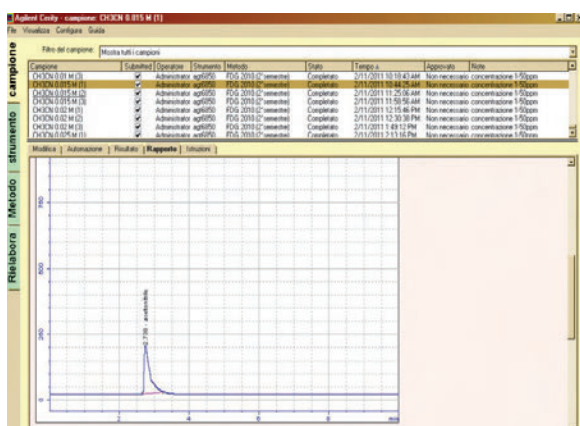


Figure 7: An [<sup>18</sup>F]FDG GC report

In GC, the mobile phase is an inert carrier gas and the stationary phase is usually a polymer on an inert solid support. The principles of this technique are similar to those of liquid chromatography. In GC analysis, a small amount of the sample is injected into the column, which is placed in an oven. Different compounds are retained from the stationary phase absorbed on the column, depending on their chemical and physical properties. At column exit the

compounds are identified with a detector. The most common detector used in GC is a flame ionisation detector (FID), which is able to work with a wide range of compounds and concentrations.

In order to investigate the chemical purity of a product, different tests can be used to research the presence of a specific impurity. One example is the determination of the amount of Kryptofix often present in most F-18 labelled PET radiopharmaceuticals, such as [<sup>18</sup>F]FDG. The technique used for this purpose is a colorimetric test. A small aliquot of the product is placed on a test paper pretreated with an iodoplatinate reagent and the spot is compared with that of a reference solution obtained using a sample of Kryptofix at the limit concentration of Kryptofix [7].

### Radionuclidic purity

Radionuclidic purity is evaluated for investigation of the isotopic forms present in a radioactive substance. As reported in the “radiopharmaceutical preparations” monograph, radionuclidic purity is the ratio, expressed as a percentage, of the radioactivity of the radionuclide concerned to the total radioactivity of the radiopharmaceutical preparations. Radionuclidic purity can be calculated using gamma spectrometry. It can be also calculated, in case of short life impurities, by determination of the isotope half-life.

### Biological tests

Biological tests are useful to ensure the sterility of radiopharmaceuticals and to detect and quantify the presence of bacterial endotoxins. The aim of these tests is to ensure product safety.

#### *Sterility*

Radiopharmaceuticals for human administration must be tested to evaluate sterility. However, owing to the duration of the test (usually 15 days), it is not possible to obtain results before the release of the product since the most commonly used PET tracers are labelled with short half-life isotopes. To ensure sterility it is necessary to operate with methods that minimize microbial contamination, which then have to be validated. A suitable test to validate the aseptic operations is the media fill test, which represents a simulation of the whole preparation process or a part of it. This test is performed by replacing the solutions, diluents and materials typically used during the preparation or the dispensing of the radiopharmaceuticals with culture media, which are then incubated for a suitable time.

#### *Bacterial endotoxin*


A test for bacterial endotoxins must be carried out on radiopharmaceuticals for human administration. Various methods are useful for this purpose:

- the gel clot method;
- the turbidimetric method;
- the chromogenic method.

These tests are based on the use of amoebocyte lysate from the horseshoe crab (*Limulus polyphemus*). For short-life radiopharmaceuticals, like [<sup>11</sup>C]methionine, according to the specific monograph it is possible to release the batch before completion of the test. For [<sup>18</sup>F]FDG, commercial kits are available for determination of the presence of bacterial endotoxins within a suitable time.

All the radiopharmaceutical quality controls should be carried out according to the specific monograph for each product. Table 2 shows quality control tests, methods and limits for [<sup>18</sup>F]FDG according to the European Pharmacopoeia (EuPh) and the United States Pharmacopoeia (USP).





Type of quality control	EuPh	USP	Analytical method
Radiochemical purity	>95%	>90%	Radio-TLC scanner/HPLC with radio-flow detector
Chemical purity	>95%	>90%	HPLC with UV or amperometric detector
Residual solvents (acetonitrile)	<4.1 mg/V <sub>max</sub>	<0.04%	Gas chromatography with an FID detector
pH	4.5-8.5	4.5-7.5	Colorimetric test
Residual Kryptofix	<2.2 mg	<50 µg/ml	Colour spot test
Sterility test	Sterile	Sterile	Microbiological test
Bacterial endotoxin	<175 IU	<175 EU	LAL test
Radionuclidic purity (half-life)	105-115 min	105-115 min	Gamma-ray spectrometry

Table 2: Common quality control tests for [<sup>18</sup>F]FDG and limits according to different pharmacopoeia



## References Chapter 1.2

### References

1. Saha GB. Fundamentals of nuclear pharmacy. New York: Springer; 2004.
2. Fawdry RM. Radiolysis of 2- $^{18}\text{F}$ fluoro-2-deoxy-D-glucose (FDG) and the role of reductant stabiliser. *Appl Radiat Isot* 2007;65:1193-201.
3. Jacobson MS, Dankwart HR, Mahoney DW. Radiolysis of 2- $^{18}\text{F}$ fluoro-2-deoxy-d-glucose ( $^{18}\text{F}$ FDG) and the role of ethanol and radioactive concentration. *Appl Radiat Isot* 2009;67:990-5.
4. Koziorowski J. A simple method for the quality control of  $^{18}\text{F}$ FDG. *Appl Radiat Isot* 2010;69:649-716.
5. Nakao R, Furutuka K, Yamaguchi M, Suzuki K. Quality control of PET radiopharmaceuticals using HPLC with electrochemical detection. *Nucl Med Biol* 2006;33:441-7.
6. Nakao R, Ito T, Yamaguchi M, Suzuki K. Improved quality control of  $^{18}\text{F}$ FDG by HPLC with UV detection. *Nucl Med Biol* 2005;32:907-12.
7. Yu S. Review of  $^{18}\text{F}$ FDG synthesis and quality control. *Biomed Imaging Intervent J* 2006;2(4):e5.

### Suggested reading

European pharmacopoeia monographs (Radiopharmaceutical preparation, 0125).



# Chapter 1 – Principles of PET radiochemistry

## 1.3 Basics of $^{18}\text{F}$ and $^{11}\text{C}$ radiopharmaceutical chemistry

Philip H. Elsinga

### Introduction

This section addresses basic and practical aspects of the synthesis of  $^{18}\text{F}$ - and  $^{11}\text{C}$ -labelled radiopharmaceuticals and the most common ways of producing a radiopharmaceutical with a short-lived positron-emitting radioisotope. In the pioneering phase of PET radiochemistry (late 1970s to early 1980s), the focus was primarily on the development of small synthons and exploring the scope and limitations of radiochemical reactions. During recent decades, however, a shift occurred towards the application of a limited number of radiochemical reactions and their optimisation to prepare new PET radiopharmaceuticals.

### Preparation of a radiopharmaceutical – general aspects

Many synthetic routes to prepare PET radiopharmaceuticals have been developed during recent decades. The great majority of PET tracers are labelled with the positron-emitting radioisotopes  $^{11}\text{C}$  and  $^{18}\text{F}$  (radioactivity decay: half-lives of 20 and 110 min, respectively). The half-lives of  $^{13}\text{N}$  and  $^{15}\text{O}$  (10 and 2 min, respectively) are too short to perform radiochemical syntheses of more than one reaction step. In most cases, [ $^{15}\text{O}$ ]radiopharmaceuticals are limited to radio-labelled water, butanol and gases for inhalation studies ( $\text{C}^{15}\text{O}$ ,  $\text{C}^{15}\text{O}_2$ ). In the case of  $^{13}\text{N}$ , this radioisotope is incorporated into nitrite/nitrate and ammonia. In addition, other positron-emitting radionuclides such as  $^{89}\text{Zr}$ ,  $^{124}\text{I}$ ,  $^{68}\text{Ga}$  and  $^{64}\text{Cu}$  have been applied mainly in the production of peptides and larger biomolecules [1].

Of the many possible radiochemical preparation methods, few have been extensively developed, and these are applied by many PET centres since they are extremely versatile and reliable. Using two preparation methods – nucleophilic substitution with [ $^{18}\text{F}$ ]fluoride and [ $^{11}\text{C}$ ]methylation – a large variety of biologically active compounds can be prepared. Important PET radiopharmaceuticals have also been prepared by electrophilic [ $^{18}\text{F}$ ]fluorination. Widespread use of these specific methods has been encouraged by the appearance of commercially available synthesis modules. Using these modules, radiochemical preparations are relatively easily performed, including by PET centres without extensive radiochemical expertise. Other radiochemical preparation methods have usually been limited to research groups and are not frequently adopted by others because they require specific expertise.

Certain general aspects in PET radiochemistry have to be considered: Firstly, the synthesis of a short-lived PET radiopharmaceutical is a fight against time because of the rapid decay of the applied radioisotopes. Preparation times of three half-lives are acceptable to obtain sufficient amounts of radiotracer for clinical studies.

A second pertinent aspect is the amount of reagent that is used. In Table 1, an estimate is shown of the absolute amounts that are used in a radiochemical synthesis. It is clear that the non-radioactive precursor is present in a large excess as compared with the radioactive reagent.

Another important aspect is isotopic dilution of the produced radioisotopes, which can lead to decreased specific activities (compare theoretical and practical specific activity in Table 1). Stable  $^{12}\text{C}$  and  $^{19}\text{F}$  isotopes are introduced in the cyclotron target or during work-up of the radioactivity prior to the actual synthesis. The main sources of carbon are carbon dioxide from the air or carbon impurities from the target materials. Fluoride sources are the  $^{18}\text{O}$ -enriched water and reagents that are used during the work-up.

In recent years, production of radiopharmaceuticals under conditions complying with Good Manufacturing Practice (GMP) is mandatory in many countries. The main focus of GMP is to control preparation of pharmaceuticals during all stages of the manufacturing process. Traceability of the product and of all production parameters needs to be assured. Guidelines for GMP especially for PET radiopharmaceuticals have been formulated by the EANM radiopharmacy committee [2].

## Radiochemistry with $^{18}\text{F}$

### *Nucleophilic fluorinations*

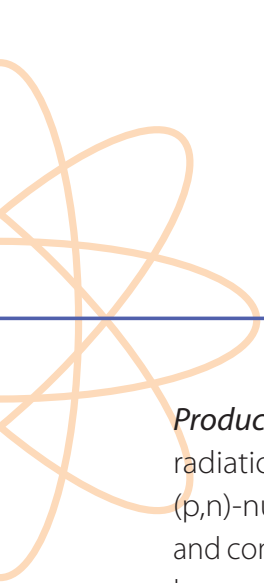
Using this preparation method, a wide variety of radiopharmaceuticals can be prepared in high radiochemical yields and high specific activities [3,4]. An advantage of  $^{18}\text{F}$  is the possibility it affords to distribute radiopharmaceuticals to sites without access to a cyclotron. The best-known example is the preparation of 2- $^{18}\text{F}$ fluoro-2-deoxy-D-glucose (FDG), which

is the work horse of PET for the investigation of glucose consumption in tumours and is commercially distributed in many countries. To increase the efficiency of FDG production, much effort has been put into scaling up the production of  $^{18}\text{F}$ fluoride and speeding up the  $^{18}\text{F}$ fluorination process. Knowledge gained from FDG production has been transferred to nucleophilic  $^{18}\text{F}$ fluorinations in general. Different suppliers offer automated synthesis modules for nucleophilic  $^{18}\text{F}$ fluorinations, and for  $^{18}\text{F}$ FDG in particular.

After the first steps of the synthesis procedure, i.e. cyclotron production and workup of  $^{18}\text{F}$ fluoride, different synthetic options are possible:

1. Direct substitution of an appropriate leaving group by  $^{18}\text{F}$ fluoride, which can be followed by hydrolysis of protective groups. Examples are the preparation of  $^{18}\text{F}$ FDG (Fig. 1) and  $^{18}\text{F}$ -3-fluoro-3-deoxy-thymidine (FLT).
2. Preparation of a reactive  $^{18}\text{F}$ fluorinated intermediate by nucleophilic substitution, followed by a second reaction, such as an alkylation. Finally, a deprotection reaction may be required. Examples of a  $^{18}\text{F}$ fluoroalkylation are the synthesis of  $^{18}\text{F}$ fluorocholeline and  $^{18}\text{F}$ fluoroethyltyrosine (FET).

During or after the preparation, purification steps are usually employed using solid-phase extraction techniques or high-performance liquid chromatography.



**Production of [<sup>18</sup>F]fluoride.** The cyclotron irradiation of <sup>18</sup>O-enriched water using the (p,n)-nuclear reaction is the most effective and convenient way to produce [<sup>18</sup>F]fluoride in large quantities up to a few hundreds of GBq.

**Work-up of [<sup>18</sup>F]fluoride.** After the irradiation, [<sup>18</sup>F]fluoride is separated from <sup>18</sup>O-enriched water. This separation has two purposes: recovery of the <sup>18</sup>O-water and the first step in the creation of reactive fluoride in an anhydrous environment. Commercially available cartridges, such as QMA-SepPak, are available. These cartridges, when conditioned into the CO<sub>3</sub><sup>2-</sup> form, trap >95% of the fluoride, whereas the <sup>18</sup>O-water is collected. The fluoride is eluted from the cartridge with a solution containing K<sub>2</sub>CO<sub>3</sub>. For some reactions other potassium salts, such as KHCO<sub>3</sub> and potassium oxalate, are used in order to decrease the basicity of the reaction medium, so avoiding side reactions.

Since K<sup>18</sup>F is not soluble in organic solvents suitable for nucleophilic fluorination reactions, a phase transfer catalyst is needed. For this purpose, tetraalkyl ammonium salts or aminopolyethers (Kryptofix 2.2.2) are used. [<sup>18</sup>F] Fluoride is reactive in water-free media only. Small amounts of water will generate a hydration shield around the fluoride anion. By means of a few successive evaporations with dry acetonitrile, the fluoride anion is stripped from its surrounding water molecules.

**Nucleophilic substitution.** Once the [<sup>18</sup>F]fluoride is dried and solubilised in the presence of the phase transfer catalyst, the actual nucleophilic substitution can take place. The reaction conditions that are applied are: heating for 10–30 min at temperatures varying from 80° to 160°C in a polar, aprotic solvent. Acetonitrile is the common solvent. Other possibilities are DMSO or DMF. Acetonitrile has the advantage that it can easily be removed by evaporation, in contrast to DMSO and DMF. Removal of the solvent is important in many production methods because its presence hampers the subsequent HPLC purification. DMSO and DMF have the advantage that the pressure in closed reaction vessels even at higher temperatures is low and therefore leakage is a minor problem.

The precursor molecule should contain a leaving group at the position where the <sup>18</sup>F radioisotope is desired. One should take into account that inversion of the stereochemistry will occur. In the case of aliphatic nucleophilic substitutions, sulphonic esters are used as suitable leaving groups. There are several groups that can be used, such as triflates, tosylates, mesylates and nosylates. The choice of a particular leaving group is determined by its reactivity, stability and ease of incorporation in a certain precursor. Aromatic nucleophilic substitutions need to be carried out with nitro- or trimethyl ammonium groups that are activated by electron-withdrawing groups in the *para*- or *ortho*-position. An example is the

preparation of the 5-HT<sub>1A</sub> antagonist *p*-[ $^{18}\text{F}$ ]MPPF or the  $^{18}\text{F}$ -prosthetic group for peptide labelling, [ $^{18}\text{F}$ ]SFB.

### *Electrophilic fluorinations*

The use of elemental fluorine  $\text{F}_2$  as an [ $^{18}\text{F}$ ]fluorinating agent originates from the very beginning of the development of the PET radiopharmaceutical chemistry [4]. Neon-20 containing 0.1–0.3%  $\text{F}_2$  is used as the target gas. Because  $\text{F}_2$  is very reactive, it is necessary to add inactive  $\text{F}_2$  to the target to prevent adsorption of  $^{18}\text{F}$  to the target wall and transport tubing. This so-called passivation process is essential and sometimes critical to obtain a sufficient yield of [ $^{18}\text{F}$ ] $\text{F}_2$ . The disadvantage of using electrophilic [ $^{18}\text{F}$ ]fluoride is its low specific activity.

Possible reactions that can be performed are additions to double bonds or aromatic substitution. The most common reaction nowadays is an electrophilic aromatic substitution of a trialkyl tin or mercury group. A well-known example is the preparation of L-[ $^{18}\text{F}$ ]-fluoro-DOPA. The first FDG productions in the years 1970–1980 were also performed using the electrophilic fluorination technique.

### **Radiochemistry with $^{11}\text{C}$**

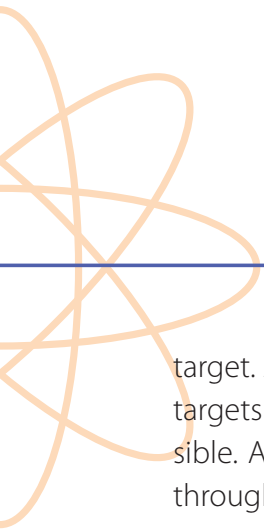
Whereas in  $^{18}\text{F}$  chemistry the first step is always a substitution reaction, in  $^{11}\text{C}$  chemistry a wide variety of small  $^{11}\text{C}$  molecules have been developed [3]. An advantage of  $^{11}\text{C}$  is that carbon is a naturally occurring nuclide; it is therefore possible to label molecules without affecting

these properties.  $^{11}\text{C}$  can be produced in the target as [ $^{11}\text{C}$ ] $\text{CO}_2$  or [ $^{11}\text{C}$ ] $\text{CH}_4$ , both via the  $^{14}\text{N}(\text{p},\text{n})^{11}\text{C}$  nuclear reaction. The advantage of [ $^{11}\text{C}$ ] $\text{CH}_4$  is that theoretically a higher specific activity can be achieved than for [ $^{11}\text{C}$ ] $\text{CO}_2$ . The natural abundance of  $\text{CO}_2$  in air is 330 ppm, whereas that of methane is 1.6 ppm. This means that precautions should be taken to exclude air from synthesis modules and solutions that start with [ $^{11}\text{C}$ ] $\text{CO}_2$ .

In Fig. 2, examples are shown of small  $^{11}\text{C}$  molecules that can be prepared from either [ $^{11}\text{C}$ ] $\text{CO}_2$  or [ $^{11}\text{C}$ ] $\text{CH}_4$  and can be further used in the synthesis of biologically interesting PET radiopharmaceuticals. The majority of  $^{11}\text{C}$  preparations use [ $^{11}\text{C}$ ]methyl iodide ( $\text{CH}_3\text{I}$ ) and [ $^{11}\text{C}$ ]methyl triflate ( $\text{CH}_3\text{OTf}$ ). An  $^{11}\text{C}$ -methylation reaction is simple, reliable and yields many biologically interesting radiopharmaceuticals. Commercial synthesis modules are available from several suppliers.

### *Production of $^{11}\text{C}$*

For the production of  $^{11}\text{C}$ , the targets are made from pure aluminium or an aluminium alloy. The target should be as small as possible to achieve a high specific activity and rapid emptying. The target gas must be very pure and not contain carbon impurities. For the production of [ $^{11}\text{C}$ ] $\text{CO}_2$ , traces of oxygen are needed to form  $\text{CO}_2$  by hot atom chemistry. Percentages of up to 1–2% of  $\text{O}_2$  in nitrogen are suitable for this purpose. To reduce the amount of ‘cold’  $\text{CO}_2$  in the target gas, an ascarite trap can be inserted between the gas supply and the



target. Another precaution is to maintain the targets under overpressure as much as possible. After irradiation, the target is emptied through stainless steel tubing.

$^{11}\text{C}$ -labelled methane is produced using the same target but with the target gas  $\text{N}_2$  and 5–10%  $\text{H}_2$ . Using a Porapak tube immersed in liquid nitrogen/argon,  $[^{11}\text{C}]\text{CH}_4$  is trapped. By warming to room temperature and using helium,  $[^{11}\text{C}]\text{CH}_4$  is transferred to the synthesis module.

#### **Preparation of $[^{11}\text{C}]\text{methyl iodide}$**

There are two common ways to prepare  $[^{11}\text{C}]$  methyl iodide, i.e. the ‘wet’ method, via reduction of  $[^{11}\text{C}]\text{CO}_2$  to  $[^{11}\text{C}]\text{methanol}$  by  $\text{LiAlH}_4$ , followed by treatment with  $\text{HI}$ , and the ‘gas phase’ method using iodine vapour and  $[^{11}\text{C}]\text{CH}_4$ . For both methods, synthesis modules are commercially available.

**The ‘wet’ method.**  $[^{11}\text{C}]\text{CO}_2$  is trapped in a solution of  $\text{LiAlH}_4$  in tetrahydrofuran (THF). The preparation of this solution should be carried out with extreme caution in order to prevent the presence of ‘cold’ carbon dioxide. Parameters that affect the amount of ‘cold’  $\text{CO}_2$  are atmosphere (argon is recommended), absolute amount of  $\text{LiAlH}_4$  and volume of the solution. The trapped  $[^{11}\text{C}]\text{CO}_2$  is reduced to  $[^{11}\text{C}]\text{methanol}$  as an  $\text{Li}$  salt. The THF is evaporated and  $\text{HI}$  (57%) is slowly added to the precipitate. The formed  $[^{11}\text{C}]\text{methyl iodide}$  is distilled via tubing containing an ascarite/phosphorous pentoxide

trap into the solution containing the precursor. Ascarite is used to remove excess of  $\text{HI}$ , whereas phosphorous pentoxide removes traces of water. Removal of acid and water is necessary for a good  $^{11}\text{C}$ -methylation yield.

**The ‘gas phase’ method.**  $[^{11}\text{C}]\text{methyl iodide}$  is directly prepared from  $[^{11}\text{C}]\text{methane}$  in the presence of iodine vapour. This method is more simple and eliminates the problems associated with the preparation of the  $\text{LiAlH}_4$  solution (specific activity) and the use of  $\text{HI}$  (deterioration of tubing and valves). A quartz tube of about 40 cm is prepared containing ascarite at both ends, iodine and an empty part. The tube is positioned in a module in such a way that the empty part will be heated at 650–750°C and the iodine part at 70–95°C.  $^{11}\text{C}$ -labelled methane is passed through the iodine, which is slowly sublimated upon heating. This gaseous mixture is passed through the empty part of the tube. Because of the high temperature, a part of  $[^{11}\text{C}]\text{methane}$  is converted into  $[^{11}\text{C}]\text{methyl iodide}$ . Alternative production methods using bromine instead of iodine have been developed, thereby avoiding the iodine evaporation step.

Because the conversion efficiency is usually 20–30%, many PET centres use a circulation pump in order to pass the reaction mixture several times through the iodine tube to increase the radiochemical yield. In the circulation, a trap must be installed to collect the  $[^{11}\text{C}]\text{methyl iodide}$ . Several traps are possible: Porapak N, glass tube in liquid argon or Car-

bosphere. By elevating the temperature as compared with the trapping conditions,  $[^{11}\text{C}]$  methyl iodide can be released from the trap using a gentle gas flow.

### Preparation of $[^{11}\text{C}]$ methyl triflate

The use of  $[^{11}\text{C}]$ methyl triflate in methylation reactions has several advantages over  $[^{11}\text{C}]$ methyl iodide. Because  $[^{11}\text{C}]$ methyl triflate is far more reactive, methylations can be performed using lower reaction temperatures, lower amounts of precursor and shorter reaction times.  $[^{11}\text{C}]$ Methyl triflate can easily be prepared by passing  $[^{11}\text{C}]$  methyl iodide through a column containing silver triflate heated at  $200^\circ\text{C}$ . Usually the silver triflate is impregnated on a carrier. The column containing the silver triflate needs to be stored in the dark and the column material should be free from oxygen.

### Methylations

A large number of radiopharmaceuticals have been labelled with N-, O- and S-nucleophiles. Well-known examples are the preparation of  $[^{11}\text{C}]$ methionine and  $[^{11}\text{C}]$ raclopride (Fig. 3). Different ways of carrying out methylations have been reported in the literature:

1. In solution: This is mostly used in practice. The precursor is dissolved in a suitable solvent, sometimes in the presence of a base. The  $[^{11}\text{C}]$ methylating agent is bubbled through the solution.
2. On solid phase support: The precursor is coated on a solid support, such as an HPLC

loop or a solid phase extraction cartridge. The  $[^{11}\text{C}]$ methylating agent is passed through the solid support. The product is eluted from the support by a solvent or HPLC mobile phase.

When methylations are carried out in solution, solvents like DMSO, DMF, acetone and acetonitrile are used. In many cases, a base is needed for deprotonation. Common bases are  $\text{K}_2\text{CO}_3$ , TBOH, NaOH and NaH. Further reaction conditions are shown in Table 2.

Trapping of  $[^{11}\text{C}]$ methyl iodide in the solution is not quantitative, so a trap at the vent line is recommended for radiation safety reasons. Active charcoal is very effective for this purpose. The trapping efficiency of  $[^{11}\text{C}]$ methyl triflate is usually almost quantitative.

### Concluding remarks

The production of  $^{11}\text{C}$  and  $^{18}\text{F}$  radiopharmaceuticals is becoming more widespread since the availability of commercially available synthesis modules for  $^{18}\text{F}$ -fluorination and  $^{11}\text{C}$ -methylations, covering most of the PET radiopharmaceuticals. Appropriate training of staff remains crucial to reliable operation of the equipment and development of new PET radiopharmaceuticals.

Several PET radiopharmaceuticals are routinely available and are prepared under GMP conditions. Radiochemistry development will further enhance the assortment of PET radiopharmaceuticals.



## References Chapter 1.3

### References

1. Holland JP, Williamson MJ, Lewis JS. Unconventional nuclides for radiopharmaceuticals. *Mol Imaging* 2010;9:1-20.
2. Elsinga PH, Todde S, Penuelas I, Meyer GJ, Farstad B, Faivre-Chauvet A, et al. Guidance on current good radiopharmacy practice (cGRPP) for the small-scale preparation of radiopharmaceuticals. *Eur J Nucl Med Mol Imaging* 2010;37:1049-62.
3. Miller PW, Long NJ, Vilar R, Gee AD. Synthesis of  $^{11}\text{C}$ ,  $^{18}\text{F}$ ,  $^{15}\text{O}$ , and  $^{13}\text{N}$  radiolabels for positron emission tomography. *Angew Chem Int Ed Engl* 2008;47:8998-9033.
4. Coenen HH. Fluorine-18 labeling methods: features and possibilities of basic reactions. *Ernst Schering Res Found Workshop* 2007;62:15-50.

Table 1: Features of  $^{18}\text{F}$  and  $^{11}\text{C}$  labelling: isotope dilution and typical reagent amounts

	<b>Theoretical SA (TBq/mmol)</b>	<b>Practical SA (TBq/mmol)</b>	<b>Amount of radiotracer (nmol)</b>	<b>Amount of precursor (nmol)</b>
$^{11}\text{C}$	$3.7 \cdot 10^5$	50	8	2500
$^{18}\text{F}$	$6.6 \cdot 10^4$	200	2	1000

SA, specific activity

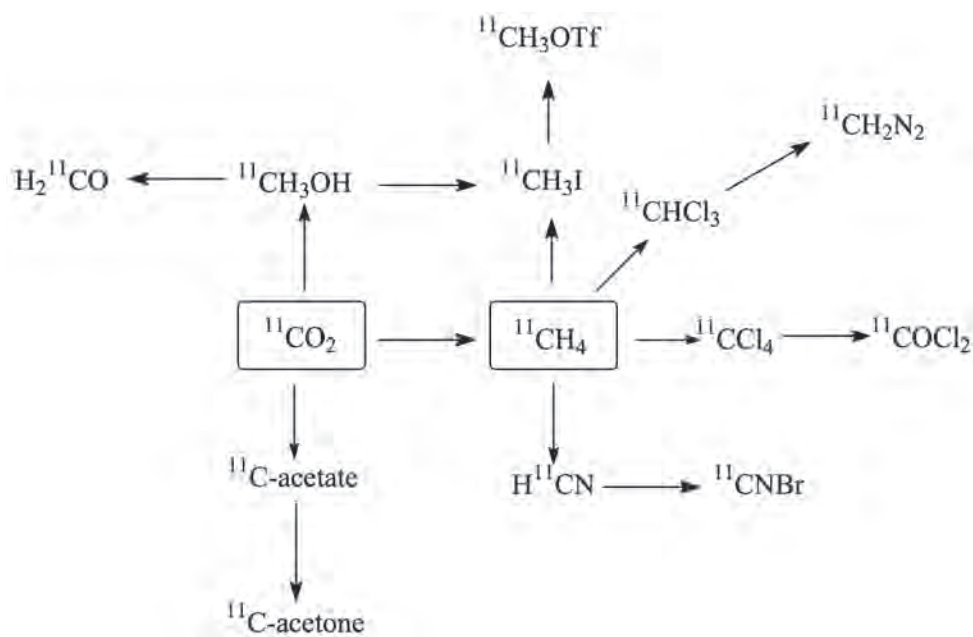
Table 2: Typical reaction conditions of [ $^{11}\text{C}$ ]methylations

	<b>[<math>^{11}\text{C}</math>]CH<sub>3</sub>I</b>	<b>[<math>^{11}\text{C}</math>]CH<sub>3</sub>OTf</b>
Temperature (°C)	20–60	80–130
Reaction time (min)	1	2–10
Precursor (mg)	< 1	1–10



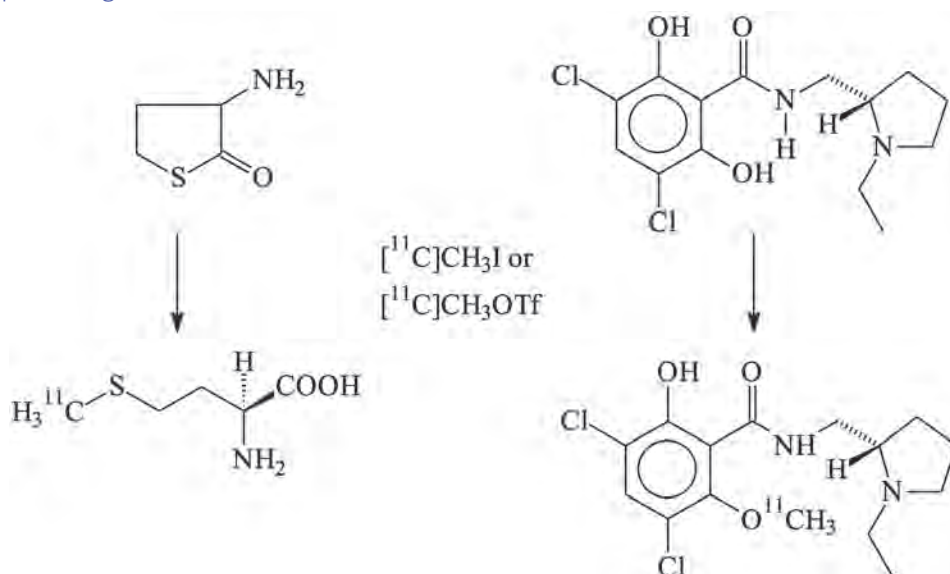
Figures and figure legends (see following pages for Figs. 1 and 2):

Figure 1: Production of  $^{11}\text{C}$  building blocks from cyclotron-produced  $[^{11}\text{C}]\text{CO}_2$  and  $[^{11}\text{C}]\text{CH}_4$ , including the methylating agents  $[^{11}\text{C}]\text{methyl iodide}$  and  $[^{11}\text{C}]\text{methyl triflate}$



© P. Elsinga

Figure 2: Two common  $^{11}\text{C}$ -methylation reactions: production of  $[^{11}\text{C}]\text{methionine}$  (left) and  $[^{11}\text{C}]\text{raclopride}$  (right)



© P. Elsinga

# Chapter 1 – Principles of PET radiochemistry

## 1.4 [<sup>18</sup>F]FDG synthesis

Francesca Giurgola, Ilaria Vaccaro and Giorgio Testanera

Thirty years have passed since [<sup>18</sup>F]FDG was first synthesised for studies in humans [1]. Today, it is still the most widely used radiotracer for PET scans. While oncological studies account for the majority of applications, [<sup>18</sup>F]FDG is also used electively for cardiological and neurological indications.

### What is 2-deoxy-2-(<sup>18</sup>F)fluoro-D-glucose?

[<sup>18</sup>F]FDG is a glucose analogue in which the OH group in the C2 position of the molecule is substituted by an <sup>18</sup>F group (fluoride). It is able to pass through the cellular membrane by facilitated transport following the same pathway as the glucose molecule. Inside the cell it is phosphorylated by hexokinase.

Since [<sup>18</sup>F]FDG, unlike glucose, lacks the OH group in the C2 position, it is not a substrate for subsequent enzymes of the glycolytic pathway and cannot be further metabolised by cells.

[<sup>18</sup>F]FDG reconversion owing to glucose-6-phosphatase entails a very slow transformation and, due to the negative polarisation, the reaction product ([<sup>18</sup>F]FDG-6P) is not able to pass through the cellular membrane. These biochemical features mean that the molecule is unable to return to the blood circulation, allowing the tracer to accumulate in cells that become visible on a PET scan owing to their beta-plus emissivity.

### [<sup>18</sup>F]fluoride

[<sup>18</sup>F]fluoride is commonly produced by a cyclotron and it is the radionuclidic component

in [<sup>18</sup>F]FDG. For more detailed information on how radionuclides are produced, the reader is referred to [2].

- Fluoride, especially in its F<sub>2</sub> form, is the most reactive and electronegative element in nature, allowing many possibilities for chemical combinations. Physical features are shown in Table 1.

T <sub>1/2</sub>	109.6 min
Decay	β+ 97% EC 3%
Energy	β+ 635 keV γ 511 keV

Table 1. Physical features of [<sup>18</sup>F]

The relatively long half-life of [<sup>18</sup>F] is very helpful for chemical and medical purposes: it allows complex synthesis, long-duration scans and late pharmacokinetic evaluations.

The [<sup>18</sup>F] radioisotope may be produced by two different types of nuclear reaction:

- <sup>20</sup>Ne(d, α)<sup>18</sup>F, which leads to F<sub>2</sub> in a gaseous form, used in electrophilic substitution reactions [3];
- <sup>18</sup>O(p, n)<sup>18</sup>F, which leads to formation of <sup>18</sup>F<sup>-</sup>, used in nucleophilic substitution reactions.

The second of these reactions is the most commonly used production system for radiopharmaceutical purposes.

### [<sup>18</sup>F]FDG synthesis

#### *Trapping and elution of [<sup>18</sup>F]*

The synthesis starts with [<sup>18</sup>F] coming from the cyclotron, usually pushed by gas into transport lines and then into the synthesis module, where it needs to be trapped on anion exchange cartridges intended to separate the water component <sup>18</sup>O. QMA Sep-Pak and Chromafix 30-PS-HCO<sub>3</sub> are the most commonly used cartridges for this purpose.

- The elution of [<sup>18</sup>F] from the cartridge to the reactor is achieved using a solution of Kryptofix/K<sub>2</sub>CO<sub>3</sub> in CH<sub>3</sub>CN. This solution works as a catalyst that increases the solubility of nucleophilic fluoride. Kryptofix is a crown ether capable of binding K<sup>+</sup> ions in order to avoid [<sup>18</sup>F]KF formation, thus allowing K<sup>+</sup> to work as an anti-ion for [<sup>18</sup>F]. This process helps to increase fluoride reactivity without interfering with the synthesis process. It should be noted that it is also possible to use TBA (tetrabutylammonium salt) with the same function as Kryptofix.

#### *Evaporation*

- For a correct synthesis process, the H<sub>2</sub>O excess still in the fluoride needs to be removed by evaporation. This is achieved through the addition of CH<sub>3</sub>CN, which forms an

azeotropic mixture with water, lowering its boiling point, and under a flux of inert gas (like He or N<sub>2</sub>). This process occurs under reduced pressure and temperature to avoid decomposition of the crown ethers.

#### *Substitution reaction*

As stated above, use of different cyclotron targets for [<sup>18</sup>F] production leads to two different types of substitution reaction:

- Electrophilic with gaseous F<sub>2</sub>
- Nucleophilic in S<sub>N</sub>2 with <sup>18</sup>F<sup>-</sup>
- Initially, FDG synthesis was performed with <sup>18</sup>F<sub>2</sub> in gaseous form and electrophilic substitution, but this technique is no longer used owing to very low specific activity and yield. It is also very difficult, technically speaking, to manage a gas target in a cyclotron and <sup>18</sup>F<sub>2</sub> in gas form for the purpose of synthesis.

In the nucleophilic reaction, after the evaporation a precursor is added. Mannose triflate (1,3,4,6-O-acetyl-2-O-trifluoromethanesulphonyl-β-D-mannopyranose) is most commonly used for this purpose, since its structure is similar to that of FDG: there is a triflate group in the C2 position and acetyl groups in the C1, C3, C4 and C6 positions, and their molecular bonds are very easy to break as a result of an increase or decrease in pH. The function of the acetyl groups is to ensure that fluorination will occur only in the C2 position, where triflate is found, which is a good leaving group.

The  $S_N2$  reaction will continue for 5 min with a reactor temperature of 85°C and the precursor concentration needs to be equimolar with Kryptofix// $K_2CO_3$ .

### Hydrolysis

Hydrolysis consists in removal of the protective acetyl groups in the C1, C3, C4 and C6 positions and can be of two types:

- Acid hydrolysis, using HCl: Hydrolysis occurs at a reactor temperature of 125°C and lasts 5–10 min. It may yield only a partially

hydrolysed product and also formation of 2-chloro-2-deoxy-D-glucose (2-CIDG) as a side reaction, but it has the great advantage of not leading to epimerisation.

- Basic hydrolysis, using NaOH: Hydrolysis occurs with the reactor at room temperature and takes a very short time (less than 1 min); chemically speaking, it is instantaneous. Perfect timing and NaOH concentration are very important for this kind of hydrolysis. Using NaOH can lead to formation of epimers such as [ $^{18}F$ ]FDM.

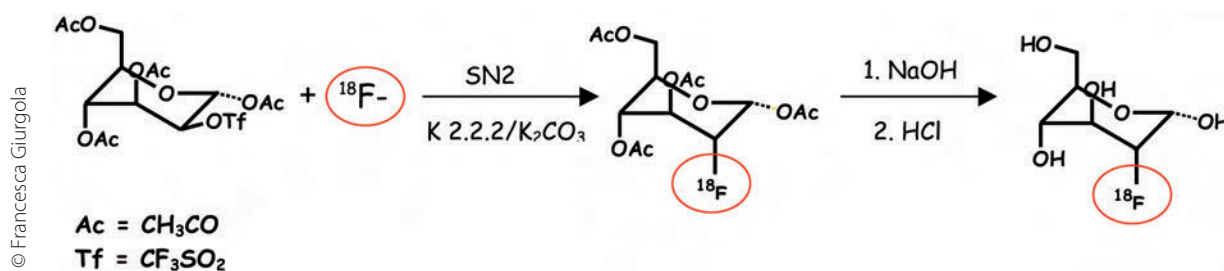


Figure 1: Synthesis of [ $^{18}F$ ]FDG

### Purification

The subsequent reaction steps give rise to many residues that need to be purified:

- Free [ $^{18}F$ ]fluoride
- Kryptofix/ $K_2CO_3$
- Partially hydrolysed [ $^{18}F$ ]FDG
- Mannose triflate which has not reacted

This purification process is achieved by means of chromatographic cartridges which also have the task of neutralising the hydrolysis solution.

The following are the most commonly used:

- PS-OH<sup>-</sup> and alumina to remove free fluoride
- PS-H<sup>+</sup> to remove Kryptofix/ $K_2CO_3$
- RP (reverse phase) cartridge to remove partially hydrolysed [ $^{18}F$ ]FDG and precursor.

Further details about the synthesis process can be found in references [4] and [5].

### [ $^{18}F$ ]FDG synthesis today

Nowadays [ $^{18}F$ ]FDG production is achieved using synthesis modules made of tubes and valves

able to connect different vials. Inside these modules, [<sup>18</sup>F]fluoride from the cyclotron is eluted into a reactor vial and undergoes all the different synthesis steps. These modules have the great advantage of usually being closed systems, which not only ensures product protection but also minimizes radiation exposure of staff. They are usually small and compact to allow adaptation to the small spaces inside the hot cells. Their ventilation system permits control radioactive and inert gas emissions during the synthesis process. Practical synthesis procedures depend on the type of module used. Generally sterile and single-use synthesis kits or cassettes are available for every module.

Single-use kits contain separately all the different component and cartridges needed to perform synthesis. The operator's tasks are to activate and correctly position them inside the modules, connecting different vials with transfer lines and valves.

There are two different types of cassette:

- "Not ready" cassettes: as in kits, reagents need to be activated while positioning is fixed, reducing operator dependence.
- "Ready to use" cassettes: Reagent positioning is completely predetermined and cassettes need only to be inserted into modules. Activation and dilution are performed by the module itself with a standardised procedure. This is considered an almost fully automatic synthesis procedure.

The great advantage in using cassettes is the reduction in possible operator-dependent errors, which increases the reproducibility and safety of the procedure. Modules with cassettes are also able to perform rinsing after synthesis, allowing cleaning of the module from residual radioactivity. This process is very useful for execution of subsequent syntheses within short time periods.

Before starting [<sup>18</sup>F]FDG synthesis, a sequence of tests must be carried out regarding pressure, flux, temperature, and leak tightness to ensure that the process will occur in safety. All control and reaction process are fully automated, but usually there is also limited possibility for manual intervention to solve problems during synthesis.

The synthesis process parameters, including temperature, pressure, flux and radiation activity, are monitored and graphically displayed on the control PC screen. Process parameters are also registered for further subsequent analysis. It is common to print a report of all data regarding the production process for documentation and archival purposes.

The development of fully automatic modules has brought about a sensible reduction in preparation and "cleaning" time for [<sup>18</sup>F]FDG synthesis. It has also made maintenance easier and rendered the synthesis process more reliable owing to the increase in standardisation.





Courtesy of Department of Nuclear Medicine,  
IRCCS Humanitas, Rozzano (Milan)

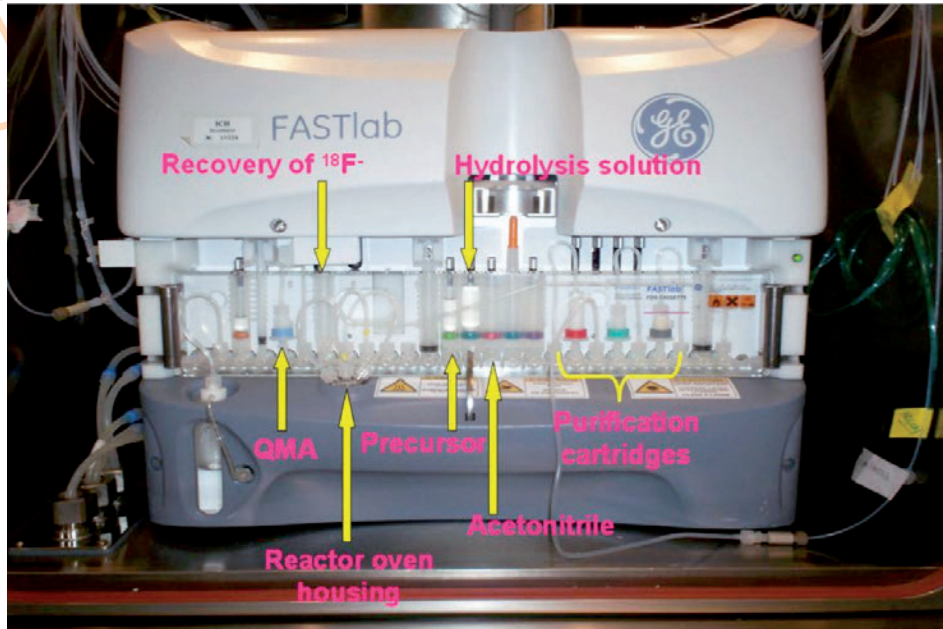


Figure 2: An example of an [ $^{18}\text{F}$ ]FDG module equipped with cassette: Fastlab GE

Courtesy of Department of Nuclear Medicine,  
IRCCS Humanitas, Rozzano (Milan)

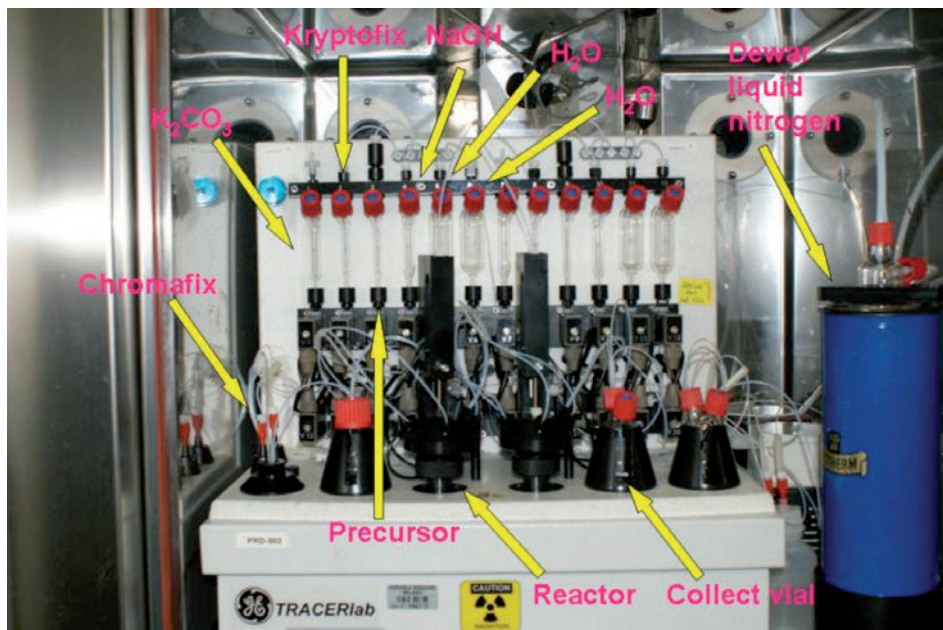


Figure 3: An example of an [ $^{18}\text{F}$ ]FDG double module: TRACERlab FX GE

## References Chapter 1.4

### References

1. Ido T, Wang C-N, Casella V et al. Labeled 2-deoxy-D-glucose analogs.  $^{18}\text{F}$ -labeled 2-deoxy-2-fluoro-D-glucose, 2-deoxy-2-fluoro-D-mannose and  $^{14}\text{C}$ -2-deoxy-2-fluoro-D-glucose. *J Label Compd Radiopharm* 1978;XIV:175-83.
2. Szczepura K. Chapter 6: PET isotope production. In : *Principles and practice of PET/CT. Part 1: A technologist's guide*. EANM, Vienna, 2010
3. Casella V, Ido T, Wolf AP et al. Anhydrous F-18 labeled elemental fluorine for radiopharmaceutical preparation. *J Nucl Med* 1980;21:750.
4. Bogni A, Pascali C. *Radiofarmaci marcati con isotopi emettitori di positroni*. Bologna: Patron, 2003.
5. Pascali C, Bogni A, Crippa F, Bombardieri E. *Concetti generali sulla produzione di radio farmaci emettitori di positroni*. Aretrè: 1999.



# Chapter 1 – Principles of PET radiochemistry

## 1.5 $^{68}\text{Ga}$ -peptide tracers

Jamshed B. Bomanji and Nikolaos D. Papathanasiou

### Introduction

Somatostatin receptor (SSTR) radionuclide tracers are of particular interest in oncology and their use is expanding worldwide. These tracers are synthetic analogues of a natural cyclic neuropeptide, somatostatin (SST), which exerts inhibitory and regulatory effects in various parts of the body such as the brain, peripheral neurons, endocrine pancreas, gut and immune system. The activities of SST are mediated through specific, G-coupled receptors (SSTRs) expressed on cell surfaces; to date, five different SSTR subtypes have been recognised. Neuroendocrine tumours (NETs) are neoplasms with distinct biological and clinical features; in particular they express high densities of SSTRs at their cell membranes. Thus, they can be effectively targeted with SSTR radionuclide probes: the tracer is injected and selectively binds to these receptors, then the receptor–tracer complex is internalised within tumour cells and accumulates in high concentrations compared with the concentrations in adjacent tissues. Thereafter, the emitted signal from the radionuclide is detected by gamma-cameras or hybrid PET-SPECT/CT scanners and maps the location and extent of tumour (Fig. 1).

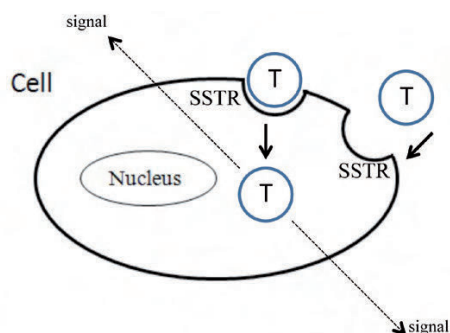


Figure 1

Figure 1: Principles of SSTR-based imaging. The radiolabelled tracer (T), with high affinity for SSTRs, is injected and binds avidly to SSTRs expressed in high densities on the cell surface. The receptor–tracer complex is then internalised within the cell. Subsequently, the signal emitted from the tracer radionuclide maps the distribution of tracer within the body

The basis for the development of SSTR tracers is the synthetic cyclic octapeptide octreotide. Octreotide retains the pharmacological profile of SST, but unlike natural SST is metabolically stable and has a relatively long biological half-life (~2 h), which enables its use in clinical practice. This analogue has been conjugated with a chelator, diethylene triamine penta-acetic acid (DTPA), which allowed successful binding of  $^{111}\text{In}$  molecule to obtain the first commercially available agent ( $^{111}\text{In}$ -DTPA<sup>0</sup>-octreotide, Octreoscan) in the early 1990s [1]. Whole-body and SPECT studies with Octreoscan have dominated the functional imaging of NETs until recently. Such studies are, however, limited by inherently suboptimal spatial resolution for the detection of small or deeply seated deposits or lesions in organs with high physiological tracer uptake (e.g. liver). Moreover, Octreoscan shows only moderate binding affinity for the SSTR-2 subtype (expressed by the majority of NETs), while DTPA, as a chelator, cannot form stable complexes with  $\beta$ -emitters ( $^{90}\text{Y}$  or  $^{177}\text{Lu}$ ) for the purpose of obtaining SSTR therapeutic agents.



The shortcomings of Octreoscan have been overcome with the advent of novel  $^{68}\text{Ga}$ -labelled peptides for SSTR PET/CT imaging. These tracers have advantageous pharmacological properties, including in particular a severalfold increase in binding affinity to SSTR-2. Applied in PET imaging they have brought about considerable improvements in spatial resolution and lesion localisation. With newer hybrid PET/CT scanners, high-quality, combined anatomical and functional information can be obtained within the same session, enhancing diagnostic accuracy. First clinical results obtained using a  $^{68}\text{Ga}$ -peptide,  $^{68}\text{Ga}$ -DOTA-TOC, in a small group of patients with carcinoid tumours were published in 2001 [2]. Since then, the number of published papers has multiplied and  $^{68}\text{Ga}$ -peptide PET/CT is becoming clinical routine in an increasing number of specialised centres. The accumulated evidence shows that it offers superior diagnostic performance compared with conventional Octreoscan, including when the latter yields negative or equivocal findings [3].  $^{68}\text{Ga}$ -peptide PET/CT is the state of the art functional imaging modality for NETs and is now replacing traditional Octreoscan in places where a PET facility is available.

### $^{68}\text{Ga}$ -peptide labelling

$^{68}\text{Ga}$  is a  $^{68}\text{Ge}/^{68}\text{Ga}$  generator product. The relatively long-lived (half-life  $\sim 270$  days) parent  $^{68}\text{Ge}$  decays by electron capture to  $^{68}\text{Ga}$ .  $^{68}\text{Ga}$  is an abundant short-lived (half-life 68 min) positron emitter, with 89% positron branch-

ing ( $\beta^+$  max. energy 1.89 MeV; 2.9 mm mean range in water), which subsequently decays to stable  $^{68}\text{Zn}$ .

$^{68}\text{Ge}$  is loaded on an  $\text{SnO}_2$  or  $\text{TiO}_2$  column;  $^{68}\text{Ga}$ , in ionic +3 oxidation state, is eluted as chloride using HCl solution. Prepurification of the eluate is often employed to minimize  $^{68}\text{Ge}$  breakthrough and to reduce the amount and volume of HCl in the solution. Afterwards, 10–50  $\mu\text{g}$  of the peptide (e.g. DOTA-TOC, DOTA-TATE) is dissolved in a suitable buffer (commonly sodium acetate or HEPES) and mixed with 200–800 MBq  $^{68}\text{Ga}$ . The role of the buffer is to keep  $\text{Ga}^{3+}$  in its ionic state and adjust pH to 3.5–4, which facilitates the formation of stable complexes of  $^{68}\text{Ga}$  with DOTA-conjugated peptides [4]. The buffered solution is incubated for  $\sim 10$  min at  $90^\circ\text{C}$  in a heating block and then subjected to sterile filtration. A high radiolabelling yield ( $>95\%$ ) of  $^{68}\text{Ga}$ -peptide tracer is achieved, which is analysed by instant thin-layer chromatography and high-performance liquid chromatography. By means of semi-automated systems, the whole process is carried out on-site within 12–25 min, obviating the need for manual handling of relatively high amounts of radioactivity and thus reducing radiation exposure to personnel. The radiolabelling procedure has been described in its basic principles and taking into account our department's protocol and experience; there is notable variation among centres worldwide regarding implemented methods of radiosynthesis [5].

### <sup>68</sup>Ga-peptides: tracers, properties and advantages

<sup>68</sup>Ga-peptides share the same basic structure, which resembles that of “conventional” Octreoscan: a synthetic SST analogue is conjugat-

ed with the chelator tetraazacyclododecane tetraacetic acid (DOTA) and this peptide–chelator complex is labelled with the positron emitter <sup>68</sup>Ga (Fig. 2).

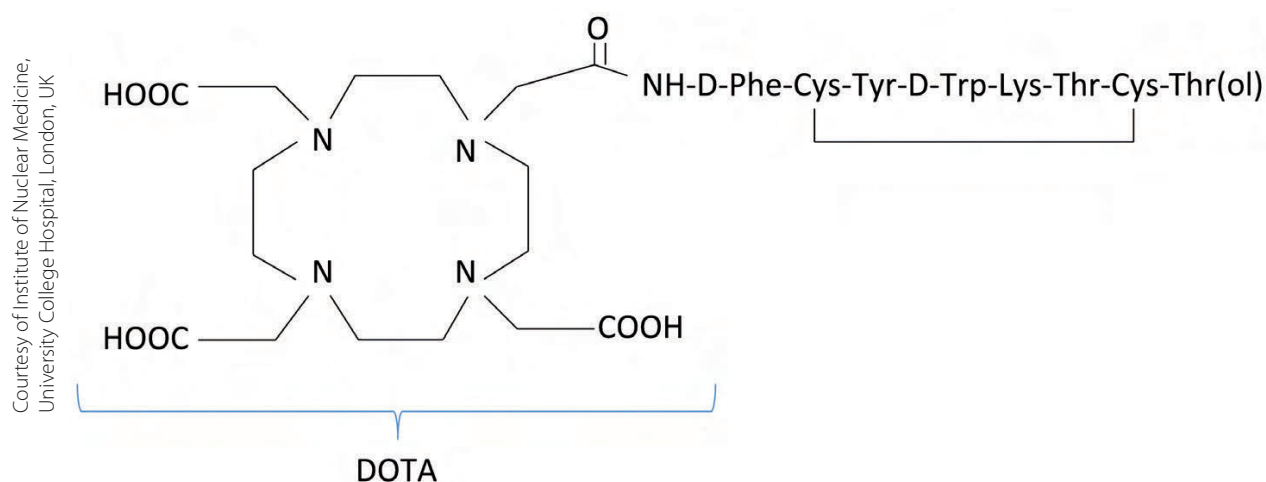


Figure 2: Chemical structure of <sup>68</sup>Ga-DOTA-Tyr<sup>3</sup>-octreotide. The macrocyclic chelator DOTA is conjugated with the octreotide SST analogue and this complex is labelled with <sup>68</sup>Ga

DOTA is an excellent macrocyclic chelator which forms stable complexes with metal radiotracers, such as <sup>68</sup>Ga, <sup>90</sup>Y or <sup>177</sup>Lu. <sup>68</sup>Ga-DOTA<sup>0</sup>-Tyr<sup>3</sup>-octreotide (<sup>68</sup>Ga-DOTA-TOC) was one of the first studied tracers, with tenfold higher binding affinity for SSTR-2 and an increased cell internalisation rate compared with Octreoscan. By replacing the C-terminal threoninol of the octreotide molecule with the natural amino acid threonine (i.e. changing octreotide to octreotate) we get the tracer <sup>68</sup>Ga-DOTA<sup>0</sup>-Tyr<sup>3</sup>-octreotate (<sup>68</sup>Ga-DOTA-TATE). <sup>68</sup>Ga-DOTA-TATE is a hyperselective SSTR-2

tracer, having the highest affinity among <sup>68</sup>Ga-peptides for SSTR-2 [6]. Another tracer, <sup>68</sup>Ga-DOTA<sup>0</sup>-1NaI<sup>3</sup>-octreotide (<sup>68</sup>Ga-DOTA-NOC) shows the broadest affinity profile, with high affinities for SSTR-2 and SSTR-5 and to a lesser extent for SSTR-3; this profile has been suggested to be coupled with enhanced diagnostic performance [7]. Figure 3 shows the basic structure of principal <sup>68</sup>Ga-labelled peptides and Table 1, their affinity profiles.

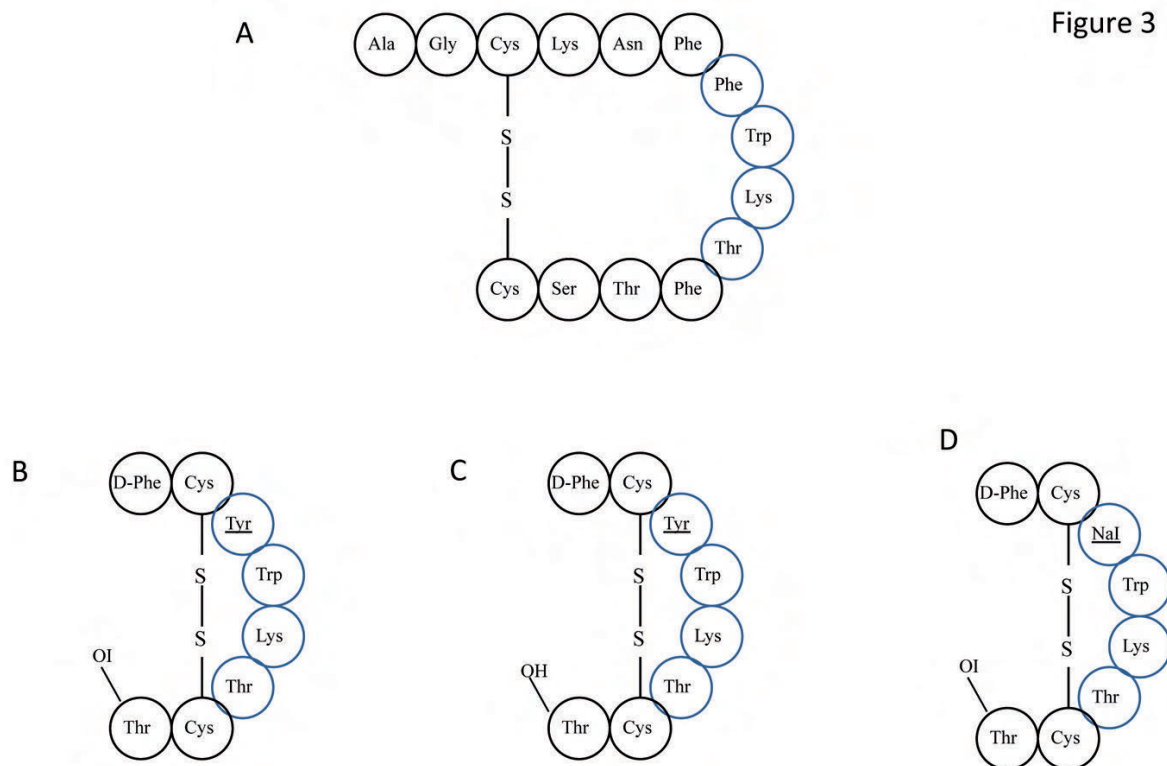
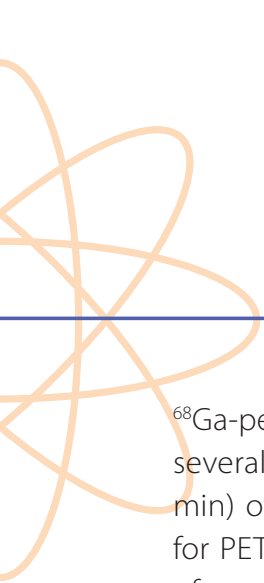


Figure 3

Figure 3A–D: Basic structure of SST and the main SST analogues. A Amino acid sequence of SST. B Amino acid sequence of the octapeptide Tyr<sup>3</sup>-octreotide (-TOC), obtained from octreotide by replacing Phe with Tyr at the C-3 position. C Octreotate (-TATE) sequence. This analogue is obtained by replacing the C-terminal threoninol of octreotide [see amino acid sequence in B] with the natural amino acid threonine (Thr). D The Nal<sup>3</sup>-octreotide (-NOC) sequence is produced by “inserting” Nal at the C-3 position of the octreotide molecule. -S-S- represents disulphide bonds between cystein (Cys) amino acids

There is a paucity of evidence regarding comparisons of the clinical efficacy of these various tracers. Such studies are difficult to perform, given the rarity and heterogeneity of NETs. All tracers bind to SSTR-2, but they do so with different affinities and exhibit various binding profiles for the other SSTR subtypes. The choice of tracer depends on the centre’s ex-

perience and preference. It seems reasonable, however, to choose either <sup>68</sup>Ga-DOTA-TOC or <sup>68</sup>Ga-DOTA-TATE if their respective <sup>90</sup>Y or <sup>177</sup>Lu counterparts are subsequently going to be used for therapy, so that the imaging peptide mimics as closely as possible the therapeutic peptide.



$^{68}\text{Ga}$ -peptides are particularly attractive for several reasons. The physical half-life (68 min) of  $^{68}\text{Ga}$  positron decay is convenient for PET imaging and matches the kinetics of peptides, with fast blood clearance and rapid target localisation.  $^{68}\text{Ga}$  is readily available on an everyday basis, independently of a nearby cyclotron. The long half-life (270 days) of parent  $^{68}\text{Ge}$  enables the use of the commercially available generator for up to 9–12 months or even longer and allows timely routine manufacture and shipment to nuclear medicine departments. The synthesis and labelling of peptides is relatively easy, with high radiolabelling yield (>95%). These tracers have favourable pharmacokinetic properties compared with Octreoscan, and enhanced diagnostic performance and clinical efficacy.

#### $^{68}\text{Ga}$ -peptides: protocol, biodistribution and pitfalls

$^{68}\text{Ga}$ -peptides show rapid blood clearance and tumoral accumulation. They are almost entirely excreted by the kidneys. The injected activities are in the range of 100–270 MBq depending on the applied tracer and the department's protocol. Images are acquired ~60 min p.i. with a dedicated PET/CT scanner in 3-D acquisition mode [8].

The physiological distribution of  $^{68}\text{Ga}$ -peptides reflects normal SSTR expression throughout the body. In general, there is intense tracer activity in the spleen, kidneys, pituitary and liver,

followed by adrenals, thyroid, salivary glands and bowel. Normal standardised uptake values in various organs show a wide range [9]. Physiological tracer accumulation in clusters of pancreatic islets (expressing SSTR-2) may mimic a focal lesion (most often in the pancreatic head) and is a potential source of pitfalls. Non-malignant, reactive nodes may show low-grade uptake owing to SSTR expression in activated lymphocytes [9]. Diffuse, low-grade uptake can be seen in the prostate gland and breast glandular tissue.

#### Clinical applications of $^{68}\text{Ga}$ -peptides

##### *Neuroendocrine tumours (NETs)*

NETs are a heterogeneous group of rare neoplasms (incidence 2.5–5 cases/100,000) that arise from neuroendocrine cells, mainly in the gastro-entero-pancreatic tract (GEP NETs) and less often in the bronchopulmonary system (pulmonary carcinoids). The incidence and prevalence of NETs has multiplied over the last 30 years owing to advances in endoscopic and imaging methods, either anatomical or functional, which have led to an increase in detection rates. NETs exhibit a striking variability in clinical behaviour and outcome. In a minority of cases (functional NETs), peptides or biogenic amines secreted by the tumour lead to distinct clinical syndromes, such as carcinoid or Zollinger-Ellison syndrome. Most often, tumours are non-functional and show a silent clinical course until late presentation

with mass effect and hepatic or skeletal metastases. There are serum markers with diagnostic and prognostic value for NETs. The proliferation marker Ki-67 is utilised to assess tumour grade and prognosis. Chromogranin A is increased in 60–80% of GEP NETs, is correlated with tumour burden, and is useful in diagnosing non-functioning tumours and later in assessing the response to therapy/follow-up. Imaging modalities are essential for accurate staging and subsequent proper clinical management. Treatment requires a multidisciplinary approach. It should be patient tailored, depending on tumour burden, symptoms and final intent: either curative, to arrest tumour growth, or palliative, to ameliorate symptoms by decreasing the secretion of bioactive agents [10].

Fluorine-18 fluorodeoxyglucose (<sup>18</sup>F-FDG) is the mainstay for the vast majority of oncological PET/CT; however, it is less well-suited for NETs. In general, these tumours are well differentiated, with low growth rate and metabolic turnover; hence they show low sensitivity for <sup>18</sup>F-FDG. In a study of 38 NET patients, Kayani et al. found that <sup>18</sup>F-FDG had inferior sensitivity compared with <sup>68</sup>Ga-DOTA-TATE (66% vs. 82%). However, patients with high-grade tumours and a higher proliferation rate (Ki-67 index >20%) showed higher uptake of <sup>18</sup>F-FDG than of <sup>68</sup>Ga-DOTA-TATE [11]. SSTRs, mainly of 2 and 5 subtypes, are located on the membrane of NET cells. This has been proven by preclinical, in vitro studies which demonstrated SSTR

expression (with in situ mRNA hybridisation) and measured the densities of these receptor proteins (with autoradiography and immunohistochemistry). The presence of SSTRs as well as their increased density provided the molecular basis for efficient targeting of NETs with radiolabelled peptides and an emerging number of imaging and therapeutic applications. <sup>18</sup>F-FDG is reserved for the minority of less well-differentiated NETs, with increased glucose metabolism and more aggressive behaviour.

Regarding the clinical management of NETs, the main applications of <sup>68</sup>Ga-peptide PET/CT are:

- Detection of primary tumours and initial staging of loco-regional and distant metastatic disease.
- Restaging of patients with known NETs to detect residual, recurrent or progressive disease.
- Determination of SSTR status and subsequent selection of patients with metastatic disease who are eligible for therapy with radionuclide SST analogues (<sup>177</sup>Lu or <sup>90</sup>Y-DOTA peptides) or “cold” octreotide.

Since <sup>68</sup>Ga-peptide imaging accurately detects and delineates tumour burden, it has been tested in monitoring response to therapy [12]. Such studies should be interpreted with caution because serial changes in the number or intensity of positive lesions indicate changes





in SSTR status – not tumoral metabolic activity as with  $^{18}\text{F}$ -FDG – and such changes do not necessarily correspond to a therapeutic response.

An increasing number of published reports show the diagnostic efficacy of  $^{68}\text{Ga}$ -peptide PET/CT. In a prospective study of 84 proven or suspected NETs,  $^{68}\text{Ga}$ -DOTA-TOC PET showed superior per-patient sensitivity (97%) than CT (61%) and SSTR-SPECT (52%).  $^{68}\text{Ga}$ -DOTA-TOC detected more lesions than the other modalities and was very effective in the detection of bone lesions [13]. Putzer et al. also found that  $^{68}\text{Ga}$ -DOTA-TOC detected bone metastases at a significantly higher rate than CT [14]. This is very important, since skeletal involvement in NETs carries a dismal prognosis and precludes extensive surgical resection. In two recent studies, with a total of 38 biopsy-proven NETs,  $^{68}\text{Ga}$ -peptide was superior (positive in 37/38) to  $^{18}\text{F}$ -DOPA (positive in 23/38 patients) PET/CT [15, 16]. The limitations of such studies include the small numbers of evaluated patients (reflecting the rarity of NETs), possible referral bias and the fact that imaging results are not validated with a standard reference method, something which frequently is not feasible or ethical.

Accurate lesion detection by  $^{68}\text{Ga}$ -peptide PET/CT has a significant impact on therapeutic management. Surgery with curative intent is the treatment method of choice for localised NETs.  $^{68}\text{Ga}$ -peptide imaging is

valuable before such a treatment approach is considered because it can accurately determine tumour extent (localising the primary tumour and identifying small or unsuspected, loco-regional nodal metastases) and guide subsequent surgical resection. Otherwise it can effectively rule out patients with distant metastatic disease, especially in the skeleton, from inappropriate surgical treatment (Fig. 4).

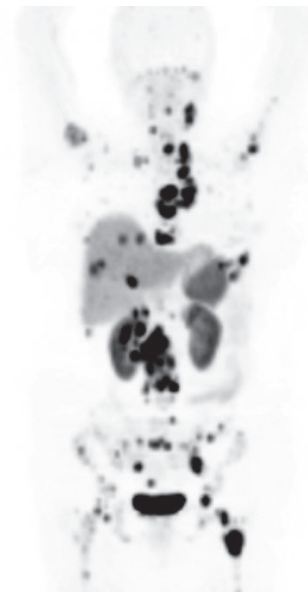


Figure 4: Patient with ileal carcinoid tumour, with multiple soft tissue and bone metastases above and below the diaphragm. This patient is unsuitable for surgical treatment; a systemic approach would be more appropriate

Frilling et al. found that  $^{68}\text{Ga}$ -DOTA-TOC contributed to clinical decision-making prior to liver surgery with curative intent [17]. It could identify patients eligible for such treatment



by determining disease extent and helped in planning the surgical strategy. In the same series, 7/15 patients evaluated for liver transplantation were excluded from further screening owing to detection of extrahepatic deposits not detected by CT or MRI. In another clinical setting, with 59 patients having metastatic NET and an unknown primary, <sup>68</sup>Ga-DOTA-NOC localised the primary site in 60% of cases [18]. The majority were ileal/jejunal and pancreatic NETs. Management change was reported in a small but considerable proportion (10%), with surgical resection of primary tumour.

The most important contribution of imaging peptides in clinical management lies in the selection of patients eligible for treatment with “cold” octreotide or SSTR radionuclide therapy. Patients who demonstrate sufficient tracer uptake on imaging can be further targeted with the corresponding <sup>90</sup>Y- or <sup>177</sup>Lu-labelled therapeutic analogues. The receptor–therapeutic peptide complex is internalised in a way similar to that during imaging, and the β-emitter then causes irreparable DNA damage and cell death. The therapeutic benefit is enhanced via direct radiation damage beyond the target cell to nearby cells and associated release of toxic metabolites (“bystander effect”). This mode of treatment has limited toxicity, induces partial responses in patients with progressive metastatic disease and shows a survival benefit compared with historical data.

### *Paraganglioma and phaeochromocytoma*

Paragangliomas are rare chromaffin cell tumours at extra-adrenal sites along the sympathetic and/or parasympathetic chain; phaeochromocytoma is the corresponding term for tumours originating from the adrenal gland. More than 10% of these tumours are malignant, with metastases to lymph nodes, liver, bones and lungs. The noradrenaline analogue MIBG is the radiopharmaceutical of choice. It enters the chromaffin cell via an active uptake mechanism and is then stored in intracellular granules or in the cytoplasm. MIBG is less sensitive for paragangliomas than for phaeochromocytomas. There are small series showing that <sup>68</sup>Ga-peptide PET/CT can be very useful for depicting paragangliomas, especially in MIBG-negative cases. If these show sufficient <sup>68</sup>Ga-peptide uptake, they can be further targeted with SSTR radionuclide β-emitters.

### *Medullary thyroid carcinoma (MTC)*

Owing to their neuroendocrine origin and behaviour, MTC cells express SSTR-2 and -5 on their surface, but with a lower and more heterogeneous density than in other NETs. In a small series of 18 MTC patients evaluated simultaneously with <sup>68</sup>Ga-DOTA-TATE and <sup>18</sup>F-FDG, none of the tracers was found to be accurate in mapping the whole tumour burden [19]. However, <sup>68</sup>Ga-peptide imaging should be applied if treatment with radionuclide analogues is considered.



### ***Meningiomas and other tumours***

Meningiomas are the most frequent extra-axial primary brain tumours and show high SSTR-2 expression.  $^{68}\text{Ga}$ -peptide PET/CT has been applied in meningiomas to detect potential skull base involvement and to help design radiotherapy treatment planning volumes.

Apart from DOTA-peptides for SSTR imaging,  $^{68}\text{Ga}$  has been used to label various other peptides, bombesin being the most important. Bombesin is an amino acid originally purified from the skin of frog which stimulates gastrin release from G cells. Bombesin receptors are overexpressed in prostate and breast cancer. Bombesin-based ligands are still a research issue at specialised centres and have not achieved broad use.

### ***Potential future applications***

For the time being  $^{68}\text{Ga}$ -based tracers are dominated by  $^{68}\text{Ga}$ -peptides applied in NETs and neural crest tumours. However, other ongoing tracer developments have notable diagnostic potential.  $^{68}\text{Ga}$ -citrate shares a similar uptake pathway to conventional  $^{67}\text{Ga}$ -citrate. It is a promising tracer for infection/inflammation, and accumulates in inflammatory lesions owing to increased capillary permeability, uptake by leucocytes and bacteria and binding to lactoferrin and bacterial siderophores[20].  $^{68}\text{Ga}$ -labelled macroaggregated albumin and

aerosol may be developed for lung perfusion/ventilation studies.  $^{68}\text{Ga}$ -biphosphonates for skeletal imaging has been reported [21] and  $^{68}\text{Ga}$ -DOTA-RGD has been used to image angiogenesis. Although this statement may sound somewhat ambitious and premature, it appears that  $^{68}\text{Ge}/^{68}\text{Ga}$  generator has the potential to evolve as “the  $^{99}\text{Mo}/^{99\text{m}}\text{Tc}$  generator” for PET imaging.

### **Key points – “take-home” message**

- $^{68}\text{Ga}$ -DOTA-peptide PET/CT is the contemporary functional method of choice for somatostatin receptor imaging of NETs.
- The most widely applied tracers are  $^{68}\text{Ga}$ -DOTA-TOC,  $^{68}\text{Ga}$ -DOTA-NOC and  $^{68}\text{Ga}$ -DOTA-TATE
- $^{68}\text{Ga}$ -peptides show excellent affinities for somatostatin receptors and are available on an everyday basis from an in-house generator
- $^{68}\text{Ga}$ -peptides have an impact on clinical management and are applied in initial staging, in re-staging and, most importantly, in the selection of eligible patients for targeted radionuclide therapy.



## References Chapter 1.5

### References

1. Krenning EP, Kwekkeboom DJ, Bakker WH, Breeman WA, Kooij PP, Oei HY, et al. Somatostatin receptor scintigraphy with [ $^{111}\text{In}$ -DTPA-D-Phe $^1$ ]- and [ $^{123}\text{I}$ -Tyr $^3$ ]-octreotide: the Rotterdam experience with more than 1000 patients. *Eur J Nucl Med* 1993;20:716-31.
2. Hofmann M, Maecke H, Borner R, Weckesser E, Schoffski P, Oei L, et al. Biokinetics and imaging with the somatostatin receptor PET radioligand ( $^{68}\text{Ga}$ -DOTATOC: preliminary data. *Eur J Nucl Med* 2001;28:1751-7.
3. Srirajaskanthan R, Kayani I, Quigley AM, Soh J, Caplin ME, Bomanji J. The role of  $^{68}\text{Ga}$ -DOTATATE PET in patients with neuroendocrine tumors and negative or equivocal findings on  $^{111}\text{In}$ -DTPA-octreotide scintigraphy. *J Nucl Med* 2010;51:875-82.
4. Bauwens M, Chekol R, Vanbilloen H, Bormans G, Verbruggen A. Optimal buffer choice of the radiosynthesis of ( $^{68}\text{Ga}$ -Dotatoc for clinical application. *Nucl Med Commun* 2010;31:753-8.
5. Breeman WA, de Jong M, de Blois E, Bernard BF, Konijnenberg M, Krenning EP. Radiolabelling DOTA-peptides with  $^{68}\text{Ga}$ . *Eur J Nucl Med Mol Imaging* 2005;32:478-85.
6. Reubi JC, Schar JC, Waser B, Wenger S, Heppeler A, Schmitt JS, et al. Affinity profiles for human somatostatin receptor subtypes SST1-SST5 of somatostatin radiotracers selected for scintigraphic and radiotherapeutic use. *Eur J Nucl Med* 2000;27:273-82.
7. Wild D, Bomanji JB, Reubi JC, Maecke HR, Caplin ME, Ell PJ. Comparison of  $^{68}\text{Ga}$ -DOTANOC and  $^{68}\text{Ga}$ -DOTATATE PET/CT in the detection of GEP NETs (OP231). *Eur J Nucl Med Mol Imaging* 2009;36 (Suppl 2):S201.
8. Virgolini I, Ambrosini V, Bomanji JB, Baum RP, Fanti S, Gabriel M, et al. Procedure guidelines for PET/CT tumour imaging with  $^{68}\text{Ga}$ -DOTA-conjugated peptides:  $^{68}\text{Ga}$ -DOTA-TOC,  $^{68}\text{Ga}$ -DOTA-NOC,  $^{68}\text{Ga}$ -DOTA-TATE. *Eur J Nucl Med Mol Imaging* 2010;37:2004-10.
9. Shastri M, Kayani I, Wild D, Caplin M, Visvikis D, Gacinovic S, et al. Distribution pattern of  $^{68}\text{Ga}$ -DOTATATE in disease-free patients. *Nucl Med Commun* 2010;31:1025-32.
10. Modlin IM, Oberg K, Chung DC, Jensen RT, de Herder WW, Thakker RV, et al. Gastroenteropancreatic neuroendocrine tumours. *Lancet Oncol* 2008;9:61-72.
11. Kayani I, Bomanji JB, Groves A, Conway G, Gacinovic S, Win T, et al. Functional imaging of neuroendocrine tumors with combined PET/CT using  $^{68}\text{Ga}$ -DOTATATE (DOTA-DPhe $^1$ ,Tyr $^3$ -octreotate) and  $^{18}\text{F}$ -FDG. *Cancer* 2008;112:2447-55.
12. Haug AR, Auernhammer CJ, Wangler B, Schmidt GP, Uebles C, Goke B, et al.  $^{68}\text{Ga}$ -DOTATATE PET/CT for the early prediction of response to somatostatin receptor-mediated radionuclide therapy in patients with well-differentiated neuroendocrine tumors. *J Nucl Med* 2010;51:1349-56.
13. Gabriel M, Decristoforo C, Kendler D, Dobrozemsky G, Heute D, Uprimny C, et al.  $^{68}\text{Ga}$ -DOTA-Tyr $^3$ -octreotide PET in neuroendocrine tumors: comparison with somatostatin receptor scintigraphy and CT. *J Nucl Med* 2007;48:508-18.
14. Putzer D, Gabriel M, Henninger B, Kendler D, Uprimny C, Dobrozemsky G, et al. Bone metastases in patients with neuroendocrine tumor:  $^{68}\text{Ga}$ -DOTA-Tyr $^3$ -octreotide PET in comparison to CT and bone scintigraphy. *J Nucl Med* 2009;50:1214-21.
15. Haug A, Auernhammer CJ, Wangler B, Tiling R, Schmidt G, Goke B, et al. Intraindividual comparison of  $^{68}\text{Ga}$ -DOTATATE and  $^{18}\text{F}$ -DOPA PET in patients with well-differentiated metastatic neuroendocrine tumours. *Eur J Nucl Med Mol Imaging* 2009;36:765-70.
16. Ambrosini V, Tomassetti P, Castellucci P, Campana D, Montini G, Rubello D, et al. Comparison between  $^{68}\text{Ga}$ -DOTA-NOC and  $^{18}\text{F}$ -DOPA PET for the detection of gastroentero-pancreatic and lung neuro-endocrine tumours. *Eur J Nucl Med Mol Imaging* 2008;35:1431-8.
17. Frilling A, Sotiropoulos GC, Radtke A, Malago M, Bockisch A, Kuehl H, et al. The impact of  $^{68}\text{Ga}$ -DOTATOC positron emission tomography/computed tomography on the multimodal management of patients with neuroendocrine tumors. *Ann Surg* 2010;252:850-6.



18. Prasad V, Ambrosini V, Hommann M, Hoersch D, Fanti S, Baum RP. Detection of unknown primary neuroendocrine tumours (CUP-NET) using (68)Ga-DOTA-NOC receptor PET/CT. *Eur J Nucl Med Mol Imaging* 2010;37:67-77.
19. Conry BG, Papathanasiou ND, Prakash V, Kayani I, Caplin M, Mahmood S, et al. Comparison of (68)Ga-DOTATATE and (18)F-fluorodeoxyglucose PET/CT in the detection of recurrent medullary thyroid carcinoma. *Eur J Nucl Med Mol Imaging* 2010;37:49-57.
20. Nanni C, Errani C, Boriani L, Fantini L, Ambrosini V, Bosch S, et al. 68Ga-citrate PET/CT for evaluating patients with infections of the bone: preliminary results. *J Nucl Med* 2010;51:1932-6.
21. Fellner M, Baum RP, Kubicek V, Hermann P, Lukes I, Prasad V, et al. PET/CT imaging of osteoblastic bone metastases with (68)Ga-bisphosphonates: first human study. *Eur J Nucl Med Mol Imaging* 2010;37:834.
22. Antunes P, Ginj M, Zhang H, Waser B, Baum RP, Reubi JC, et al. Are radiogallium-labelled DOTA-conjugated somatostatin analogues superior to those labelled with other radiometals? *Eur J Nucl Med Mol Imaging* 2007;34:982-93.

Table 1: Affinity profiles ( $IC_{50}$  values<sup>1</sup>) of peptides for SSTRs 1–5

	<b>SSTR-1</b>	<b>SSTR-2</b>	<b>SSTR-3</b>	<b>SSTR-4</b>	<b>SSTR-5</b>
SST-28	3.8±0.3	2.5±0.3	5.7±0.6	4.2±0.3	3.7±0.4
Ga-DOTA-TOC	>10,000	2.5±0.5	613±140	> 1,000	73±21
Ga-DOTA-TATE	>10,000	0.20±0.04	>1,000	300±140	377±18
Ga-DOTA-NOC	>10,000	1.9±0.4	40±5.8	260±74	7.2±1.6
In-DTPA-octreotide	>10,000	22±3.6	182±13	>1,000	237±52

<sup>1</sup> The half-maximal inhibitory concentration ( $IC_{50}$ ) is a measure of the effectiveness of a compound in inhibiting a biological or biochemical function. This quantitative measure indicates how much of a particular drug or other substance (inhibitor) is needed to inhibit a given biological process (or component of a process, i.e. an enzyme, cell, cell receptor or microorganism) by half. The lower the  $IC_{50}$  value, the higher the affinity of the tracer.

$IC_{50}$  values are in nmol/l (mean±SE). Data are exported from Reubi et al. [6] and Antunes et al [22]

# Chapter 2 – Clinical applications of PET/CT in oncology

## 2.1 Introduction

Wim J.G. Oyen and Arturo Chiti

Since the introduction of integrated PET/CT scanners approximately 10 years ago, a large number of indications for this technology in oncology have been investigated and subsequently proven. Fluorodeoxyglucose (FDG) remains the main radiopharmaceutical for PET/CT, although a revival of well-known tracers such as fluorothymidine (FLT) and  $^{11}\text{C}$ - and  $^{18}\text{F}$ -labelled choline derivatives and the development of new agents such as  $^{68}\text{Ga}$ -labelled somatostatin derivatives are enhancing the application of PET/CT even further and accelerating the use of molecular imaging in oncology.

In the following sections, the indications for and performance of PET/CT are summarised for tumour types in which PET/CT plays an established, decisive or significant role in the diagnostic process and follow-up of cancer patients and the management of their disease. Upcoming indications are discussed, as the field is rapidly evolving beyond staging and re-staging using whole-body PET/CT. Such a standard and qualitative procedure places a limited demand on patient preparation and data acquisition. When progressing towards therapy response monitoring and radiation treatment planning based on molecular imag-

ing results, the demands dramatically increase. To allow robust quantification of data and adequate incorporation of molecular imaging in radiation treatment plans, there is an absolute demand for strict standardisation, QC and QA.

EANM is leading this process through EANM Research Ltd (EARL), founded in 2006 as an initiative for Multicentre Nuclear Medicine and Research (<http://earl.eanm.org>). The project is set up as an FDG-PET/CT accreditation programme, based on the “FDG PET and PET/CT: EANM procedure guideline for tumour PET imaging: version 1.0”, published in EJNMMI in January 2010. The role of the nuclear medicine technologist in this process will be important and, indeed, crucial to its success. Correct instruction and preparation of patients, adequate set-up of scanners and other devices according to agreed procedures and strict adherence to protocols for acquisition and image processing do place higher demands on the professionalism of the nuclear medicine technologist. Ultimately, the close multidisciplinary collaboration within the field of nuclear medicine will increase the quality of our work and further enhance the impact of molecular imaging in oncology.

# Chapter 2 – Clinical applications of PET/CT in oncology

## 2.2 Head and neck cancer

Murat Fani Bozkurt

### Introduction

**Head and neck cancer** is the sixth most common malignancy worldwide and accounts for 2–5% of all cancers. The great majority of head and neck cancers are epithelial cancers, most of which are classified as oropharyngeal, nasopharyngeal or laryngeal squamous cell cancers according to their anatomical location. Since the head and neck region is quite a limited area, the diagnosis and treatment of head and neck cancers are difficult and require a team of surgeons, oncologists, radiation oncologists and imaging specialists. The treatment options consist of surgery, radiotherapy, chemotherapy or, as employed in most patients, a combination thereof. Appropriate diagnosis which leads to use of suitable treatment options is very important both for disease control and for the well-being of patients with regard to daily activities such as speaking and feeding [1].

Less than one-third of head and neck cancers present as stage I or II, i.e. most tumours are at a more advanced stage at the time of presentation. The most common sites for head and neck cancers are the tongue base and the tonsillar fossa, which together account for approximately 75% of all sites. Tobacco and alcohol are causative factors for head and neck cancers and heavy use of both tobacco and alcohol often leads to an additional primary tumour of the lung or oesophagus. Early diagnosis and appropriate treatment are of great importance for long-term survival, as in many other types of cancer [2].

### Role of PET/CT

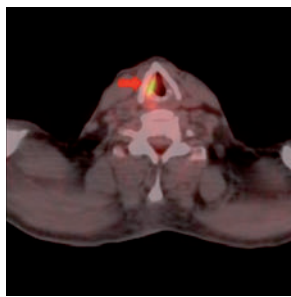
The role of PET/CT in the management of head and neck cancer is increasing. The most commonly used PET radiotracer is FDG, as in other tumours. The normal pattern of FDG uptake in the head and neck region is somewhat complex and some normal variants may mimic pathological uptake. PET/CT is a more useful imaging modality compared with PET alone since it can provide a combination of anatomical and functional information that helps to identify normal variants more clearly. The indications for PET/CT in head and neck cancer are as follows:

1. Staging of primary head and neck cancer
2. Identification of sites of recurrence
3. Distinguishing residual disease from post-operative changes
4. Assessment of the site of an unknown primary tumour
5. Therapy response evaluation
6. Evaluation of prognosis

### Patient preparation and PET/CT imaging protocol

Prior to oncological FDG PET/CT imaging, patients should be in the fasting state for at least 4–6 h. Blood glucose level is measured before FDG injection. The ideal glucose level is generally accepted to be lower than 140 mg/dl but especially for some diabetic patients, whose blood glucose levels are poorly regulated, glucose levels up to 200 mg/dl are accepted. Insulin should be avoided soon before FDG

injection but may be applied a few hours beforehand whenever needed. After intravenous FDG injection, patients are advised to lie still and rest for at least 45 min, the uptake period of FDG. Since body motion and some muscular activities such as speaking and chewing can give rise to muscular uptake which can cause confusion at scan interpretation, patients should be encouraged to avoid any unnecessary body motion, eating, drinking and speaking (Fig. 1).



Courtesy of Başkent University  
Department of Nuclear Medicine,  
Mehmet Aydın, Adana, TURKEY

Figure 1: Unilateral FDG uptake at the vocal cords (arrow), due to vocal cord paralysis

Patients should micturate following the uptake period and they are then taken into the scanning room, where they lie supine on the imaging table. The CT part of the study is generally performed first. Intravenous contrast agents are seldom used when oral agents can be administered to outline normal bowel. For head and neck cancer imaging, the scan range often includes the whole skull to the mid-thighs. Although this can differ among PET/CT scanners, images are acquired in blocks of 15 cm where five to six blocks (bed positions) are needed to complete the study. During the

scanning, immobilisation of the patient, especially the head region, is of great importance for interpretation. Arms down position is the preferred imaging position for head and neck cancer patients.

### Staging of head and neck cancer

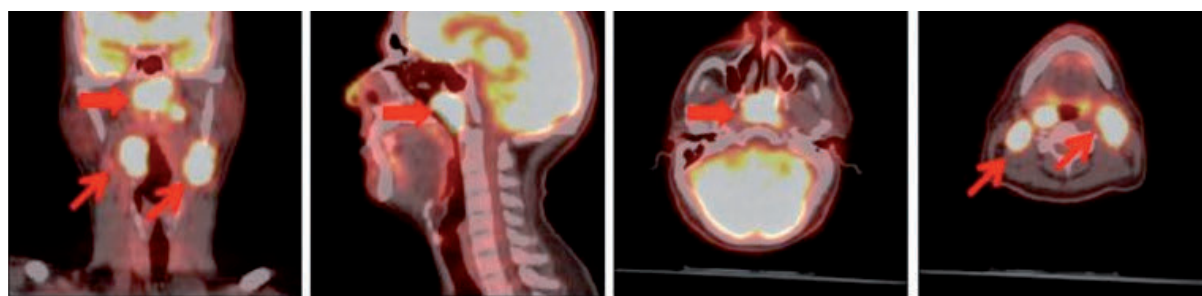
More than 95% of all head and neck cancers can be detected by PET/CT. PET/CT is very successful for assessment of tumour extent but it is less useful for the assessment of mucosal or submucosal extent owing to the limited spatial resolution.

Lymph node metastasis has prognostic value in head and neck cancer. Given the fact that more than 300 of approximately 800 lymph nodes in the entire human body are located in the head and neck region, it is very important to assess whether lymph nodes harbour metastatic disease. Anatomical imaging modalities such as ultrasonography, CT and MRI rely on lymph node size to distinguish metastatic nodes. However, it is known that nodal size alone cannot differentiate malignant involvement of lymph nodes. Small lymph nodes may harbour metastasis while large lymph nodes may only be reactive. PET/CT has been shown to be more sensitive than MRI and CT in the detection of lymph node metastasis. The success of PET/CT is size dependent but with the help of modern PET/CT cameras with improved resolution capacity, small nodes of a few millimetres can be detected. Ultrasound guided fine needle aspiration biopsy of lymph

nodes (even when smaller than 10 mm) acts as a standard diagnostic tool for metastatic lymph node involvement. PET/CT is successful in detecting occult lymph node metastasis in clinically node-negative (N0) head and neck cancers, most of which are oral or oropharyngeal cancers. Studies have reported that

PET/CT can detect occult disease in about 7% of patients. PET/CT is more helpful in patients with T1–T3 disease, among whom the use of PET can reduce the probability of occult lymph node metastasis to below 15% [3] (Figs. 2, 3).

Courtesy of Başkent University  
Department of Nuclear Medicine,  
Mehmet Aydın, Adana, TURKEY



A

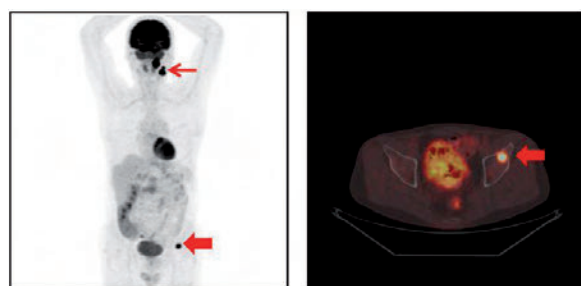
B

C

D

Figure 2A–D: Coronal (A), sagittal (B) and transaxial (C and D) FDG PET/CT images of a 45-year-old male with the diagnosis of nasopharyngeal cancer, showing the primary tumour (wide arrows) and lymph node metastasis (arrows)

Courtesy of Başkent University  
Department of Nuclear Medicine,  
Mehmet Aydın, Adana, TURKEY



A

B

Figure 3A, B: Whole-body maximum intensity projection (A) and transaxial (B) FDG PET/CT images of a 35-year-old male with the diagnosis of metastatic head and neck cancer to cervical lymph nodes (wide arrows) and iliac bone (arrow)

### PET/CT vs sentinel lymph node biopsy

Although sentinel lymph node biopsy is not yet a standard of care procedure for head and neck cancers, there are some reports which support its use in the disease management. PET/CT cannot replace sentinel lymph node biopsy in head and neck cancer because of the impact of the limited spatial resolution on detection of micrometastases. Owing to this limited spatial resolution, the sensitivity of PET/CT for detection of lymph node metastasis is lower than that of sentinel lymph node biopsy, though the specificity of PET/CT is reported to be higher. It is recommended that sentinel lymph node biopsy should be performed when PET/CT is negative and neck dissection when PET/CT is positive for lymph node metastasis. This potential use of PET/CT has been reported to reduce the number of futile neck dissections.

### Detection of synchronous primary cancer

PET/CT serves as a very useful imaging modality for the detection of synchronous primary disease in patients with head and neck cancer. Since there is a common aetiological effect of alcohol and tobacco for head and neck and respiratory tract cancers, synchronous lesions are found in nearly 20% of patients at a rate of 5% per year. Conventional imaging modalities may have a limited role compared with PET/CT, which is often capable of detecting lesions that have not been suspected. If PET only imaging is done instead of PET/CT, then combination with CT of the chest becomes crucial.

### Detection of the site of an unknown primary

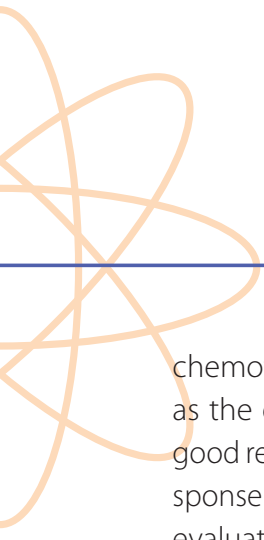
About 1 in 20 cases of head and neck cancer presents only as a metastatic lymph node without any clues regarding the primary site on conventional imaging modalities. As already mentioned, early detection and treatment are of great importance for prognosis. It has been reported that PET/CT can detect the site of an unknown primary in 20–50% of cases presenting with malignant cervical lymph nodes. The most common pitfall of PET imaging for this purpose is physiological uptake of FDG in the lingual and palatine tonsils. Any asymmetric pattern of uptake should be regarded as suggestive of an unknown primary site and the utmost care must be taken when interpreting the PET/CT scan [2,4].

### Evaluation of response to therapy

PET/CT permits not only visual but, more importantly, (semi-)quantitative evaluation. A quantitative approach makes it possible for the imaging specialist to interpret more objectively. For therapy response evaluation, the standardised uptake value (SUV) of lesions is measured before therapy and compared with the SUV measured after chemotherapy or radiation therapy. Theoretically, it is assumed that any significant reduction in metabolic uptake of a malignant lesion after therapy correlates with a good therapy response and is a predictor of a good outcome. There is still debate regarding the exact time period appropriate for evaluation of response after







chemotherapy and radiation therapy as well as the exact decrease in SUV indicative of a good response. It is generally accepted that response to chemotherapy can be appropriately evaluated several weeks after termination of the chemotherapy. Indeed, many studies recommend performance of PET/CT as early as 2 weeks after cessation of chemotherapy. As radiation therapy induces a more significant inflammatory response, it is suggested that an interval of at least 3 weeks should be allowed before evaluating treatment response. Most studies conclude that PET/CT imaging 3 months after radiation therapy can give more reliable results for evaluation of response to radiation therapy.

Some studies in the literature suggest that a better long-term outcome can be predicted on the basis of post-therapy FDG uptake with a maximum SUV of 3 or less or an 80% reduction in SUV compared with the pretherapy SUV. More data are warranted to clarify this issue [5].

### Detection of residual disease and differentiation of post-therapy changes

Conventional imaging modalities such as CT and MRI essentially depend on the morphological features of tissues. Therefore, detection of residual disease is mostly done by evaluation of any anatomical asymmetry in the head and neck region. Surgery and radiation therapy, however, can cause major defects in normal anatomy that usually reduce symmetry. For this reason, it is not always possible to detect residual disease or to differentiate post-therapy changes from residual or recurrent disease with conventional imaging modalities. PET/CT is reported to be a more sensitive and reliable tool to detect residual disease after therapy and to differentiate post-therapy changes from disease if a suitable time period is allowed to elapse so that postoperative or postradiotherapy changes can diminish. Studies generally advocate performance of PET/CT at least 4 months after major surgery, and it has been reported that by 6 months after therapy, negative FDG PET/CT has a very high negative predictive value in ruling out malignant disease [5,6].



## References Chapter 2.2

### References

1. Goerres GW, Von Schultess GK, Hany TF. Positron emission tomography and PET/CT of the head and neck: FDG uptake in normal anatomy, in benign lesions and in changes resulting from treatment. *AJR Am J Roentgenol* 2002;179:1337-43.
2. Chisin R, Macapinlac HA. The indications of FDG-PET in neck oncology. *Radiol Clin North Am* 2000;38:999-1012.
3. Stuckensen T, Kovacs AF, Adams S, Baum RP. Staging of the neck in patients with oral cavity squamous cell carcinomas: a prospective comparison of PET, ultrasound, CT and MRI. *J Craniomaxillofac Surg* 2000;28:319-24.
4. Kole AC, Niewig OE, Pruijm J. Detection of unknown occult primary tumors using positron emission tomography. *Cancer* 1998;82:1160-6.
5. Kostakoglu L, Goldsmith SJ. PET in the assessment of therapy response in patients with carcinoma of head and neck and the esophagus. *J Nucl Med* 2004;45:56-68.
6. Schoder H, Yeung HW. Positron emission imaging of head and neck cancer including thyroid carcinoma. *Semin Nucl Med* 2004;34:180-97.



# Chapter 2 – Clinical applications of PET/CT in oncology

## 2.3 Lung cancer

Francesco Giammarile and Claire Houzard

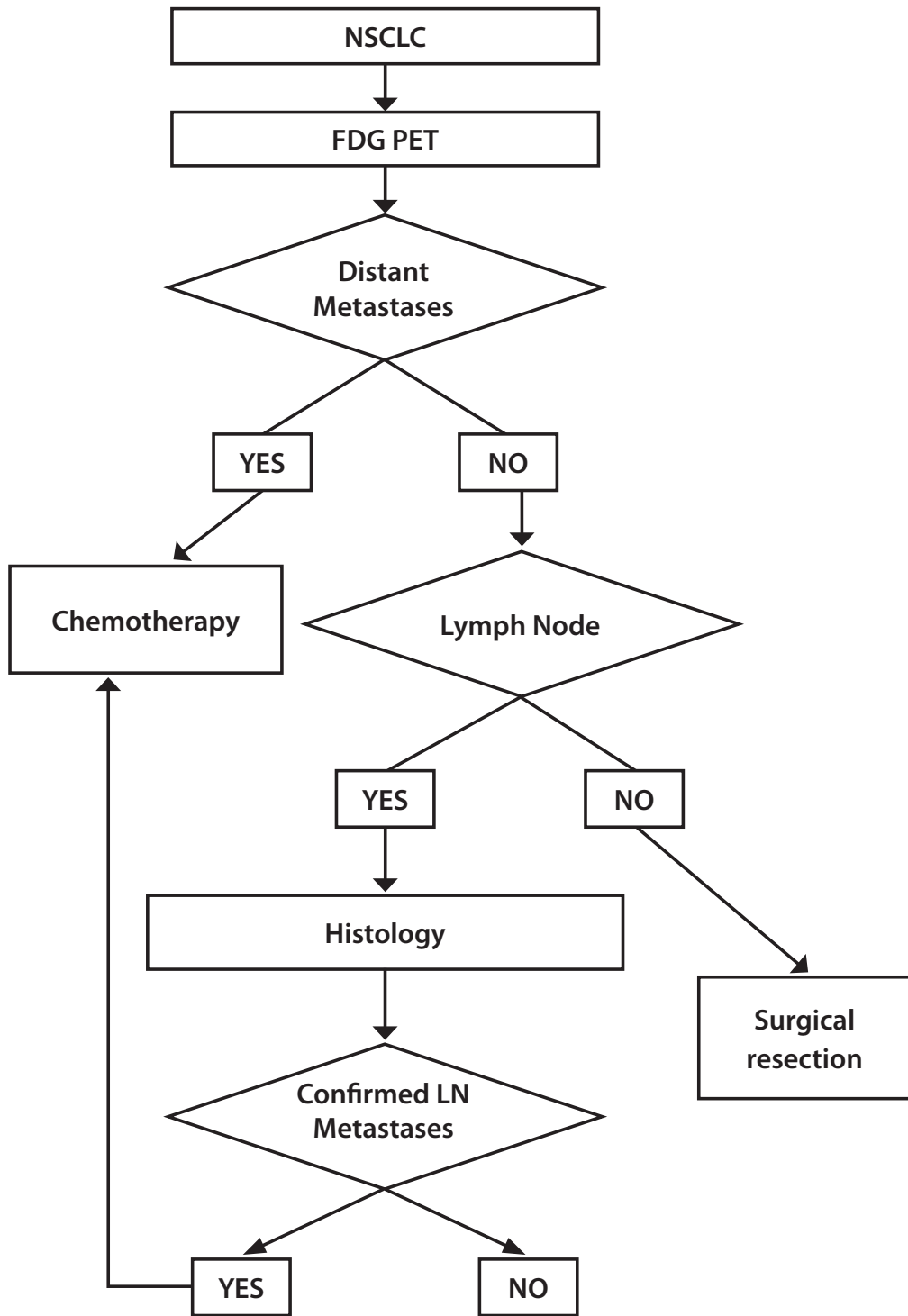
### Introduction

Lung cancer is the most common cancer worldwide, accounting for 12.3% of all new cases; it is also the leading cause of death globally. Histologically, lung cancer is classified into two main categories: non-small cell lung cancer (NSCLC, 80% of cases) and small cell lung cancer (SCLC, 20%). NSCLC occurs in several histological variants, including squamous cell carcinoma (30%), adenocarcinoma (30%), large cell carcinoma (10%) and less frequent types such as adenosquamous carcinoma, carcinoid tumours, mucoepidermoid carcinoma and adenoid cystic carcinoma.

The average survival time for untreated NSCLC and SCLC is only 6 months and 2 months, respectively. If diagnosed at an early stage, NSCLC can be cured by surgical resection. Locally advanced disease is treated by preoperative chemoradiotherapy followed by surgical resection. In contrast, the primary therapy of SCLC is systemic chemotherapy, since this tumour type has usually metastasised at the time of diagnosis. Because of this difference in the treatment strategies, it is essential to correctly diagnose, stage and restage patients [1,2].

### Initial staging

Despite many advances in the diagnosis, staging and treatment of NSCLC, the overall 5-year survival rate of patients with resectable NSCLC is less than 50%. This suboptimal survival rate is likely due to many factors, including the aggressiveness of the specific phenotype, locally advanced disease at presentation and inaccurate pretreatment staging. It is plausible that undetected locoregional and distant micrometastatic disease at the time of presentation results in inappropriate treatment and, therefore, decreased stage-specific survival. Accurate clinical staging is important in order to determine the best possible therapeutic option and to assess prognosis. The anatomical extent of the disease at the time of diagnosis is defined using the TNM system. An algorithm for the staging of NSCLC with the implementation of  $^{18}\text{F}$ -FDG PET imaging is shown in Fig. 1 [3].



Adapted with permission from De Wever et al. [3]. Eur Respir J 2009; 33: 201-212

Figure 1: Algorithm for the staging of NSCLC with the implementation of <sup>18</sup>F-FDG PET imaging

### Tumour assessment: T-stage

About 75% of pulmonary nodules are found incidentally. A solitary pulmonary nodule (SPN), or coin lesion, is a non-spiculated round lesion smaller than 3 cm in diameter without associated atelectasis or adenopathy. Larger lesions are likely to be cancerous and prompt pathological diagnosis; subsequent resection is usually indicated. Twenty to thirty percent of patients present with SPN, and differentiation of benign lesions from malignancy may be difficult with conventional imaging modalities such as chest radiography and computed tomography (CT) [1,2,4].

$^{18}\text{F}$ -fluorodeoxyglucose ( $^{18}\text{F}$ -FDG) positron emission tomography (PET) can provide additional information. The sensitivity, specificity and accuracy of  $^{18}\text{F}$ -FDG PET in differentiating benign from cancerous lesions larger than 1 cm are more than 95%, 75% and 90%, respectively. For SPN smaller than 1 cm, only strong uptake of  $^{18}\text{F}$ -FDG may be of diagnostic value (Fig. 2) [3,5].

Courtesy of  
Médecine Nucléaire -  
Centre Hospitalier  
Lyon Sud, France

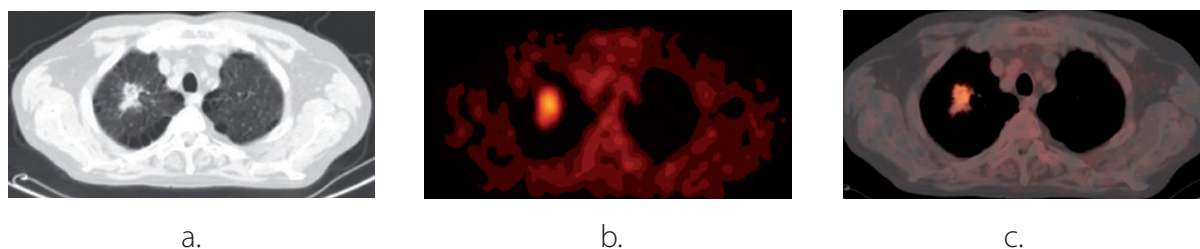


Figure 2a–c: SPN characterisation:  $^{18}\text{F}$ -FDG uptake in a suspicious nodule. a CT of a 59-year-old man showing a 23-mm spiculated SPN in the right superior lobe. b  $^{18}\text{F}$ -FDG PET image with intense uptake in the nodule. c  $^{18}\text{F}$ -FDG PET/CT fused image (true positive)

False-positive results are due to conditions where  $^{18}\text{F}$ -FDG accumulation occurs in metabolically active tissue that is not cancerous. Most benign pulmonary nodules do not accumulate  $^{18}\text{F}$ -FDG. However, active granulomatous inflammations or infections like tuberculosis, sarcoidosis (Fig. 3), aspergillosis, histoplasmosis and coccidioidomycosis can

demonstrate increased  $^{18}\text{F}$ -FDG uptake. Since generally malignant nodules show increased  $^{18}\text{F}$ -FDG uptake over time, while pulmonary nodules of benign origin have a declining pattern of uptake with time, some authors have proposed performing delayed  $^{18}\text{F}$ -FDG PET images or dual-time-point imaging [6].

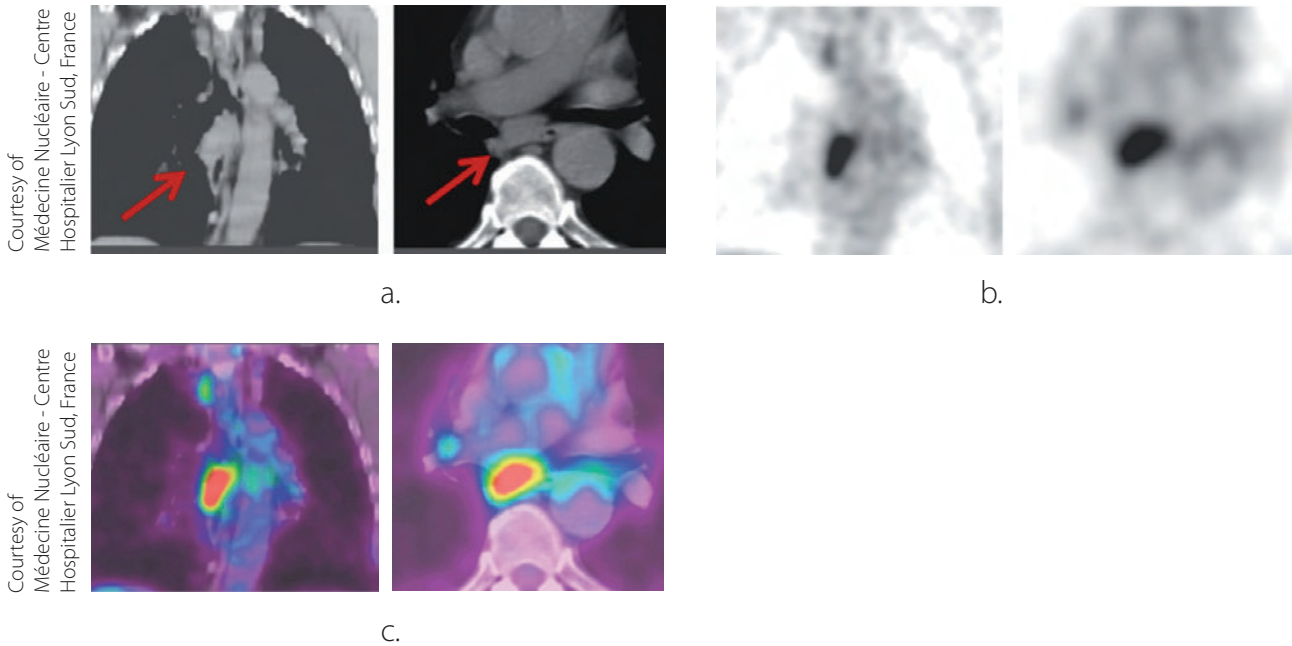


Figure 3a–c: Tissue characterisation:  $^{18}\text{F}$ -FDG uptake in sarcoidosis. a CT of a 55-year-old woman showing mediastinal nodes (red arrows). b  $^{18}\text{F}$ -FDG PET image with intense uptake in the nodes. c  $^{18}\text{F}$ -FDG PET/CT fused image (false positive)

False-negative PET images can occur for low-metabolism tumours such as bronchioloalveolar carcinomas or squamous cell carcinomas (up to 60%) and bronchial carcinoid tumours (up to 85%). In addition, very small lesions (less than 5 mm) can be missed because of the partial volume effect and motion artefacts [5,7].

Overall,  $^{18}\text{F}$ -FDG PET is more accurate than CT for correct prediction of the T-stage of malignant tumours; however, differences are not significant, and CT is fundamental to assess lesion size, used for the determination of T-stage [8].

#### ***Nodal assessment: N-stage***

The involvement of regional lymph nodes has a significant impact on prognosis and influences treatment in NSCLC. The size, number and nodal levels involved influence survival. Only patients with limited mediastinal lymph node metastases (stage IIIa) should proceed to surgical resection. CT provides good anatomical definition but significant over- and understaging.  $^{18}\text{F}$ -FDG PET has been shown to be more accurate than CT for staging mediastinal nodes since detection is dependent not on size but on metabolic activity of nodes (Fig. 4).

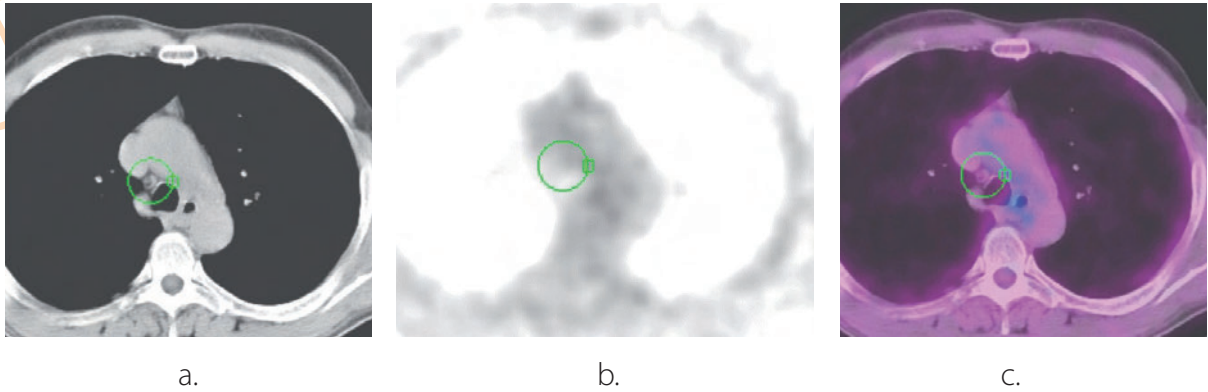


Figure 4a–c: N staging: downstaging with <sup>18</sup>F-FDG. a CT of a 62-year-old man showing a pathological node in the mediastinum (green circle). b <sup>18</sup>F-FDG PET image with no uptake in the node. c <sup>18</sup>F-FDG PET/CT fused image (true negative)

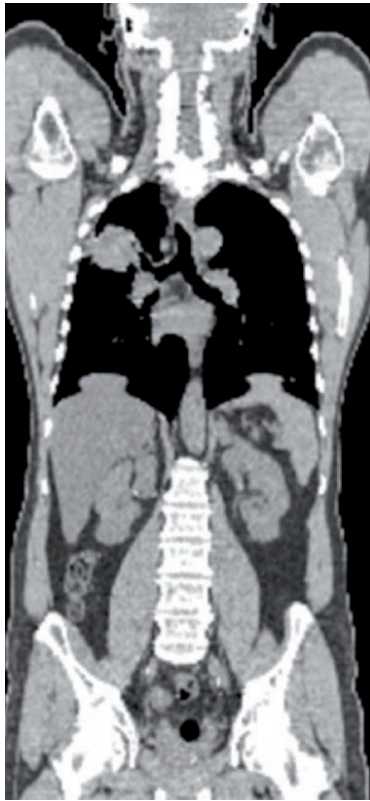
As in primary tumours, false positive uptake in nodes occurs in tuberculosis, sarcoidosis, histoplasmosis, Wegener's granulomatosis, amyloidosis, anthracosis and organising pneumonias. The clinical importance of <sup>18</sup>F-FDG PET lies in the high negative predictive value in lymph node staging. False-negative results can occur in micrometastases. Therefore, a positive <sup>18</sup>F-FDG PET for mediastinal nodes requires pathological confirmation (to ensure that no potentially curable patient is refused appropriate treatment) while a negative <sup>18</sup>F-FDG PET/CT may negate the requirement for mediastinoscopy [9].

#### **Assessment of distant metastases: M-stage**

The detection of distant metastases implies palliative treatment. At presentation, the commonest sites for metastatic disease in NSCLC are, in decreasing order, brain, bone, liver and adrenals. <sup>18</sup>F-FDG PET is a whole-body imaging system that will identify unsuspected metastases (Fig. 5).



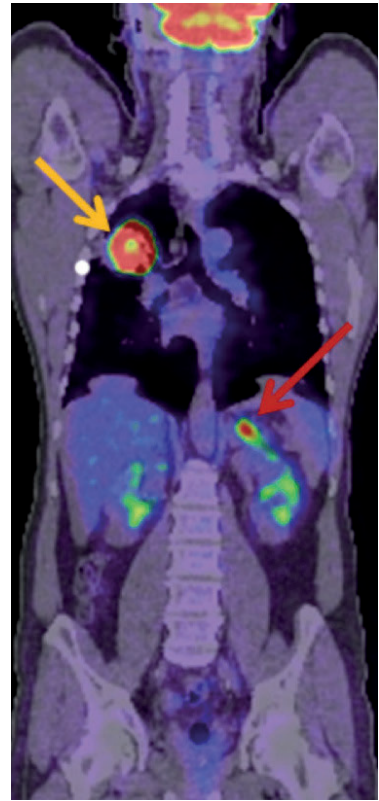
Courtesy of Médecine Nucléaire - Centre Hospitalier Lyon Sud, France



a.

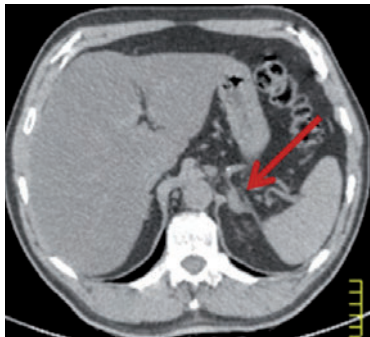


c.

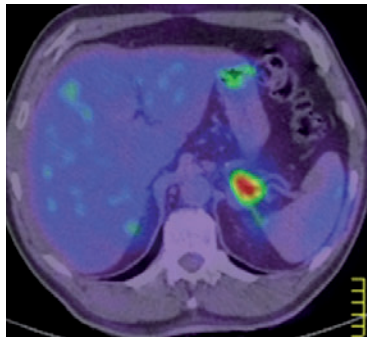


d.

Courtesy of Médecine Nucléaire - Centre Hospitalier Lyon Sud, France



b.



e.

Figure 5a–e. M staging: upstaging with  $^{18}\text{F}$ -FDG. a,b CT of a 60-year-old man showing lung cancer and normal left adrenal (red arrow). c  $^{18}\text{F}$ -FDG PET image with necrotic primitive neoplastic pulmonary tumour (yellow arrow) and adrenal metastasis (red arrow). d,e  $^{18}\text{F}$ -FDG PET/CT fused image (true positive)



It is significantly better than CT in detecting extrathoracic metastases, but is limited in assessing brain metastases because of the high rate of glucose uptake by brain cells (in this case, additional CT or MRI is performed) [10,11].

### Follow-up

#### Prognosis

There are numerous reports on the prognostic value of  $^{18}\text{F}$ -FDG PET using the SUV of the primary tumour although the values used are very variable [12].

#### Response to treatment

Neoadjuvant chemoradiation therapy followed by curative resection is an acceptable treatment for resectable stage IIIa NSCLC. Owing to a lack in survival benefit, in stage IIIb and unresectable stage IIIa patients only chemoradiation is proposed.

Assessment of response to these treatments may result in alteration of the course of management and provide prognostic information. Since changes in metabolism always precede changes in morphology,  $^{18}\text{F}$ -FDG PET can determine early response to therapy (Fig. 6).

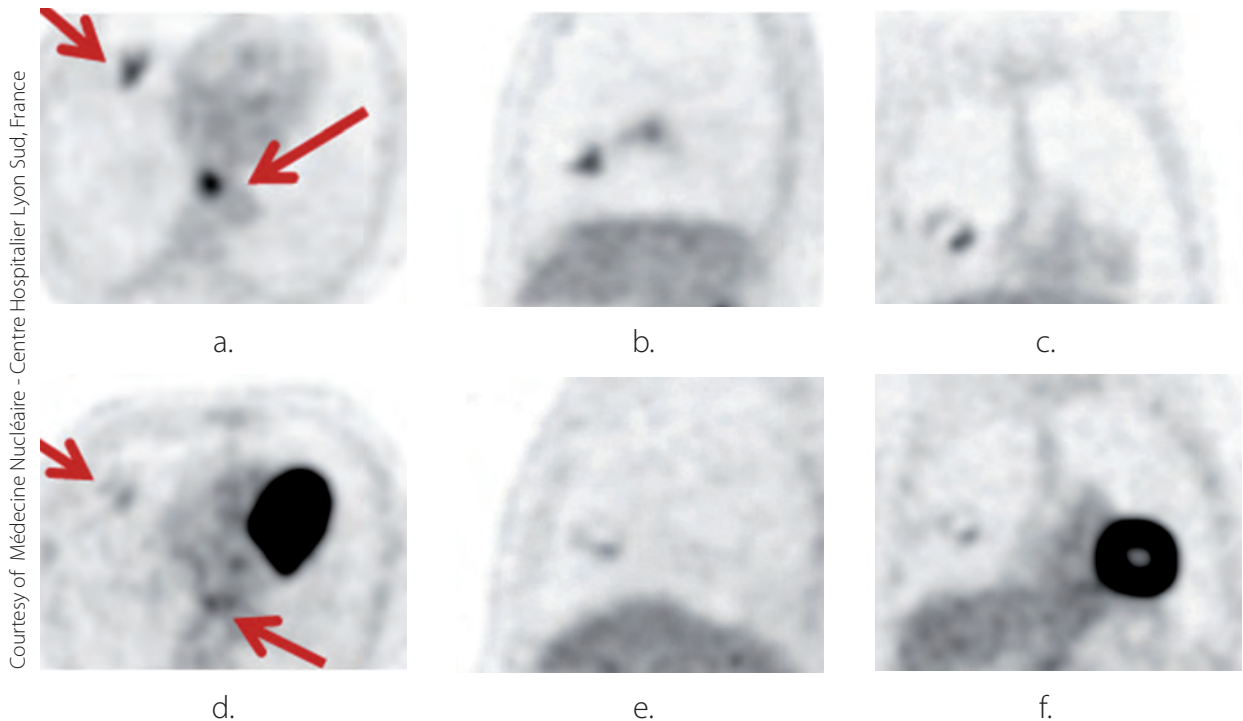


Figure 6a–f. Response assessment with  $^{18}\text{F}$ -FDG: axial  $^{18}\text{F}$ -FDG PET views (a,d), sagittal  $^{18}\text{F}$ -FDG PET views (b,e) and coronal  $^{18}\text{F}$ -FDG PET views (c,f) in a stage IIIb NSCLC (red arrows: primary tumour and mediastinal lymph node) before (a–c) and after (d–f) radiochemotherapy (good response with lower intensity metabolism)

Courtesy of Médecine Nucléaire - Centre Hospitalier Lyon Sud, France

A reduction in tumour  $^{18}\text{F}$ -FDG uptake by more than 20%, as assessed by SUV, is used as a criterion for a metabolic response in NSCLC [13].

### **Recurrent disease**

After curative treatment of NSCLC, most of the conventional imaging techniques are sensitive for structural changes but have limited ability to distinguish scars from viable tumours.  $^{18}\text{F}$ -FDG PET is both sensitive and specific for recurrent disease, with a high negative predictive value, and will alter treatment plans in up to 63% of patients. However, the clinical significance of this potential superiority is still unknown [14].

### **Future applications and developments**

#### **Radiation treatment planning**

In localised NSCLC,  $^{18}\text{F}$ -FDG PET has been widely explored and has been recommended as a standard means of evaluation for patients undergoing radiotherapy or surgery [2,3]. It permits assessment of stage with a higher sensitivity and specificity than standard morphological imaging and is therefore of major importance for therapeutic strategy [4-7]. The potential impact of  $^{18}\text{F}$ -FDG PET on radiotherapy patient management may be particularly important as it may upstage the extent of disease, change the treatment intent from curative to palliative, increase the radiation field size owing to the finding of unsuspected

mediastinal node involvement not seen on CT scans, decrease the treatment field size owing to better localisation of the tumour in areas of associated atelectasis or postobstructive pneumonitis and decrease inter-observer variation in target definition [11,15].

The addition of 4D  $^{18}\text{F}$ -FDG PET (i.e. images acquired with respiratory gating) will improve image quality since 3D PET images suffer from motion blurring due to breathing. Whether the resulting modifications in treatment plan will significantly improve tumour control and quality of life has still to be demonstrated [11,15,16].

#### **New radiopharmaceuticals for PET imaging**

Proliferation and metabolic activity could be analysed with  $^{18}\text{F}$ -fluorothymidine and  $^{18}\text{F}$ -fluorocholine. Apoptosis is studied with  $^{18}\text{F}$ -annexin V and hypoxia with  $^{18}\text{F}$ -fluoromisonidazole. However, to date, none of these markers under development has proved superior to  $^{18}\text{F}$ -FDG in published studies and no tumour-specific radiopharmaceutical for NSCLC has been identified [17].

#### **Economic aspects**

Several studies have evaluated the cost-effectiveness of PET/CT in NSCLC. All the authors have concluded that  $^{18}\text{F}$ -FDG PET is cost-effective in the management of SPN and in the pretreatment staging of NSCLC [18].



---

## Conclusion

$^{18}\text{F}$ -FDG PET is an imaging technology with evolving potential. The advantage of  $^{18}\text{F}$ -FDG PET lies in its ability to detect metabolic changes in cancer cells before anatomical changes (commonly identified by conventional imaging modalities). This advantage may help to achieve more accurate staging than is possible with conventional imaging. It may also identify tumours at an earlier stage, assess their response to neoadjuvant therapy and help with follow-up surveillance. The potential capability of PET in assessing the tumour responsiveness to chemotherapy can be used as a prognostic factor, thereby influencing the direction of further management. Furthermore,  $^{18}\text{F}$ -FDG PET can be used in conformal radiotherapy planning in order to reduce the radiation dose to normal tissue and deliver higher tumour dose.

## References Chapter 2.3

### References

1. Pfister DG, Johnson DH, Azzoli CG. American Society of Clinical Oncology treatment of unresectable non-small-cell lung cancer guideline: update 2003. *J Clin Oncol* 2004;22:330-53.
2. Ost D, Fein AM, Feinsilver SH. The solitary pulmonary nodule. *N Engl J Med* 2003;348:2535-42.
3. De Wever W, Stroobants S, Coolen J, Verschakelen JA. Integrated PET/CT in the staging of nonsmall cell lung cancer: technical aspects and clinical integration. *Eur Respir J* 2009;33:201-12.
4. Tan BB, Flaherty KR, Kazerooni EA, Iannettoni MD. The solitary pulmonary nodule. *Chest* 2003;123:89-96.
5. Kim BT, Kim Y, Lee KS, Yoon SB, Cheon EM, Kwon OJ, et al. Localized form of bronchioloalveolar carcinoma: FDG PET findings. *Am J Roentgenol* 1998;170:935-9.
6. Gould MK, Maclean CC, Kuschner WG, Rydzac CE, Owens DK. Accuracy of positron emission tomography for diagnosis of pulmonary nodules and mass lesions: a meta-analysis. *JAMA* 2001;285:936-7.
7. Hashimoto Y, Tsujikawa T, Kondo C, Maki M, Momose M, Nagai A, et al. Accuracy of PET for diagnosis of pulmonary lesions with 18-FDG uptake below the standardized uptake value of 2.5. *J Nucl Med* 2006;47:426-31.
8. Gupta NC, Graeber GM, Rogers JS, Bishop HA. Comparative efficacy of positron emission tomography with FDG and computed tomographic scanning in preoperative staging of non-small cell lung cancer. *Ann Surg* 1999;229:286-91.
9. Weng E, Tran L, Rege S, Safa A, Sadeghi A, Juillard G, et al. Accuracy and clinical impact of mediastinal lymph node staging with FDG-PET imaging in potentially resectable lung cancer. *Am J Clin Oncol* 2000;23:47-52.
10. Lee J, Aronchick JM, Alavi A. Accuracy of 18-fluorodeoxyglucose positron emission tomography for the evaluation of malignancy in patients presenting with new lung abnormalities. *Chest* 2001;120:1791-7.
11. MacManus MP, Hicks RJ, Matthews JP. High rate of detection of unsuspected distant metastases by PET in apparent stage III non-small-cell lung cancer: implications for radical radiation therapy. *Int J Radiat Oncol Biol Phys*. 2001;50:287-93.
12. Eschmann SM, Friedel G, Paulsen F. Impact of staging with 18F-FDG-PET on outcome of patients with stage III non-small cell lung cancer: PET identifies potential survivors. *Eur J Nucl Med Mol Imaging* 2007;34:54-9.
13. Kalff V, Hicks RJ, MacManus MP. Clinical impact of (18) F fluorodeoxyglucose positron emission tomography in patients with non-small-cell lung cancer: a prospective study. *J Clin Oncol* 2001;19:111-8.
14. Hillner BE, Siegel BA, Liu D. Impact of positron emission tomography/computed tomography and positron emission tomography (PET) alone on expected management of patients with cancer: initial results from the National Oncologic PET Registry. *J Clin Oncol* 2008;26:2155-61.
15. MacManus MP, Hicks RJ, Ball DL. F-18 fluorodeoxyglucose positron emission tomography staging in radical radiotherapy candidates with nonsmall cell lung carcinoma: powerful correlation with survival and high impact on treatment. *Cancer* 2001;92:886-95.
16. Vanuytsel LJ, Vansteenkiste JF, Stroobants SG, De Leyn PR, De Wever W, Verbeken EK, et al. The impact of (18)F-fluoro-2-deoxy-D-glucose positron emission tomography (FDG-PET) lymph node staging on the radiation treatment volumes in patients with non-small cell lung cancer. *Radiother Oncol* 2000;55:317-24.
17. Spiro SG, Buscombe J, Cook G. Ensuring the right PET scan for the right patient. *Lung Cancer* 2008;59:48-56.
18. Remonnay R, Morelle M, Pommier P, Giammarile F, Carrère MO. Assessing short-term effects and costs at an early stage of innovation: The use of positron emission tomography on radiotherapy treatment decision making. *Int J Technol Assess Health Care* 2008; 24:212-20.

# Chapter 2 – Clinical applications of PET/CT in oncology

## 2.4 Breast cancer

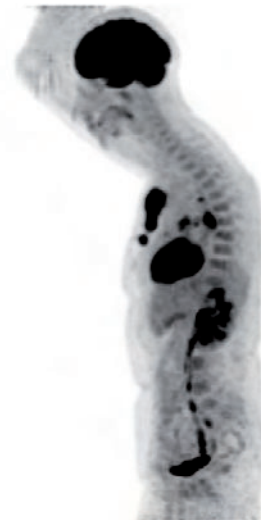
Leonne Prompers, Emiel Beijer, Christian Urbach, Servé Halders and Felix Manuel Mottaghy

### Introduction

Breast cancer is the most common malignancy in women [1]. In 2008, 429,000 new cases of breast cancer were diagnosed in Europe, and 129,000 women died from breast cancer in the same year [2]. It is a cancer originating from breast tissue, most commonly either from milk ducts or from the lobules that supply the ducts with milk. Cancers originating from milk ducts are called ductal carcinomas, while cancers originating from the lobules are known as lobular carcinomas. Some breast cancers have receptors that are sensitive to hormones such as oestrogen and progesterone. Some are characterised by an overexpression of human epidermal growth factor receptor 2 (HER2). The advent of targeted antibody therapy with trastuzumab (Herceptin) targeting this HER2 receptor has been a major breakthrough in breast cancer treatment. Breast cancers that do not express the genes for oestrogen receptor, progesterone receptor or HER2 are called triple-negative tumours. These triple-negative tumours have a poorer prognosis owing to their lack of susceptibility to targeted therapy. In addition to the histological subtype of the tumour, the most essential prognostic factor in breast cancer is the presence and extent of axillary or other (lymph node) metastases. The survival rate drops sharply if malignant axillary nodes are present and it drops even more if distant metastases are found. Treatment has developed considerably in the past decade and this has had an impact on survival. Certainly in patients with no metastases,

loco-regional surgery and systemic treatments have a curative aim.

Various imaging tools, including mammography, MRI, bone scans, CT, PET and PET/CT, are widely available for breast cancer imaging. The role of 2-[<sup>18</sup>F]fluoro-2-deoxy-D-glucose (<sup>18</sup>F-FDG) PET/CT in breast cancer imaging will be the topic of this chapter.



Courtesy of Department of Nuclear Medicine, Maastricht University Medical Center

### <sup>18</sup>F-FDG avidity

Infiltrating ductal carcinomas are <sup>18</sup>F-FDG avid and <sup>18</sup>F-FDG uptake is significantly higher compared with lobular carcinomas [3-5]. The limited uptake in lobular carcinomas restricts the indication for <sup>18</sup>F-FDG PET/CT in these breast cancers. <sup>18</sup>F-FDG uptake also increases with histological grade and depends on hormone receptor status: oestrogen receptor-negative, progesterone receptor-negative and triple-negative tumours show higher <sup>18</sup>F-FDG avidity than hormone receptor-positive tumours. In addition, a high maximum standardised

uptake value is associated with a higher TNM stage [3-6]. The TNM classification is a cancer staging system that describes the extent of cancer: T describes the size of the tumour, N whether lymph nodes are involved and M whether metastases are present.

### Procedure

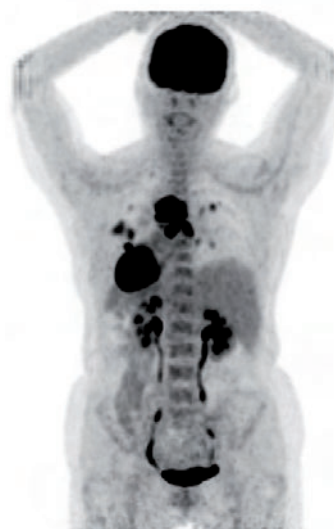
Technical protocols concerning  $^{18}\text{F}$ -FDG administration, patient preparation and scan procedure in breast cancer imaging are largely equivalent to other (standard) whole-body tumour imaging protocols. Of special note is that breast cancer patients should be injected in the arm contralateral to the side of interest. In the case of bilateral breast lesions, a foot injection should be administered. The PET/CT scan should be acquired with the patient's arms raised above the head.

### Indications

#### *Detection of primary breast tumours*

Previous data show that the sensitivity of PET for detecting small breast tumours (<1 cm) and in situ lesions is rather low [7, 8]. The reason for this may be related to tumour biology since in situ cancers may be associated with decreased vascularity and glycolytic activity [3]. Nevertheless, more recently Heusner et al. showed a similar accuracy of PET/CT to MRI for the detection of breast cancer lesions using a PET/CT mammography protocol [9]. This protocol utilises a special breast-positioning aid that allows a pendant breast position similar

to that for the MRI breast coil used in clinical routine. However, also in this study the MRI seemed more accurate when assessing the T-stage. Taking into account the rather high sensitivity of MRI in the detection of breast tumours, the accuracy of T-staging, the relatively low cost and the absence of ionising radiation, MRI will probably remain the cornerstone in the initial detection and T-staging of breast tumours.



#### *Assessment of axillary lymph node status*

The assessment of regional lymph node involvement by  $^{18}\text{F}$ -FDG PET/CT is quite good, although micrometastases are often missed, which diminishes the utility of PET/CT in defining the axillary lymph node status [10-12]. It seems clear that  $^{18}\text{F}$ -FDG PET/CT cannot replace sentinel lymph node biopsy or axillary lymph node dissection [12].





### ***Staging of breast cancer***

Adequate staging is essential in breast cancer patients in order to select the appropriate therapeutic strategy and thereby enhance the likelihood and duration of survival. Conventional staging of breast cancer consists of chest x-ray, liver ultrasonography or CT and bone scintigraphy. In recent years, several studies have highlighted the superiority of  $^{18}\text{F}$ -FDG PET/CT over such conventional modalities in the staging of initial and recurrent breast cancer [13-27]. The higher diagnostic value of  $^{18}\text{F}$ -FDG PET/CT resides in the more accurate detection of distant metastases. Its superiority particularly relates to small sites of nodal disease. Furthermore, numerous studies have pointed out the additional value of  $^{18}\text{F}$ -FDG PET/CT in altering treatment management. Up to 42% of patients have been reported to be up- or downstaged by  $^{18}\text{F}$ -FDG PET/CT [18, 20, 23, 24, 26], with consequences for treatment in up to 30% of patients [18, 19, 23]. PET/CT is clearly superior to bone scanning in demonstrating osteolytic metastases [28, 29]. Bone scanning seems to have a better sensitivity in the detection of osteoblastic metastases, and it has therefore been suggested that the two scans should have a complementary role [30, 31].

Another advantage of  $^{18}\text{F}$ -FDG PET/CT over conventional staging is the higher patient comfort compared with conventional multi-step examinations. Conventional imaging takes at least three examinations (bone scintigraphy, chest x-ray and ultrasound or CT

of the liver), whereas  $^{18}\text{F}$ -FDG PET/CT is performed in a single examination. In addition, given the relatively low specificity of conventional imaging, supplementary examinations are often needed to confirm abnormalities, causing anxiety and delaying the start of treatment [32]. One of the disadvantages of  $^{18}\text{F}$ -FDG PET/CT is that the costs of PET/CT are still about 3-4 times higher than those of conventional imaging. Whether the use of PET/CT in breast cancer staging is cost-effective is not clear at present [33]. However, several renowned clinics now use PET/CT for staging of patients with locally advanced or recurrent breast cancer because of its superiority over conventional staging.

### ***Therapy management***

PET/CT has a role in assessing response to systemic therapy [34]. In the neo-adjuvant setting, PET/CT can early identify non-responders or chemotherapy-resistant patients, thus determining timing of surgery [35]. The optimal date for an interim PET/CT to evaluate chemotherapy response is probably immediately before the third cycle of chemotherapy [36, 37]. PET/CT might also be useful in predicting response to therapy as it detects metabolic changes that usually precede anatomical changes [38].

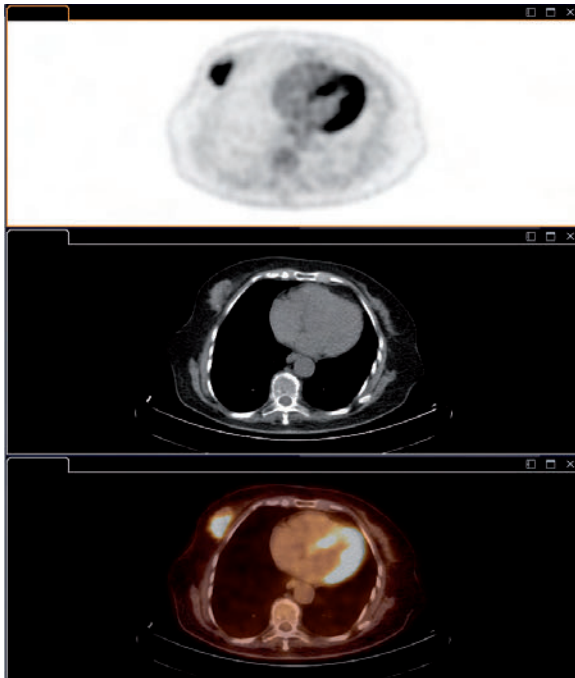
### ***Detection of suspected recurrences***

In patients who have had previous lumpectomies, mammography assessment and CT assessment can be very difficult owing to sur-



gical scars and the effect of radiation therapy [39]. In these cases, PET/CT demonstrates an excellent ability to detect local recurrences.

In asymptomatic breast cancer patients with rising serum tumour markers or in patients with clinical symptoms, PET/CT is superior to conventional imaging in detecting metastatic disease [25, 39-44].



Courtesy of Department of Nuclear Medicine, Maastricht University Medical Center

### Positron emission mammography

MRI has been successfully implemented in many medical centres as a valuable tool to diagnose breast cancer and is recommended as a supplemental screening tool to mammography in women considered to be at high risk for developing breast cancer [45]. One of the important issues with MRI, however, is the rather high false-positive rate.

In the United States, approximately 1 million surgical and needle breast biopsies performed each year yield benign findings [46]. As stated before, the use of whole-body  $^{18}\text{F}$ -FDG PET/CT is restricted in the primary diagnosis of breast cancer. High-resolution PET, also known as positron emission mammography (PEM), is a small organ-specific PET device with a reported spatial resolution of 2 mm. In addition it has the capability of providing PET biopsy guidance that facilitates percutaneous sampling of identified lesions [47, 48]. Recent data show that PEM and breast MRI have the same overall sensitivity for depiction of index cancerous lesions, including invasive cancer and DCIS [49, 50]. Furthermore, these studies show a trend towards higher specificity of PEM. PEM is therefore less likely to prompt unnecessary biopsies, which warrants future investigations.

### Conclusions

The lack of recommendations to guide appropriate use of PET/CT imaging is one of the factors currently limiting its application in breast cancer. It seems clear that PET/CT is superior to conventional imaging in the primary staging of breast cancer patients. PET/CT also has a role in assessing response to systemic therapy and in detecting local recurrences or metastatic disease. The role of PET/CT in the detection of primary breast tumours is rather limited. However, PEM could be an alternative for women who cannot tolerate MRI and may play a more important role in the future because of its high specificity.




## References Chapter 2.4

### References

1. Jemal A, Murray T, Ward E, Samuels A, Tiwari RC, Ghafoor A, et al. Cancer statistics, 2005. CA: Cancer J Clin 2005;55:10-30.
2. Ferlay J, Shin HR, Bray F, Forman D, Mathers C, Parkin DM. Estimates of worldwide burden of cancer in 2008: GLOBOCAN 2008. Int J Cancer 2010;127:2893-917.
3. Heudel P, Cimarelli S, Montella A, Bouteille C, Mognetti T. Value of PET-FDG in primary breast cancer based on histopathological and immunohistochemical prognostic factors. Int J Clin Oncol 2010;15:588-93.
4. Inoue T, Yutani K, Taguchi T, Tamaki Y, Shiba E, Noguchi S. Preoperative evaluation of prognosis in breast cancer patients by [(18)F]2-Deoxy-2-fluoro-D-glucose-positron emission tomography. J Cancer Res Clin Oncol 2004;130:273-8.
5. Crowe JP Jr, Adler LP, Shenk RR, Sunshine J. Positron emission tomography and breast masses: comparison with clinical, mammographic, and pathological findings. Ann Surg Oncol 1994;1:132-40.
6. Basu S, Chen W, Tchou J, Mavi A, Cermik T, Czerniecki B, et al. Comparison of triple-negative and estrogen receptor-positive/progesterone receptor-positive/HER2-negative breast carcinoma using quantitative fluorine-18 fluorodeoxyglucose/positron emission tomography imaging parameters: a potentially useful method for disease characterization. Cancer 2008;112:995-1000.
7. Avril N, Rose CA, Schelling M, Dose J, Kuhn W, Bense S, et al. Breast imaging with positron emission tomography and fluorine-18 fluorodeoxyglucose: use and limitations. J Clin Oncol 2000;18:3495-502.
8. Uematsu T, Kasami M, Yuen S. Comparison of FDG PET and MRI for evaluating the tumor extent of breast cancer and the impact of FDG PET on the systemic staging and prognosis of patients who are candidates for breast-conserving therapy. Breast Cancer 2009;16:97-104.
9. Heusner TA, Kuemmel S, Umutlu L, Koeninger A, Freudenberg LS, Hauth EA, et al. Breast cancer staging in a single session: whole-body PET/CT mammography. J Nucl Med. 2008;49:1215-22.
10. Wahl RL, Siegel BA, Coleman RE, Gatsonis CG. Prospective multicenter study of axillary nodal staging by positron emission tomography in breast cancer: a report of the staging breast cancer with PET Study Group. J Clin Oncol 2004;22:277-85.
11. Veronesi U, De Cicco C, Galimberti VE, Fernandez JR, Rotmensz N, Viale G, et al. A comparative study on the value of FDG-PET and sentinel node biopsy to identify occult axillary metastases. Ann Oncol 2007;18:473-8.
12. Heusner TA, Kuemmel S, Hahn S, Koeninger A, Otterbach F, Hamami ME, et al. Diagnostic value of full-dose FDG PET/CT for axillary lymph node staging in breast cancer patients. Eur J Nucl Med Mol Imaging 2009;36:1543-50.
13. van der Hoeven JJ, Krak NC, Hoekstra OS, Comans EF, Boom RP, van Geldere D, et al. 18F-2-fluoro-2-deoxy-d-glucose positron emission tomography in staging of locally advanced breast cancer. J Clin Oncol 2004;22:1253-9.
14. van Oost FJ, van der Hoeven JJ, Hoekstra OS, Voogd AC, Coebergh JW, van de Poll-Franse LV. Staging in patients with locoregionally recurrent breast cancer: current practice and prospects for positron emission tomography. Eur J Cancer 2004;40:1545-53.
15. Port ER, Yeung H, Gonen M, Liberman L, Caravelli J, Borgen P, et al. 18F-2-fluoro-2-deoxy-D-glucose positron emission tomography scanning affects surgical management in selected patients with high-risk, operable breast carcinoma. Ann Surg Oncol 2006;13:677-84.
16. Mahner S, Schirrmacher S, Brenner W, Jenicke L, Habermann CR, Avril N, et al. Comparison between positron emission tomography using 2-[fluorine-18]fluoro-2-deoxy-D-glucose, conventional imaging and computed tomography for staging of breast cancer. Ann Oncol 2008;19:1249-54.
17. Eubank WB, Mankoff DA, Takasugi J, Vesselle H, Eary JF, Shanley TJ, et al. 18fluorodeoxyglucose positron emission tomography to detect mediastinal or internal mammary metastases in breast cancer. J Clin Oncol 2001;19:3516-23.
18. Dizendorf EV, Baumert BG, von Schulthess GK, Lutolf UM, Steinert HC. Impact of whole-body 18F-FDG PET on staging and managing patients for radiation therapy. J Nucl Med 2003;44:24-9.

19. Groheux D, Moretti JL, Baillet G, Espie M, Giacchetti S, Hindie E, et al. Effect of (18)F-FDG PET/CT imaging in patients with clinical stage II and III breast cancer. *Int J Radiat Oncol Biol Phys* 2008;71:695-704.
20. Fuster D, Duch J, Paredes P, Velasco M, Munoz M, Santamaria G, et al. Preoperative staging of large primary breast cancer with [18F]fluorodeoxyglucose positron emission tomography/computed tomography compared with conventional imaging procedures. *J Clin Oncol* 2008;26:4746-51.
21. Dose J, Bleckmann C, Bachmann S, Bohuslavizki KH, Berger J, Jenicke L, et al. Comparison of fluorodeoxyglucose positron emission tomography and „conventional diagnostic procedures“ for the detection of distant metastases in breast cancer patients. *Nucl Med Commun* 2002;23:857-64.
22. Isasi CR, Moadel RM, Blaufox MD. A meta-analysis of FDG-PET for the evaluation of breast cancer recurrence and metastases. *Breast Cancer Res Treat* 2005;90:105-12.
23. Eubank WB, Mankoff D, Bhattacharya M, Gralow J, Linden H, Ellis G, et al. Impact of FDG PET on defining the extent of disease and on the treatment of patients with recurrent or metastatic breast cancer. *AJR Am J Roentgenol* 2004;183:479-86.
24. Jager JJ, Keymeulen K, Beets-Tan RG, Hupperets P, van Kroonenburgh M, Houben R, et al. FDG-PET-CT for staging of high-risk breast cancer patients reduces the number of further examinations: A pilot study. *Acta Oncol* 2010;49:185-91.
25. Radan L, Ben-Haim S, Bar-Shalom R, Guralnik L, Israel O. The role of FDG-PET/CT in suspected recurrence of breast cancer. *Cancer* 2006;107:2545-51.
26. Dirisamer A, Halpern BS, Flory D, Wolf F, Beheshti M, Mayerhoefer ME, et al. Performance of integrated FDG-PET/contrast-enhanced CT in the staging and restaging of colorectal cancer: comparison with PET and enhanced CT. *Eur J Radiol* 2010;73:324-8.
27. Segaert I, Mottaghy F, Ceysens S, De Wever W, Stroobants S, Van Ongeval C, et al. Additional value of PET-CT in staging of clinical stage IIB and III breast cancer. *Breast J* 2010;16:617-24.
28. Cook GJ, Houston S, Rubens R, Maisey MN, Fogelman I. Detection of bone metastases in breast cancer by 18FDG PET: differing metabolic activity in osteoblastic and osteolytic lesions. *J Clin Oncol* 1998;16:3375-9.
29. Du Y, Cullum I, Illidge TM, Ell PJ. Fusion of metabolic function and morphology: sequential [18F]fluorodeoxyglucose positron-emission tomography/computed tomography studies yield new insights into the natural history of bone metastases in breast cancer. *J Clin Oncol* 2007;25:3440-7.
30. Ben-Haim S, Israel O. Breast cancer: role of SPECT and PET in imaging bone metastases. *Semin Nucl Med* 2009;39:408-15.
31. Costelloe CM, Rohren EM, Madewell JE, Hamaoka T, Theriault RL, Yu TK, et al. Imaging bone metastases in breast cancer: techniques and recommendations for diagnosis. *Lancet Oncol* 2009;10:606-14.
32. Gerber B, Seitz E, Muller H, Krause A, Reimer T, Kundt G, et al. Perioperative screening for metastatic disease is not indicated in patients with primary breast cancer and no clinical signs of tumor spread. *Breast Cancer Res Treat* 2003;82:29-37.
33. Pennant M, Takwoingi Y, Pennant L, Davenport C, Fry-Smith A, Eisinga A, et al. A systematic review of positron emission tomography (PET) and positron emission tomography/computed tomography (PET/CT) for the diagnosis of breast cancer recurrence. *Health Technol Assess* 2010;14:1-103.
34. Avril N, Sassen S, Roylance R. Response to therapy in breast cancer. *J Nucl Med* 2009;50 Suppl 1:55S-63S.
35. Krak NC, Boellaard R, Hoekstra OS, Twisk JW, Hoekstra CJ, Lammertsma AA. Effects of ROI definition and reconstruction method on quantitative outcome and applicability in a response monitoring trial. *Eur J Nucl Med Mol Imaging* 2005;32:294-301.
36. Rousseau C, Devillers A, Sagan C, Ferrer L, Bridji B, Champion L, et al. Monitoring of early response to neoadjuvant chemotherapy in stage II and III breast cancer by [18F] fluorodeoxyglucose positron emission tomography. *J Clin Oncol* 2006;24:5366-72.

- 
37. Martoni AA, Zamagni C, Quercia S, Rosati M, Cacciari N, Bernardi A, et al. Early (18)F-2-fluoro-2-deoxy-d-glucose positron emission tomography may identify a subset of patients with estrogen receptor-positive breast cancer who will not respond optimally to preoperative chemotherapy. *Cancer* 2010;116:805-13.
38. Duch J, Fuster D, Munoz M, Fernandez PL, Paredes P, Fontanillas M, et al. 18F-FDG PET/CT for early prediction of response to neoadjuvant chemotherapy in breast cancer. *Eur J Nucl Med Mol Imaging* 2009;36:1551-7.
39. Siggelkow W, Rath W, Buell U, Zimny M. FDG PET and tumour markers in the diagnosis of recurrent and metastatic breast cancer. *Eur J Nucl Med Mol Imaging* 2004;31 Suppl 1:S118-24.
40. Lind P, Igerc I, Beyer T, Reinprecht P, Hausegger K. Advantages and limitations of FDG PET in the follow-up of breast cancer. *Eur J Nucl Med Mol Imaging* 2004;31 Suppl 1:S125-34.
41. Suarez M, Perez-Castejon MJ, Jimenez A, Domper M, Ruiz G, Montz R, et al. Early diagnosis of recurrent breast cancer with FDG-PET in patients with progressive elevation of serum tumor markers. *Q J Nucl Med* 2002;46:113-21.
42. Gallowitsch HJ, Kresnik E, Gasser J, Kumnig G, Igerc I, Mikosch P, et al. F-18 fluorodeoxyglucose positron-emission tomography in the diagnosis of tumor recurrence and metastases in the follow-up of patients with breast carcinoma: a comparison to conventional imaging. *Invest Radiol* 2003;38:250-6.
43. Tatsumi M, Cohade C, Mourtzikos KA, Fishman EK, Wahl RL. Initial experience with FDG-PET/CT in the evaluation of breast cancer. *Eur J Nucl Med Mol Imaging* 2006;33:254-62.
44. Zangheri B, Messa C, Picchio M, Gianolli L, Landoni C, Fazio F. PET/CT and breast cancer. *Eur J Nucl Med Mol Imaging* 2004;31 Suppl 1:S135-42.
45. Enriquez L, Listinsky J. Role of MRI in breast cancer management. *Cleve Clin J Med* 2009;76:525-32.
46. Tafra L, Fine R, Whitworth P, Berry M, Woods J, Ekblom G, et al. Prospective randomized study comparing cryo-assisted and needle-wire localization of ultrasound-visible breast tumors. *Am J Surg* 2006;192:462-70.
47. Weinberg IN, Beylin D, Zavarzin V, Yarnall S, Stepanov PY, Anashkin E, et al. Positron emission mammography: high-resolution biochemical breast imaging. *Technol Cancer Res Treat* 2005;4:55-60.
48. Weinberg IN. Applications for positron emission mammography. *Phys Med* 2006;21 Suppl 1:132-7.
49. Schilling K, Narayanan D, Kalinyak JE, The J, Velasquez MV, Kahn S, et al. Positron emission mammography in breast cancer presurgical planning: comparisons with magnetic resonance imaging. *Eur J Nucl Med Mol Imaging* 2011;38:23-36.
50. Berg WA, Madsen KS, Schilling K, Tartar M, Pisano ED, Larsen LH, et al. Breast cancer: comparative effectiveness of positron emission mammography and MR imaging in presurgical planning for the ipsilateral breast. *Radiology* 2011;258:59-72.

# Chapter 2 – Clinical applications of PET/CT in oncology

## 2.5 Prostate cancer

Sarah Schwarzenboeck, Michael Souvatzoglou and Bernd J. Krause

### Introduction

Prostate cancer is among the carcinomas with the highest prevalence in men. Within the European Union, there were 301,500 incident cases of prostate cancer in 2006 (24.1% of all cases), and it was one of the leading causes of carcinoma-associated death in men (10.4%) [1]. Commonly used diagnostic tools in the evaluation of prostate cancer are digital rectal examination, measurement of serum levels of prostate-specific antigen (PSA), transrectal ultrasound and ultrasound-guided biopsies [2]. Besides these diagnostic methods, morphological and functional imaging methods such as computed tomography (CT), magnetic resonance imaging (MRI) and positron emission tomography (PET, PET/CT) are used.  $^{18}\text{F}$ -fluorodeoxyglucose ( $^{18}\text{F}$ -FDG) has shown limited sensitivity in various studies for the detection of differentiated prostate carcinomas and imaging of recurrent prostate cancer [3–5].  $^{18}\text{F}$ -FDG accumulation is mostly observed in dedifferentiated, aggressive and metastasised prostate cancer. Further PET and PET/CT tracers that have been introduced for the diagnosis of prostate carcinoma are  $^{18}\text{F}$ -fluorodihydrotestosterone,  $^{11}\text{C}$ -acetate,  $^{11}\text{C}$ -methionine and  $^{11}\text{C}$ - or  $^{18}\text{F}$ -labelled choline derivatives [5–11]. Promising results have been obtained using PET and PET/CT with  $^{11}\text{C}$ - and  $^{18}\text{F}$ -labelled choline derivatives; for an overview see Krause et al. [12]. Choline is an essential constituent of the cell membrane phospholipids. The use of choline to image prostate cancer is based on increased phos-

phorylcholine levels and an elevated phosphatidylcholine turnover in prostate cancer cells [13,14]. After uptake into the tumour cell via a high-affinity transporter system, choline is phosphorylated by choline kinase – which is the first step in the Kennedy pathway – and is incorporated into the phosphatidyl membrane. Key enzymes of the choline metabolism, such as choline kinase, are up-regulated in prostate cancer cells [15,16]. Additionally, increased expression of choline transporters and an elevated choline transportation rate have been detected [16–19]. This chapter reviews the use of PET and PET/CT using radioactively labelled choline derivatives in prostate cancer, with special emphasis on patients with biochemical recurrence.

### Imaging of primary prostate cancer

The value of PET and PET/CT using  $^{11}\text{C}$ - and  $^{18}\text{F}$ -labelled choline derivatives for the diagnosis of primary prostate cancer has been examined in several studies with partially controversial results [8, 11, 20–37]. The mean sensitivity and specificity for the detection of local prostate cancer are 91% and 73% respectively. The majority of reported sensitivities have been based on per patient analyses, which have shown better results (98–100%) than lesion-based analyses. Some of the studies with selected patient groups have shown high sensitivities for the detection of primary prostate cancer [26, 30, 36], while others have reported lower detection rates [23, 24, 29, 31] (Table 1). The detection rate of primary pros-

tate cancer using  $^{11}\text{C}$ -choline PET and PET/CT may be influenced by the tumour configuration: The detection of small and partly 'rind-like' carcinomas (onion ring form of growth) is of-

ten not possible. Furthermore, differentiation between benign prostatic hyperplasia, prostatitis and high-grade intraepithelial neoplasia is not always possible [23, 24, 29, 33, 35–37].

Courtesy of Department of Nuclear  
Medicine, University Hospital Rostock,  
University of Rostock

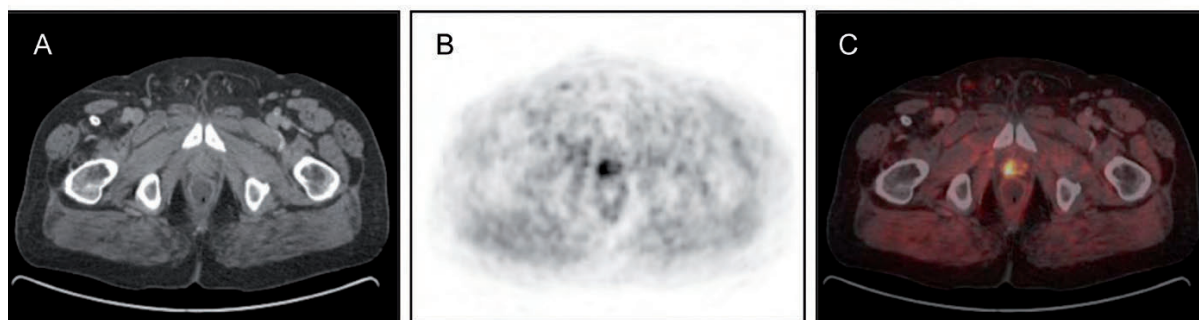


Figure 1. 65 year old patient with prostate cancer and status after radiation therapy 11/03, referred for  $^{11}\text{C}$ -choline PET/CT due to increasing PSA up to 3,34 ng/ml.  $^{11}\text{C}$ -choline PET/CT at 11/10 revealed local recurrence (A) CT scan, (B) PET scan, (C) PET/CT fused images

With respect to lymph node staging, only a few studies have reported results for sensitivity and specificity. De Jong et al. showed that  $^{11}\text{C}$ -choline PET identified metastatic pelvic lymph nodes with a size between 0.5 and 3 cm [38]. The authors reported 19 correct negative findings in 19 patients without lymph node metastases and one instance of false positive  $^{11}\text{C}$ -choline enhancement in a lymph node with inflammatory changes. Schiavina et al. examined 57 patients with biopsy-proven prostate cancer and an intermediate or high risk for lymph node metastases using  $^{11}\text{C}$ -choline PET/CT prior to prostatectomy and extended pelvic lymph node dissection [32].  $^{11}\text{C}$ -choline PET/CT showed a sensitivity of 60% and a specificity of 98% for the detection of lymph node metastases. Comparing  $^{11}\text{C}$ -

choline PET/CT findings with nomograms, no statistically significant difference was found in sensitivity and specificity (Briganti nomogram: 60% and 74%; Kattan nomogram: 60% and 64%). Poulsen et al. examined 25 consecutive patients with primary prostate cancer using  $^{18}\text{F}$ -choline PET/CT. The sensitivity and specificity of  $^{18}\text{F}$ -choline PET/CT for patient-based lymph node staging of prostate cancer were 100% and 95% respectively [39].

$^{11}\text{C}$ -choline PET/CT has also been successfully used in patients with advanced prostate cancer [40]. In these patients, PET/CT allowed a more precise assessment of disease localisation and extent within a single examination (lymph nodes, bones and other organs, e.g. lung) and demonstrated additional value for



the detection of bone metastases, thereby influencing individualised therapy planning.

### Imaging of recurrent prostate cancer

A number of studies have been performed on the use of  $^{11}\text{C}$ - and  $^{18}\text{F}$ -labelled choline deriva-

tives for the diagnosis of recurrent prostate cancer, showing an increasingly valuable potential of this hybrid imaging technique for the detection of local, regional and systemic disease [22, 25, 33, 41–59].

Courtesy of Department of Nuclear  
Medicine, University Hospital Rostock,  
University of Rostock

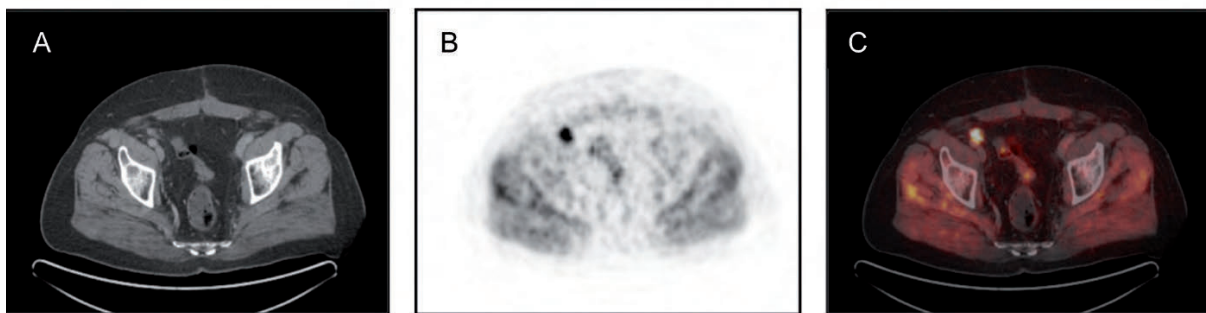


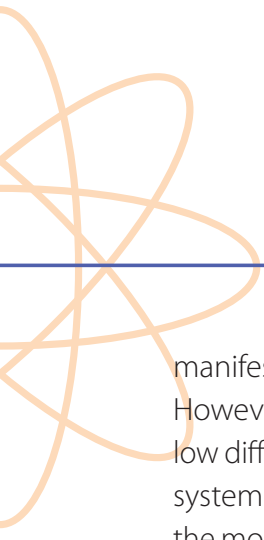
Figure 2. 72 year old patient with prostate cancer and status after salvage prostatectomy and radiation therapy 01/99, status after local recurrence and anti-androgen therapy 11/05, referred for  $^{11}\text{C}$ -choline PET/CT due to increasing PSA up to 3 ng/ml.  $^{11}\text{C}$ -choline PET/CT at 12/10 revealed lymphnode metastasis. (A) CT scan, (B) PET scan, (C) PET/CT fused images

Table 2 shows a summary of relevant publications regarding the diagnostic efficacy of PET and PET/CT using  $^{11}\text{C}$ - and  $^{18}\text{F}$ -labelled choline derivatives in patients with recurrent prostate cancer after primary therapy. Overall, the results of 22 groups and 1731 patients were analysed. The majority of patients were examined after radical prostatectomy, while the others were initially treated with conformal radiation therapy and/or anti-androgen therapy. The mean interval between first local treatment and PET/CT at the time of biochemical recurrence was 42 months. The mean serum PSA value at the time of PET or PET/CT was 8.0 ng/ml. Mean sensitivity and specificity were calcu-

lated as 69.1% and 69.2% for the detection of local recurrence, lymph node metastases and bone metastases. Only a few patients were under anti-androgen therapy during PET/CT scanning (Table 2).

Recurrence of prostate cancer can be found in 20%–50% of patients within 10 years after radical prostatectomy as primary treatment [60,61] and in up to 53% within 10 years after conformal radiation therapy [62]. In most of the patients, recurrence is suspected as a result of an increase in the serum PSA level, which is a sensitive biomarker for recurrence of prostate cancer and often precedes clinical





manifestation by months or even years [63]. However, increase in serum PSA does not allow differentiation between local, regional and systemic disease. Lymph nodes and bone are the most common sites of metastases of prostate cancer. About 50% of patients develop local recurrence while the remainder suffer from metastatic disease with or without local recurrence [64]. It is crucial to distinguish between local, regional and systemic recurrence for the purpose of individualised treatment. At present, conventional imaging methods such as transrectal ultrasound, CT and MRI are not sufficiently accurate in the localisation of recurrence of prostate cancer. This clinical situation demands a diagnostic procedure with a high sensitivity and specificity for early and exact detection of disease localisation. This is a key challenge that needs to be met in order to improve diagnostic performance and accuracy.

Picchio et al. compared  $^{18}\text{F}$ -FDG and  $^{11}\text{C}$ -choline for re-staging in 100 prostate cancer patients with biochemical recurrence and a mean serum PSA level of 6.6 ng/ml. In 47% of patients, lesions with pathological  $^{11}\text{C}$ -choline accumulation were found [51]. Cimitan et al. performed an  $^{18}\text{F}$ -fluorocholine PET/CT study in 100 patients with biochemical recurrence after primary therapy. A positive  $^{18}\text{F}$ -fluorocholine PET/CT scan was obtained in 54 of the patients (54%). Negative  $^{18}\text{F}$ -fluorocholine PET/CT imaging without pathological uptake was demonstrated in 89% of patients with a PSA

<4 ng/ml [44]. Rinnab et al. [54] performed  $^{11}\text{C}$ -choline PET/CT in 50 patients who had previously undergone primary therapy. Most of the pathological  $^{11}\text{C}$ -choline PET/CT findings were compared with histopathology as the gold standard. The investigators reported that the sensitivity of PET/CT at PSA values of less than 2.5 ng/ml was 91%, though with a lower specificity of 50%. Scattoni et al. examined 25 patients with biochemical recurrence and lymph node metastases with  $^{11}\text{C}$ -choline PET/CT and reported a high positive predictive value even at low PSA concentrations. The negative predictive value, on the other hand, was low; this was most likely related not to lymph node metastases but to microscopic lesions [57]. Reske et al. [52] performed  $^{11}\text{C}$ -choline PET/CT in 49 patients with biochemical recurrence and suspicion of local recurrence of prostate cancer. Local recurrence was biopsy proven in 36 of the 49 patients (74%), and  $^{11}\text{C}$ -choline PET/CT correctly predicted local recurrence in 71% of these 36 patients. Husarik et al. evaluated the value of  $^{18}\text{F}$ -fluorocholine PET/CT in 111 patients with prostate cancer, 68 of whom were restaged because of biochemical recurrence. The authors showed a sensitivity of 86% for the diagnosis of recurrent prostate cancer [25]. Krause et al. [48] examined 63 patients with biochemical failure after primary therapy. Pathological areas were detected in 35 of the patients (56%). The detection rate for PSA values <1 ng/ml was 36%. Furthermore, the authors demonstrated a linear correlation between  $^{11}\text{C}$ -choline PET/CT detection rate

and serum PSA value. Castellucci et al. [42] assessed the effect of total PSA, PSA velocity and PSA doubling time on the  $^{11}\text{C}$ -choline PET/CT detection rate in 190 patients with biochemical recurrence of prostate cancer. The investigators confirmed the linear correlation between PSA value and  $^{11}\text{C}$ -choline PET/CT detection rate. A multivariate analysis showed that PSA doubling time and PSA velocity were additional independent predictive factors for PET positivity. Giovacchini et al. [45] examined 358 patients with biochemical recurrence after radical prostatectomy. The percentage of positive scans was 19% in those with a PSA concentration between 0.2 and 1 ng/ml, 46% in those with a PSA of 1–3 ng/ml and 82% in those with a PSA >3 ng/ml. The authors concluded that a PSA value of 1 ng/ml might be a reasonable threshold when considering a choline PET/CT scan. Castellucci et al. evaluated the potential of  $^{11}\text{C}$ -choline PET/CT in re-staging of prostate cancer patients after radical prostatectomy who presented a mild increase in PSA (<1.5 ng/ml) during follow-up. The authors showed positive findings in 29 of 102 patients (28%) [43].

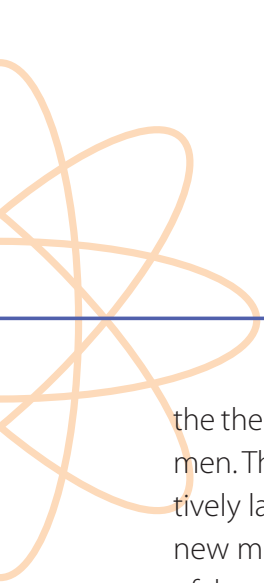
Nevertheless, study results regarding the value of choline PET/CT in patients with recurrence have to be interpreted carefully owing to the low numbers of patients in some studies, the lack of histopathology in most studies, the use of retrospective data analysis in most studies, and the use of different tracers and different PET and PET/CT systems. Moreover, small

lymph nodes might and micrometastases will not be detectable by PET and PET/CT owing to the partial volume effect. In the future, adequately designed, prospective studies with exact definition of patient groups and comparison of imaging results with histology, as well as multicentre trials, will be needed to corroborate the data and define the clinical efficacy of PET/CT in the re-staging of prostate cancer.

Imaging results using  $^{11}\text{C}$ - and  $^{18}\text{F}$ -labelled choline derivatives might influence the therapeutic management. Distant metastases have to be excluded before choosing the treatment modality, e.g. salvage radiation therapy, salvage radical prostatectomy or lymphadenectomy. Therapy could also be optimised using choline PET/CT. For example, a single-site local lymph node metastasis could be treated by radiation therapy with an extended field or by salvage lymphadenectomy, while systemic therapy could be initiated in the case of disseminated disease.

#### Therapy response assessment

Systemic therapy of advanced prostate cancer comprises androgen deprivation by LHRH agonists/antagonists and anti-androgen therapy, chemotherapy, bisphosphonates, and – within clinical studies – anti-neovascular agents and tyrosine kinase inhibitors. Methods of conventional follow-up such as clinical response, serum PSA level and conventional imaging modalities have been insufficient for assessing



the therapeutic efficacy of any treatment regimen. The use of PET and PET/CT with radioactively labelled choline derivatives may offer a new method for early and precise prediction of therapy response and outcome of a chosen therapy regimen. Preclinical studies show that  $^{11}\text{C}$ -choline PET can be used to monitor effects of a cytotoxic therapy in prostate cancer xenograft models [65]. In an *in vivo* study of prostate cancer mouse xenograft models with xenotransplanted PC3 cells in NMRI (nu/nu) mice under docetaxel treatment which were imaged with  $^{11}\text{C}$ -choline small animal PET/CT, the authors showed that docetaxel therapy led to a significant reduction in mean  $^{11}\text{C}$ -choline uptake of 45%, paralleled by significant tumour growth inhibition. Prospective clinical studies are necessary to evaluate the usefulness of PET and PET/CT imaging with  $^{11}\text{C}$ - and  $^{18}\text{F}$ -labelled choline for therapy response assessment. These clinical studies will have to elucidate the best tracer, time of scanning and clinical significance of the magnitude of signal changes [66]. Currently, few data have been published regarding use of PET/CT for therapy monitoring of prostate cancer patients among whom a relevant number are under anti-androgen treatment. Preliminary results with  $^{18}\text{F}$ -fluorocholine PET [9] and  $^{11}\text{C}$ -choline PET/CT [24] showed a significant reduction in choline uptake after initiation of anti-androgen therapy. Giovacchini et al. used  $^{11}\text{C}$ -choline PET/CT to monitor a group of six patients with localised prostate cancer under bicalutamide treatment (150 mg/day) for a median duration

of 4 months (range 3–12 months). The authors found a significant reduction in choline uptake and a high inter-patient variability. The imaging biomarker signal decrease was paralleled by a decrease in PSA values of 78% [24].

### Conclusion/Outlook

Choline PET/CT is a clinically valuable tool for re-staging of patients with increasing PSA serum levels after definitive local therapy. At the present time, however, choline PET/CT cannot be recommended as a first-line screening procedure for primary prostate cancer in men at risk, though it may be of value for the detection of clinically suspected prostate cancer in patients with multiple negative prostate biopsies. Preliminary studies evaluating the use of choline PET/CT for therapy response assessment after anti-hormonal therapy have revealed partially promising results, and clinical studies of the use of choline PET/CT for therapy monitoring in patients with metastases under docetaxel chemotherapy are being launched.

Although considerable progress has been made in recent years with PET/CT using  $^{11}\text{C}$ - and  $^{18}\text{F}$ -labelled choline derivatives, diagnostic performance still needs to be improved. Many strategies for prostate cancer imaging with novel radiotracers such as bombesin-based tracers or tracers for androgen receptor imaging are being assessed in preclinical studies and in some cases in initial clinical feasibility studies. In the future more tumour-specific

tracers may increase the sensitivity and specificity of multimodality imaging for the diagnosis of prostate cancer. Advances in hybrid imaging, especially PET/MRI, could also lead to improvements in diagnostic accuracy by

combining the molecular imaging properties of PET with the high resolution and soft tissue contrast of MRI and the functional and molecular MRI techniques.

Table 1

Tracer	Ref.	Author	Year	Modality	Pts. (n)	Local tumour		Lymph nodes	
						Sensitivity (%)	Specificity (%)	Sensitivity (%)	Specificity (%)
<sup>18</sup> F-choline	[26]	Kwee	2005	PET	17	100	-	-	-
	[33]	Schmid	2005	PET/CT	19	100	-	-	-
	[27]	Kwee	2006	PET	26	100	-	-	-
	[25]	Husarik	2008	PET/CT	43	98	-	33	100
	[34]	Steuber	2010	PET/CT	20	-	-	0	100
	[20]	Beheshti	2010	PET/CT	130	n.c.	n.c.	45	96
<sup>11</sup> C-choline	[39]	Poulsen	2010	PET/CT	25	-	-	100	95
	[8]	Kotzerke	2000	PET	23	100	-	50	90
	[21]	de Jong	2002	PET	25	100	-	80	95
	[38]	de Jong	2003	PET	67	-	-	80	96
	[35]	Sutinen	2004	PET	14	100	-	-	-
	[36]	Yamaguchi	2005	PET	20	100	-	-	-
	[37]	Yoshida	2005	PET	13	-	-	-	-
	[23]	Farsad <sup>1</sup>	2005	PET/CT	36	66	81	-	-
	[30]	Reske <sup>1</sup>	2006	PET/CT	26	100	-	-	-
	[31]	Scher	2007	PET/CT	58	86	70	-	-
	[29]	Martorana <sup>1</sup>	2006	PET/CT	43	66	84	-	-
[24]	Giovacchini <sup>1</sup>	2008	PET/CT	19	72	43	-	-	
[32]	Schiavina	2008	PET/CT	57	-	-	60	98	
[28]	Li <sup>2</sup>	2008	PET/CT	49	90	86	-	-	

Tracer	Ref.	Author	Year	Modality	Pts. (n)	Local tumour		Lymph nodes	
						Sensitivity (%)	Specificity (%)	Sensitivity (%)	Specificity (%)
	[11]	Watanabe	2010	PET	43	73	59	-	-
	[67]	Souvatzoglou	2011	PET/CT	43	79	-	-	-
<b>Sum</b>					<b>816</b>				
<b>Mean</b>						<b>89.4</b>	<b>70.5</b>	<b>56</b>	<b>96.2</b>
<b>Median</b>						<b>99</b>	<b>75.5</b>	<b>55</b>	<b>96</b>

Table 1: Diagnostic efficacy of <sup>18</sup>F-choline and <sup>11</sup>C-choline PET and PET/CT in patients with primary prostate cancer (modified and updated from [12])

<sup>1</sup> Sextant-based comparison with histology

<sup>2</sup> Uptake ratio of lesion to muscle was compared with histology

Table 2

Tracer	Ref.	Author	Year	Modus	Pts. (n)	Pts. (n)	Pts. (n)	Pts. (n)	Time (Mo)	PSA (ng/mL)	Sens. (%)	Spec. (%)
					all	RP	RT	ADT				
<sup>18</sup> F-choline	[47]	Heinisch	2006	PET/CT	34	31	3	4	-	17.1	41	-
	[33]	Schmid	2005	PET/CT	9	8	1	-	49	14.1	100	-
	[44]	Cimitan	2006	PET/CT	100	58	21	21	-	48.3	54	-
	[25]	Husarik	2008	PET/CT	68	68	-	13	-	10.8	86	-
	[59]	Vees	2007	PET	20	20	-	-	35	0.4	50	-
	[50]	Pelosi	2008	PET/CT	56	56	-	-	-	-	43	-
	[58]	Steiner	2009	PET/CT	47	17	30	-	67	3.3	81	-
<sup>11</sup> C-choline	[51]	Picchio <sup>1</sup>	2003	PET	100	77	23	-	-	6.6	47	-

Tracer	Ref.	Author	Year	Modus	Pts.	Pts.	Pts.	Pts.	Time (Mo)	PSA	Sens.	Spec.
					(n)	(n)	(n)	(n)				
					all	RP	RT	ADT	Tx-PET/CT	(ng/mL)	(%)	(%)
	[22]	de Jong <sup>1</sup>	2003	PET	36	20	16	-	-	12.0	55	100
	[49]	Ohlmann	2007	PET/CT	45	0	45	-	-	7.8	65	-
	[54]	Rinnab	2007	PET/CT	50	40	10	4	22	3.6	95	40
	[57]	Scattoni	2007	PET/CT	25	25	-	-	-	4.0	100	66
	[41]	Breeuwsma <sup>1</sup>	2010	PET	80	0	70	-	-	12.3	81	100
	[48]	Krause	2008	PET/CT	63	42	21	17	47	5.9	56	-
	[55]	Rinnab	2008	PET/CT	15	15	-	-	24	2.3	100	0
	[52]	Reske	2008	PET/CT	49	49	-	9	59	2.0	73	88
	[56]	Rinnab	2009	PET/CT	41	41	-	-	24	2.8	93	36
	[42]	Castellucci	2009	PET/CT	190	190	-	-	46	4.2	39	-
	[45]	Giovacchini	2010	PET/CT	358	358		155		3.8	85	93
	[46]	Giovacchini	2010	PET/CT	170	170			45	3.2	87	89
	[53]	Richter <sup>1</sup>	2010	PET	73	49	24	15		2.7	61	80
	[43]	Castellucci	2011	PET/CT	102	102	-	16		0.9	28	-
<b>Sum</b>					<b>1731</b>	<b>1436</b>	<b>264</b>	<b>254</b>				
<b>Mean</b>									<b>42</b>	<b>8.0</b>	<b>69.1</b>	<b>69.2</b>
<b>Median</b>									<b>45.5</b>	<b>4.0</b>	<b>69</b>	<b>88</b>

Table 2: Diagnostic efficacy of <sup>18</sup>F-choline and <sup>11</sup>C-choline PET and PET/CT in patients with recurrent prostate cancer (modified and updated from [12])

RP, radical prostatectomy;  
 RT, radiotherapy;  
 ADT, androgen deprivation therapy;  
 Tx, therapy

<sup>1</sup> PET only

## References Chapter 2.5

### References

1. Ferlay J, Autier P, Boniol M, Heanue M, Colombet M, Boyle P. Estimates of the cancer incidence and mortality in Europe in 2006. *Ann Oncol* 2007;18:581-92.
2. Smith RA, Cokkinides V, Eyre HJ. Cancer screening in the United States, 2007: a review of current guidelines, practices, and prospects. *CA Cancer J Clin* 2007;57:90-104.
3. Hofer C, Laubenbacher C, Block T, Breul J, Hartung R, Schwaiger M. Fluorine-18-fluorodeoxyglucose positron emission tomography is useless for the detection of local recurrence after radical prostatectomy. *Eur Urol* 1999;36:31-5.
4. Morris MJ, Akhurst T, Osman I, Nunez R, Macapinlac H, Siedlecki K, et al. Fluorinated deoxyglucose positron emission tomography imaging in progressive metastatic prostate cancer. *Urology* 2002;59:913-8.
5. Nunez R, Macapinlac HA, Yeung HW, Akhurst T, Cai S, Osman I, et al. Combined 18F-FDG and 11C-methionine PET scans in patients with newly progressive metastatic prostate cancer. *J Nucl Med* 2002;43:46-55.
6. Albrecht S, Buchegger F, Soloviev D, Zaidi H, Veas H, Khan HG, et al. (11C)-acetate PET in the early evaluation of prostate cancer recurrence. *Eur J Nucl Med Mol Imaging* 2007;34:185-96.
7. Dehdashti F, Picus J, Michalski JM, Dence CS, Siegel BA, Katzenellenbogen JA, et al. Positron tomographic assessment of androgen receptors in prostatic carcinoma. *Eur J Nucl Med Mol Imaging* 2005;32:344-50.
8. Kotzerke J, Prang J, Neumaier B, Volkmer B, Guhlmann A, Kleinschmidt K, et al. Experience with carbon-11 choline positron emission tomography in prostate carcinoma. *Eur J Nucl Med* 2000;27:1415-9.
9. Larson SM, Morris M, Gunther I, Beattie B, Humm JL, Akhurst TA, et al. Tumor localization of 16beta-18F-fluoro-5alpha-dihydrotestosterone versus 18F-FDG in patients with progressive, metastatic prostate cancer. *J Nucl Med* 2004;45:366-73.
10. Toth G, Lengyel Z, Balkay L, Salah MA, Tron L, Toth C. Detection of prostate cancer with 11C-methionine positron emission tomography. *J Urol* 2005;173:66-9; discussion 9.
11. Watanabe H, Kanematsu M, Kondo H, Kako N, Yamamoto N, Yamada T, et al. Preoperative detection of prostate cancer: a comparison with 11C-choline PET, 18F-fluorodeoxyglucose PET and MR imaging. *J Magn Reson Imaging* 2010;31:1151-6.
12. Krause BJ, Souvatzoglou M, Treiber U. Imaging of prostate cancer with PET/CT and radioactively labeled choline derivatives. *Urol Oncol* 2011;in press.
13. Ackerstaff E, Glunde K, Bhujwala ZM. Choline phospholipid metabolism: a target in cancer cells? *J Cell Biochem* 2003;90:525-33.
14. Casciani E, Gualdi GF. Prostate cancer: value of magnetic resonance spectroscopy 3D chemical shift imaging. *Abdom Imaging* 2006;31:490-9.
15. Ramirez de Molina A, Penalva V, Lucas L, Lacal JC. Regulation of choline kinase activity by Ras proteins involves Ral-GDS and PI3K. *Oncogene* 2002;21:937-46.
16. Ratnam S, Kent C. Early increase in choline kinase activity upon induction of the H-ras oncogene in mouse fibroblast cell lines. *Arch Biochem Biophys* 1995;323:313-22.
17. Ackerstaff E, Pflug BR, Nelson JB, Bhujwala ZM. Detection of increased choline compounds with proton nuclear magnetic resonance spectroscopy subsequent to malignant transformation of human prostatic epithelial cells. *Cancer Res* 2001;61:3599-603.
18. Hara T, Bansal A, DeGrado TR. Choline transporter as a novel target for molecular imaging of cancer. *Mol Imaging* 2006;5:498-509.
19. Katz-Brull R, Degani H. Kinetics of choline transport and phosphorylation in human breast cancer cells; NMR application of the zero trans method. *Anticancer Res* 1996;16(3B):1375-80.
20. Beheshti M, Imamovic L, Broinger G, Vali R, Waldenberger P, Stoiber F, et al. 18F choline PET/CT in the preoperative staging of prostate cancer in patients with intermediate or high risk of extracapsular disease: a prospective study of 130 patients. *Radiology* 2010;254:925-33.
21. de Jong IJ, Pruijm J, Elsinga PH, Vaalburg W, Mensink HJ. Visualization of prostate cancer with 11C-choline positron emission tomography. *Eur Urol* 2002;42:18-23.



22. de Jong IJ, Pruim J, Elsinga PH, Vaalburg W, Mensink HJ. 11C-choline positron emission tomography for the evaluation after treatment of localized prostate cancer. *Eur Urol* 2003;44:32-8; discussion 8-9.
23. Farsad M, Schiavina R, Castellucci P, Nanni C, Corti B, Martorana G, et al. Detection and localization of prostate cancer: correlation of (11)C-choline PET/CT with histopathologic step-section analysis. *J Nucl Med* 2005;46:1642-9.
24. Giovacchini G, Picchio M, Coradeschi E, Scattoni V, Bettinardi V, Cozzarini C, et al. [(11)C]choline uptake with PET/CT for the initial diagnosis of prostate cancer: relation to PSA levels, tumour stage and anti-androgenic therapy. *Eur J Nucl Med Mol Imaging* 2008;35:1065-73.
25. Husarik DB, Miralbell R, Dubs M, John H, Giger OT, Gelet A, et al. Evaluation of [(18)F]-choline PET/CT for staging and restaging of prostate cancer. *Eur J Nucl Med Mol Imaging* 2008;35:253-63.
26. Kwee SA, Coel MN, Lim J, Ko JP. Prostate cancer localization with 18fluorine fluorocholine positron emission tomography. *J Urol* 2005;173:252-5.
27. Kwee SA, Wei H, Sesterhenn I, Yun D, Coel MN. Localization of primary prostate cancer with dual-phase 18F-fluorocholine PET. *J Nucl Med* 2006;47:262-9.
28. Li X, Liu Q, Wang M, Jin X, Yao S, Liu S, et al. C-11 choline PET/CT imaging for differentiating malignant from benign prostate lesions. *Clin Nucl Med* 2008;33:671-6.
29. Martorana G, Schiavina R, Corti B, Farsad M, Salizzoni E, Brunocilla E, et al. 11C-choline positron emission tomography/computerized tomography for tumor localization of primary prostate cancer in comparison with 12-core biopsy. *J Urol* 2006;176:954-60; discussion 60.
30. Reske SN, Blumstein NM, Neumaier B, Gottfried HW, Finsterbusch F, Kocot D, et al. Imaging prostate cancer with 11C-choline PET/CT. *J Nucl Med* 2006;47:1249-54.
31. Scher B, Seitz M, Albinger W, Tiling R, Scherr M, Becker HC, et al. Value of 11C-choline PET and PET/CT in patients with suspected prostate cancer. *Eur J Nucl Med Mol Imaging* 2007;34:45-53.
32. Schiavina R, Scattoni V, Castellucci P, Picchio M, Corti B, Briganti A, et al. 11C-choline positron emission tomography/computerized tomography for preoperative lymph-node staging in intermediate-risk and high-risk prostate cancer: comparison with clinical staging nomograms. *Eur Urol* 2008;54:392-401.
33. Schmid DT, John H, Zweifel R, Cservenyak T, Westera G, Goerres GW, et al. Fluorocholine PET/CT in patients with prostate cancer: initial experience. *Radiology* 2005;235:623-8.
34. Steuber T, Schlomm T, Heinzer H, Zacharias M, Ahyai S, Chun KF, et al. [F(18)]-fluoroethylcholine combined in-line PET-CT scan for detection of lymph-node metastasis in high risk prostate cancer patients prior to radical prostatectomy: preliminary results from a prospective histology-based study. *Eur J Cancer* 2010;46:449-55.
35. Sutinen E, Nurmi M, Roivainen A, Varpula M, Tolvanen T, Lehtikoinen P, et al. Kinetics of [(11)C]choline uptake in prostate cancer: a PET study. *Eur J Nucl Med Mol Imaging* 2004;31:317-24.
36. Yamaguchi T, Lee J, Uemura H, Sasaki T, Takahashi N, Oka T, et al. Prostate cancer: a comparative study of 11C-choline PET and MR imaging combined with proton MR spectroscopy. *Eur J Nucl Med Mol Imaging* 2005;32:742-8.
37. Yoshida S, Nakagomi K, Goto S, Futatsubashi M, Torizuka T. 11C-choline positron emission tomography in prostate cancer: primary staging and recurrent site staging. *Urol Int* 2005;74:214-20.
38. de Jong IJ, Pruim J, Elsinga PH, Vaalburg W, Mensink HJ. Preoperative staging of pelvic lymph nodes in prostate cancer by 11C-choline PET. *J Nucl Med* 2003;44:331-335.
39. Poulsen MH, Bouchelouche K, Gerke O, Petersen H, Svolgaard B, Marcussen N, et al. [18F]-fluorocholine positron-emission/computed tomography for lymph node staging of patients with prostate cancer: preliminary results of a prospective study. *BJU Int* 2010;106:639-43; discussion 44.

- 
40. Tuncel M, Souvatzoglou M, Herrmann K, Stollfuss J, Schuster T, Weirich G, et al. [(11)C]Choline positron emission tomography/computed tomography for staging and restaging of patients with advanced prostate cancer. *Nucl Med Biol* 2008;35:689-95.
41. Breeuwsma AJ, Pruijm J, van den Bergh AC, Leliveld AM, Nijman RJ, Dierckx RA, et al. Detection of local, regional, and distant recurrence in patients with psa relapse after external-beam radiotherapy using (11)C-choline positron emission tomography. *Int J Radiat Oncol Biol Phys* 2010;77:160-4.
42. Castellucci P, Fuccio C, Nanni C, Santi I, Rizzello A, Lodi F, et al. Influence of trigger PSA and PSA kinetics on 11C-choline PET/CT detection rate in patients with biochemical relapse after radical prostatectomy. *J Nucl Med* 2009;50:1394-400.
43. Castellucci P, Fuccio C, Rubello D, Schiavina R, Santi I, Nanni C, et al. Is there a role for (11)C-choline PET/CT in the early detection of metastatic disease in surgically treated prostate cancer patients with a mild PSA increase <1.5 ng/ml? *Eur J Nucl Med Mol Imaging* 2011;38:55-63.
44. Cimitan M, Bortolus R, Morassut S, Canzonieri V, Garbeglio A, Baresic T, et al. [18F]fluorocholine PET/CT imaging for the detection of recurrent prostate cancer at PSA relapse: experience in 100 consecutive patients. *Eur J Nucl Med Mol Imaging* 2006;33:1387-98.
45. Giovacchini G, Picchio M, Coradeschi E, Bettinardi V, Gianolli L, Scattoni V, et al. Predictive factors of [(11)C]choline PET/CT in patients with biochemical failure after radical prostatectomy. *Eur J Nucl Med Mol Imaging* 2010;37:301-9.
46. Giovacchini G, Picchio M, Scattoni V, Garcia Parra R, Briganti A, Gianolli L, et al. PSA doubling time for prediction of [(11)C]choline PET/CT findings in prostate cancer patients with biochemical failure after radical prostatectomy. *Eur J Nucl Med Mol Imaging* 2010;37:1106-16.
47. Heinisch M, Dirisamer A, Loidl W, Stoiber F, Gruy B, Haim S, et al. Positron emission tomography/computed tomography with F-18-fluorocholine for restaging of prostate cancer patients: meaningful at PSA <5 ng/ml? *Mol Imaging Biol* 2006;8:43-8.
48. Krause BJ, Souvatzoglou M, Tuncel M, Herrmann K, Buck AK, Praus C, et al. The detection rate of [11C]choline-PET/CT depends on the serum PSA-value in patients with biochemical recurrence of prostate cancer. *Eur J Nucl Med Mol Imaging* 2008;35:18-23.
49. Ohlmann C, Pfister D, Thüer D, Wille S, Engelmann UH, Heidenreich A. 11C-choline-positron emission tomography/computerized tomography (11C-PET/CT) for tumour localization of locally recurrent prostate cancer after radiation therapy. *Eur Urol Suppl* 2007;6:229.
50. Pelosi E, Arena V, Skanjeti A, Pirro V, Douroukas A, Pupi A, et al. Role of whole-body 18F-choline PET/CT in disease detection in patients with biochemical relapse after radical treatment for prostate cancer. *Radiol Med* 2008;113:895-904.
51. Picchio M, Messa C, Landoni C, Gianolli L, Sironi S, Brioschi M, et al. Value of [11C]choline-positron emission tomography for re-staging prostate cancer: a comparison with [18F]fluorodeoxyglucose-positron emission tomography. *J Urol* 2003;169:1337-40.
52. Reske SN, Blumstein NM, Glatting G. [11C]choline PET/CT imaging in occult local relapse of prostate cancer after radical prostatectomy. *Eur J Nucl Med Mol Imaging* 2008;35:9-17.
53. Richter JA, Rodriguez M, Rioja J, Penuelas I, Marti-Climent J, Garrastachu P, et al. Dual tracer 11C-choline and FDG-PET in the diagnosis of biochemical prostate cancer relapse after radical treatment. *Mol Imaging Biol* 2010;12:210-7.
54. Rinnab L, Mottaghy FM, Blumstein NM, Reske SN, Hautmann RE, Hohl K, et al. Evaluation of [11C]-choline positron-emission/computed tomography in patients with increasing prostate-specific antigen levels after primary treatment for prostate cancer. *BJU Int* 2007;100:786-93.
55. Rinnab L, Mottaghy FM, Simon J, Volkmer BG, de Petriconi R, Hautmann RE, et al. [11C]Choline PET/CT for targeted salvage lymph node dissection in patients with biochemical recurrence after primary curative therapy for prostate cancer. Preliminary results of a prospective study. *Urol Int* 2008;81:191-7.

56. Rinnab L, Simon J, Hautmann RE, Cronauer MV, Hohl K, Buck AK, et al. [(11C)Choline PET/CT in prostate cancer patients with biochemical recurrence after radical prostatectomy. *World J Urol* 2009;27:619-25.
57. Scattoni V, Picchio M, Suardi N, Messa C, Freschi M, Roscigno M, et al. Detection of lymph-node metastases with integrated [11C]choline PET/CT in patients with PSA failure after radical retropubic prostatectomy: results confirmed by open pelvic-retroperitoneal lymphadenectomy. *Eur Urol* 2007;52:423-9.
58. Steiner C, Veas H, Zaidi H, Wissmeyer M, Berrebi O, Kossovsky MP, et al. Three-phase 18F-fluorocholine PET/CT in the evaluation of prostate cancer recurrence. *Nuklearmedizin* 2009;48:1-9; quiz N2-3.
59. Veas H, Buchegger F, Albrecht S, Khan H, Husarik D, Zaidi H, et al. 18F-choline and/or 11C-acetate positron emission tomography: detection of residual or progressive subclinical disease at very low prostate-specific antigen values (<1 ng/mL) after radical prostatectomy. *BJU Int* 2007;99:1415-20.
60. Freedland SJ, Presti JC Jr, Amling CL, Kane CJ, Aronson WJ, Dorey F, et al. Time trends in biochemical recurrence after radical prostatectomy: results of the SEARCH database. *Urology* 2003;61:736-41.
61. Han M, Partin AW, Zahurak M, Piantadosi S, Epstein JI, Walsh PC. Biochemical (prostate specific antigen) recurrence probability following radical prostatectomy for clinically localized prostate cancer. *J Urol* 2003;169:517-23.
62. Chism DB, Hanlon AL, Horwitz EM, Feigenberg SJ, Pollack A. A comparison of the single and double factor high-risk models for risk assignment of prostate cancer treated with 3D conformal radiotherapy. *Int J Radiat Oncol Biol Phys* 2004;59:380-5.
63. Roberts SG, Blute ML, Bergstralh EJ, Slezak JM, Zincke H. PSA doubling time as a predictor of clinical progression after biochemical failure following radical prostatectomy for prostate cancer. *Mayo Clin Proc* 2001;76:576-81.
64. Bott SR. Management of recurrent disease after radical prostatectomy. *Prostate Cancer Prostatic Dis* 2004;7:211-6.
65. Krause BJ, Souvatzoglou M, Herrmann K, Weber AW, Schuster T, Buck AK, et al. [11C]Choline as pharmacodynamic marker for therapy response assessment in a prostate cancer xenograft model. *Eur J Nucl Med Mol Imaging* 2010;37:1861-8.
66. Contractor KB, Aboagye EO. Monitoring predominantly cytostatic treatment response with 18F-FDG PET. *J Nucl Med* 2009;50 Suppl 1:97-105.
67. Souvatzoglou M, Weirich G, Schwarzenboeck S, et al. The sensitivity of [11C]choline PET/CT to localize prostate cancer depends on the tumour configuration. *Clin. Cancer Res.* 2011

# Chapter 2 – Clinical applications of PET/CT in oncology

## 2.6 Lymphomas

Roberto C. Delgado-Bolton and José L. Carreras Delgado

### Introduction

<sup>18</sup>F-FDG PET has a main role in the management of patients with lymphoma. It has demonstrated a higher efficacy than conventional imaging methods such as CT, MRI and gallium scans, providing a more accurate distinction between scar or fibrosis and active tumour. Studies have evaluated the performance of <sup>18</sup>F-FDG PET in pretreatment staging, monitoring response to therapy and post-therapy surveillance, among other applications. <sup>18</sup>F-FDG PET has a major role in monitoring response to therapy and has allowed the introduction of the concept of risk-adapted therapy. This is discussed more fully in this section, which reviews the role of PET in the management of lymphoma.

### Initial staging

Based on the fact that most lymphomas show high levels of <sup>18</sup>F-FDG uptake, many studies analysing the performance of PET in the staging of lymphomas have shown very high sensitivity in patients with Hodgkin's lymphoma (HL) and high-grade non-Hodgkin's lymphoma (NHL). <sup>18</sup>F-FDG PET improved the performance of conventional imaging methods (including CT) in the detection of nodal and extranodal disease as well as in the characterisation of lesions considered equivocal on other imaging methods [1]. The additional information supplied by <sup>18</sup>F-FDG PET improves the accuracy of the staging of the disease, resulting in the upstaging or downstaging of the disease when compared

with conventional imaging methods [1,2]. Therefore, <sup>18</sup>F-FDG PET has a potential impact on management decisions as therapy is based on the stage of the disease. In addition, the advent of multimodality imaging with <sup>18</sup>F-FDG PET/CT has further improved upon the performance of <sup>18</sup>F-FDG PET alone, as is reflected by the higher specificity of the combined technique in recent studies [1].

An interesting issue is whether intravenous contrast must be used in PET/CT. Preliminary data suggest that intravenous contrast allows a more accurate assessment of the liver and spleen compared with unenhanced CT [3]. A review of the published data concluded that intravenous contrast-enhanced low-dose PET/CT may represent a reasonable choice as a single imaging modality for staging FDG-avid lymphomas [4].

Efficacy studies have evidenced the superior performance of <sup>18</sup>F-FDG PET in the initial staging of lymphomas, but there is very little evidence regarding its impact on patient outcomes. Even so, <sup>18</sup>F-FDG PET/CT has become the cornerstone of the staging imaging procedures in the state-of-the-art management in FDG-avid lymphomas (HL and aggressive NHL) [1]. In low-grade or indolent lymphomas, where <sup>18</sup>F-FDG PET has shown a variable diagnostic performance and impact on management, <sup>18</sup>F-FDG PET/CT is used sporadically or in clinical trials with frequently encouraging results [1].

## Therapy response evaluation

### *Concept of risk-adapted therapy*

Without doubt the most promising clinical application of  $^{18}\text{F}$ -FDG PET is in the early monitoring of response to therapy: new possibilities for risk stratification and individualisation of therapy have emerged based on the results of interim  $^{18}\text{F}$ -FDG PET [1,5,6]. The concept of risk-adapted therapy in lymphoma is increasingly accepted as a way to achieve higher cure rates with a lower or equal risk of treatment-related morbidity and mortality. Tailoring and individualising therapy according to the need of the patient is a therapeutic option which could perhaps soon become the standard of care. However, it is still not proven that modifying therapy on the basis of interim PET can improve patient outcomes. Therefore, this issue must be analysed in appropriately designed clinical trials.  $^{18}\text{F}$ -FDG PET enables evaluation of the early metabolic changes rather than the morphological changes which occur later during therapy. In lymphoma these early metabolic changes are highly predictive of the final treatment response. PET performed after a few courses of standard chemotherapy is a reliable prognostic tool to identify poor responders to therapy. Interim PET is a powerful prognostic tool when compared with other well-established clinical parameters in lymphoma [1,5,6].

### *Risk stratification and evaluation of response to therapy: prognostic indexes and imaging procedures*

For both HL and NHL there are well-defined pretreatment prognostic indexes that have demonstrated a prognostic value and the prediction of survival in prospective studies [1,7–10]. The therapeutic strategy is determined mainly by the clinical stage and these prognostic indexes. However, tumour response to therapy is an important surrogate for other assessments of clinical benefit, including progression-free survival and overall survival [1,5,6].

Several prognostic indexes have been developed for HL and NHL. The indexes developed for advanced HL have demonstrated a limited clinical utility and their predictive value has been questioned [11–13]. All these indexes take into account different risk factors (age, stage, etc.) to establish the prognosis and risk of recurrence. However, the values obtained are based on a group of patients who had been analysed retrospectively. Therefore, they do not necessarily reflect the risk in the individual patient [6]. Recently, the concept of risk-adapted therapy has been proposed, based on the fact that the chemosensitivity of the tumour or early response to therapy in the individual patient would allow risk stratification and, possibly, help with the therapeutic decisions as it predicts the probability of achieving control of the disease [1,5,6,11].



Until recently, CT and MRI have had a main role in diagnostic imaging in oncology. In recent years, however, there has been a change in this paradigm, as  $^{18}\text{F}$ -FDG PET has demonstrated a superior efficacy compared with conventional imaging methods in the evaluation of the oncological disease, especially in monitoring response to therapy, where the functional information supplied by  $^{18}\text{F}$ -FDG PET allows assessment of the early metabolic changes instead of the morphological changes which occur later during therapy [1,5]. Many studies in which  $^{18}\text{F}$ -FDG PET has been performed after one to three courses of chemotherapy in aggressive NHL [14–22] and HL [11,23–26] have evidenced that these early metabolic changes have a high predictive value for the response at the end of the treatment and progression-free survival [1]. A meta-analysis by Terasawa et al. concludes that  $^{18}\text{F}$ -FDG PET is a reliable prognostic tool to identify patients with a bad response to therapy in HL [27].

***Differences between HL and NHL: repercussions on therapy response evaluation with PET***

The histopathological and physiopathological characteristics of the neoplastic tissue are different for HL and NHL. In HL, the Reed-Sternberg cells represent less than 1% of the neoplastic tissue, whereas in diffuse large B cell lymphoma (DLBCL) they represent more than 90% of the total cell population [28]. In HL, the accompanying non-neoplastic lymphomononuclear cells produce an interconnected network by

cytokines that assure the immortality of the Reed-Sternberg cells and work as an amplifier of the capacity of PET to detect response [5,29–31]. This non-neoplastic compartment is disconnected very early by chemotherapy, giving rise to a situation denominated “complete metabolic response” [5,28,31–33]; this phenomenon explains the impressive prognostic value of PET in HL. This is the reason why, in around 80% of patients with HL, normalisation of the PET scan is achieved after two courses of ABVD [24,26,31]. On the other hand, in DLBCL chemotherapy progressively destroys a fraction of neoplastic cells, the percentage of cellular destruction being predictive of the response at the end of the chemotherapy [28]. In DLBCL the accompanying non-neoplastic lymphomononuclear cells do not seem to have a role in  $^{18}\text{F}$ -FDG uptake [28,34]. Instead,  $^{18}\text{F}$ -FDG uptake reflects the metabolic situation and represents the balance between the cellular destruction of the chemosensitive components and the growth of the resistant components [35]. It is characteristic in DLBCL that the metabolic activity decreases in a continuous way, as a fraction of neoplastic cells dies progressively. Owing to this progressive behaviour, the significance and predictive value of the early assessment of response probably differ depending on the timing of the PET scan [35]. At the beginning of the treatment (after one or two courses) PET assesses chemosensitivity as the prevailing phenomenon is the destruction of the most chemosensitive cells, whereas after three or four courses PET evaluates resistance



to therapy as FDG uptake depends more on the growth of the resistant components of the tumour [5,35].

### ***Evaluation of $^{18}\text{F}$ -FDG PET-CT: visual or semiquantitative?***

Based on the histopathological and physiopathological differences between HL and NHL discussed in the previous section, it seems that a visual analysis would be preferable in HL (because of its dichotomous response), whereas in DLBCL a semiquantitative analysis (using the maximum standardised uptake value or  $\text{SUV}_{\text{max}}$ ) would be preferable (because of its progressive response) [5,28]. However, when applying a semiquantitative analysis it must be taken into account that SUV depends on many factors (patient preparation and blood glucose levels,  $^{18}\text{F}$ -FDG administration protocol,  $^{18}\text{F}$ -FDG uptake time, PET scanner, image reconstruction, etc.). Therefore, it is necessary to standardise the  $^{18}\text{F}$ -FDG PET procedure in order to obtain PET images which will be comparable between different centres and will also permit comparison of successive studies within each centre, especially when using PET for response assessment [1,36].

### ***Considerations regarding the concept of minimal residual disease***

The concept of minimal residual uptake (MRU) has been defined as the presence of low-grade  $^{18}\text{F}$ -FDG uptake (just above background) in a location where previously there was disease. This concept was first described


for HL in 2005 [23], although it was later applied for both HL and NHL. The definition of MRU has changed since then, a consensus being achieved in 2009. Gallamini et al. [31] reviewed the evolution of the concept of MRU, which can be summarised in three points:

1. In 2005 Hutchings et al. considered MRU to reflect unspecific inflammatory processes related to cell destruction [23,31,37].
2. In 2007 Gallamini et al. [11] defined MRU as low  $^{18}\text{F}$ -FDG uptake similar to the mediastinal blood pool [31].
3. In 2008 Barrington et al. [36,38] defined MRU as a residual  $^{18}\text{F}$ -FDG uptake with an intensity lower than or equal to the liver uptake [31].

The evolution of the definition of MRU has extended the limits of what is considered MRU. These modifications have been aimed at increasing specificity and reducing the number of false positives when PET is used to predict the response to therapy and patient outcome [5,31,39].

However, these modifications in the definition of MRU have had consequences, especially in the design of clinical trials, as several of those currently under way are using different criteria for the interpretation of interim PET [31]. Therefore, in April 2009 an international meeting took place in Deauville (France), where uniform criteria were established for interim PET scan interpretation. The conclusions of this meeting are presented in the next section.





### ***Evaluation of response to therapy: Is there a consensus?***

The response evaluation criteria with  $^{18}\text{F}$ -FDG PET differ depending on the timing of the PET scan, i.e. whether it is performed early during therapy or after its completion.

Interim PET. When applying PET in the evaluation of response to therapy, the main problem is the absence of uniform criteria in studies available in the literature. The use of different criteria has led to a great variability in the reported sensitivity and specificity [28]. In some studies the International Harmonization Project criteria were applied, although these were designed to evaluate response after completion of therapy [3,40]. Another issue to take into account is the concept of MRU and its limits [23]. Recently, with many new clinical trials dedicated to this subject, the need for standard criteria for PET interpretation has become even more important, in order to obtain reproducible results all over the world [28].

In this context an international meeting was organised with experts in nuclear medicine and haematology. The First International Workshop on Interim PET in Lymphoma took place in Deauville (France) in April 2009, with the aim of establishing uniform criteria for interim PET scan interpretation and launching international validation studies, as had been done previously in the International Harmonization Project in 2007 [3,5,28,40]. The conclusions of the Deauville meeting were published

recently [28]. Gallamini et al. [31] revised the conclusions of the meeting and indicated that the criteria for the interpretation of interim PET can be summarised in three main statements: (a) visual analysis is preferable, although in some cases  $\text{SUV}_{\text{max}}$  can be used; (b) interim PET must be analysed comparing the focal  $^{18}\text{F}$ -FDG uptakes with those described in the pretherapy study; and (c) the intensity of  $^{18}\text{F}$ -FDG uptake must be categorised using a five-point scale where the reference organ is the liver [5,31]. The proposed five-point scale is:

1. Absence of uptake
2. Uptake  $\leq$  mediastinum
3. Uptake  $>$  mediastinum but  $\leq$  liver
4. Uptake moderately higher than the liver uptake, in any location
5. Marked increased uptake in any location and new focal lesions

During this meeting, international validation studies were designed for HL and NHL to validate these interpretation criteria [28,31]. A follow-up meeting, entitled the Second International Workshop on Interim PET in Lymphoma, took place in Menton (France) in April 2010. The conclusions of this second meeting had not been published at the time of submission of this manuscript.

### ***Evaluation of response after completion of therapy.***

The International Harmonization Project established standard criteria to evaluate response

after completion of therapy. The conclusions of the International Harmonization Project were published in 2007 [3,40] and can be summarised in the following recommendations:

1. Use of  $^{18}\text{F}$ -FDG PET for response assessment at the conclusion of therapy: Many studies have demonstrated the value of PET for response assessment of HL and DLBCL at the conclusion of front-line, salvage or high-dose therapy. The role of PET for response assessment of aggressive NHL subtypes other than DLBCL and of indolent and mantle cell lymphomas is less clear [3].
2. Requirement for pretherapy  $^{18}\text{F}$ -FDG PET scan for response assessment of lymphoma at the conclusion of therapy: Pretherapy PET is not compulsory for assessment of response after treatment of patients with HL, DLBCL, follicular lymphoma or mantle cell lymphoma because these lymphomas are routinely FDG avid. However, pretherapy PET is definitely encouraged for these subtypes because it can facilitate the interpretation of post-therapy PET. In contrast, pretherapy PET is obligatory for variably FDG-avid lymphomas if PET is to be used to assess their response to treatment. These include aggressive NHL subtypes other than DLBCL, such as T-cell lymphomas, and all subtypes of indolent NHL other than follicular lymphoma. If PET is to be used for response assessment of patients with these histological subtypes, there needs to be evidence that PET was positive at all disease sites with a diameter  $\geq 1.5$  cm detected by CT [3].
3. Timing of  $^{18}\text{F}$ -FDG PET performed for response assessment at the conclusion of therapy: To minimize the frequency of post-therapy inflammatory changes, which potentially confuse the interpretation of PET scans, PET should not be performed earlier than 3 weeks after chemotherapy and preferably 8–12 weeks after completion of radiotherapy [3].
4. Interpretation of  $^{18}\text{F}$ -FDG PET scans performed for response assessment at the conclusion of therapy: Visual assessment alone appears to be sufficient to decide whether PET is positive or negative at the conclusion of therapy, and semiquantitative analysis (using  $\text{SUV}_{\text{max}}$ ) does not seem necessary. The generally accepted definition of a positive or abnormal PET finding when using visual assessment is focal or diffuse FDG uptake above background in a location incompatible with normal anatomy or physiology [3]. This definition looks as if it is suitable in most instances, although there are some exceptions.

These recommendations established by the International Harmonization Project were designed to standardise the interpretation of PET in the evaluation of response to therapy in the clinical setting as well as in clinical trials [3,5,40].



### Follow-up and early detection of recurrent disease

The available literature is very limited regarding the value of  $^{18}\text{F}$ -FDG PET in the follow-up setting. Therefore the role of  $^{18}\text{F}$ -FDG PET in the detection of preclinical relapse is not clear, although it could be discussed that  $^{18}\text{F}$ -FDG PET could perhaps allow patients to be treated with salvage therapy when they present minimal disease instead of an overt relapse. Further studies are needed to assess the efficacy of  $^{18}\text{F}$ -FDG PET in the follow-up setting [1].

### Response prediction before high-dose chemotherapy and autologous stem cell transplantation

Available evidence indicates that  $^{18}\text{F}$ -FDG PET performed after induction chemotherapy and just before autologous stem cell transplantation can predict which patients will achieve long-term remission after the high-dose salvage regimen. Patients with persistent disease on  $^{18}\text{F}$ -FDG PET present short progression-free survival, although the published studies have also reported a higher rate of false-positive results compared with when PET is performed early during front-line therapy. The role of  $^{18}\text{F}$ -FDG PET in this setting is unclear, and available data do not support a change in treatment intent despite a suboptimal metabolic response to induction therapy [1].

### Conclusions

$^{18}\text{F}$ -FDG PET has a key role in the management of patients with lymphoma. Efficacy studies have evidenced the superior performance of

$^{18}\text{F}$ -FDG PET in the initial staging of lymphomas, but there is very little evidence regarding its impact on patient outcomes. Even so,  $^{18}\text{F}$ -FDG PET/CT has become the cornerstone of the staging imaging procedures in state-of-the-art management of FDG-avid lymphomas.

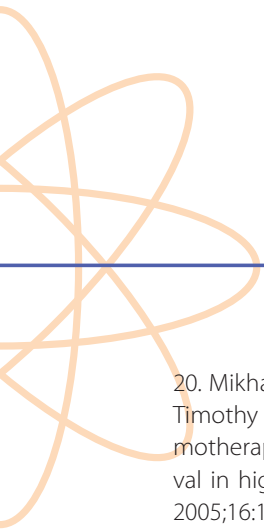
$^{18}\text{F}$ -FDG PET has a main role in monitoring response to therapy and has allowed the introduction of the concept of risk-adapted therapy. The concept of risk-adapted therapy in lymphoma is increasingly accepted as a way to achieve higher cure rates with a lower or equal risk of treatment-related morbidity and mortality. Tailoring and individualising therapy according to the need of the patient is a therapeutic option which could perhaps soon become the standard of care. However, it is still not proven that modification of therapy based on interim PET can improve patient outcomes. Therefore, this issue must be analysed in appropriately designed clinical trials.

Recent meetings have developed recommendations for the assessment of PET for monitoring response to therapy in lymphomas. In 2009 an international meeting in Deauville established uniform criteria for interim PET scan interpretation. In 2007 the International Harmonization Project published recommendations and standard criteria for the evaluation of response after completion of therapy.

## References Chapter 2.6

### References

1. Hutchings M, Barrington SF. PET/CT for therapy response assessment in lymphoma. *J Nucl Med* 2009;50:215–305.
2. Isasi CR, Lu P, Blaufox MD. A metaanalysis of 18F-2-deoxy-2-fluoro-D-glucose positron emission tomography in the staging and restaging of patients with lymphoma. *Cancer* 2005;104:1066–74.
3. Juweid ME, Stroobants S, Hoekstra OS, et al. Use of positron emission tomography for response assessment of lymphoma: consensus of the Imaging Subcommittee of International Harmonization Project in Lymphoma. *J Clin Oncol* 2007;25:571–8.
4. Seam P, Juweid ME, Cheson BD. The role of FDG-PET scans in patients with lymphoma. *Blood* 2007;110:3507–16.
5. Delgado-Bolton RC, Carreras Delgado JL. Évaluation de la réponse au traitement du lymphome avec la TEP 18F-FDG: existe-t-il un consensus dans l'évaluation de la réponse? [18F-FDG PET-CT for therapy response evaluation in lymphoma: Is there a consensus regarding evaluation of response?] *Médecine Nucléaire* 2011;35:29–37.
6. Basu S. Early FDG-PET response—adapted risk stratification and further therapeutic decision-making in lymphoma: will this replace the established prognostic indices and be the standard-of-care in clinical management? *Eur J Nucl Med Mol Imaging* 2009;36:2089–90.
7. The International Non-Hodgkin's Lymphoma Prognostic Factors Project. A predictive model for aggressive non-Hodgkin's lymphoma. *N Engl J Med* 1993;329:987–94.
8. Solal-Celigny P, Roy P, Colombat P, et al. Follicular lymphoma international prognostic index. *Blood* 2004;104:1258–65.
9. Hasenclever D, Diehl V. A prognostic score for advanced Hodgkin's disease: international prognostic factors project on advanced Hodgkin's disease. *N Engl J Med* 1998;339:1506–14.
10. Lister TA, Crowther D, Sutcliffe SB, et al. Report of a committee convened to discuss the evaluation and staging of patients with Hodgkin's disease: Cotswolds meeting. *J Clin Oncol* 1989;7:1630–6.
11. Gallamini A, Hutchings M, Rigacci L, et al. Early interim 2-[18F]fluoro-2-deoxy-D-glucose positron emission tomography is prognostically superior to international prognostic score in advanced-stage Hodgkin's lymphoma: a report from a joint Italian–Danish study. *J Clin Oncol* 2007;25:3746–52.
12. Gobbi PG, Zinzani PL, Brogna C, et al. Comparison of prognostic models in patients with advanced Hodgkin disease: promising results from integration of the best three systems. *Cancer* 2001;91:1467–78.
13. Hasenclever D. The disappearance of prognostic factors in Hodgkin's disease. *Ann Oncol* 2002;13 (Suppl):75–8.
14. Jerusalem G, Beguin Y, Fassotte MF, et al. Persistent tumor 18F-FDG uptake after a few cycles of polychemotherapy is predictive of treatment failure in non-Hodgkin's lymphoma. *Haematologica* 2000;85:613–8.
15. Mikhaeel NG, Timothy AR, O'Doherty MJ, Hain S, Maisey MN. 18-FDG PET as a prognostic indicator in the treatment of aggressive non-Hodgkin's lymphoma: comparison with CT. *Leuk Lymphoma* 2000;39:543–53.
16. Spaepen K, Stroobants S, Dupont P, et al. Early restaging positron emission tomography with 18F-fluorodeoxyglucose predicts outcome in patients with aggressive non-Hodgkin's lymphoma. *Ann Oncol* 2002;13:1356–63.
17. Hoekstra OS, Ossenkuppele GJ, Golding R, et al. Early treatment response in malignant lymphoma, as determined by planar fluorine-18-fluorodeoxyglucose scintigraphy. *J Nucl Med* 1993;34:1706–10.
18. Kostakoglu L, Coleman M, Leonard JP, Kuji I, Zoe H, Goldsmith SJ. PET predicts prognosis after 1 cycle of chemotherapy in aggressive lymphoma and Hodgkin's disease. *J Nucl Med* 2002;43:1018–27.
19. Torizuka T, Nakamura F, Kanno T, et al. Early therapy monitoring with FDG-PET in aggressive non-Hodgkin's lymphoma and Hodgkin's lymphoma. *Eur J Nucl Med Mol Imaging* 2004;31:22–8.



20. Mikhaeel NG, Hutchings M, Fields PA, O'Doherty MJ, Timothy AR. FDG-PET after two to three cycles of chemotherapy predicts progression-free and overall survival in high-grade non-Hodgkin lymphoma. *Ann Oncol* 2005;16:1514–23.
21. Haioun C, Itti E, Rahmouni A, et al. [18F]fluoro-2-deoxy-D-glucose positron emission tomography (FDG-PET) in aggressive lymphoma: an early prognostic tool for predicting patient outcome. *Blood* 2005;106:1376–81.
22. Kostakoglu L, Goldsmith SJ, Leonard JP, et al. FDG-PET after 1 cycle of therapy predicts outcome in diffuse large cell lymphoma and classic Hodgkin disease. *Cancer* 2006;107:2678–87.
23. Hutchings M, Mikhaeel NG, Fields PA, Nunan T, Timothy AR. Prognostic value of interim FDG-PET after two or three cycles of chemotherapy in Hodgkin lymphoma. *Ann Oncol* 2005;16:1160–8.
24. Hutchings M, Loft A, Hansen M, et al. FDG-PET after two cycles of chemotherapy predicts treatment failure and progression-free survival in Hodgkin lymphoma. *Blood* 2006;107:52–9.
25. Zinzani PL, Tani M, Fanti S, et al. Early positron emission tomography (PET) restaging: a predictive final response in Hodgkin's disease patients. *Ann Oncol* 2006;17:1296–300.
26. Gallamini A, Rigacci L, Merli F, et al. The predictive value of positron emission tomography scanning performed after two courses of standard therapy on treatment outcome in advanced stage Hodgkin's disease. *Haematologica* 2006;91:475–81.
27. Terasawa T, Lau J, Bardet S, et al. Fluorine-18-fluoro-deoxyglucose positron emission tomography for interim response assessment of advanced-stage Hodgkin's lymphoma and diffuse large B-cell lymphoma: a systematic review. *J Clin Oncol* 2009;27:1906–14.
28. Meignan M, Gallamini A, Haioun C. Report on the First International Workshop on Interim-PET-Scan in Lymphoma. *Leuk Lymphoma* 2009;50:1257–60.
29. Canellos GP. Residual mass in lymphoma may not be residual disease. *J Clin Oncol* 1988;6:931–933.
30. Skinnider BF, Mak TW. The role of cytokines in classical Hodgkin lymphoma. *Blood* 2002;99:4283–97.
31. Gallamini A, Fiore F, Sorasio R, Meignan M. Interim positron emission tomography scan in Hodgkin lymphoma: definitions, interpretation rules, and clinical validation. *Leuk Lymphoma* 2009;50:1761–4.
32. Kostakoglu L. Early prediction of response to therapy: the clinical implications in Hodgkin's and non-Hodgkin's lymphoma. *Eur J Nucl Med Mol Imaging* 2008;35:1413–20.
33. MacManus MP, Seymour JF, Hicks RJ. Overview of early response assessment in lymphoma with FDG-PET. *Cancer Imaging* 2007;7:10–8.
34. Gallamini A. The prognostic role of positron emission tomography scan in Hodgkin's lymphoma. *Haematologica* 2009;3:144–50.
35. Meignan M, Itti E, Gallamini A, Haioun C. Interim 18F-fluorodeoxyglucose positron emission tomography in diffuse large B-cell lymphoma: qualitative or quantitative interpretation – where do we stand? *Leuk Lymphoma* 2009;50:1753–6.
36. Barrington SF, Qian W, Somer EJ, et al. Concordance between four European centres of PET reporting criteria designed for use in multicentre trials in Hodgkin lymphoma. *Eur J Nucl Med Mol Imaging* 2010;37:1824–33.
37. Spaepen K, Stroobants S, Dupont P, et al. [18F]FDG PET monitoring of tumour response to chemotherapy: does [18F]FDG uptake correlate with the viable tumour cell fraction? *Eur J Nucl Med Mol Imaging* 2003;30:682–8.
38. Barrington SF, Qian W, Somer EJ, et al. Concordance between four European centres of PET reporting criteria designed for use in multicentre trials in Hodgkin lymphoma. *Eur J Nucl Med Mol Imaging* 2009;36 (Suppl.2):S252.
39. Gallamini A, Hutchings M, Avigdor A, Polliack A. Early interim PET scan in Hodgkin lymphoma: where do we stand? *Leuk Lymphoma* 2008;49:659–62.
40. Cheson BD, Pfistner B, Juweid ME, et al. Revised response criteria for malignant lymphoma. *J Clin Oncol* 2007;25:579–86.

# Chapter 2 – Clinical applications of PET/CT in oncology

## 2.7 Digestive tract tumours

Jolanta Kunikowska and Leszek Królicki

### Introduction

In 1924, Warburg showed that cancer cells are characterised by a particular phenotype: glucose in cancer cells is metabolised mainly by an anaerobic pathway. The major tracer used for PET is fluorodeoxyglucose (FDG), an analogue of glucose. Deoxyglucose can be easily labelled with radioactive fluorine, a positron emitter ( $^{18}\text{F}$ ). It is transported by the same mechanisms as are involved in intracellular transport, and it is phosphorylated in the first reaction of the Krebs cycle (as a result of hexokinase). However, the product of phosphorylation (6-deoxyglucose-phosphate), owing to changes in structure, is accumulated in the cell. Thus, the measured radioactivity of  $^{18}\text{F}$ -FDG is an indicator of metabolic pathways for glucose (or rather, an indicator of the mechanisms of glucose transport activity and hexokinase activity). Cellular  $^{18}\text{F}$ -FDG uptake is related to the expression of the glucose transport protein GLUT1. Overexpression of GLUT1 is not specific for malignancy; it is also seen in, for instance, inflammation, brown adipose tissue and muscles. This is the reason why this radiopharmaceutical is not a specific marker. Currently, almost 90% of research techniques are performed using  $^{18}\text{F}$ -FDG PET. Novel radiotracers using other metabolic pathways or knowledge of receptor overexpression have been introduced, including labelled amino acids,  $^{18}\text{F}$ -fluorothymidine ( $^{18}\text{F}$ -FLT),  $^{18}\text{F}$ -choline and somatostatin analogues such as  $^{68}\text{Ga}$ -DOTATATE.

### Oesophageal cancer

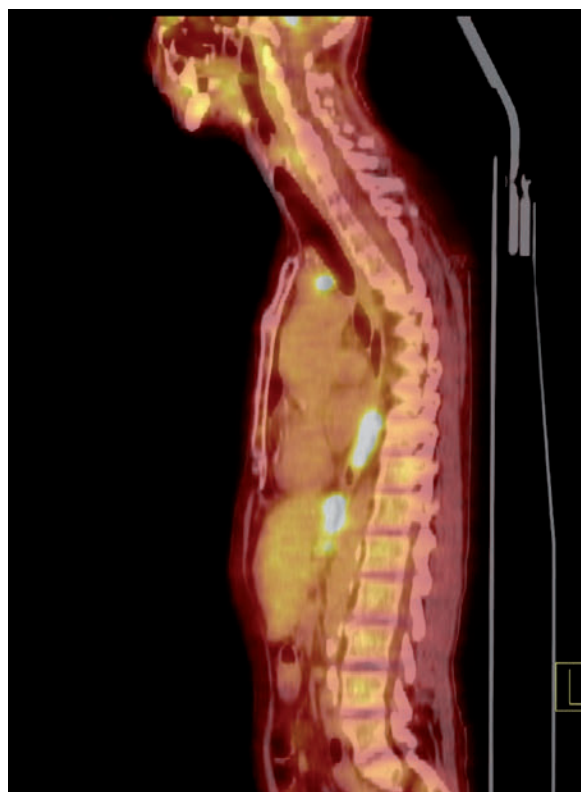
Oesophageal cancer appears in two principal subtypes: squamous cell cancer and adenocarcinoma. Squamous cell cancer arises from the cells that line the upper part of the oesophagus, while adenocarcinoma arises from glandular cells that are present at the junction of the oesophagus and stomach. The typical oesophageal tumour symptoms are dysphagia and pain.

Endoscopy with biopsy plays the main role in the diagnosis of oesophageal cancer. Additional testing is usually performed to estimate the tumour stage. CT of the chest, abdomen and pelvis is used to evaluate whether the cancer has spread to adjacent tissues or distant organs (especially regional lymph nodes). The sensitivity of CT is, however, limited by the fact that its ability to detect masses is generally restricted to those larger than 1 cm.

PET/CT can play a role in primary tumour detection, with reported sensitivities of between 91% and 100% [1–3]. False positive uptake can occur due to inflammation. The reported accuracy of  $^{18}\text{F}$ -FDG PET/CT in the staging of regional lymph nodes is 24–90%, while the accuracy of CT is 40–73% [1–5]. The specificity of  $^{18}\text{F}$ -FDG PET/CT in the detection of regional nodal metastases is between 82% and 100% [1,2,5]. The major limitation of  $^{18}\text{F}$ -FDG PET/CT in the detection of nodal metastases adjacent to the primary tumour is its relatively poor spatial resolution (approximately 6 mm), which reduces the sensitivity.



PET/CT is strictly recommended to improve the accuracy of detection of distant metastases, thereby facilitating treatment planning (Fig. 1).



Courtesy of Nuclear Medicine Department,  
Medical University of Warsaw

Figure 1: Oesophageal cancer with metastasis to paratracheal lymph node

Distant metastatic disease has a significant impact on patient management because these patients are no longer eligible for surgical resection. For the detection of distant metastases,  $^{18}\text{F}$ -FDG PET has a reported sensitivity of 69–100%, a specificity of 84–90% and an accuracy of 84–91%, while the sensitivity is lower [4, 6].  $^{18}\text{F}$ -FDG PET has been reported to reveal more than 20% of unsuspected distant

metastases [6].  $^{18}\text{F}$ -FDG PET/CT scans can also exclude metastatic disease at sites considered abnormal on conventional imaging.

For the diagnosis of regional and distant recurrences  $^{18}\text{F}$ -FDG PET/CT has a sensitivity of 94%, a specificity of 82% and an accuracy of 87% (compared with 81%, 82% and 81%, respectively, for conventional imaging) [7]. Other tracers such as  $^{18}\text{F}$ -FLT could be used, but data are still limited.

### Gastric cancer

Stomach cancer is often asymptomatic or in its early stage causes only non-specific symptoms like loss of appetite and abdominal discomfort. The cancer has often reached an advanced stage by the time that further symptoms occur, including abdominal pain, loss of weight and bleeding resulting in anaemia. If clinical symptoms suggest gastric cancer, endoscopy is the best imaging method. Additionally, CT scanning of the abdomen may reveal gastric cancer, but it is more useful in determining invasion into adjacent tissues or the presence of spread to local lymph nodes.

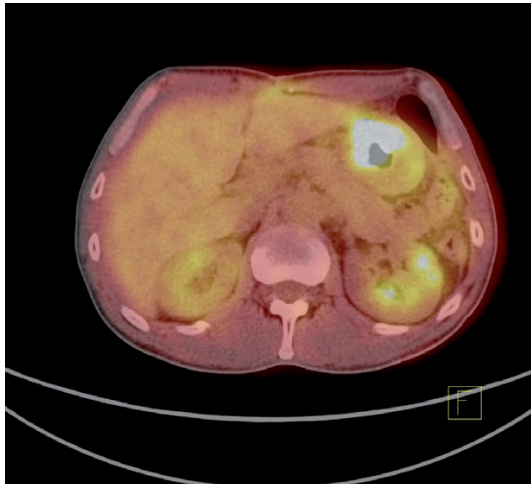
In gastric cancer,  $^{18}\text{F}$ -FDG PET/CT may be used for staging, diagnosis of recurrent disease, prognosis and therapy monitoring. However, different types of cancer are characterised by a variety of types of  $^{18}\text{F}$ -FDG uptake, and the clinical role of  $^{18}\text{F}$ -FDG PET/CT in this setting is currently not well defined.



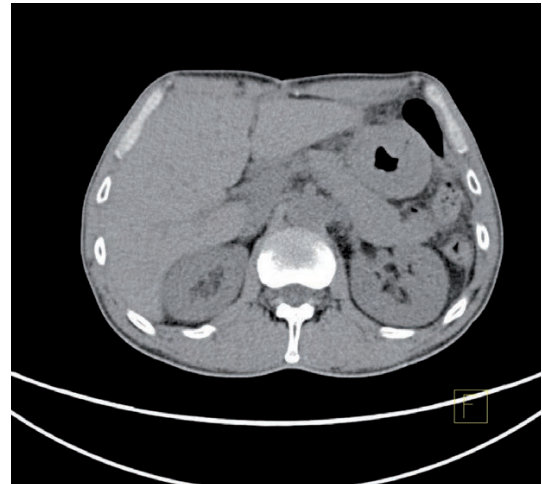
The sensitivity of  $^{18}\text{F}$ -FDG PET for the detection of primary tumours is 58–94% and the specificity, 78–100% [8–12], the rates depend-

ing on tumour size, depth of invasion and cell type (Fig. 2).

Courtesy of Nuclear Medicine Department,  
Medical University of Warsaw



a.



b.

Figure 2a,b: Gastric cancer. There is increased uptake of  $^{18}\text{F}$ -FDG (a) and thickening of the gastric wall (b)

Its reported detection rate for tumours measuring less than 30 mm is 17% while for tumours of more than 30 mm the rate rises to 77% [9]. In the diffuse type of gastric cancer, according to Lauren's classification, the detection rate with  $^{18}\text{F}$ -FDG PET is 41%, which is significantly lower than that for the intestinal type (83%) [13]. Mucinous carcinoma and signet ring cell carcinoma typically show low uptake of  $^{18}\text{F}$ -FDG.

$^{18}\text{F}$ -FDG PET has a lower sensitivity than CT in the detection of regional lymph node metastases, mainly owing to its poor spatial resolution [14], while the reported sensitivity is 17–46% [9,10,15]. Yoshioka et al. reported

that the sensitivity and specificity of  $^{18}\text{F}$ -FDG PET were, respectively, 85% and 74% for liver metastases, 67% and 88% for lung metastases, 24% and 76% for ascites, 30% and 82% for bone metastases and 4% and 100% for pleural metastases [12].

$^{18}\text{F}$ -FDG PET/CT could play a role in the diagnosis of distant lesions, but the low metabolic activity seen in most primary tumours could also be anticipated in metastases.

Because of the limited usefulness of  $^{18}\text{F}$ -FDG in gastric cancer owing to the relatively high number of primary tumours that are not glucose avid, other tracers have been inves-

tingated. Measurement of tumour growth and DNA synthesis in vivo might be superior for imaging malignancies of the gastrointestinal tract. In a study by Herrmann et al. using  $^{18}\text{F}$ -FLT, the sensitivity for the detection of primary tumours was 100% whereas that of  $^{18}\text{F}$ -FDG was 69% [16].

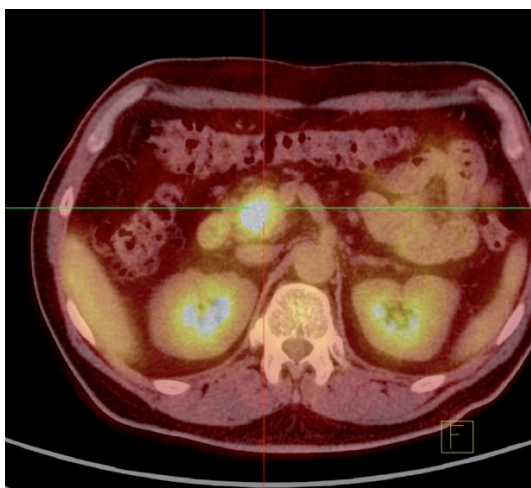
### Pancreatic cancer

Pancreatic cancer has a very poor prognosis, with the survival rate being only 5% at 5 years following diagnosis. About 95% of exocrine pancreatic cancers are adenocarcinomas; the remaining 5% include adenosquamous carcinomas, signet ring cell carcinomas, hepatoid

carcinomas, colloid carcinomas, undifferentiated carcinomas, and undifferentiated carcinomas with osteoclast-like giant cells. Exocrine pancreatic tumours are far more common than pancreatic endocrine tumours, which account for only 1% of all cases. Pancreatic cancer is sometimes called a “silent killer” because in its early form it is symptomless, and later symptoms are usually non-specific and varied. Therefore, pancreatic cancer is often not diagnosed until it is advanced.

The sensitivity of PET in the diagnosis of pancreatic adenocarcinoma is 67–97%, and the specificity, 61–97% [17–27] (Fig. 3).

Courtesy of Nuclear Medicine Department,  
Medical University of Warsaw



a.



b.

Figure 3a,b: Pancreatic cancer. There is increased uptake of  $^{18}\text{F}$ -FDG in the head of the pancreas (a), in the visualised CT lesion (b)

Hypoxia accompanying tumours and inflammatory processes limits the value of examination. As its sensitivity and specificity are similar to those of other methods, PET imaging is now

considered a supplementary examination if the results of other studies do not allow for unequivocal identification.

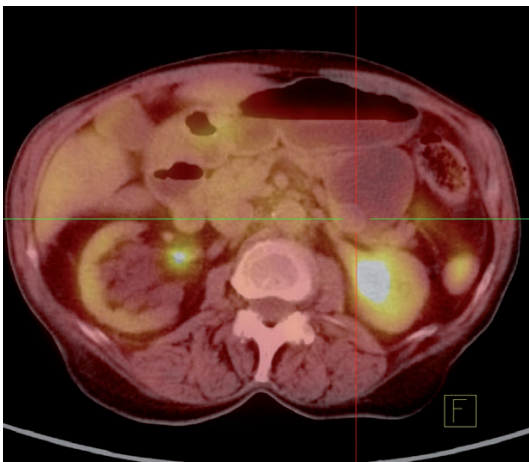
Since neuroendocrine tumours of the pancreas are known to be  $^{18}\text{F}$ -FDG negative, a different tracer should be used when such a lesion is suspected; for example,  $^{68}\text{Ga}$ -DOT-ATATE may be used owing to the expression of somatostatin receptors on such tumours, or  $^{18}\text{F}$ -DOPA may be employed to target catecholamine pathways.

$^{18}\text{F}$ -FDG PET/CT is significantly more sensitive than conventional CT imaging in detecting

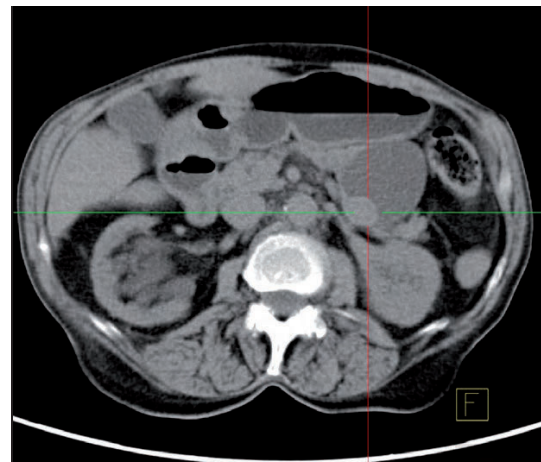
metastatic disease in patients with pancreatic cancer, and its use has been reported to lead to treatment changes in 12–69% of such patients [21,22,25,28].

Another issue is the characterisation of cystic lesions in the pancreas (differentiation between benign and proliferative changes) (Fig. 4).

Courtesy of Nuclear Medicine Department, Medical University of Warsaw



a.



b.

Figure 4a,b: Cystic lesion of the pancreas. Decreased uptake of  $^{18}\text{F}$ -FDG is present in the tail of the pancreas (a), in the visualised CT lesion (b)

In this application, the additional functional assessment is very useful. The sensitivity of PET is higher than that of CT; however, the specificity of the two methods is comparable.

In conclusion,  $^{18}\text{F}$ -FDG PET/CT is a complementary study to assess the nature of focal lesions in the pancreas. Moreover, it is a particularly useful modality in the diagnosis of metastases.



## Hepatocellular carcinoma

Hepatocellular carcinoma (HCC) is a primary malignancy of the liver. Most cases of HCC appear in patients with chronic viral hepatitis infection (hepatitis B or C, ca. 20% of cases) or cirrhosis (ca. 80% of cases, alcoholism being the most common cause). HCC may present with jaundice, bloating from ascites, easy bruising from blood clotting abnormalities, loss of appetite, unintentional weight loss, abdominal pain, especially in the upper right part, nausea, emesis or fatigue. Owing to its cost-effectiveness, ultrasound (US) is usually the first examination. In patients with a high suspicion of HCC but negative US, the best method of diagnosis is a CT scan of the abdomen using an intravenous contrast agent and three-phase scanning.

Owing to the high background of  $^{18}\text{F}$ -FDG uptake by the normal liver and the low metabolic activity of HCC, only 50–55% of HCCs can be visualised by  $^{18}\text{F}$ -FDG PET [29–32]. For this reason,  $^{18}\text{F}$ -FDG PET/CT is not recommended in the diagnosis of HCC.  $^{18}\text{F}$ -FDG PET can, however, play a role in prognostic assessment since poorly differentiated tumours are able to accumulate  $^{18}\text{F}$ -FDG. Overall survival is lower among patients with positive  $^{18}\text{F}$ -FDG PET/CT findings for all indexed lesions than among those with  $^{18}\text{F}$ -FDG negative or partially positive findings [33].  $^{18}\text{F}$ -FDG may show extra-hepatic metastases or residual activity after interventional therapy [34].

Recently,  $^{11}\text{C}$ - or  $^{18}\text{F}$ -choline and  $^{11}\text{C}$ -acetate have been introduced as new tumour-seeking agents for the evaluation of a variety of malignant tumours.  $^{11}\text{C}$ -acetate, a tracer of lipid metabolism, is a promising radiopharmaceutical for the diagnosis of HCC. The reported sensitivity in the detection of low- or intermediate-grade HCC is 87% [35].

The accumulation of  $^{18}\text{F}$ -FDG and  $^{11}\text{C}$ -acetate depends on the biological activity of the cancer. High-grade tumours exhibit uptake of  $^{11}\text{C}$ -acetate, but not of  $^{18}\text{F}$ -FDG, whereas low-grade tumours accumulate  $^{18}\text{F}$ -FDG but show no or low accumulation of  $^{11}\text{C}$ -acetate. Tumours of intermediate grade exhibit variable accumulation of the two tracers. With respect to the use of PET/CT for detection of primary tumours, Park et al. reported an overall sensitivity of 61% with  $^{11}\text{C}$ -acetate and 75% with  $^{18}\text{F}$ -FDG as single tracers, rising to 83% for dual-tracer imaging [33]. Accumulation of  $^{11}\text{C}$ -acetate was significantly greater than that of  $^{18}\text{F}$ -FDG in well-differentiated HCCs, with positive lesions in 71.4% and 50% of cases, respectively [33]. Owing to the short half-life of  $^{11}\text{C}$  ( $t_{1/2}=20$  min),  $^{11}\text{C}$ -acetate is only available in nuclear medicine departments equipped with a cyclotron.

Choline is the main component of phosphatidylcholines, an important constituent of cell membrane phospholipids. Malignant tumours may show high proliferation and increased metabolism of cell membrane

components, which will lead to increased uptake of choline.

As demonstrated in spectroscopic studies, HCC is characterised by significantly higher concentrations of choline than normal liver cells. It seems that  $^{18}\text{F}$ -choline is as good a marker as  $^{11}\text{C}$ -acetate in the diagnosis of HCC, and it is much easier to use. Currently, however, no sufficiently large studies have been performed to identify the role of this marker in clinical practice. Talbot et al. reported a sensitivity of 88% for  $^{18}\text{F}$ -fluorocholine and 68% for  $^{18}\text{F}$ -FDG [36] in a study of 81 patients. Of 11 patients with well-differentiated HCC, six had a positive result with  $^{18}\text{F}$ -fluorocholine alone, whereas  $^{18}\text{F}$ -FDG was never positive alone. In non-malignant lesions,  $^{18}\text{F}$ -fluorocholine appears less specific than  $^{18}\text{F}$ -FDG (62% vs 91%) because of uptake by focal nodular hyperplasia [36].

In conclusion, patients with suspected HCC should be examined using  $^{18}\text{F}$ -choline or  $^{11}\text{C}$ -acetate, while an additional study using  $^{18}\text{F}$ -FDG is recommended when a negative or ambiguous result is obtained. Owing to the resolution of the images, changes with a diameter of less than 7 mm cannot always be assessed.

### Colorectal cancer

Colorectal cancer is the most common cancer of the digestive tract and the third leading cause of cancer-related death in the Western

world [37]. It arises from adenomatous polyps in the colon. These mushroom-shaped growths are usually benign, but some develop into cancer over time. Localised colon cancer is usually diagnosed through colonoscopy.

PET is recommended in the staging and re-staging of colorectal cancer. The sensitivity of  $^{18}\text{F}$ -FDG PET/CT in staging is 96–100%, and higher than that of other diagnostic techniques, but specificity is limited to 58–95% [38,39]. The sensitivity depends on the histological type of the carcinoma: lower sensitivity, 58%, is noted for the detection of mucinous cancer, while for non-mucinous cancer sensitivity reaches 92% [40].

For the detection of lymph node involvement,  $^{18}\text{F}$ -FDG PET/CT has low sensitivity but high specificity. In a study by Abdel-Nabi et al., sensitivity was 29% and specificity was 96% [38]; Mukai et al. [39] found a similar sensitivity (22.2%). Owing to the effectiveness of other diagnostic methods (particularly endoscopy) and limitations in the assessment of micro-metastases in regional lymph nodes, PET is of limited significance in the initial staging of the disease.

PET has a high sensitivity in the evaluation of distant metastases. The reported sensitivity of PET in the detection of liver metastasis is between 85% and 100% (mean 88%) while that of CT is 82%; similarly, the specificity of PET is 96% and that of CT, 84% [38, 41–48].





The likelihood of false-negative findings depends on the size of metastases (for lesions <1 cm, sensitivity is only 25%) [41] and the histological type. Other distant metastases may be recognised with <sup>18</sup>F-FDG PET/CT. Overall, PET has 91% sensitivity and 76–95% specificity for metastatic disease, and is thus superior to CT (61% sensitivity and 91% specificity) [45].

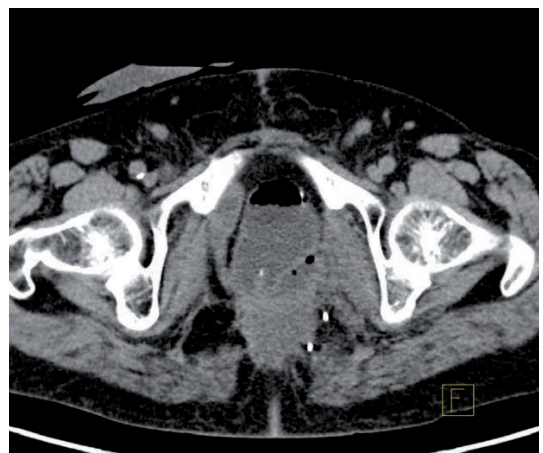
The results of <sup>18</sup>F-FDG PET change the treatment plan in 31% (range 20–58%) of patients [42,45,46].

<sup>18</sup>F-FDG PET/CT is a useful tool in the recognition of local recurrences: differentiation between postoperative or post-radiation therapy scar/fibrotic tissue and vital tumour in rectal cancer is difficult or impossible when using morphology-based imaging modalities (Fig. 5).

Courtesy of Nuclear Medicine Department,  
Medical University of Warsaw



a.



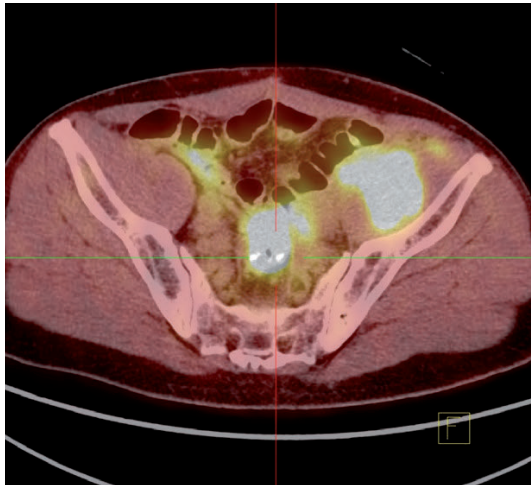
b.

Figure 5a,b: Colon cancer after surgery and radiotherapy. There is absence of increased uptake of <sup>18</sup>F-FDG (a) in the visualised CT lesion (b). Typical scar is present after radiotherapy

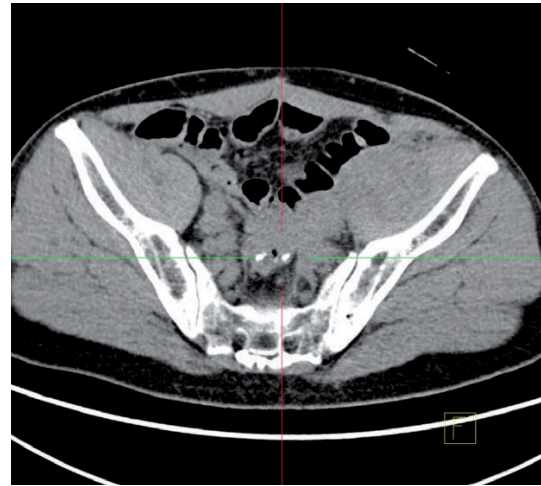
In a meta-analysis, the sensitivity of <sup>18</sup>F-FDG PET/CT in detecting local recurrence was found to be 98% and the specificity, 76% [49]. A review of the literature for evaluation of recurrence shows that the sensitivity of PET is

94% and that of CT, 79% (2,244 patient studies); specificity is 87% for PET and 73% for CT (2,244 patient studies), and PET leads to a change in treatment in 32% (915 patient studies) (Fig. 6).

Courtesy of Nuclear Medicine Department,  
Medical University of Warsaw



a.



b.

Figure 6a,b: Colon cancer after surgery. There is increased uptake of  $^{18}\text{F}$ -FDG at the site of surgery and metastasis to pelvic lymph nodes (a), in the visualised CT lesions (b)

$^{18}\text{F}$ -FDG PET/CT has been found to be successful in localising the site of relapse in patients with elevated CEA, with a reported sensitivity of nearly 100% and a specificity of 71% [50].


### Gallbladder carcinoma and cholangiocarcinoma

Cholangiocarcinoma is a malignant primary tumour of the biliary duct system that may originate in the intrahepatic/extrahepatic bile ducts and terminate at the ampulla of Vater. This is the reason it can involve three regions of the biliary system: intrahepatic, perihilar and distal extrahepatic. The most common localisation is perihilar; such tumours are also called Klatskin tumours. Intrahepatic tumours are the least common. More than 95% of these tumours are ductal adenocarcinomas; many patients present with unresectable or metastatic disease.

Usually, like most malignancies, cholangiocarcinoma cells have high glucose uptake, and the sensitivity of  $^{18}\text{F}$ -FDG PET/CT in carcinoma of the gallbladder and cholangiocarcinoma is quite high, although it seems to be dependent on the tumour subtype. The sensitivity of  $^{18}\text{F}$ -FDG PET/CT for the detection of gallbladder carcinoma is 78%, and in nodular cholangiocarcinoma it rises to 85%; however, sensitivity is only 18% in infiltrating cholangiocarcinoma [51]. Detection of cholangiocarcinoma depends on localisation. The sensitivity and specificity of  $^{18}\text{F}$ -FDG PET/CT for intrahepatic cholangiocarcinoma are 93% and 80%, respectively, and better than the values for CT. For extrahepatic cholangiocarcinoma, the sensitivity of  $^{18}\text{F}$ -FDG PET/CT is 55% and specificity is 33%, which is comparable to CT [52].







$^{18}\text{F}$ -FDG PET/CT can identify distant metastases of peripheral cholangiocarcinoma that are not detected with MRI and CT. The sensitivity of  $^{18}\text{F}$ -FDG PET/CT for detection of distant metastases has been reported to be 94–100%, with 100% specificity; however, the sensitivity for detection of regional lymph nodes metastases was only 12%, with 96% specificity [52,53]. The ability of PET to detect distant metastases may alter the surgical management plan in up to 30% of cases [51,54].

### Gastrointestinal stroma tumours

Gastrointestinal stroma tumours (GISTs) are the most common mesenchymal tumours of the gastrointestinal tract (1–3% of all gastrointestinal malignancies). The tumours most often arise in the stomach (70%), followed by the small intestine (20%), large intestine (5%) and oesophagus (5%). The biology of the tumour is defined by mutations in the c-kit gene. In 1998, Hirota et al. reported a mutation of the c-kit proto-oncogene that activates tyrosine kinase in the absence of a stem cell factor, leading to uncontrolled cell proliferation [55].

$^{18}\text{F}$ -FDG PET has been shown to be highly sensitive in detecting early response to treatment with the tyrosine kinase inhibitor imatinib: 1 month after initiation of therapy, the response was accurately predicted in 95% with PET/CT

in comparison to only 44% with CT [56,57];  $^{18}\text{F}$ -FDG PET/CT could predict response as early as 24 h after the start of treatment, whereas CT only did so several weeks later [56]. This ability to predict the long-term treatment response is useful [57, 58]. An absolute  $\text{SUV}_{\text{max}}$  threshold of 3.4 and a 40% reduction in  $\text{SUV}_{\text{max}}$  have been found to be more predictive of time to treatment failure than the  $\text{SUV}_{\text{max}}$  threshold of 2.5 and 25% reduction reported in a previous trial [59,60].

Unfortunately, access to PET is still limited for patients with GISTs because the glucose uptake before treatment is not sufficient to be detected by  $^{18}\text{F}$ -FDG PET/CT in some lesions.

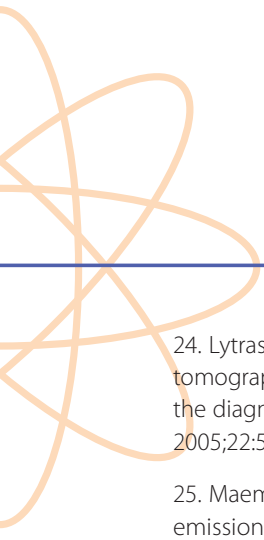
### Conclusion

PET/CT is a very useful technique in the imaging of oncological disease. The commonly available radiotracer  $^{18}\text{F}$ -FDG is well established as a diagnostic tool for a variety of gastrointestinal cancers. It is not a specific radiotracer and further developments of specific radiotracers will improve the modality. Labelled acetate and choline are now well developed tracers in the diagnosis of hepatocellular carcinoma. Novel reconstruction software and new technical ideas such as time of flight with new radiotracers will be the future of oncological imaging.

## References Chapter 2.7

### References

1. Flanagan FL, Dehdashti F, Siegel BA, et al. Staging of esophageal cancer with 18F-fluorodeoxyglucose positron emission tomography. *AJR Am J Roentgenol* 1997;168:417–24.
2. Rankin SC, Taylor H, Cook GJ, Mason R. Computed tomography and positron emission tomography in the pre-operative staging of oesophageal carcinoma. *Clin Radiol* 1998;53:659–65.
3. Kole AC, Plukker JT, Nieweg OE, Vaalburg W. Positron emission tomography for staging of oesophageal and gastroesophageal malignancy. *Br J Cancer* 1998;78:521–27.
4. Skehan SJ, Brown AL, Thompson M, et al. Imaging features of primary and recurrent esophageal cancer at FDG PET. *Radiographics* 2000;20:713–23.
5. Luketich JD, Schauer PR, Meltzer CC, et al. Role of positron emission tomography in staging esophageal cancer. *Ann Thorac Surg* 1997;64:765–9.
6. Lowe VJ, Naunheim KS. Current role of positron emission tomography in thoracic oncology. *Thorax* 1998;53:703–12.
7. Flamen P, Lerut A, Van Cutsem E, et al. The utility of positron emission tomography for the diagnosis and staging of recurrent esophageal cancer. *J Thorac Cardiovasc Surg* 2000;120:1085–92.
8. Yun M, Lim JS, Noh SH et al. Lymph node staging of gastric cancer using (18)F-FDG PET: a comparison study with CT. *J Nucl Med* 2005;46:1582–8.
9. Mukai K, Ishida Y, Okajima K, et al. Usefulness of preoperative FDG-PET for detection of gastric cancer. *Gastric Cancer* 2006;9:192–6.
10. Mochiki E, Kuwano H, Katoh H, et al. Evaluation of 18F-2-deoxy-2-fluoro-d-glucose positron emission tomography for gastric cancer. *World J Surg* 2004;28:247–53.
11. Yeung HW, Macapinlac H, Karpehet M, et al. Accuracy of FDG-PET in gastric cancer. Preliminary experience. *Clin Positron Imaging* 1998;4:213–21.
12. Yoshioka T, Yamaguchi K, Kubota K, et al. Evaluation of 18F-FDG PET in patients with advanced, metastatic, or recurrent gastric cancer. *J Nucl Med* 2003;44:690–9.
13. Stahl A, Ott K, Weber WA, et al. FDG PET imaging of locally advanced gastric carcinomas: correlation with endoscopic and histopathological findings. *Eur J Nucl Med Mol Imaging* 2003;30:288–95.
14. McAteer D, Wallis F, Couper G, et al. Evaluation of 18F-FDG positron emission tomography in gastric and oesophageal carcinoma. *Br J Radiol* 1999;72:525–9.
15. Chen J, Cheong JH, Yun MJ, et al. Improvement in pre-operative staging of gastric adenocarcinoma with positron emission tomography. *Cancer* 2005;103:2383–90.
16. Herrmann K, Ott K, Buck AK, et al. Imaging gastric cancer with PET and the radiotracers 18F-FLT and 18F-FDG: a comparative analysis. *J Nucl Med* 2007;48:1945–50.
17. Giorgi MC, Cunha RM, Soares J Jr, et al. Dual-head gamma camera coincidence imaging in pancreatic cancer. *Rev Esp Med Nucl* 2004;23:90–4.
18. Nishiyama Y, Yamamoto Y, Monden T, et al. Evaluation of delayed additional FDG PET imaging in patients with pancreatic tumour. *Nucl Med Commun* 2005;26:895–901.
19. Rasmussen I, Sorensen J, Langstrom B, et al. Is positron emission tomography using 18F-fluorodeoxyglucose and 11C-acetate valuable in diagnosing indeterminate pancreatic masses? *Scand J Surg* 2004;93:191–7.
20. van Kouwen MC, Jansen JB, van Goor H, et al. FDG PET is able to detect pancreatic carcinoma in chronic pancreatitis. *Eur J Nucl Med Mol Imaging* 2005;32:399–404.
21. Bang S, Chung HW, Park SW, et al. The clinical usefulness of 18-fluorodeoxyglucose positron emission tomography in the differential diagnosis, staging, and response evaluation after concurrent chemoradiotherapy for pancreatic cancer. *J Clin Gastroenterol* 2006;40:923–9.
22. Heinrich S, Goerres GW, Schafer M, et al. Positron emission tomography/computed tomography influences on the management of resectable pancreatic cancer and its cost-effectiveness. *Ann Surg* 2005;242:235–43.
23. Lemke AJ, Niehues SM, Hosten N, et al. Retrospective digital image fusion of multidetector CT and 18F-FDG PET: clinical value in pancreatic lesions -- a prospective study with 104 patients. *J Nucl Med* 2004;45:1279–86.



24. Lytras D, Connor S, Bosonnet L, et al. Positron emission tomography does not add to computed tomography for the diagnosis and staging of pancreatic cancer. *Dig Surg* 2005;22:55–62.
25. Maemura K, Takao S, Shinchi H, et al. Role of positron emission tomography in decisions on treatment strategies for pancreatic cancer. *J Hepatobil Pancreat Surg* 2006;13:435–41.
26. Sperti C, Bissoli S, Pasquali C, et al. 18-Fluorodeoxyglucose positron emission tomography enhances computed tomography diagnosis of malignant intraductal papillary mucinous neoplasms of the pancreas. *Ann Surg* 2007;246:932–9.
27. Casneuf V, Delrue L, Kelles A, et al. Is combined [18F]fluorodeoxyglucose-positron emission tomography/computed tomography superior to positron emission tomography or computed tomography alone for diagnosis, staging and restaging of pancreatic lesions? *Acta Gastro-Ent Belg* 2007;70:331–8.
28. Nishiyama Y, Yamamoto Y, Yokoe K, et al. Contribution of whole body FDG-PET to the detection of distant metastasis in pancreatic cancer. *Ann Nucl Med* 2005;19:491–7.
29. Iwata Y, Shiomi S, Sasaki N, et al. Clinical usefulness of positron emission tomography with fluorine-18-fluorodeoxyglucose in the diagnosis of liver tumors. *Ann Nucl Med* 2000;14:121–6.
30. Khan M, Combs C, Brunt E, et al. Positron emission tomography scanning in the evaluation of hepatocellular carcinoma. *J Hepatol* 2000;32:792–7.
31. Delbeke D, Martin WH, Sadler MP, et al. Evaluation of benign vs malignant hepatic lesions with positron emission tomography. *Arch Surg* 1998;133:510–6.
32. Trojan J, Schroeder O, Raedle J, et al. Fluorine-18 FDG positron emission tomography for imaging of hepatocellular carcinoma. *Am J Gastroenterol* 1999;94:3314–9.
33. Park JW, Kim JH, Kim SK, et al. A prospective evaluation of 18FDG and 11C acetate PET/CT for detection of primary and metastatic hepatocellular carcinoma. *J Nucl Med* 2008;49:1912–21.
34. Torizuka T, Tamaki N, Inokuma T, et al. Value of fluorine-18-FDG-PET to monitor hepatocellular carcinoma after interventional therapy. *J Nucl Med* 1994;35: 1965–9.
35. Ho CL, Yu SC, Yeung DW. 11C-acetate PET imaging in hepatocellular carcinoma and other liver masses. *J Nucl Med* 2003;44:213–21.
36. Talbot J, Fartoux L, Balogova S, et al. Detection of hepatocellular carcinoma with PET/CT: a prospective comparison of <sup>18</sup>F-fluorocholine and <sup>18</sup>F-FDG in patients with cirrhosis or chronic liver disease. *J Nucl Med* 2010;51:1699–706.
37. Cancer. National Cancer Institute. 2009. <http://www.cancer.gov/cancertopics/commoncancers>.
38. Abdel-Nabi H, Doerr RJ, Lamonica DM, et al. Staging of primary colorectal carcinomas with fluorine-18 fluorodeoxyglucose whole-body PET: correlation with histopathologic and CT findings. *Radiology* 1998;206:755–60.
39. Mukai M, Sadahiro S, Yasuda S, et al. Preoperative evaluation by whole-body 18F-fluorodeoxyglucose positron emission tomography in patients with primary colorectal cancer. *Oncol Rep* 2000;7:85–7.
40. Whiteford MH, Whiteford HM, Yee LF, et al. Usefulness of FDG-PET scan in the assessment of suspected metastatic or recurrent adenocarcinoma of the colon and rectum. *Dis Colon Rectum* 2000 ;43 :759–67.
41. Fong Y, Saldinger PF, Akhurst T, et al. Utility of 18F-FDG positron emission tomography scanning on selection of patients for resection of hepatic colorectal metastases. *Am J Surg* 1998;178:282–7.
42. Ogunbiyi OA, Flanagan FL, Dehdashti F, et al. Detection of recurrent and metastatic colorectal cancer: comparison of positron emission tomography and computed tomography. *Ann Surg Oncol* 1997;4:613–20.
43. Rohren EM, Paulson EK, Hagge R, et al. The role of F-18 FDG positron emission tomography in preoperative assessment of the liver in patients being considered for curative resection of hepatic metastases from colorectal cancer. *Clin Nucl Med* 2002;27:550–5.
44. Boykin KN, Zibari GB, Lilien DL, et al. The use of FDG-positron emission tomography for the evaluation of colorectal metastases of the liver. *Am Surg* 1999;65:1183–5.

45. Wiering B, Krabbe PF, Jager GJ, et al. The impact of fluor-18-deoxyglucose-positron emission tomography in the management of colorectal liver metastases. *Cancer* 2005;104:2658–70.
46. Delbeke D, Vitola JV, Sandler MP, et al. Staging recurrent metastatic colorectal carcinoma with PET. *J Nucl Med* 1997;38:1196–201.
47. Lai DT, Fulham M, Stephen MS, et al. The role of whole-body positron emission tomography with [18F]fluorodeoxyglucose in identifying operable colorectal cancer metastases the liver. *Arch Surg* 1996;131:703–7.
48. Beets G, Pennickx F, Schiepers C, et al. Clinical value of whole-body positron emission tomography with [18F]fluorodeoxyglucose in recurrent colorectal cancer. *Br J Surg* 1994;81:1666–70.
49. Huebner RH, Park JE, Shepard JE, et al. Meta-analysis of the literature for whole body FDG-PET detection of recurrent colorectal cancer. *J Nucl Med* 2000;41:1177–89.
50. Tutt ANJ, Plunkett TA, Barrington SF, et al. The role of positron emission tomography in the management of colorectal cancer [review]. *Colorectal Dis* 2004;6:2–9.
51. Anderson CD, Rice MH, Pinson CW, et al. Fluorodeoxyglucose PET imaging in the evaluation of gallbladder carcinoma and cholangiocarcinoma. *J Gastrointest Surg* 2004;8:90–7.
52. Petrowsky H, Wildbrett P, Husarik DB, et al. Impact of integrated positron emission tomography and computed tomography on staging and management of gallbladder cancer and cholangiocarcinoma. *J Hepatol* 2006;45:43–50.
53. Jadvar H, Henderson RW, Conti PS. F-18]fluorodeoxyglucose positron emission tomography and positron emission tomography: computed tomography in recurrent and metastatic cholangiocarcinoma. *J Comput Assist Tomogr* 2007;31:223–8.
54. Fritscher-Ravens A, Bohuslavizki KH, Broering DC, et al. FDG PET in the diagnosis of hilar cholangiocarcinoma. *Nucl Med Commun* 2001;22:1277–85.
55. Hirota S, Isozaki K, Moriyama Y, et al. Gain-of-function mutations of C-kit in human gastrointestinal stromal tumors. *Science* 1998;279:577–80.
56. Stroobants S, Goeminne J, Seegers M, et al. 18FDG-positron emission tomography for the early prediction of response in advanced soft tissue sarcoma treated with imatinib mesylate (Gleevec). *Eur J Cancer* 2003;39:2012–20.
57. Antoch G, Kanja J, Bauer S, et al. Comparison of PET, CT, and dual-modality PET/CT imaging for monitoring of imatinib (STI-571) therapy in patients with gastrointestinal stromal tumors. *J Nucl Med* 2004;45:357–65.
58. Therasse P, Arbuck SG, Eisenhauer EA, et al. New guidelines to evaluate the response to treatment in solid tumors: European Organization for Research and Treatment of Cancer, National Cancer Institute of the United States, National Cancer Institute of Canada. *J Natl Cancer Inst* 2000;92:205–16.
59. Van den Abbeele AD. The lessons of GIST — PET and PET/CT: a new paradigm for imaging. *The Oncologist* 2008;13:8–13.
60. Holdsworth CH, Manola J, Badawi RD, et al. Use of computerized tomography (CT) as an early prognostic indicator of response to imatinib mesylate (IM) in patients with gastrointestinal stromal tumors (GIST). *Proc Am Soc Clin Oncol* 2004;22:197.



# Chapter 2 – Clinical applications of PET/CT in oncology

## 2.8 Neuroendocrine tumour

Valentina Ambrosini and Stefano Fanti

### Introduction

Over past decades, nuclear medicine procedures have acquired a relevant role in the detection of neuroendocrine tumours (NET), and the recent introduction of specific PET tracers for NET studies has further increased nuclear physicians' diagnostic and therapeutic (peptide receptor radionuclide therapy, PRRT) interest in this subset of tumours.

Knowledge of the biological features of NET is of crucial importance in understanding the mechanism of action and the potential clinical relevance of the radiotracers currently used in NET imaging, since nuclear medicine compounds have been designed taking into account the specific characteristics of NET cells.

NET are heterogeneous slow-growing neoplasms that occur in 1-4/100,000 people per year [1,2]. Derived from endocrine cells originating from the neural crest [3], NET are characterised by an endocrine metabolism and a typical pathological pattern. Moreover, NET can produce a large variety of substances, and as they belong to the APUD cell system (amine precursor uptake and decarboxylation), NET can take up, accumulate and decarboxylate amine precursors such as dihydroxyphenylalanine (DOPA) and hydroxytryptophan. The presence of hormone syndromes related to amine/hormone production allows the differentiation of NET in functional (33–50% of cases) and non-functional tumours. Another

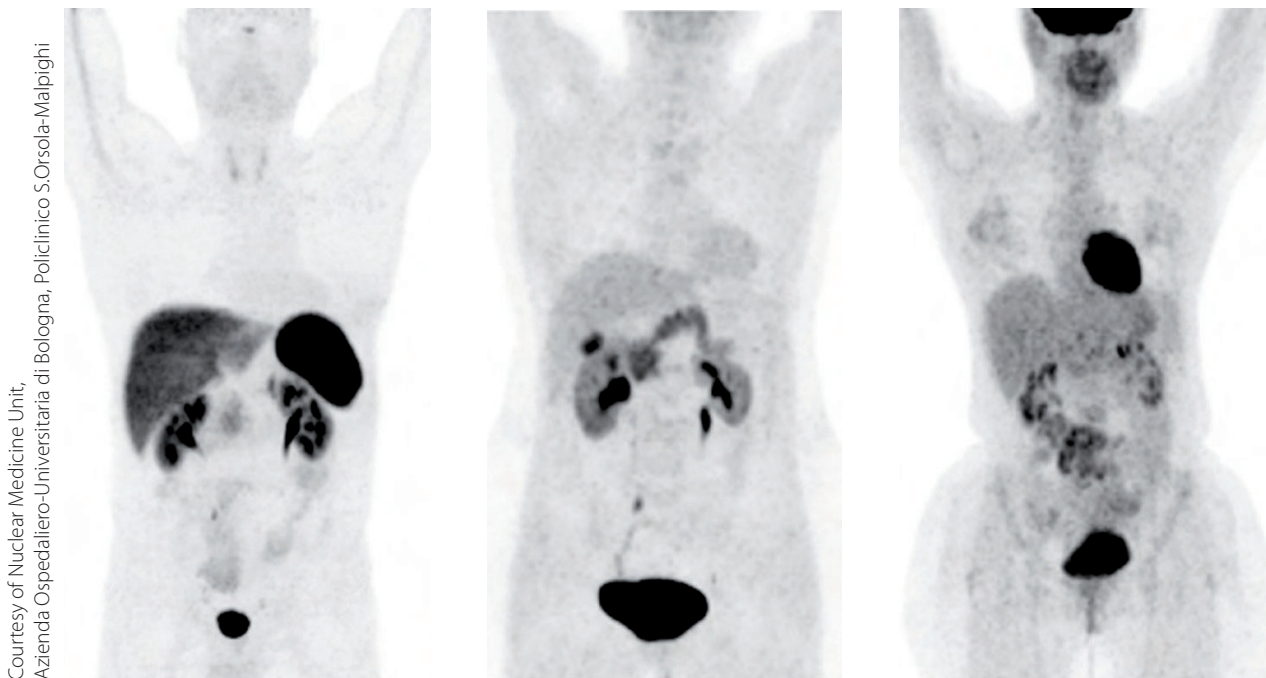
typical feature of NE cells is the expression of several receptors in high quantities [3]; somatostatin receptor (SST) subtypes are the ones mostly represented.

As regards disease staging, a TNM staging system has been proposed for tumours of the fore-gut, mid-gut and hind-gut [4,5] by the European Neuroendocrine Tumour Society (ENETS), taking into account the most recent WHO classifications and the need for a better prognostic assessment of NET. Histological grading identifies three categories based on the Ki-67 levels (G1: Ki-67 <2%; G2: Ki-67 between 3% and 20%; G3: Ki-67 >20%) [4,5]. Although traditionally the TNM staging classification has not been applied to lung NET, the TNM has been demonstrated to be useful in these patients; therefore the International Association for the Study of Lung Cancer (IASLC) recently recommended that the TNM be applied to pulmonary NET [6].

From a diagnostic point of view, NET have represented a diagnostic challenge since they can present as small lesions with variable anatomical localisation. The diagnostic flow-chart of NET has traditionally included ultrasound, computed tomography (CT), magnetic resonance imaging and somatostatin receptor scintigraphy (SRS) [7,8]. SRS has played a major role in the functional assessment of NET, since it has been reported to have a higher accuracy than conventional imaging procedures [9]. However, more recently, the introduction

of specific PET tracers for NET assessment completely revolutionised the diagnostic approach to this subset of tumours owing to the better spatial resolution of PET as compared to scintigraphy.

Currently the most relevant PET tracers for well-differentiated NET tumours (Fig. 1) are  $^{68}\text{Ga}$ -DOTA peptides (DOTATOC, DOTANOC, DOTATATE) and  $^{18}\text{F}$ -DOPA while  $^{18}\text{F}$ -FDG is employed in selected cases with undifferentiated lesions or variable expression of SST [10].



Courtesy of Nuclear Medicine Unit, Azienda Ospedaliero-Universitaria di Bologna, Policlinico S.Orsola-Malpighi

Figure 1a–c: PET coronal images showing the physiological differences in tracer biodistribution. a  $^{68}\text{Ga}$ -DOTA peptides (DOTANOC); b  $^{18}\text{F}$ -DOPA; c  $^{18}\text{F}$ -FDG

### $^{68}\text{Ga}$ -DOTA peptides

$^{68}\text{Ga}$ -DOTA peptides are a group of positron-emitting tracers that specifically bind to SST over-expressed on NET cells. Six different SST have been identified (SST1, SST2A, SST2B, SST3, SST4, SST5) in humans. All tracers belonging to this group have a common structure that includes the active part binding to

SST (TOC, NOC, TATE), a chelant (DOTA) and the beta-emitting isotope ( $^{68}\text{Ga}$ ). These compounds show variable binding affinity to SST receptor subtypes [11]: all can bind to SST2 and SST5, but only DOTANOC also presents good affinity for SST3. There is nevertheless at present no indication that these differences in SST binding affinity are associated with a





direct clinical correlate and/or advantages in clinical employment. The uptake of  $^{68}\text{Ga}$ -DOTA peptides is an indirect measure of the presence of SST on NET cells, which are over-expressed in well-differentiated tumours, and is not dependent on cell metabolism (unlike, for example, uptake of  $^{18}\text{F}$ -DOPA or  $^{18}\text{F}$ -FDG). Therefore,  $^{68}\text{Ga}$ -DOTA peptide PET/CT not only provides data on disease extension but also allows non-invasive assessment of the presence of SST on NET cells; this has direct therapeutic implications, since NET are treated with cold or 'hot' (PRRT) somatostatin analogues. Antunes et al. also reported how the labelling with  $^{68}\text{Ga}$  presents advantages over other employed isotopes [11].

Indications for  $^{68}\text{Ga}$ -DOTA peptide PET/CT include staging, re-staging after therapy, identification of the site of an unknown primary tumour (in patients with proven NET secondary lesions) and selection of cases eligible for therapy with either cold or hot (PRRT) somatostatin analogues.

At present,  $^{68}\text{Ga}$ -DOTA peptides are employed in specialised centres as part of clinical trials for the diagnostic work-up of NET and they have not yet been registered for routine clinical use. The most commonly employed tracers are  $^{68}\text{Ga}$ -DOTATOC,  $^{68}\text{Ga}$ -DOTANOC (Fig. 2) and  $^{68}\text{Ga}$ -DOTATATE.

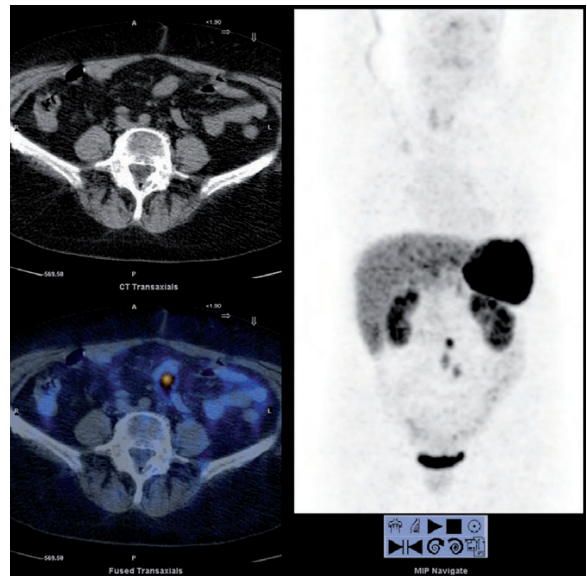


Figure 2:  $^{68}\text{Ga}$ -DOTANOC PET/CT images of a patient with biopsy-proven NET metastatic lesions and unknown primary tumour. PET/CT allowed the detection of a focal area of tracer uptake in the ileum wall suspicious for tumour primary site, one abdominal node, one mesenteric nodule and a focal area at the liver level (first segment).  $^{68}\text{Ga}$ -DOTANOC PET/CT showed that all the detected lesions presented an increased expression of SST

In the past few years, the employment of  $^{68}\text{Ga}$ -DOTA peptides in well-differentiated NET has increased exponentially, and the published results confirm their higher accuracy as compared with CT and SRS for the identification of both the primary tumour and metastatic sites [12,13]. The study with the largest patient population with NET (84 patients) reported a superior sensitivity of DOTATOC (97%) in comparison to CT (61%) and SRS (52%) [13].  $^{68}\text{Ga}$ -



DOTA peptides have been reported [14–17] to accurately visualise well-differentiated NET lesions at lymph nodes, bone and liver and to be of value in detection of the unknown primary tumour. A recent paper [18] also described how the maximum standardised uptake value ( $SUV_{max}$ ) may have prognostic value in patients with NET: in a population of 44 patients, the  $SUV_{max}$  was significantly higher in cases with stable disease or partial response at follow-up. These data reflect the observation that well-differentiated lesions (characterised by higher SST expression and therefore tracer uptake) are associated with a slower growth rate. Recently, an evaluation of the clinical impact of  $^{68}Ga$ -DOTANOC PET/CT on patient management was performed in a population of 90 subjects:  $^{68}Ga$ -DOTANOC PET/CT affected either the staging or the therapy in half the patients, with modification of the therapeutic approach being the most frequently observed impact [19].

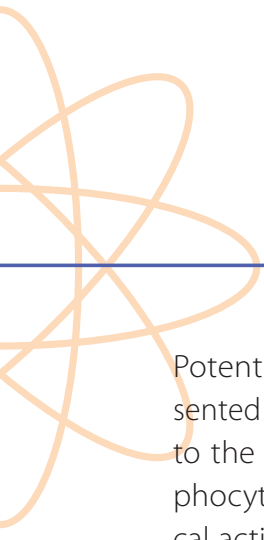
From a technical point of view,  $^{68}Ga$ -DOTA peptides present several advantages. The labelling with  $^{68}Ga$  is relatively easy and inexpensive:  $^{68}Ga$  can be easily eluted from a commercially available  $^{68}Ge/^{68}Ga$  generator and does not require an on-site cyclotron. However it should be noticed that all generators available so far are not GMP compliant. The long half-life of the mother radionuclide  $^{68}Ge$  (270.8 days) makes it possible to use the generator for approximately 9–12 months depending on requirement.  $^{68}Ga$  ( $t_{1/2}=68$  min) is

a positron emitter with 89% positron emission and negligible gamma emission (1077 keV) of 3.2% only. For labelling, the  $^{68}Ga$  eluate is first concentrated and purified using a microchromatography method [20]. Radiolabelling yields of >95% can usually be achieved within 15 min.

$^{68}Ga$ -DOTA peptide PET/CT image acquisition (skull base to the middle of the thigh) should be performed following currently available guidelines [21]. Intravenous injected doses ( $^{68}Ga$ -DOTATOC,  $^{68}Ga$ -DOTANOC,  $^{68}Ga$ -DOTATATE) vary between 100 and 200 MBq. The amount of injected radioactivity strictly depends on the daily production of the generator for each single elution (usually ranging from 300 to 700 MBq) and, of course, the number of patients scanned per day. Uptake time varies between 45 and 90 min after injection; although there is no generally accepted acquisition time in the literature, best results at most centres are achieved acquiring the images at 60 min. Considering the prognostic relevance of  $SUV_{max}$  measures, it is important that uptake time is standardised among patients.

Images should be reconstructed using the iterative reconstruction algorithm implemented in the system and with the system settings.

Sites of physiological SST receptor expression include the liver, spleen, pituitary, thyroid, kidneys, adrenal glands, salivary glands, stomach wall and bowel.



Potential false positive findings are represented by the presence of inflammation (due to the expression of SST on activated lymphocytes), accessory spleen or physiological activity at the adrenal level. The head of the pancreas may show variable  $^{68}\text{Ga}$ -DOTA peptide uptake and represents a potential pitfall in image interpretation since it is not necessarily associated with the presence of active disease. Its clinical significance and the mechanism of uptake in the pancreatic head are still debated.

### $^{18}\text{F}$ -DOPA

Originally employed for the diagnosis of movement disorders and in cases of hypoglycaemia of the newborn,  $^{18}\text{F}$ -DOPA also may be used in patients with NET. In fact, as they belong to the APUD cell system, NET cells are easily visualised on  $^{18}\text{F}$ -DOPA PET/CT images.

$^{18}\text{F}$ -DOPA has been reported to show a higher accuracy for the detection of NET lesions compared with CT and SRS [9]. Currently, there are only two studies comparing  $^{68}\text{Ga}$ -DOTA peptides (DOTANOC and DOTATATE) with  $^{18}\text{F}$ -DOPA in NET: in both papers a higher sensitivity was reported for  $^{68}\text{Ga}$ -DOTA peptides [22,23].

From a technical point of view, the relatively difficult synthesis process [24] and higher costs have limited widespread use of  $^{18}\text{F}$ -DOPA in favour of  $^{68}\text{Ga}$ -DOTA peptides.  $^{18}\text{F}$ -DOPA im-

age acquisition is performed after an uptake time of 60 min from injection (intravenous injection of 370 MBq). Oral premedication with carbidopa has been reported to increase image quality [25]. Regions of physiological  $^{18}\text{F}$ -DOPA uptake include the striatum and pancreas with subsequent elimination through the biliary, digestive and urinary tracts.

### $^{18}\text{F}$ -FDG

It is generally accepted that  $^{18}\text{F}$ -FDG is not the tracer of choice to visualise well-differentiated NET. However, the evidence that NET lesions may present areas with variable tracer uptake within the same lesion supported the hypothesis of employing  $^{18}\text{F}$ -FDG in undifferentiated NET forms. In fact, less differentiated NET lesions present a higher growth rate and therefore higher glucose consumption and can be visualised on  $^{18}\text{F}$ -FDG PET/CT. From a clinical point of view, the presence of  $^{18}\text{F}$ -FDG-avid NET lesions is associated with a worse prognosis and a significantly higher risk of death [26]. In addition,  $^{18}\text{F}$ -FDG may contribute to the identification of NET histological subtypes that are characterised by variable expression of SST (e.g. medullary thyroid carcinoma).

### Conclusions

Several PET tracers are currently available to study NET.  $^{68}\text{Ga}$ -DOTA peptides seem to be the most promising owing to their practical advantages (easy synthesis process, potentially lower costs, patient friendliness) and higher sensitivity for the detection of well-

differentiated lesions. Moreover,  $^{68}\text{Ga}$ -DOTA peptides non-invasively provide information on SST expression on NET cells, with a direct impact on treatment decisions (selection of eligible candidates for either 'hot' or 'cold' somatostatin analogue therapy).  $^{18}\text{F}$ -DOPA also has a relevant role, being more accurate than SRS and CT; the main advantage as compared to  $^{68}\text{Ga}$ -DOTA peptides is related to commercial availability of the tracer while limitations are relatively high cost and incomplete diffusion throughout Europe. The role of  $^{18}\text{F}$ -FDG in NET imaging is mainly limited to undifferentiated NET forms and cases presenting a variable SST expression (e.g. medullary thyroid carcinoma).



## References Chapter 2.8

### References

1. Modlin IM, Kidd M, Latich I, Zikusoka MN, Shapiro MD. Current status of gastrointestinal carcinoids. *Gastroenterology* 2005;128:1717–51.
2. Taal BG, Visser O. Epidemiology of neuroendocrine tumours. *Neuroendocrinology* 2004;80 Suppl 1:3–7.
3. Reubi JC. Neuropeptide receptors in health and disease: the molecular basis for in vivo imaging. *J Nucl Med* 1995;36:1825–35.
4. Rindi G, Klöppel G, Alhman H, Caplin M, Couvelard A, de Herder WW, et al. TNM staging of foregut (neuro)endocrine tumors: a consensus proposal including a grading system. *Virchows Arch* 2006;449:395–401.
5. Rindi G, Klöppel G, Couvelard A, Komminoth P, Körner M, Lopes JM, et al. TNM staging of midgut and hindgut (neuro) endocrine tumors: a consensus proposal including a grading system. *Virchows Arch* 2007;451:757–62.
6. Travis WD; IASLC Staging Committee. Reporting lung cancer pathology specimens. Impact of the anticipated 7th Edition TNM classification based on recommendations of the IASLC Staging Committee. *Histopathology* 2009;54:3–11.
7. Sundin A, Garske U, Orlefors H. Nuclear imaging of neuroendocrine tumours. *Best Pract Res Clin Endocrinol Metab* 2007;21:69–85.
8. Ramage JK, Davies AH, Ardill J, Bax N, Caplin M, Grossman A, et al. UKNETwork for neuroendocrine tumours. Guidelines for the management of gastroenteropancreatic neuroendocrine (including carcinoid) tumours. *Gut* 2005;54 Suppl 4:iv1–16.
9. Krenning EP, Kwekkeboom DJ, Bakker WH, Breeman WA, Kooij PP, Oei HY, et al. Somatostatin receptor scintigraphy with [111In-DTPA-D-Phe1]- and [123I-Tyr3]-octreotide: the Rotterdam experience with more than 1000 patients. *Eur J Nucl Med* 1993;20:716–31.
10. Adams S, Baum R, Rink T, Schumm-Dräger PM, Usadel KH, Hör G. Limited value of fluorine-18 fluorodeoxyglucose positron emission tomography for the imaging of neuroendocrine tumors. *Eur J Nucl Med* 1998;25:79–83.
11. Antunes P, Ginj M, Zhang H, Waser B, Baum RP, Reubi JC, et al. Are radiogallium-labelled DOTA-conjugated somatostatin analogues superior to those labelled with other radiometals? *Eur J Nucl Med Mol Imaging* 2007;34:982–93.
12. Kowalski J, Henze M, Schuhmacher J, Mäcke HR, Hofmann M, Haberkorn U. Evaluation of positron emission tomography imaging using [68Ga]-DOTA-D Phe(1)-Tyr(3)-octreotide in comparison to [111In]-DTPAOC SPECT. First results in patients with neuroendocrine tumors. *Mol Imaging Biol* 2003;5:42–8.
13. Gabriel M, Decristoforo C, Kendler D, Dobrozemsky G, Heute D, Uprimny C, et al. [68Ga]DOTA-Tyr3-octreotide PET in neuroendocrine tumors: comparison with somatostatin receptor scintigraphy and CT. *J Nucl Med* 2007;48:508–18.
14. Putzer D, Gabriel M, Henninger B, Kendler D, Uprimny C, Dobrozemsky G, et al. Bone metastases in patients with neuroendocrine tumor: 68Ga-DOTA-Tyr3-octreotide PET in comparison to CT and bone scintigraphy. *J Nucl Med* 2009;50:1214–21.
15. Ambrosini V, Tomassetti P, Castellucci P, Campana D, Montini G, Rubello D, et al. Comparison between [68Ga]DOTA-NOC and [18F]DOPA PET for the detection of gastroentero-pancreatic and lung neuro-endocrine tumours. *Eur J Nucl Med Mol Imaging* 2008;35:1431–8.
16. Fanti S, Ambrosini V, Tomassetti P, Castellucci P, Montini G, Allegri V, et al. Evaluation of unusual neuroendocrine tumours by means of [68Ga]DOTA-NOC PET. *Biomed Pharmacother* 2008;62:667–71.
17. Prasad V, Ambrosini V, Hommann M, Hoersch D, Fanti S, Baum RP. Detection of unknown primary neuroendocrine tumours (CUP-NET) using (68)Ga-DOTA-NOC receptor PET/CT. *Eur J Nucl Med Mol Imaging* 2010;37:67–77.
18. Campana D, Ambrosini V, Pezzilli R, Fanti S, Labate AM, Santini D, et al. Standardized uptake values of (68)Ga-DOTANOC PET: a promising prognostic tool in neuroendocrine tumors. *J Nucl Med*. 2010;51:353–9.
19. Ambrosini V, Campana D, Bodei L, Nanni C, Castellucci P, Allegri V, et al. 68Ga-DOTANOC PET/CT clinical impact in patients with neuroendocrine tumors. *J Nucl Med* 2010;51:669–73.

20. Zhernosekov KP, Filosofov DV, Baum RP, Aschoff P, Bihl H, Razbash AA, et al. Processing of generator-produced  $^{68}\text{Ga}$  for medical application. *J Nucl Med* 2007;48:1741–8.

21. Virgolini I, Ambrosini V, Bomanji JB, Baum RP, Fanti S, Gabriel M, et al. Procedure guidelines for PET/CT tumour imaging with  $^{68}\text{Ga}$ -DOTA-conjugated peptides:  $^{68}\text{Ga}$ -DOTA-TOC,  $^{68}\text{Ga}$ -DOTA-NOC,  $^{68}\text{Ga}$ -DOTA-TATE. *Eur J Nucl Med Mol Imaging* 2010;37:2004–10.

22. Ambrosini V, Tomassetti P, Castellucci P, Campana D, Montini G, Rubello D, et al. Comparison between [ $^{68}\text{Ga}$ ]DOTA-NOC and [ $^{18}\text{F}$ ]DOPA PET for the detection of gastroentero-pancreatic and lung neuro-endocrine tumours. *Eur J Nucl Med Mol Imaging* 2008;35:1431–8.

23. Haug A, Auernhammer CJ, Wängler B, Tiling R, Schmidt G, Göke B, et al. Intraindividual comparison of [ $^{68}\text{Ga}$ ]DOTA-TATE and [ $^{18}\text{F}$ ]DOPA PET in patients with well-differentiated metastatic neuroendocrine tumours. *Eur J Nucl Med Mol Imaging* 2009;36:765–70.

24. DeVries EFJ, Luurtsema G, Brussermann M, Elsinga PH, Vaalburg W. Fully automated synthesis module for the high yield one-pot preparation of 6- $^{18}\text{F}$ fluoro-L-DOPA. *Appl Radiat Isot* 1999;51:389–94.

25. Orlefors H, Sundin A, Lu L, Oberg K, Langstrom B, Eriksson B, et al. Carbidopa pretreatment improves image interpretation and visualisation of carcinoid tumours with  $^{11}\text{C}$ -5-hydroxytryptophan positron emission tomography. *Eur J Nucl Med Mol Imaging* 2006;33:60–5.

26. Binderup T, Knigge U, Loft A, Federspiel B, Kjaer A.  $^{18}\text{F}$ -fluorodeoxyglucose positron emission tomography predicts survival of patients with neuroendocrine tumors. *Clin Cancer Res* 2010;16:978–85.



# Chapter 3 – Clinical applications of PET/CT in infection and inflammation

François-Xavier Hanin and François Jamar

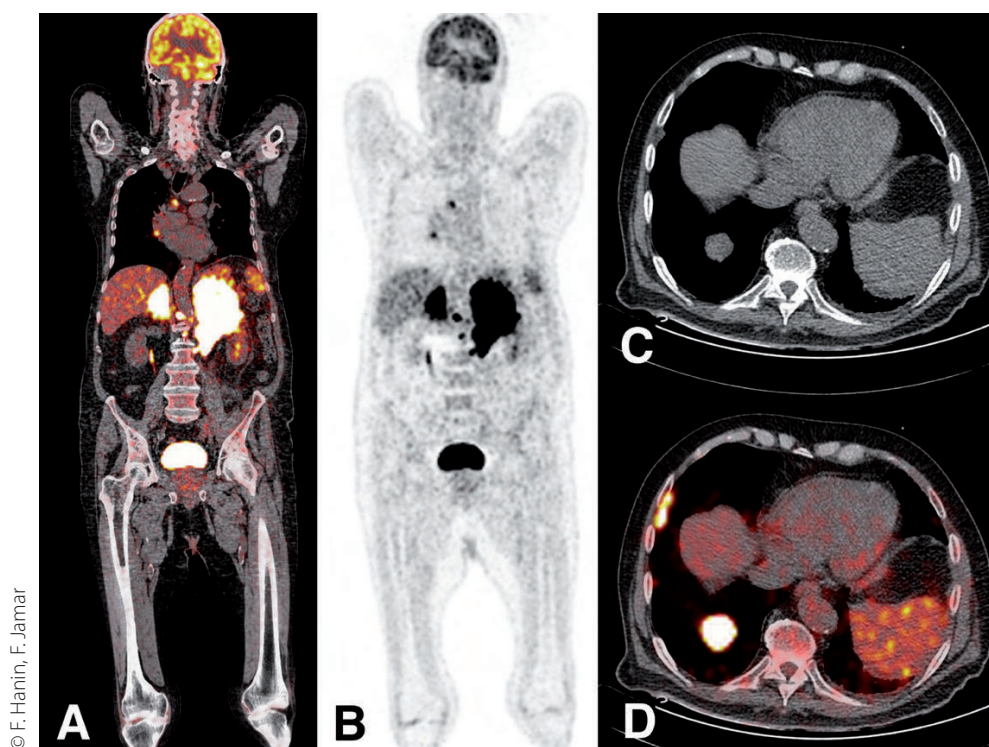
## Introduction

$^{18}\text{F}$ -FDG PET and PET/CT now have proven high diagnostic accuracy in disease assessment in oncology, neurology and cardiology. In the field of inflammation and infection, nuclear medicine offers several techniques allowing detection and follow-up of disease, such as labelled white blood cell (WBC) scintigraphy, anti-granulocyte monoclonal antibody (MoAb) immunoscintigraphy and  $^{18}\text{F}$ -FDG PET and PET/CT. During the past decade, PET/CT has become a commonly accepted tool in the detection of infection and inflammation, but WBC scintigraphy remains a more accurate diagnostic procedure in specific cases. This chapter reviews the main indications for  $^{18}\text{F}$ -FDG PET/CT in

this field and discusses its advantages and pitfalls compared with WBC scintigraphy.

## Fever of unknown origin

Fever or pyrexia of unknown origin (PUO) poses a difficult challenge. True PUO is defined as a temperature of more than  $38.3^{\circ}\text{C}$  that lasts for 3 weeks or more and remains undiagnosed after 3 days in hospital or 1 week of outpatient evaluation (Petersdorf's criteria adapted according to Durack et al. [1]). There are more than 200 possible diagnoses. They are usually classified as infections, non-infectious inflammatory diseases or tumours, each of these accounting for one-third of the final diagnoses (Fig. 1: cancer in PUO).



© F. Hanin, F. Jamar




Figure 1A–D: An 84-year old male was referred for fever of unknown origin. A,B: Coronal fused PET/CT image (A) and coronal PET image (B) showing intense uptake in two large adrenal masses. Note the two foci of uptake in the right hilar and mediastinal lymph nodes. C,D: Axial CT slice (C) showing a pulmonary mass in the right lower lobe with intense  $^{18}\text{F}$ -FDG uptake on the fusion image (D). The conjunction of a lung nodule, pleural and mediastinal foci and large adrenal masses was suggestive of metastatic lung cancer. Pathology, however, finally revealed a large B-cell lymphoma mimicking lung cancer

In up to one-third of cases, however, no diagnosis is finally obtained [2]. Besides classic PUO, other entities were defined by Durack et al.: nosocomial PUO, neutropenic PUO and PUO in patients with the human immunodeficiency virus (HIV) infection. Other conditions associated with immunocompromised patients and postoperative fever constitute further entities that have not been explored separately. Whatever the definition, the ability to reach a final diagnosis varies from one hospital to another, depending, for instance, on whether a diagnostic work-up can be performed in less than 3 days [3]. Because of this wide heterogeneity and differences in inclusion criteria, results from different publications are hard to compare. Considering the long-standing role of labelled WBCs in diagnosing infection, this technique remains preferred by many centres when there is a diagnostic

clue suggestive of infection. This preference is not, however, supported by comparative data since direct comparisons with WBC scanning are not available for  $^{18}\text{F}$ -FDG PET/CT and comparisons with  $^{18}\text{F}$ -FDG PET have been performed in only a limited number of patients [4].

The initial studies dealing with classic PUO were performed using  $^{18}\text{F}$ -FDG PET alone and only a few studies have been reported since  $^{18}\text{F}$ -FDG PET/CT became the standard for imaging. All but one of those studies have been single-centre and about half of them have been retrospective. According to a recent meta-analysis [5], nine studies (including four with CT) met the criteria for classic PUO, covering 388 patients in total. A final diagnosis was reached in 242 of them (62%) and  $^{18}\text{F}$ -FDG PET was positive in 240 (62%) and considered helpful in 177 (46%). The statistical analysis of the five  $^{18}\text{F}$ -FDG PET studies without CT gave a pooled sensitivity of 83% (95% CI: 73–90%) and a pooled specificity of 58% (95% CI: 49–66%). This was improved when CT was added in the last four studies, where the pooled sensitivity and specificity were 98% (95% CI: 94–100%) and 86% (95% CI: 75–93%), respectively. Interestingly, the benefit with CT was mainly related to a reduction in the number of false-positive cases, rather than to the improved anatomical accuracy. Overall,  $^{18}\text{F}$ -FDG PET seemed to perform particularly well in cases of neoplasia (23 cases) and was slightly less sensitive in infection and non-in-



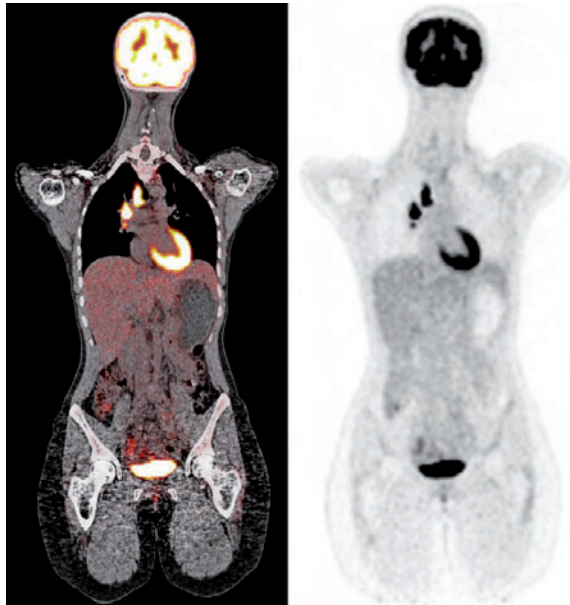
fectious inflammation. In the only prospective multicentre study published so far, with a very rigorous diagnostic algorithm [6], the analysis of 70 patients, among whom a final diagnosis was obtained in 35, showed that  $^{18}\text{F}$ -FDG PET had a positive and negative predictive value of 70% and 92%, respectively, and was useful in 33% of the entire population. Although the number of evaluable studies remains limited, there is now evidence that  $^{18}\text{F}$ -FDG PET/CT should be considered as one of the first diagnostic tools in patients with PUO in whom conventional diagnostic procedures have not been successful. The additional value of combining the  $^{18}\text{F}$ -FDG PET study with a whole-body CT study with iodinated contrast injection remains to be prospectively evaluated, although retrospective data reported by Ferda et al. [7] are convincing. A prospective study of  $^{18}\text{F}$ -FDG PET combined with full CT scan in intensive care unit patients with fever demonstrated a high diagnostic yield as a first-line tool [8].  $^{18}\text{F}$ -FDG PET has also proved useful in the other types of PUO although the number of reported studies remains small.

In AIDS, there are typical and well-defined anatomical steps for the appearance of the

$^{18}\text{F}$ -FDG-avid lymph nodes, starting from the upper part of the torso and then involving the lower part of the body [9]. In addition, the degree of uptake is related to viral load [10] and increases in the event of treatment withdrawal [2]. In addition,  $^{18}\text{F}$ -FDG PET can play a role in the management of infectious and oncological complications of AIDS, such as opportunistic infections, lymphoma, Kaposi's sarcoma and AIDS-related dementia complex [9]. Nevertheless, the involvement of lymph nodes related to viral load may complicate the interpretation of results [11].

#### **Granulomatous and inflammatory diseases**

$^{18}\text{F}$ -FDG PET has not been widely used in tuberculosis. An interesting pilot study [12] developed a two-time point method to better characterise tuberculosis involvement in HIV-negative patients.  $^{18}\text{F}$ -FDG PET has emerged as a very valuable tool in evaluating sarcoidosis. The whole-body tomographic capability together with the physical properties of  $^{18}\text{F}$ -FDG PET as compared with  $^{67}\text{Ga}$  scintigraphy explains why the latter has been almost completely abandoned in this indication [13]. The method is well suited for whole-body evaluation of this very polymorphic disorder (Fig. 2).



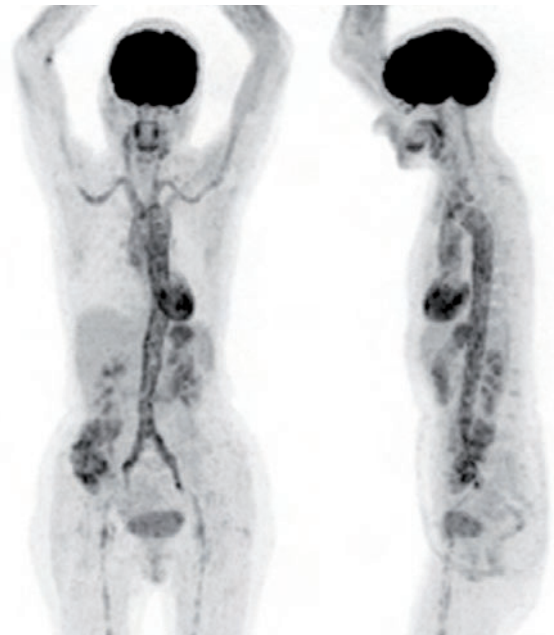
© F. Hanin, F. Jamar

Figure 2: Coronal fused PET/CT (left) and coronal PET (right) images of a 34-year-old woman previously treated for melanoma. Foci of intense uptake in right hilar and mediastinal lymph nodes led to a biopsy, which revealed granulomatous inflammatory lymph nodes without malignant cells. Patient was therefore treated for sarcoidosis and the repeat  $^{18}\text{F}$ -FDG PET 6 months later showed complete disappearance of abnormal uptake

It is useful for the diagnosis and staging of the disease in a number of anatomical sites [14, 15] and seems to be helpful for assessing the effect of treatment, especially with steroids [16]. It is, however, essential to keep in mind that  $^{18}\text{F}$ -FDG PET/CT will not substitute for pathology: in particular, the differential diagnosis with lymphoma is impossible with certitude and, therefore, a pathological diagnosis will be required in patients with enlarged lymph

nodes.  $^{18}\text{F}$ -FDG PET/CT may, however, help to identify the right and easiest node to biopsy.

In inflammatory or immune conditions,  $^{18}\text{F}$ -FDG PET has proved very promising for assessing large-vessel arteritides, such as giant-cell arteritis (GCA) and Takayasu's disease. This has been observed in dedicated studies and in subsets of studies in patients with PUO [17]. The sensitivity (77–92%) and specificity (89–100%) were found to be high in untreated patients with GCA and inflammatory markers (Fig. 3).



© F. Hanin, F. Jamar

Figure 3: Coronal (left) and sagittal (right) maximal intensity projections of a 59-year-old woman referred for weight loss, increased C-reactive protein and asthenia.  $^{18}\text{F}$ -FDG PET/CT reveals intense uptake in the aorta and large vessels, consistent with vasculitis

A lower sensitivity was observed under immunosuppressive therapy (e.g. steroids). Further, in GCA,  $^{18}\text{F}$ -FDG PET has proved useful in assessing the extent of the disease and in monitoring the disease activity during therapy. It must be noted that  $^{18}\text{F}$ -FDG PET does not allow reliable diagnosis and monitoring of localised temporal arteritis [18]. Use of  $^{18}\text{F}$ -FDG PET in other inflammatory or immune conditions (e.g. rheumatoid arthritis) has been shown to be feasible but its relevance remains to be determined in daily practice.

#### Infection of vascular grafts

The incidence of vascular graft infection ranges from 0.25% to 6%, but such infection is

often severe and leads to high mortality rates (20–70%) if diagnosis is delayed [19]. These infections can appear up to several years after placement and are challenging to diagnose early as the clinical course is often indolent.

The role of WBC scintigraphy has been well documented in the past, showing a sensitivity from 53% to 100% and a specificity from 50% to 100% [20].  $^{18}\text{F}$ -FDG PET/CT is a promising tool for the early detection of vascular graft infection by virtue of the combination of morphological and functional imaging information (Fig. 4).

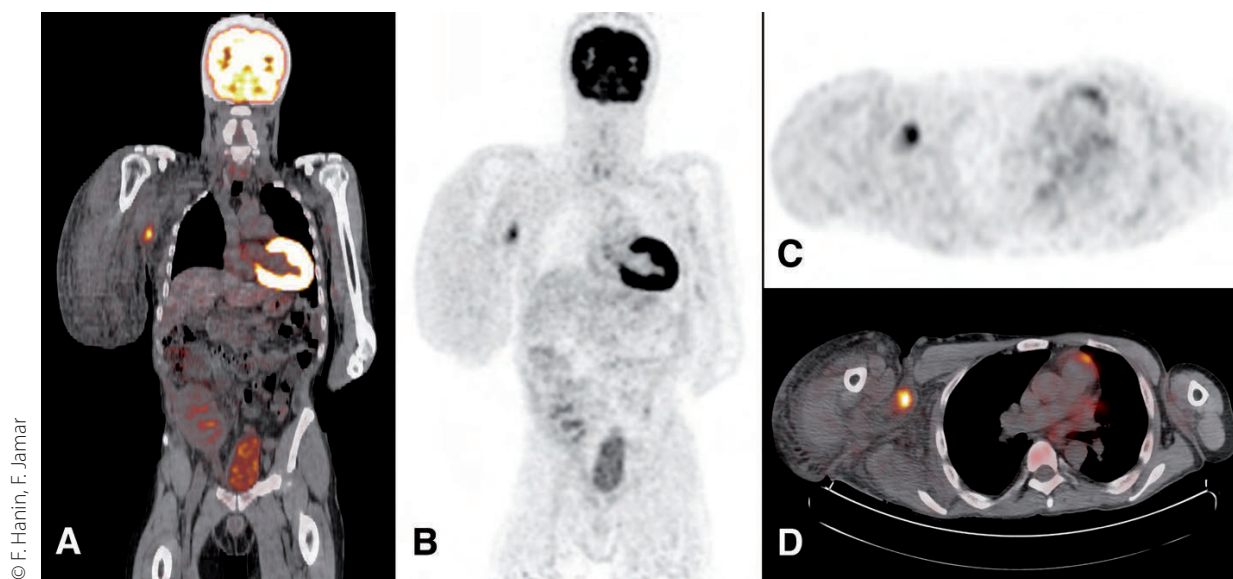


Figure 4A–D: A 37-year-old patient with multiple vascular grafts showing multiple septic foci due to *Staphylococcus aureus*. Coronal (A, B) and axial (C, D) views of PET/CT fused images (A, D) and PET images (B, C) revealing focal uptake of FDG in the right axillary region, allowing accurate localization on the infected vascular graft

In addition, fusion of CT and PET imaging is mandatory for the correct localisation of intense uptake. In the past,  $^{18}\text{F}$ -FDG PET alone was described to show better accuracy than CT alone [20, 21], while more recent data suggest that  $^{18}\text{F}$ -FDG PET/CT furthermore results in an increase in specificity and therefore global accuracy [22]. False positive uptake has been described in the early postoperative period, especially as haematomas, bleeding or thrombosis.

The physiological uptake of FDG on non-infected graft has led some authors to define criteria, qualitative as well as quantitative, to better discriminate infected graft from inflammatory reaction to a foreign body. An interesting study by Spacek et al. in 96 patients showed that an irregular FDG uptake and an irregular graft boundary on CT were predictive criteria for infection [23]. In contrast, diffuse, smooth and regular uptake along the graft is likely to be related to inflammation around a foreign body, without infection. To date, semi-quantitative analysis of focal uptake has not shown any predictive value for vascular graft infection.

#### Bone infection

WBC scintigraphy (using either  $^{99\text{m}}\text{Tc}$ -HMPAO or  $^{111}\text{In}$ -oxine [or tropolonate] labelling) has shown very good results for detecting osteomyelitis (overall accuracy of about 90% [20]), but is of very limited value in two specific indications.

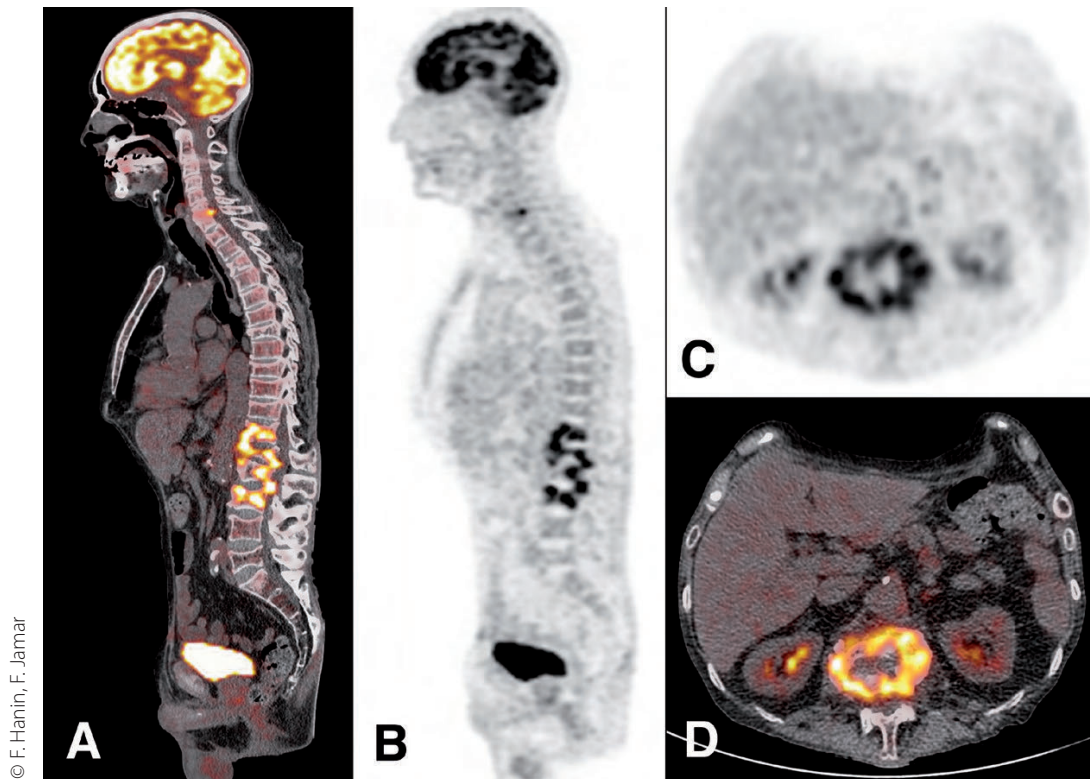
First, it is poorly effective for detecting spinal infection, i.e. vertebral osteomyelitis and/or spondylodiscitis. Typically, these pathological cases appear as photopenic lesions on WBC scintigraphy owing to the absence of leucocyte migration related to an encapsulation of the infection and vascular spasm. The specificity of this photopenic picture is very low since tumours, Paget's disease and infarction can show a similar pattern [24].

Secondly, WBC scintigraphy shows poor accuracy, ranging from 53% to 76%, for chronic osteomyelitis or suspected recurrence [25]. In addition, it shows better sensitivity and specificity for peripheral chronic osteomyelitis imaging (84% and 80%, respectively) than for chronic osteomyelitis of the axial skeleton (21% and 60%, respectively) [26].

As a result of these limitations of WBC scintigraphy,  $^{18}\text{F}$ -FDG PET/CT has attracted increasing interest in this field: for acute osteomyelitis, a sensitivity of 98% and a specificity ranging from 75% to 99% have been reported [25], while a sensitivity of 94–100% and a specificity of 87–100% have been reported in vertebral osteomyelitis and spondylodiscitis (Fig. 5).







© F. Hanin, F. Jamar

Figure 5: A 75-year-old patient hospitalized for back pain. Sagittal (A, B) and axial (C, D) views of fused PET/CT images (A, D) and PET images (B, C) revealed intense uptake in the lumbar spine, further diagnosed as *Mycobacterium avium*-related spondylodiscitis

This excellent accuracy of  $^{18}\text{F}$ -FDG PET/CT has a major impact on the clinical management of patients with (disco)-vertebral infection, by modifying treatment in 52% of cases [27]. A meta-analysis of chronic osteomyelitis imaging in 2005 by Termaat et al. reported aggregated sensitivity and specificity of 96% and 91%, respectively [26].

In conclusion, WBC scanning remains the first-line technique for acute infection in peripheral osteomyelitis, whereas  $^{18}\text{F}$ -FDG PET/CT has become the preferred tool, along with MRI,

in spondylodiscitis; in this latter indication,  $^{18}\text{F}$ -FDG PET/CT is especially to be preferred when MRI is hampered by the presence of metallic hardware.

#### Orthopaedic prosthesis infection: hip and knee

Hip and knee joint replacement is subject to two major potential complications: infection and loosening. In both cases, the clinical symptoms will usually be limited to a painful arthroplasty.  $^{18}\text{F}$ -FDG PET is a relatively new tool in these indications, while three-phase



bone scan (TPBS) and WBC scintigraphy are the traditional investigative tools.

### ***Patterns and quantitative approach***

The uptake of FDG around a prosthesis can be related to the exudation of immunologically active cells, especially leucocytes and macrophages [25], but in the case of aseptic loosening, metallic and polyethylene particles are likely to induce FDG uptake as well [28]. Therefore, criteria allowing differentiation have been sought in order to better discriminate causes of painful arthroplasty.

A first approach is to analyse the characteristics of FDG uptake around a hip prosthesis, evaluating the correlation with the clinical outcome. A scale of uptake was proposed by Reinartz et al. [29]: this scale relies essentially on the distribution of the uptake, with several patterns from no uptake (pattern 1) to FDG uptake in the periprosthetic soft tissues (pattern 5).

The second approach is the use of semi-quantitative analysis of the standardised uptake value (SUV) as a potential discriminative factor. In a group of 92 arthroplasties [29], no significant difference in SUV between aseptic loosening and infection was noted, although there was a significant difference between pathological and non-pathological arthroplasties.

The overall sensitivity, specificity and accuracy of  $^{18}\text{F}$ -FDG PET in patients with a painful arthroplasty using qualitative criteria are 85%,

90% and 89%, respectively, for the hip, and 98%, 75% and 83%, respectively, for the knee [29]. Nevertheless, more precise criteria are mandatory to improve discrimination of mechanical loosening from infection [30].

### ***Role of $^{18}\text{F}$ -FDG PET vs WBC and TPBS***

WBC scintigraphy remains the best technique for detection of prosthetic infection [20], showing higher accuracies (91% for hip and 84% for knee) than either PET (89% for hip and 83% for knee) or TPBS (80% for hip and 81% for knee). Although from combined series  $^{18}\text{F}$ -FDG PET shows a higher accuracy in the diagnosis of prosthetic infection and loosening, it remains a costly and less accessible technique compared with TPBS. Its main advantages are a better accuracy than TPBS and the fact that it is a one-day procedure (while WBC scintigraphy is more complex and time-consuming). Therefore,  $^{18}\text{F}$ -FDG PET can be considered highly effective for diagnosing complications of joint replacement, while more specific criteria need to be developed to better discriminate infection from loosening.  $^{18}\text{F}$ -FDG PET should not be used routinely in patients with painful arthroplasty as a first-line tool. To date, there are no data in the literature on the added value of  $^{18}\text{F}$ -FDG PET/CT compared with  $^{18}\text{F}$ -FDG PET alone.

Finally, it is undisputed that in departments where there is little or no access to WBC scanning or PET, TPBS remains a valuable alternative as it is accessible, fast and non-invasive.



### The infected diabetic foot

The clinical diagnosis, treatment and follow-up of diabetic foot infections remain difficult owing to several diabetic-specific causes: neuropathy, higher susceptibility to infection and vascular impairments. It is often of major clinical importance to distinguish between soft tissue and underlying bone infection since osteomyelitis leads to a more aggressive treatment.

As stated in the section on bone infection, WBC scintigraphy is the modality of choice in the diagnosis of peripheral infection, the reported sensitivity and specificity being between 72% and 100% and between 67% and 98%, respectively [31]. The main disadvantage of WBC scintigraphy is the poor image quality, which leads to difficulties in assessing whether abnormal activity in the foot is attributable to a bone or a soft tissue infection. More recently it has been possible to address this pitfall by using SPECT/CT detection cameras, which allow better localisation of the hotspots.

Recent data, however, show high sensitivity, specificity and accuracy (81%, 93% and 90%, respectively) for  $^{18}\text{F}$ -FDG PET. Interestingly, comparisons of these values with MRI in the same indication have shown MRI to have a better sensitivity (91%) but a lower specificity (78%) and a global accuracy of 81%. The authors concluded that the two techniques are complementary in that the high sensitivity of MRI is combined with the higher specificity of  $^{18}\text{F}$ -FDG PET, which better discriminates between osteomyelitis and

uninfected Charcot's neuroarthropathy [32].  $^{18}\text{F}$ -FDG PET/CT was initially found in a series of 14 patients to be accurate in assessing diabetic foot [33]. Others, however, have found  $^{18}\text{F}$ -FDG PET/CT to have a much lower accuracy. In addition, whether combination with CT has an added diagnostic value remains undetermined. Therefore,  $^{18}\text{F}$ -FDG PET/CT cannot fully replace WBC scintigraphy, especially when the latter is acquired in combination with bone marrow scintigraphy and using SPECT-CT [20].

### Technical issues<sup>1</sup>

- The clinical indication must be reviewed with care in order to choose the correct imaging protocol
- Whole-body imaging is necessary in PUO but a limited field of view can be sufficient in answering specific questions
- Diabetic patients must be checked carefully for hyperglycaemia, although this may not preclude valid imaging in infection and inflammation as it does in tumours [34]
- Careful examination of possible pregnancy is always necessary
- Interpretation should consider potential false positive results related to physiological or tumour uptake

---

<sup>1</sup> Detailed EANM guidelines will be available shortly and will cover all issues

## References Chapter 3

### References

1. Durack DT, Street AC. Fever of unknown origin--reexamined and redefined. *Curr Clin Top Infect Dis* 1991;11:35-51.
2. Bleeker-Rovers CP, Vos FJ, Corstens FH, Oyen WJ. Imaging of infectious diseases using [18F] fluorodeoxyglucose PET. *Q J Nucl Med Mol Imaging* 2008;52:17-29.
3. Habibzadeh F, Yadollahie M. Time for a change in the definition of fever of unknown origin. *J Infect* 2008;57:166-7.
4. Kjaer A, Lebech AM, Eigtved A, Hojgaard L. Fever of unknown origin: prospective comparison of diagnostic value of 18F-FDG PET and 111In-granulocyte scintigraphy. *Eur J Nucl Med Mol Imaging* 2004;31:622-6.
5. Dong MJ, Zhao K, Liu ZF, Wang GL, Yang SY, Zhou GJ. A meta-analysis of the value of fluorodeoxyglucose-PET/PET-CT in the evaluation of fever of unknown origin. *Eur J Radiol* 2010; Dec 3. [Epub ahead of print]
6. Bleeker-Rovers CP, Vos FJ, Mudde AH, et al. A prospective multi-centre study of the value of FDG-PET as part of a structured diagnostic protocol in patients with fever of unknown origin. *Eur J Nucl Med Mol Imaging* 2007;34:694-703.
7. Ferda J, Ferdova E, Zahlava J, Matejovic M, Kreuzberg B. Fever of unknown origin: a value of (18)F-FDG-PET/CT with integrated full diagnostic isotropic CT imaging. *Eur J Radiol* 2010;73:518-25.
8. Simons KS, Pickkers P, Bleeker-Rovers CP, Oyen WJ, van der Hoeven JG. F-18-fluorodeoxyglucose positron emission tomography combined with CT in critically ill patients with suspected infection. *Intensive Care Med* 2010;36:504-11.
9. Sathekge M, Goethals I, Maes A, van de Wiele C. Positron emission tomography in patients suffering from HIV-1 infection. *Eur J Nucl Med Mol Imaging* 2009;36:1176-84.
10. Sathekge M, Maes A, Kgomo M, Van de Wiele C. Fluorodeoxyglucose uptake by lymph nodes of HIV patients is inversely related to CD4 cell count. *Nucl Med Commun* 2010;31:137-40.
11. Sathekge M, Maes A, Kgomo M, Pottel H, Stolz A, Van De Wiele C. FDG uptake in lymph-nodes of HIV+ and tuberculosis patients: implications for cancer staging. *Q J Nucl Med Mol Imaging* 2010;54:698-703.
12. Sathekge M, Maes A, Kgomo M, Stoltz A, Pottel H, Van de Wiele C. Impact of FDG PET on the management of TBC treatment. A pilot study. *Nuklearmedizin* 2010;49:35-40.
13. Nishiyama Y, Yamamoto Y, Fukunaga K, et al. Comparative evaluation of 18F-FDG PET and 67Ga scintigraphy in patients with sarcoidosis. *J Nucl Med* 2006;47:1571-6.
14. Bonardel G, Carmoi T, Gontier E, et al. [Use of positron emission tomography in sarcoidosis]. *Rev Med Interne* 2011;32:101-8.
15. Teirstein AS, Machac J, Almeida O, Lu P, Padilla ML, Iannuzzi MC. Results of 188 whole-body fluorodeoxyglucose positron emission tomography scans in 137 patients with sarcoidosis. *Chest* 2007;132:1949-53.
16. Keijsers RG, Verzijlbergen FJ, Oyen WJ, et al. 18F-FDG PET, genotype-corrected ACE and sIL-2R in newly diagnosed sarcoidosis. *Eur J Nucl Med Mol Imaging* 2009;36:1131-7.
17. Meller J, Sahlmann CO, Gurocak O, Liersch T, Meller B. FDG-PET in patients with fever of unknown origin: the importance of diagnosing large vessel vasculitis. *Q J Nucl Med Mol Imaging* 2009;53:51-63.
18. Bossert M, Prati C, Balblanc JC, Lohse A, Wendling D. Aortic involvement in giant cell arteritis: Current data. *Joint Bone Spine* 2010; doi:10.1016/j.jbspin.2010.09.013
19. Ben-Haim S, Gacinovic S, Israel O. Cardiovascular infection and inflammation. *Semin Nucl Med* 2009;39:103-14.
20. Glaudemans AW, Signore A. FDG-PET/CT in infections: the imaging method of choice? *Eur J Nucl Med Mol Imaging* 2010;37:1986-91.
21. Bruggink JL, Glaudemans AW, Saleem BR, et al. Accuracy of FDG-PET-CT in the diagnostic work-up of vascular prosthetic graft infection. *Eur J Vasc Endovasc Surg* 2010;40:348-54.
22. Keidar Z, Nitecki S. FDG-PET for the detection of infected vascular grafts. *Q J Nucl Med Mol Imaging* 2009;53:35-40.
23. Spacek M, Belohlavek O, Votrubova J, Sebesta P, Stadler P. Diagnostics of "non-acute" vascular prosthesis infection using 18F-FDG PET/CT: our experience with 96 prostheses. *Eur J Nucl Med Mol Imaging* 2009;36:850-8.



24. Palestro CJ, Love C, Bhargava KK. Labeled leukocyte imaging: current status and future directions. *Q J Nucl Med Mol Imaging* 2009;53:105-23.
25. Stumpe KD, Strobel K. 18F FDG-PET imaging in musculoskeletal infection. *Q J Nucl Med Mol Imaging* 2006;50:131-42.
26. Termaat MF, Raijmakers PG, Scholten HJ, Bakker FC, Patka P, Haarman HJ. The accuracy of diagnostic imaging for the assessment of chronic osteomyelitis: a systematic review and meta-analysis. *J Bone Joint Surg Am* 2005;87:2464-71.
27. Ito K, Kubota K, Morooka M, Hasuo K, Kuroki H, Mimori A. Clinical impact of (18)F-FDG PET/CT on the management and diagnosis of infectious spondylitis. *Nucl Med Commun* 2010;31:691-8.
28. DeHeer DH, Engels JA, DeVries AS, Knapp RH, Beebe JD. In situ complement activation by polyethylene wear debris. *J Biomed Mater Res* 2001;54:12-9.
29. Reinartz P, Mumme T, Hermanns B, et al. Radionuclide imaging of the painful hip arthroplasty: positron-emission tomography versus triple-phase bone scanning. *J Bone Joint Surg Br* 2005;87:465-70.
30. van der Bruggen W, Bleeker-Rovers CP, Boerman OC, Gotthardt M, Oyen WJ. PET and SPECT in osteomyelitis and prosthetic bone and joint infections: a systematic review. *Semin Nucl Med* 2010;40:3-15.
31. Palestro CJ, Love C. Nuclear medicine and diabetic foot infections. *Semin Nucl Med* 2009;39:52-65.
32. Nawaz A, Torigian DA, Siegelman ES, Basu S, Chryssikos T, Alavi A. Diagnostic performance of FDG-PET, MRI, and plain film radiography (PFR) for the diagnosis of osteomyelitis in the diabetic foot. *Mol Imaging Biol* 2010;12:335-42.
33. Keidar Z, Militianu D, Melamed E, Bar-Shalom R, Israel O. The diabetic foot: initial experience with 18F-FDG PET/CT. *J Nucl Med* 2005;46:444-9.
34. Rabkin Z, Israel O, Keidar Z. Do hyperglycemia and diabetes affect the incidence of false-negative 18F-FDG PET/CT studies in patients evaluated for infection or inflammation and cancer? A comparative analysis. *J Nucl Med* 2010;51:1015-20.

# Chapter 4 – Clinical applications of PET/CT in cardiology

Oliver Gaemperli and Philipp A. Kaufmann

## Introduction


Since its first days, positron emission tomography (PET) has generated great interest as a non-invasive tool for the assessment of a variety of cardiac conditions, and has greatly enhanced our pathophysiological understanding of cardiac pathologies. Owing to its unique physical and technical characteristics, PET allows quantification of radiotracer uptake using dynamic acquisition and mathematical models of tracer kinetics. Its superior spatial and temporal resolution compared with conventional nuclear methods and its high detection sensitivity for radiotracers have enabled groundbreaking insights into the regulation of myocardial blood flow (MBF) and metabolic health and substrate utilisation of the heart [1,2].

Despite its undisputed advantages, the widespread dissemination of cardiac PET into clinical diagnostic services has been constrained by the complexity of production and short physical half-lives of positron-emitting radioligands, the need for an on-site cyclotron facility for the production of most perfusion tracers, the limited availability of PET scanners and the high costs of PET imaging. Nonetheless, PET is gaining acceptance among cardiac diagnostic services. The development and introduction of novel radiolabelled compounds [e.g. rubidium-82 ( $^{82}\text{Rb}$ ) or  $^{18}\text{F}$ -BMS-747158-02], the accrued number of studies document-

ing their clinical use and the ever-increasing availability of PET devices fostered mainly by the great clinical success of PET in oncology have contributed to a steady growth in cardiac imaging. Recent developments include the combination of PET with high-end CT scanners into hybrid scanners which have opened new avenues for future applications and will further promote the use of PET in cardiovascular research and clinical practice [3].

## Technical characteristics of PET relevant to cardiac applications

A number of technical and instrumental properties allow PET to operate as a highly accurate technique for cardiac applications. Owing to coincidence detection and PET detector design, the spatial resolution of current PET devices reaches 4 mm in the centre of the field of view compared with 10–12 mm for single-photon emission computed tomography (SPECT) [4], although in cardiac imaging resolution is slightly degraded by respiratory and cardiac wall movement. The recent introduction of new detector materials (e.g. lutetium oxyorthosilicate) and detector systems with reduced detection dead-time [4] as well as the increasing use of three- rather than two-dimensional acquisitions [5] are important milestones in the development of PET technology and have significantly contributed to its increasing use in nuclear cardiology.



Despite the high photon energy released in annihilation of positrons (511 keV), PET is more susceptible to photon attenuation than SPECT, where photon energies from cardiac applications range from 70 to 140 keV. The reason for this seemingly paradoxical finding is that coincidence registration with PET requires two photons to travel through the whole cross-section of the body before a true event is recorded. This, however, makes photon attenuation more predictable than with SPECT as it is uniform along a given line of response between two detectors and independent from the origin of the positron along this line, and therefore allows for more robust means of attenuation correction. As a result, attenuation correction is now widely accepted for PET imaging and has proven indispensable for quantitative assessment of MBF [6].

Image acquisition in list mode is widely available for clinical use and allows images to be reconstructed retrospectively using different rebinning criteria [7]. This provides high flexibility in data processing and reconstruction of images using ECG or respiratory gating, dynamic image frames for quantitative analysis or simple addition of information into static images. In cardiology, this approach facilitates quantification of blood flow by applying dynamic tracer kinetic modelling or assessment of left ventricular volumes and function from ECG-gated data.

### Radiopharmaceuticals

The most common radiolabelled compounds available for cardiac PET applications are summarised in Table 1. All compounds listed in Table 1 [except for  $^{18}\text{F}$ -fluorodeoxyglucose ( $^{18}\text{F}$ -FDG)] are used for myocardial perfusion imaging, the most common imaging application in nuclear cardiology. Radiokinetic properties of these compounds should ideally fulfil a number of requirements to allow their use as perfusion tracers (Table 2). It should be noted, however, that all currently available perfusion tracers listed in Table 1 have relative advantages and disadvantages: none of them meets all the radiokinetic requirements to be considered the ideal perfusion tracer. However, promising new agents are currently in preclinical and clinical evaluation with the potential to overcome most of the limitations of currently used compounds [8].

### *Radiolabelled water*

Radiolabelled water ( $^{15}\text{O}$ - $\text{H}_2\text{O}$ ) is a metabolically inert and freely diffusible perfusion tracer. Consequently, myocardial uptake is linearly related to MBF, which allows accurate quantification of MBF over a wide range of values (Fig. 1) [9–11].



Adapted from Knutti J et al. J Nucl Cardiol 2009; 16:497

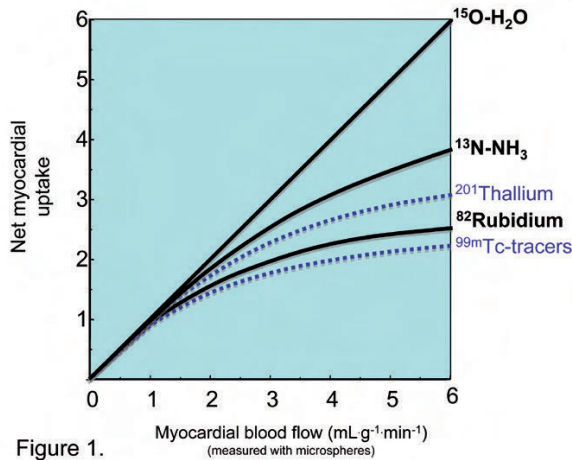


Figure 1.

Figure 1: Simplified schematic representation of myocardial radiotracer extraction as a function of MBF.  $^{15}\text{O-H}_2\text{O}$  is the only perfusion tracer with a quasi-linear relationship between myocardial extraction and MBF; with all other tracers (PET and SPECT perfusion tracers) extraction tends to plateau at increasing flow values.  $^{99\text{m}}\text{Tc}$  tracers include  $^{99\text{m}}\text{Tc}$ -methoxyisobutylisonitrile and  $^{99\text{m}}\text{Tc}$ -tetrofosmin

However, since  $^{15}\text{O-H}_2\text{O}$  is not retained in the myocardial compartment, it rapidly reaches an equilibrium between myocardium and blood pool, without enough myocardial contrast to generate appropriate perfusion images. Quantitative assessment of MBF with  $^{15}\text{O-H}_2\text{O}$  requires complex mathematical processing to separate myocardial and blood pool and create anatomical images of the left ventricle [12,13]. These radiokinetic features have limited the ample use of  $^{15}\text{O-H}_2\text{O}$  for clinical PET perfusion imaging. For research purposes, however, this tracer

has gained wide popularity. Indeed, the very short physical half-life of the  $^{15}\text{O}$  isotope (2 min) allows repeated measurements of MBF under different biological conditions in the same session.

### $^{13}\text{N}$ -ammonia

$^{13}\text{N}$ -ammonia ( $^{13}\text{N-NH}_3$ ) has a high first-pass extraction rate of up to 80% and myocardial uptake is linear over a wide range of MBF, except at very high flow rates (Fig. 1) [14–16]. Upon internalisation,  $^{13}\text{N-NH}_3$  is trapped in the intracellular compartment after metabolic conversion into  $^{13}\text{N}$ -glutamine, thereby creating high myocardial contrast images (Fig. 2).

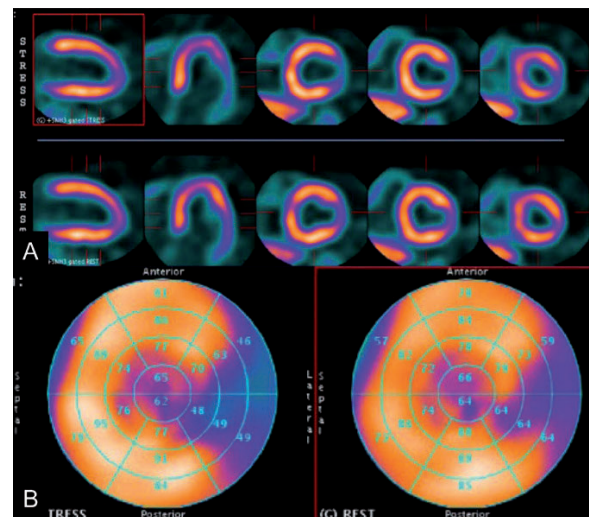


Figure 2.

Figure 2A,B: Example of stress/rest  $^{13}\text{N-NH}_3$  perfusion PET in a 77-year-old patient with an occluded left circumflex artery. The paired stress and rest perfusion images (A) and perfusion polar maps (B) show a partially reversible perfusion defect of the laterobasal wall

Courtesy of the Cardiac Imaging Department, University Hospital Zurich, Switzerland

However, its short physical half-life (10 min) necessitates an on-site cyclotron for production and immediate administration. A similar performance of  $^{13}\text{N-NH}_3$  compared to  $^{15}\text{O-H}_2\text{O}$  for quantification of MBF has been demonstrated in experimental animal [10] and human studies [17]. Its ability to provide high-quality perfusion images and allow quantification of regional MBF simultaneously have advanced this compound as an excellent clinical perfusion tracer in diagnostic centres with an on-site cyclotron (Fig. 3), and an increasing number of publications underline its clinical diagnostic and prognostic value [18–21].

Figure 3A: Dynamic image acquisition (18 frames) after  $^{13}\text{N-NH}_3$  injection showing sequential activity in the right ventricle [dark blue regions of interest (ROI), frames 2–4], the left ventricle (light blue ROI, frame 5) and the left ventricular myocardium (white ROI, frames 6–18).

Figure 3B: Time-activity curves for the right ventricular cavity (RV), left ventricular cavity (LV) and left ventricular myocardial segments (myocardium).

Figure 3C: Segmental values for coronary flow reserve (CFR) calculated from time-activity curves after pixelwise tracer kinetic modelling using a three-compartment model [14]

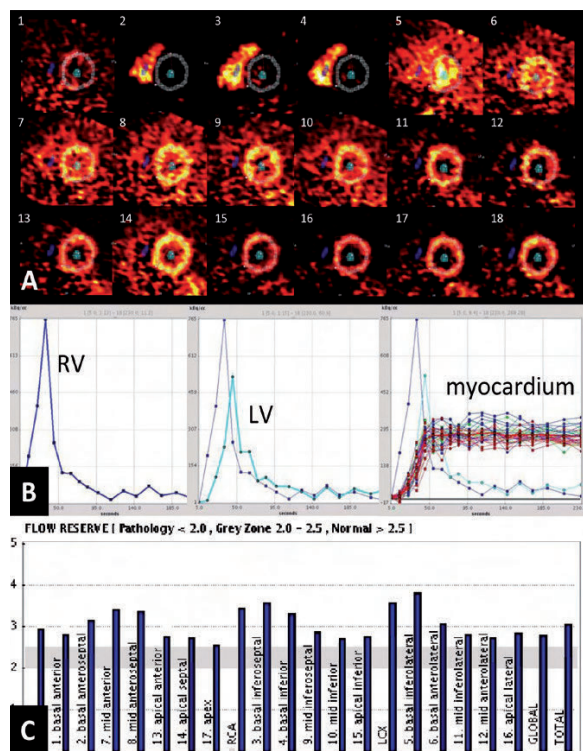


Figure 3.

### Rubidium-82

Rubidium-82 ( $^{82}\text{Rb}$ ) is an analogue of the potassium cation and undergoes cellular uptake by the Na/K-ATPase. Unlike other positron-emitting compounds which are cyclotron products,  $^{82}\text{Rb}$  can be obtained from an  $^{82}\text{Sr}/^{82}\text{Rb}$  generator by decay from  $^{82}\text{Sr}$  attached to an elution column (Table 1). Downsides of  $^{82}\text{Rb}$  are the lower myocardial extraction rate, its non-linear relationship between myocardial tracer uptake and MBF (Fig. 1) [22,23], the high positron energy (which allows the positron to travel for several millimetres before annihilation and thereby lowers spatial resolution) (Table 1) and the ultrashort half-life (leading to detector oversaturation at the beginning of the acquisition (particularly with three-dimensional acquisition protocols) and low count statistics and increased image

noise in later phases. Additionally, cellular uptake by the energy-dependent Na/K-ATPase raises concerns regarding a potential interaction with the prevailing metabolic state of the cell [24].

#### ***<sup>18</sup>F-labelled BMS-747158-02***

The relative drawbacks of available perfusion tracers have fuelled an intensive search for novel compounds with the ability to overcome the previously mentioned limitations. The <sup>18</sup>F-labelled compound BMS-747158-02 has recently been introduced as a promising novel compound for myocardial perfusion imaging with PET, and the results of current phase II and III clinical trials are eagerly awaited. The available evidence in animal studies indicates excellent biodistribution data, prolonged stable myocardial retention and high tracer extraction at variable flow rates [8]. Additionally, the long half-life allows perfusion PET imaging in centres without an on-site cyclotron.

#### ***<sup>18</sup>F-fluorodeoxyglucose***

<sup>18</sup>F-fluorodeoxyglucose (<sup>18</sup>F-FDG) – a biological analogue of glucose – is taken up by myocytes via facilitated diffusion through the glucose transporter (GLUT-1 and GLUT-4). Upon internalisation, FDG is phosphorylated to FDG-6-phosphate, but unlike glucose does not undergo further metabolism, and therefore remains trapped in the myocyte. <sup>18</sup>F-FDG is clinically used to assess myocardial glucose uptake, a surrogate for myocardial viability.

Chronically underperfused but viable myocardium characteristically shows an increased <sup>18</sup>F-FDG uptake due to upregulation of anaerobic pathways (i.e. anaerobic glycolysis), whereas in scars <sup>18</sup>F-FDG uptake is markedly reduced or absent [25,26]. The rather long physical half-life of the <sup>18</sup>F-nuclide (110 min) allows for <sup>18</sup>F-FDG to be centrally produced in a cyclotron facility and distributed to PET centres nearby on a day-to-day basis, obviating the need for an on-site cyclotron (Table 1).


### **Patient preparation and protocols**

#### ***Myocardial perfusion PET***

A full myocardial perfusion study entails acquiring images during a state of cardiac stress to elicit changes in myocardial perfusion that may not be present at rest. Several stress techniques are available for myocardial perfusion imaging. Dynamic exercise (bicycle or treadmill) is generally the stress procedure of choice in patients who are able to exercise. Inherently with PET, however, physical exercise procedures are difficult to perform owing to the temporal proximity of tracer injection and image acquisition. Therefore, pharmacological stress (with vasodilators or dobutamine) is preferred.

All stress procedures should be supervised by a qualified physician with knowledge of the available pharmacological stress agents and expertise in advanced life support techniques. Patient preparation includes obtaining the patient's in-





formed consent and a clinical history covering indications for the test, symptoms, risk factors, medication and prior diagnostic or therapeutic procedures, and finally establishing a secure intravenous line for radiopharmaceutical and stress agent administration. Haemodynamic non-invasive monitoring (including 12-lead ECG, heart rate and blood pressure) should be ensured at all times during the stress procedure. Cardiac medications which could interfere with the pharmacological stress agent should be withheld if possible. This includes nitrates for at least 24 h and beta-blockers and calcium antagonists for at least 48 h prior to the test. If a vasodilator stress agent (adenosine or dipyridamole) is used, caffeine-containing beverages (coffee, tea, cola etc.), foods (chocolate) and medications (some pain relievers, stimulants and weight-control drugs) and methylxanthine-containing medications should be discontinued for at least 12 h prior to the test [2].

***Vasodilator stress (adenosine, dipyridamole).***

Adenosine mediates direct coronary arteriolar dilation via the A<sub>2A</sub> adenosine receptor subtype, and in normal coronary arteries results in a three- to fourfold increase in MBF. Dipyridamole is an indirect coronary arteriolar dilator that increases the tissue levels of adenosine through inhibition of the intracellular reuptake and deamination of adenosine. Adenosine and dipyridamole tend to induce a modest increase in heart rate and a modest decrease in both systolic and diastolic blood pressure. Thus, both agents induce

direct near-maximal myocardial hyperaemia, thereby uncoupling MBF from myocardial oxygen demand. In myocardium served by a stenosed coronary artery, hyperaemic blood flow is reduced; this leads to heterogeneities of perfusion during vasodilation, demarcating ischaemic myocardial territories.

Dosing schemes for adenosine and dipyridamole are given in Table 3. Owing to its non-selective action on all adenosine receptor subtypes (A<sub>1</sub>, A<sub>2A</sub>, A<sub>2B</sub>, A<sub>3</sub>), vasodilators are contraindicated in patients with a history of bronchospasm, high-grade AV block of sick sinus syndrome, symptomatic aortic stenosis and hypertrophic obstructive cardiomyopathy, and hypotension [27]. Newer agents with selectivity for A<sub>2A</sub> receptors are under clinical and preclinical evaluation. Regadenoson is the first selective A<sub>2A</sub> agonist approved for use in the United States and has recently received market approval in Europe in 2010. It has a longer half-life than adenosine, can be administered as a bolus and is better tolerated than adenosine or dipyridamole [28].

***Dobutamine.***

Dobutamine is a sympathomimetic agent with high affinity to adrenergic  $\beta$ <sub>1</sub>-receptors. It causes secondary coronary vasodilation through increased myocardial oxygen demand as a result of  $\beta$ <sub>1</sub>-mediated dose-dependent increases in heart rate, blood pressure and myocardial contractility. Dobutamine is administered as a continuous intravenous infusion that

is titrated according to the patient's heart rate up to a maximal dose of 40 µg/kg/min (Table 3). Absolute contraindications to dobutamine include acute coronary syndrome, uncontrolled severe hypertension, acute aortic dissection and uncontrolled cardiac arrhythmias.

### ***<sup>18</sup>F-FDG PET***

Myocardial viability studies are often performed in conjunction with perfusion studies (PET or SPECT). The patient should be fasted overnight (at least 6h) and alcohol and smoking should be discontinued for at least 12 h. Whether the <sup>18</sup>F-FDG study is performed before or after the perfusion study depends on the logistics of each individual centre; however, if the perfusion study is performed with <sup>13</sup>N-NH<sub>3</sub> PET, the longer half-life of <sup>18</sup>F-FDG precludes performing the <sup>18</sup>F-FDG study first.

Under fasting conditions, myocardial glucose (and hence <sup>18</sup>F-FDG) uptake is low and non-uniform throughout the left ventricle, as the prevailing myocardial energy source is free fatty acids [29]. It is therefore necessary to standardise the metabolic environment in order to obtain interpretable images of myocardial glucose utilisation. The three most common methods to standardise myocardial glucose uptake are discussed below:

#### ***Oral glucose loading.***

This is the most common method of standardising myocardial glucose uptake on account of its relative convenience. Oral ad-

ministration of 25–100 g of glucose results in the release of pancreatic insulin, which in turn increases myocardial glucose and <sup>18</sup>F-FDG uptake. However, this method may lead to sub-optimal image quality in up to 25% of patients [30]. Increased myocardial insulin resistance and therefore abnormal glucose handling is common in type 2 diabetic subjects and patients with congestive heart failure, which may account for reduced image quality in a substantial proportion of patients. A modified oral glucose loading protocol with additional intravenous administration of short-acting insulin may improve image quality, particularly in patients with insulin resistance [1].

#### ***Hyperinsulinaemic euglycaemic clamp.***

The hyperinsulinaemic euglycaemic clamp consists of an intravenous protocol for simultaneous administration of glucose and insulin in order to achieve a steady state of myocardial glucose uptake. This protocol accounts for the insulin resistance of each individual subject and yields images of high quality even in type 2 diabetic patients. However, the clamp protocol is cumbersome and time-consuming and therefore reserved for a number of institutes with particular expertise. For a more detailed description of this protocol, the interested reader is referred to other sources [1,30,31].

#### ***Nicotinic acid derivatives.***

Nicotinic acid derivatives such as acipimox are inhibitors of peripheral lipolysis, thereby reducing circulating free fatty acid concen-





trations. They are effective for improving  $^{18}\text{F}$ -FDG image quality, and when combined with subcutaneous or intravenous injection of small amounts of short-acting insulin, good image quality can also be obtained in diabetic subjects. With the exception of flushing, no side-effects of acipimox have been observed.

### Image processing and reconstruction

In cardiovascular applications, PET needs to achieve a high level of quantitative accuracy to allow for a reliable comparison of myocardial perfusion in all left ventricular territories. This is accomplished by applying a number of corrections to the raw image datasets (Fig. 4):

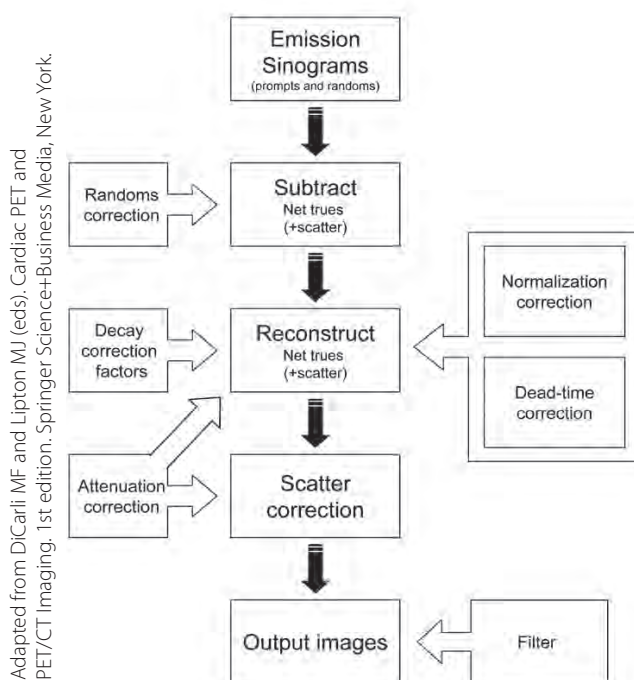


Figure 4: Flowchart for PET image processing and reconstruction

### Detector corrections

Detector normalisation and correction for dead-time loss are crystal-specific calibrations performed prior to imaging. Detector normalisation reflects the individual sensitivity of each scintillation crystal in the detector array and ensures uniform detector sensitivity. Detector dead-time loss is the fraction of counts lost to pulse pile-up and can be assessed by the count rate characteristics of the scanner. Applying dead-time loss factors ensures a linear relationship between injected activity and actual count rate.

### Randoms and scatter correction

Correction for random events recorded by PET detectors can be achieved by direct measurement using the delayed coincidence technique. This technique is based on the principle that events occurring at time intervals much longer than the detector response time are due solely to random coincidences and are therefore subtracted from the number of prompt events along a given line of response. Scatter correction can be implemented by applying a model of contribution of scattered counts based on the theory underlying Compton scatter of gamma rays. Attenuation maps can be used to provide an estimate of the expected scatter in a given subject. Major factors affecting the amount of scatter are the energy windows of acceptance set according to the energy of the radiotracer and the energy resolution of the detector and whether axial septa are used to block axially oblique scatter events.



### **Attenuation correction**

As mentioned above, photon attenuation can result in significant degradation of counts. In heavy subjects, the fraction of photons that escape the body without absorption or scatter can be as low as 2%. An interesting property of PET is that attenuation is constant along a given line of coincidence, no matter where along this line positron annihilation occurred, even if the source is placed outside the body. This characteristic feature is exploited in practice by performing a transmission shadow profile of the body with an external gamma-ray source which is used to compute attenuation maps. A number of available PET systems are equipped with transmission sources such as germanium-68 ( $^{68}\text{Ge}$ , 511 keV) rod sources or caesium-137 ( $^{137}\text{Cs}$ , 662 keV) point sources. However, nowadays, the majority of PET devices are hybrid PET/CT scanners which employ a slow helical CT scan to generate transmission data using the intrinsic CT system. This has the advantage of being considerably faster than the often time-consuming external source transmission scans and has been proven to provide reliable and reproducible attenuation correction [6]. Careful attention should be given to correct alignment of transmission and emission scans to avoid misregistration artefacts.

### **Image reconstruction algorithms**

Image reconstruction algorithms include filtered back-projection (FBP), maximum-likelihood expectation-maximisation (MLEM) and

ordered-subsets expectation-maximisation (OSEM). FBP often performs well for cardiac PET imaging since myocardial count density is often sufficient in most protocols. FBP is exact (it only involves a single backprojection step) and requires little computational time; however, it is prone to artefacts and may not produce the best quality images. If OSEM techniques are available, these algorithms are usually a better choice, particularly in situations in which extracardiac activity is present or count density is low. However, for dynamic cardiac PET imaging using tracer kinetic modelling to estimate MBF, FBP is considered the best algorithm because of its exact nature, even though image quality can be poorer.

## Clinical applications of cardiac PET imaging

### **Diagnostic value and risk stratification in coronary artery disease**

Compared with the more widely available SPECT technique, PET is considered to have a superior diagnostic accuracy for the detection of coronary artery disease (CAD). Available PET studies with  $^{13}\text{N-NH}_3$  or  $^{82}\text{Rb}$  report a high diagnostic performance with invasive coronary angiography as the standard or reference (weighted sensitivity and specificity of 90% and 89%, respectively) and compare favourably with data published for SPECT [32]. This was confirmed in three small head-to-head comparisons of PET versus SPECT which showed a higher diagnostic accuracy of PET,



which had an overall sensitivity and specificity of 93% and 82%, respectively, versus 85% and 67%, respectively, for SPECT [33–35].

Besides its diagnostic value for the detection of CAD, perfusion imaging provides relevant data for patient risk stratification and prediction of cardiac events [36,37]. Compared with SPECT, PET is a newer technique and thus prospective studies documenting the predictive value of PET data are just starting to accrue [38,39]. These reports have consistently demonstrated a graded and independent relationship between the extent of perfusion abnormalities on PET and cardiovascular outcomes during a limited follow-up of 2.7–3.5 years. Most importantly, event rates are low with normal perfusion on PET (annualised event rates 0.4%– 2.4%) but increase by a factor ranging from approximately 3 to 17 in patients with moderate to severe perfusion defects. Furthermore, functional information from gated PET has proven to have an added independent prognostic value [38, 40].

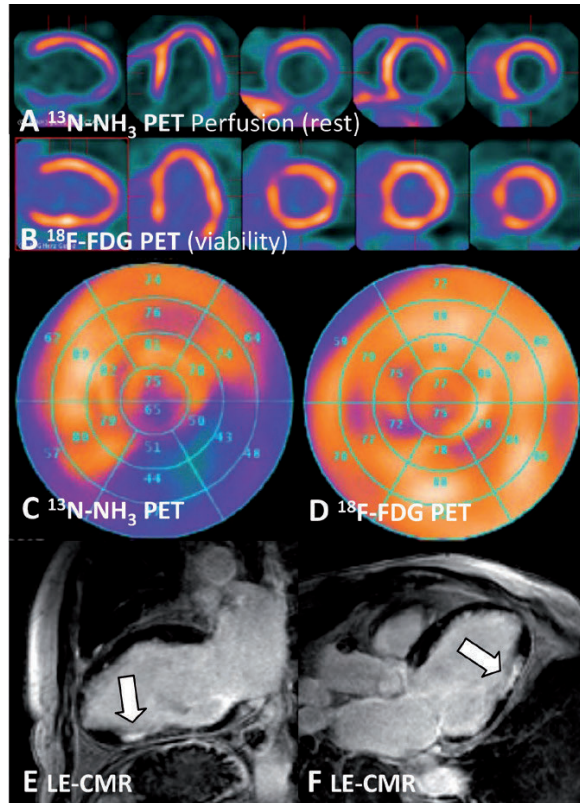
#### ***Added value of quantitative MBF and flow reserve***

The ability to provide non-invasive regional absolute quantification of MBF is a distinct and useful advantage of PET over other imaging modalities. In the presence of epicardial coronary artery stenoses, the hyperaemic response to adenosine or dipyridamole tends to de-

crease at diameter stenoses greater than 40% and is virtually nullified with stenoses greater than 80% [41]. There are insufficient data to support an added diagnostic value of quantitative MBF measurements over perfusion imaging alone [42]. However, the potential clinical utility of measuring MBF is supported by a number of prognostic studies in patients with cardiovascular risk factors [43], in patients with hypertrophic [20], dilated [21] or ischaemic cardiomyopathy [44], and in patients with suspected or known CAD [18]. The last-mentioned trial documented an independent prognostic value of myocardial perfusion abnormalities and coronary flow reserve (CFR) assessed with dynamic <sup>13</sup>N-NH<sub>3</sub> PET over a follow-up of 5.4 years. In patients with normal perfusion, abnormal CFR was independently associated with a higher annual event rate over 3 years compared with normal CFR (1.4% vs 6.3%). Similarly, in abnormal perfusion, CFR remained predictive throughout the 10-year follow-up period.

#### ***Assessment of myocardial viability***

In patients with ischaemic cardiomyopathy, dysfunctional but viable myocardium can exist in a state of hibernation (where glucose uptake is preserved or even increased but contractility impaired), and can recover contractility upon adequate restoration of blood flow (Fig. 5) [45].



Courtesy of the Cardiac Imaging Department, University Hospital Zurich, Switzerland

Figure 5A–F. Example of hibernating myocardium. Myocardial perfusion PET with  $^{13}\text{N-NH}_3$  (A and C) and  $^{18}\text{F-FDG}$  PET (B and D) demonstrate the typical pattern of perfusion–metabolism mismatch. A large inferolateral perfusion defect at rest can be seen (A and C) with preserved  $^{18}\text{F-FDG}$  uptake (B and D), indicating the presence of hibernating myocardium. The delayed enhancement cardiac magnetic resonance images (E and F) show a small area of transmurial scar in the midportion of the inferolateral wall (arrows) with a preserved viable rim in the remaining segments of the inferolateral wall.

A recent meta-analysis of  $^{18}\text{F-FDG}$  PET studies has yielded a weighted sensitivity and specificity of 92% and 63%, respectively, to predict regional functional recovery, and 83% and 64%, respectively, to predict global recovery of left ventricular function after revascularisation [46]. Patients with viable myocardium who underwent revascularisation had the best survival (annual mortality 4%), whereas the highest annualised mortality rate was observed in patients with viability receiving medical therapy (17%) [46]. Nonetheless, it should be noted that only very limited prospective data are available on the clinical value of PET and its impact on prognosis. In the PARR-2 trial, 430 patients with CAD and left ventricular ejection fraction of less than 35% were randomised to a standard therapy arm (decision regarding treatment strategy based on clinical judgement) and a PET-guided therapy arm (where  $^{18}\text{F-FDG}$  PET was used to guide treatment strategy) [47]. At 1 year, no significant differences in cardiovascular outcomes were noted between the PET-guided and the standard therapy arms. Nonetheless, if only patients who met PET recommendations for revascularisation were included, a significant difference favouring the PET guided arm could be observed, with a hazard ratio of 0.62 (95%CI 0.42–0.93).



### Hybrid PET/CT imaging: combination of morphology and function

The rapid advances in multislice CT technology have facilitated hybrid PET/CT imaging, which consists of fusion of both imaging modalities into one hybrid image. By exploiting the relative merits of each technique, i.e. ability of CT to reveal the burden of anatomical CAD and ability of PET to evaluate its physiological relevance, hybrid imaging can non-invasively provide unique information to guide management decisions in CAD patients (Fig. 6).

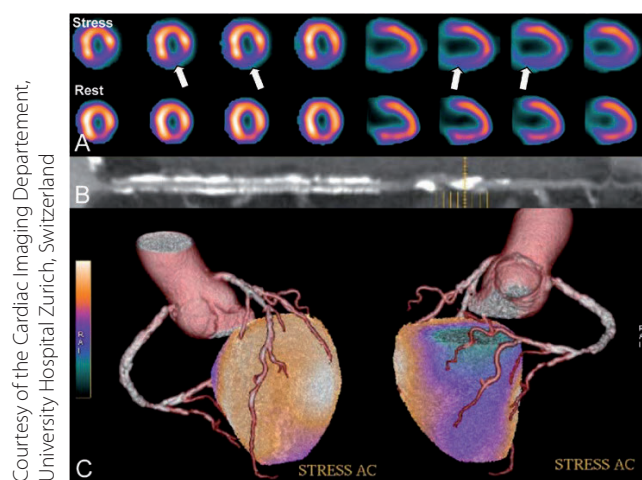


Figure 6A–C. Hybrid three-dimensional volume-rendered PET/CT images in an 80-year-old gentleman. The stress and rest perfusion images (A) document inferior ischaemia. His CT coronary angiogram (B) reveals intracoronary stents encompassing the whole right coronary artery. Hybrid imaging (C) shows superposition of the right coronary artery and the inferior perfusion defect, raising the strong suspicion of in-stent restenosis of the right coronary artery

The first pioneering report of hybrid PET with  $^{13}\text{N-NH}_3$  and CT angiography was presented by Namdar and colleagues [3]. Sensitivity, specificity and positive and negative predictive values of hybrid PET/CT for the detection of flow-limiting stenoses were 90%, 98%, 82% and 99%, respectively, compared with the clinical gold standard of PET and invasive coronary angiography. A number of similar studies using SPECT/CT hybrid imaging have followed, given the wider availability of the SPECT technique, confirming the superiority of the hybrid approach over the single modalities for the detection of CAD [48–51]. Through spatial co-localisation of perfusion defects with their subtending coronary arteries, the hybrid approach allows targeted revascularisation of haemodynamically relevant stenoses and avoids overuse of angioplasty in non-obstructive lesions [52]. First prospective data document a prognostic value of hybrid imaging [53]. A match of perfusion defect with the corresponding coronary stenosis identifies a group of patients with a very high annual event rate (6.0%) compared to those with unmatched (2.8%) or normal findings (1.3%). The clinical use of hybrid imaging has further been facilitated by the development and introduction of commercially available dedicated cardiac fusion software [54].

A recent joint position statement by the European Association of Nuclear Medicine (EANM), the European Society of Cardiac Radiology (ESCR) and the European Council

of Nuclear Cardiology (ECNC) has given recommendations on the clinical use of hybrid imaging. They support its use in patients with an intermediate pretest probability of CAD. It should be noted that hybrid imaging is a novel technique and that evidence on which patients should undergo such hybrid evaluations is therefore scarce. The incremental value of hybrid imaging and its impact on management strategies need to be evaluated in larger cohorts and in multicentre investigations. It is foreseeable, however, that the increasing availability of PET scanners equipped with high-end CT devices and the implementation of novel acquisition techniques for CT angiography, which can lower radiation exposure considerably [55], will contribute to a more widespread use of hybrid protocols in the non-invasive evaluation of CAD.





## References Chapter 4

### References

1. Dilsizian V, Bacharach SL, Beanlands RS, Bergmann SR, Delbeke D, Gropler RJ, et al. PET myocardial perfusion and metabolism imaging. [http://www.asnc.org/section\\_73.cfm](http://www.asnc.org/section_73.cfm) (accessed march 12th, 2011). 2009.
2. Hesse B, Tagil K, Cuocolo A, Anagnostopoulos C, Bardies M, Bax J, et al. EANM/ESC procedural guidelines for myocardial perfusion imaging in nuclear cardiology. *Eur J Nucl Med Mol Imaging* 2005;32:855-97.
3. Namdar M, Hany TF, Koepfli P, Siegrist PT, Burger C, Wyss CA, et al. Integrated PET/CT for the assessment of coronary artery disease: a feasibility study. *J Nucl Med* 2005;46:930-5.
4. Pichler BJ, Wehrl HF, Judenhofer MS. Latest advances in molecular imaging instrumentation. *J Nucl Med* 2008;49 Suppl 2:5S-23S.
5. Schepis T, Gaemperli O, Treyer V, Valenta I, Burger C, Koepfli P, et al. Absolute quantification of myocardial blood flow with  $^{13}\text{N}$ -ammonia and 3-dimensional PET. *J Nucl Med* 2007;48:1783-9.
6. Koepfli P, Hany TF, Wyss CA, Namdar M, Burger C, Konstantinidis AV, et al. CT attenuation correction for myocardial perfusion quantification using a PET/CT hybrid scanner. *J Nucl Med* 2004;45:537-42.
7. Bengel FM, Higuchi T, Javadi MS, Lautamaki R. Cardiac positron emission tomography. *J Am Coll Cardiol* 2009;54:1-15.
8. Nekolla SG, Reder S, Saraste A, Higuchi T, Dzewas G, Preissel A, et al. Evaluation of the novel myocardial perfusion positron-emission tomography tracer  $^{18}\text{F}$ -BMS-747158-02: comparison to  $^{13}\text{N}$ -ammonia and validation with microspheres in a pig model. *Circulation* 2009;119:2333-42.
9. Schafers KP, Spinks TJ, Camici PG, Bloomfield PM, Rhodes CG, Law MP, et al. Absolute quantification of myocardial blood flow with  $\text{H}(2)(^{15}\text{O})$  and 3-dimensional PET: an experimental validation. *J Nucl Med* 2002;43:1031-40.
10. Bol A, Melin JA, Vanoverschelde JL, Baudhuin T, Vogelers D, De Pauw M, et al. Direct comparison of  $^{13}\text{N}$ -ammonia and  $^{15}\text{O}$ -water estimates of perfusion with quantification of regional myocardial blood flow by microspheres. *Circulation* 1993;87:512-25.
11. Bergmann SR, Fox KA, Rand AL, McElvany KD, Welch MJ, Markham J, et al. Quantification of regional myocardial blood flow in vivo with  $\text{H}2^{15}\text{O}$ . *Circulation* 1984;70:724-33.
12. Araujo LI, Lammertsma AA, Rhodes CG, McFalls EO, Iida H, Rechavia E, et al. Noninvasive quantification of regional myocardial blood flow in coronary artery disease with oxygen-15-labeled carbon dioxide inhalation and positron emission tomography. *Circulation* 1991;83:875-85.
13. Hermansen F, Ashburner J, Spinks TJ, Kooner JS, Camici PG, Lammertsma AA. Generation of myocardial factor images directly from the dynamic oxygen-15-water scan without use of an oxygen-15-carbon monoxide blood-pool scan. *J Nucl Med* 1998;39:1696-702.
14. Muzik O, Beanlands RS, Hutchins GD, Mangner TJ, Nguyen N, Schwaiger M. Validation of nitrogen-13-ammonia tracer kinetic model for quantification of myocardial blood flow using PET. *J Nucl Med* 1993;34:83-91.
15. Bellina CR, Parodi O, Camici P, Salvadori PA, Taddei L, Fusani L, et al. Simultaneous in vitro and in vivo validation of nitrogen-13-ammonia for the assessment of regional myocardial blood flow. *J Nucl Med* 1990;31:1335-43.
16. Choi Y, Huang SC, Hawkins RA, Kim JY, Kim BT, Hoh CK, et al. Quantification of myocardial blood flow using  $^{13}\text{N}$ -ammonia and PET: comparison of tracer models. *J Nucl Med* 1999;40:1045-55.
17. Nitzsche EU, Choi Y, Czernin J, Hoh CK, Huang SC, Schelbert HR. Noninvasive quantification of myocardial blood flow in humans. A direct comparison of the  $^{13}\text{N}$ -ammonia and the  $^{15}\text{O}$ -water techniques. *Circulation* 1996;93:2000-6.
18. Herzog BA, Husmann L, Valenta I, Gaemperli O, Siegrist PT, Tay FM, et al. Long-term prognostic value of  $^{13}\text{N}$ -ammonia myocardial perfusion positron emission tomography added value of coronary flow reserve. *J Am Coll Cardiol* 2009;54:150-6.
19. Koepfli P, Wyss CA, Namdar M, Klainiguti M, von Schulthess GK, Luscher TF, et al. Beta-adrenergic blockade and myocardial perfusion in coronary artery disease: differential effects in stenotic versus remote myocardial segments. *J Nucl Med* 2004;45:1626-31.



20. Cecchi F, Olivetto I, Gistri R, Lorenzoni R, Chiriatti G, Camici PG. Coronary microvascular dysfunction and prognosis in hypertrophic cardiomyopathy. *N Engl J Med* 2003;349:1027-35.
21. Neglia D, Michelassi C, Trivieri MG, Sambuceti G, Giorgetti A, Pratali L, et al. Prognostic role of myocardial blood flow impairment in idiopathic left ventricular dysfunction. *Circulation* 2002;105:186-93.
22. Lautamaki R, George RT, Kitagawa K, Higuchi T, Merrill J, Voicu C, et al. Rubidium-82 PET-CT for quantitative assessment of myocardial blood flow: validation in a canine model of coronary artery stenosis. *Eur J Nucl Med Mol Imaging* 2009;36:576-86.
23. Herrero P, Markham J, Shelton ME, Weinheimer CJ, Bergmann SR. Noninvasive quantification of regional myocardial perfusion with rubidium-82 and positron emission tomography. Exploration of a mathematical model. *Circulation* 1990;82:1377-86.
24. Goldstein RA, Mullani NA, Marani SK, Fisher DJ, Gould KL, O'Brien HA Jr. Myocardial perfusion with rubidium-82. II. Effects of metabolic and pharmacologic interventions. *J Nucl Med* 1983;24:907-15.
25. Camici P, Ferrannini E, Opie LH. Myocardial metabolism in ischemic heart disease: basic principles and application to imaging by positron emission tomography. *Prog Cardiovasc Dis* 1989;32:217-38.
26. Wijns W, Vatner SF, Camici PG. Hibernating myocardium. *N Engl J Med* 1998;339:173-81.
27. Cerqueira MD, Verani MS, Schwaiger M, Heo J, Iskandrian AS. Safety profile of adenosine stress perfusion imaging: results from the Adenoscan Multicenter Trial Registry. *J Am Coll Cardiol* 1994;23:384-9.
28. Iskandrian AE, Bateman TM, Belardinelli L, Blackburn B, Cerqueira MD, Hendel RC, et al. Adenosine versus regadenoson comparative evaluation in myocardial perfusion imaging: results of the ADVANCE phase 3 multicenter international trial. *J Nucl Cardiol* 2007;14:645-58.
29. Gropler RJ, Siegel BA, Lee KJ, Moerlein SM, Perry DJ, Bergmann SR, et al. Nonuniformity in myocardial accumulation of fluorine-18-fluorodeoxyglucose in normal fasted humans. *J Nucl Med* 1990;31:1749-56.
30. Knuuti MJ, Nuutila P, Ruotsalainen U, Saraste M, Harkonen R, Ahonen A, et al. Euglycemic hyperinsulinemic clamp and oral glucose load in stimulating myocardial glucose utilization during positron emission tomography. *J Nucl Med* 1992;33:1255-62.
31. Knuuti J, Schelbert HR, Bax JJ. The need for standardisation of cardiac FDG PET imaging in the evaluation of myocardial viability in patients with chronic ischaemic left ventricular dysfunction. *Eur J Nucl Med Mol Imaging* 2002;29:1257-66.
32. Di Carli MF, Hachamovitch R. New technology for noninvasive evaluation of coronary artery disease. *Circulation* 2007;115:1464-80.
33. Go RT, Marwick TH, MacIntyre WJ, Saha GB, Neumann DR, Underwood DA, et al. A prospective comparison of rubidium-82 PET and thallium-201 SPECT myocardial perfusion imaging utilizing a single dipyridamole stress in the diagnosis of coronary artery disease. *J Nucl Med* 1990;31:1899-905.
34. Stewart RE, Schwaiger M, Molina E, Popma J, Gacioch GM, Kalus M, et al. Comparison of rubidium-82 positron emission tomography and thallium-201 SPECT imaging for detection of coronary artery disease. *Am J Cardiol* 1991;67:1303-10.
35. Tamaki N, Yonekura Y, Senda M, Yamashita K, Koide H, Saji H, et al. Value and limitation of stress thallium-201 single photon emission computed tomography: comparison with nitrogen-13 ammonia positron tomography. *J Nucl Med* 1988;29:1181-8.
36. Hachamovitch R, Hayes SW, Friedman JD, Cohen I, Berman DS. Comparison of the short-term survival benefit associated with revascularization compared with medical therapy in patients with no prior coronary artery disease undergoing stress myocardial perfusion single photon emission computed tomography. *Circulation* 2003;107:2900-7.
37. Iskander S, Iskandrian AE. Risk assessment using single-photon emission computed tomographic technetium-99m sestamibi imaging. *J Am Coll Cardiol* 1998;32:57-62.
38. Lertsburapa K, Ahlberg AW, Bateman TM, Katten D, Volker L, Cullom SJ, et al. Independent and incremental prognostic value of left ventricular ejection fraction determined by stress gated rubidium 82 PET imaging in patients with known or suspected coronary artery disease. *J Nucl Cardiol* 2008;15:745-53.



39. Yoshinaga K, Chow BJ, Williams K, Chen L, deKemp RA, Garrard L, et al. What is the prognostic value of myocardial perfusion imaging using rubidium-82 positron emission tomography? *J Am Coll Cardiol* 2006;48:1029-39.
40. Dorbala S, Hachamovitch R, Curillova Z, Thomas D, Vangala D, Kwong RY, et al. Incremental prognostic value of gated Rb-82 positron emission tomography myocardial perfusion imaging over clinical variables and rest LVEF. *JACC Cardiovasc Imaging* 2009;2:846-54.
41. Uren NG, Melin JA, De Bruyne B, Wijns W, Baudhuin T, Camici PG. Relation between myocardial blood flow and the severity of coronary-artery stenosis. *N Engl J Med* 1994;330:1782-8.
42. Kajander S, Joutsiniemi E, Saraste M, Pietila M, Ukkonen H, Saraste A, et al. Cardiac positron emission tomography/computed tomography imaging accurately detects anatomically and functionally significant coronary artery disease. *Circulation* 2010;122:603-13.
43. Schindler TH, Nitzsche EU, Schelbert HR, Olschewski M, Sayre J, Mix M, et al. Positron emission tomography-measured abnormal responses of myocardial blood flow to sympathetic stimulation are associated with the risk of developing cardiovascular events. *J Am Coll Cardiol* 2005;45:1505-12.
44. Tio RA, Dabeshlim A, Siebelink HM, de Sutter J, Hillege HL, Zeebregts CJ, et al. Comparison between the prognostic value of left ventricular function and myocardial perfusion reserve in patients with ischemic heart disease. *J Nucl Med* 2009;50:214-9.
45. Camici PG, Prasad SK, Rimoldi OE. Stunning, hibernation, and assessment of myocardial viability. *Circulation* 2008;117:103-14.
46. Schinkel AF, Bax JJ, Poldermans D, Elhendy A, Ferrari R, Rahimtoola SH. Hibernating myocardium: diagnosis and patient outcomes. *Curr Probl Cardiol* 2007;32:375-410.
47. Beanlands RS, Nichol G, Huszti E, Humen D, Racine N, Freeman M, et al. F-18-fluorodeoxyglucose positron emission tomography imaging-assisted management of patients with severe left ventricular dysfunction and suspected coronary disease: a randomized, controlled trial (PARR-2). *J Am Coll Cardiol* 2007;50:2002-12.
48. Rispler S, Keidar Z, Ghersin E, Roguin A, Soil A, Dragu R, et al. Integrated single-photon emission computed tomography and computed tomography coronary angiography for the assessment of hemodynamically significant coronary artery lesions. *J Am Coll Cardiol* 2007;49:1059-67.
49. Gaemperli O, Schepis T, Valenta I, Husmann L, Scheffel H, Duerst V, et al. Cardiac image fusion from stand-alone SPECT and CT: clinical experience. *J Nucl Med* 2007;48:696-703.
50. Santana CA, Garcia EV, Faber TL, Sirineni GK, Esteves FP, Sanyal R, et al. Diagnostic performance of fusion of myocardial perfusion imaging (MPI) and computed tomography coronary angiography. *J Nucl Cardiol* 2009;16:201-11.
51. Slomka PJ, Cheng VY, Dey D, Woo J, Ramesh A, Van Kriekinge S, et al. Quantitative analysis of myocardial perfusion SPECT anatomically guided by coregistered 64-slice coronary CT angiography. *J Nucl Med* 2009;50:1621-30.
52. Gaemperli O, Husmann L, Schepis T, Koepfli P, Valenta I, Jenni W, et al. Coronary CT angiography and myocardial perfusion imaging to detect flow-limiting stenoses: a potential gatekeeper for coronary revascularization? *Eur Heart J*. 2009;30:2921-9.
53. Pazhenkottil AP, Nkoulou RN, Ghadri JR, Herzog BA, Buechel RR, Kuest SM, et al. Prognostic value of cardiac hybrid imaging integrating single-photon emission computed tomography with coronary computed tomography angiography. *Eur Heart J*. 2011 Feb 14 [Epub ahead of print].
54. Gaemperli O, Schepis T, Kalff V, Namdar M, Valenta I, Stefani L, et al. Validation of a new cardiac image fusion software for three-dimensional integration of myocardial perfusion SPECT and stand-alone 64-slice CT angiography. *Eur J Nucl Med Mol Imaging* 2007;34:1097-106.
55. Husmann L, Valenta I, Gaemperli O, Adda O, Treyer V, Wyss CA, et al. Feasibility of low-dose coronary CT angiography: first experience with prospective ECG-gating. *Eur Heart J* 2008;29:191-7.
56. McNeill AJ, Fioretti PM, el-Said SM, Salustri A, Forster T, Roelandt JR. Enhanced sensitivity for detection of coronary artery disease by addition of atropine to dobutamine stress echocardiography. *Am J Cardiol* 1992;70:41-6.

TABLES

Table 1: Most common PET tracers for cardiac applications

Tracer	Physical half-life	Recommended activity (MBq)	Maximum positron energy (MeV)	Tissue positron range (mm) <sup>a</sup>	Uptake mechanism	Radionuclide production
<sup>15</sup> O-H <sub>2</sub> O	2 min	700 – 1,500	1.70	1.87	Free diffusion (perfusion)	Cyclotron
<sup>82</sup> Rb	78 s	1,100 – 1,500	3.15	4.10	Na/K-ATPase (perfusion)	<sup>82</sup> Sr/ <sup>82</sup> Rb generator
<sup>13</sup> N-NH <sub>3</sub>	10 min	370 – 740	1.19	1.26	Diffusion/ meta-bolic trapping (perfusion)	Cyclotron
<sup>18</sup> F-FDG	110 min	200 – 350	0.64	0.54	Glucose transport/ hexo-kinase (viability)	Cyclotron

<sup>a</sup> Calculated for soft tissue using the full width at 20% of the maximum amplitude (FW20M) method

Table 2: Radiokinetic properties of the “ideal” PET perfusion tracer

High first-pass extraction fraction at both baseline and high flow rates for maximal activity accumulation in the heart and improved image quality
Linear correlation of myocardial tracer uptake with MBF rate
Prolonged retention in the heart to give a stable distribution and high count statistics and permit ECG gating for the simultaneous assessment of perfusion and LV function
Metabolic inertness
Efficient, fast, reliable and fully automated radiochemical synthesis

Table 3: Dosing regimen for pharmacological stress agents in myocardial perfusion PET

<b>Adenosine</b>	Continuous intravenous infusion at 140 µg/kg/min over 6–7 min <sup>a</sup>
	PET tracer injection 3 min into adenosine infusion
<b>Dipyridamole</b>	Continuous intravenous infusion at 140 µg/kg/min over 4 min
	PET tracer injection 3–5 min after completion of dipyridamole infusion
<b>Dobutamine</b>	Continuous intravenous infusion starting at 5–10 µg/kg/min
	Increase by 10 µg/kg/min increments to reach target heart rate (at least 85% of the age-predicted maximal heart rate) or maximal dose of 40 µg/kg/min
	If necessary, increase heart rate with intravenous atropine (0.25 mg, repeated every 1–2 min up to a maximal dose of 1 mg) [56]
	Continue dobutamine infusion for at least 2 min after tracer injection

<sup>a</sup> For patients at risk of complications (AV conduction disturbances, borderline hypotension, inadequately controlled asthma), adenosine infusion can be started at a lower dose (50 µg/kg/min) and increased at 1-min intervals to 75, 100 and 140 µg/kg/min if tolerated. PET tracer injection can be performed 1 min into the 140 µg/kg/min dose. Shorter adenosine infusion protocols are not recommended for PET perfusion imaging, particularly if dynamic image acquisition for MBF quantification is envisaged

# Chapter 5 – Clinical applications of PET/CT in neurology

## 5.1 Introduction to brain PET

Jacques Darcourt

**Positron emission tomography** neuroimaging is a fast-growing field in nuclear medicine. This is due to the high incidence of neurodegenerative diseases as well as to the number of radiopharmaceuticals which are or will become available. The brain “targets” for molecular imaging are exceptionally rich: perfusion, metabolism, neurotransmission, amyloid plaques, tumours, microglial activation, etc. However, neuroimaging nuclear medicine procedures need to be more widely known and understood by referring physicians and their usefulness recognised by clinical guidelines in neurology, psychiatry, geriatrics and neuro-oncology. In order to achieve this recognition, technologists and nuclear medicine physicians should work together to standardise the protocols and demonstrate the usefulness of these techniques in clinical trials and daily practice. We are at the very beginning of this process.

Against this background, the EANM Neuroimaging Committee has organised this section of this Technologist’s Guide in five chapters which cover the current applications of brain PET imaging.

The first chapter addresses dementia and related disorders, which is certainly the current “driving force” of brain PET. A large body of data has supported the use of  $^{18}\text{F}$ -FDG brain PET in dementia for many years. Flavio Nobili reviews this large field, pointing out

the major currently accepted indications. He also addresses amyloid plaque imaging for Alzheimer’s disease, which should become available in the near future.

The second chapter is very different and deals with psychiatry. Marco Pagani clearly explains the current situation. It is a field of major future applications such as depression, post-traumatic stress disorders, attention deficit disorders and autism. Therefore we should be aware of these promising indications. However, the role of PET imaging is far from being as mature in these indications as in dementias for example.

In the third chapter Jan Booij reviews the applications of PET imaging for diagnosis of movement disorders. This is of major importance since it is the first well-established use of neurotransmission imaging and it illustrates elegantly the use different radiopharmaceuticals for the diagnosis.

In the fourth chapter, Klaus Tatsch describes the capabilities of PET imaging for brain tumour management. This indication is particularly representative of where brain PET stands. It adds valuable molecular information to MRI morphological data, taking advantage of biological features such as glucose or amino acid specific tumour metabolism.

The last chapter, written by Franck Semah and Gregory Petyt, reviews the use of brain





---

PET in epilepsy. The authors explain in particular how  $^{18}\text{F}$ -FDG PET images can detect metabolic abnormalities which draw attention to specific regions which can be missed on MRI.

The EANM Neuroimaging Committee along with the Technologist Committee hopes that these chapters will contribute to the further development of brain PET imaging, to increased standardisation of the techniques and to recognition of the techniques in clinical strategies for patient management.



# Chapter 5 – Clinical applications of PET/CT in neurology

## 5.2 Dementia and related disorders

Flavio Nobili

### Basic principles of brain glucose utilisation

The brain mainly utilises glucose to produce energy. Glucose enters the neuron–astrocyte unit, where it undergoes phosphorylation via hexokinase. Energy production takes place at the synaptic terminals via the tricarboxylic acid pathway, requiring oxygen and leading to high ATP availability (aerobic glycolysis). This pathway is very productive but cannot quickly meet the need for energy during brain activation. In turn, astrocytes mainly utilise anaerobic glycolysis, providing much less energy but doing so more rapidly. The lactate end-product is transferred from astrocytes to neurons and is transformed to pyruvate for more economic energy production [1].

Glucose metabolism is closely coupled to neuronal function at rest and during functional activation. Labelling glucose with [ $^{18}\text{F}$ ] fluorine allows quantitative or semi-quantitative measurement of synaptic terminal metabolism in its neuron–astrocyte functional unit, as the greater part of glucose utilisation happens at the synaptic level. The reference grey matter cerebral metabolic rate for glucose (CMR<sub>glc</sub>) ranges from about 40 to 60 mmol glucose/100 g of brain tissue/min at rest in the normal adult; in the white matter the rate is about 25–30% of that in the grey matter. The highest values are found in the thalami, basal ganglia and occipital polar and mesial cortex, while the cerebellum and medial temporal cortex show the lowest values. As compared to SPECT tracers, this topo-

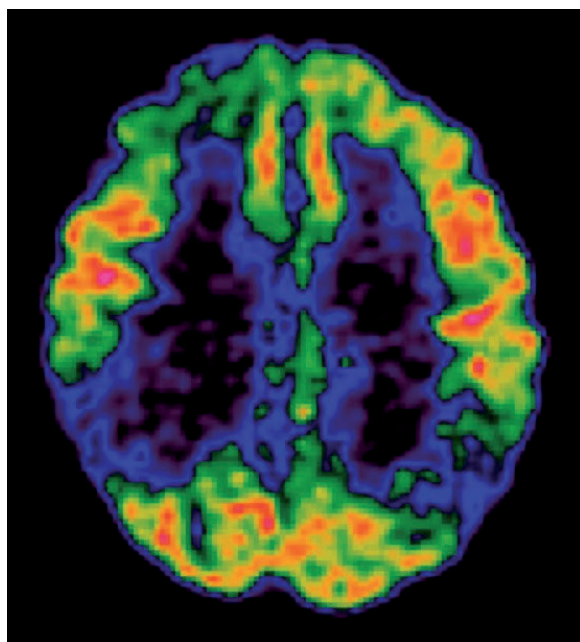
graphic distribution closely resembles that obtained with  $^{99\text{m}}\text{Tc}$ -ECD but is less than that obtained with  $^{99\text{m}}\text{Tc}$ -HMPAO. At rest, glucose uptake distribution is mainly driven by basal neuronal activity and represents general neuronal integrity. For a tissue unit, reduced glucose uptake essentially represents either a reduction in the number of synapses or reduced synaptic metabolic activity. The EANM provides guidelines for brain  $^{18}\text{F}$ -FDG PET [2].

### Mild cognitive impairment and Alzheimer's disease

Recently, the diagnostic effort in patients with Alzheimer's disease (AD) has moved to early stages of the disease, when dementia is not yet present (i.e. the subject maintains his/her autonomy in everyday occupations). This stage is known as mild cognitive impairment (MCI) and has been defined as a memory deficit confirmed by standardised cognitive tests. However, not all individuals with MCI will develop dementia. When a typical MCI patient with suspicion of AD undergoes  $^{18}\text{F}$ -FDG PET, hypometabolism is found in one or more of the following: precuneus, posterior cingulate cortex, and the lateral posterior parietal, both lateral and mesial temporal and, to a lesser extent, lateral frontal association cortices. Using re-orientation on the so-called Ohnishi transaxial plane (i.e. with the nose tilted about  $30^\circ$  upward with respect to the bicommissural plane [3]), analysis of transaxial slices is more adequate in segmenting the hippocampus and the mesial temporal lobe, which is indeed

not parallel to the bicommissural plane. The primary sensorimotor cortex, visual cortex, thalami, basal ganglia and cerebellum are relatively spared.

A very frequent feature especially evident in the early stages of disease is the strong asymmetric involvement. As a consequence, visual analysis of scans strongly relies on asymmetric evaluation of abnormalities. Early-onset AD (i.e. before the age of 60) is more often characterised by posterior parieto-temporal hypometabolism as compared to late-onset AD, in which medial temporal hypometabolism prevails. An example in a patient with early-onset AD is shown in Fig. 1.



Courtesy of Clinical Neurophysiology and Nuclear Medicine Dept., University Hospital San Martino, Genoa, Italy

Figure 1:  $^{18}\text{F}$ -FDG PET findings in a patient with early-onset AD

In a study including 284 patients, of whom 138 had a neuropathological diagnosis, a typical AD pattern (i.e. parietal and temporal hypometabolism, with or without frontal involvement) showed a sensitivity of 94% and a specificity of 73% in comparison to the neuropathological diagnosis [4]. In another study, the sensitivity of PET for Alzheimer's disease was 86% (95% CI: 76–93%) and the specificity was 86% (95% CI: 72–93%) [5]. Its high accuracy has positioned  $^{18}\text{F}$ -FDG PET as one of the biomarkers for the diagnosis of AD, even before the onset of dementia, the others being MRI and tau protein and Ab 1-42 assays in cerebrospinal fluid [6].

$^{18}\text{F}$ -FDG PET has been reported to be highly sensitive to hypometabolism in AD patients over time, in follow-up studies lasting 1 year. This means that it is a suitable marker to follow the disease evolution and to evaluate the potential effect of both symptomatic and neuroprotective agents. It has been computed that metabolism reduction in critical regions is in the order of 16–19% over 3 years, while in healthy subjects reduction is virtually absent over such a time span. In the next few years, some radiopharmaceuticals able to image the amyloid brain burden will become commercially available. Virtually all patients with AD show amyloid brain deposition (very high sensitivity), but patients with dementia with Lewy bodies (DLB) or Parkinson's disease dementia and some elderly healthy subjects are also 'amyloid positive' (moderate specificity) [7].

### Frontotemporal dementia

Frontotemporal dementia accounts for about 10% of all dementias and is mainly characterised by early behavioural disturbances, including apathy, disinhibition, altered social behaviour and stereotyped behaviour, variously mixed according to the parts of the frontal lobes maximally involved. In the left-sided variants (progressive aphasia), language complaints are found. Both the frontal lobes may be variably involved, often in an asymmetric fashion, together with the pole and the anterolateral aspect of the temporal lobes, the insula and the anterior cingulate gyrus. When the frontal lobe is severely affected, hypometabolism in the contralateral cerebellar hemisphere is found ('crossed cerebellar diaschisis') as a consequence of deafferentation via the fronto-ponto-cerebellar fibres. In the variant 'frontal lobe degeneration' (FLD), the two frontal lobes are more symmetrically affected. Figure 2 shows the  $^{18}\text{F}$ -FDG PET of a patient with FLD.

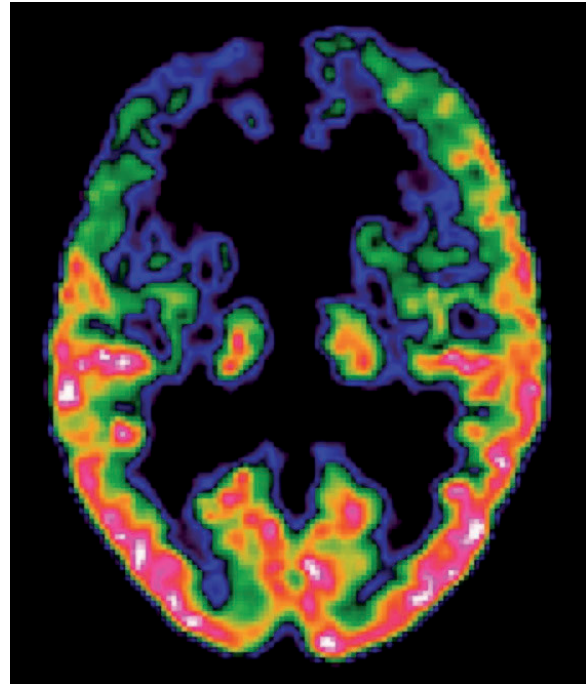


Figure 2:  $^{18}\text{F}$ -FDG PET findings in a patient with FLD

Courtesy of Clinical Neurophysiology and Nuclear Medicine Dept.,  
University Hospital San Martino, Genoa, Italy



### Dementia with Lewy bodies

Dementia with Lewy bodies accounts for about 10–15% of cases of dementia. The clinical symptoms may include spontaneous (not drug-induced) parkinsonism, early visual hallucinations, fluctuating attention and REM sleep behaviour disorders. Neuroleptic hypersensitivity (severe parkinsonism following neuroleptic administration) is a key sign. The metabolic picture is similar to that observed in AD, but occipital hypometabolism is more frequent and more severe, while medial temporal lobe hypometabolism is milder. Presynaptic dopaminergic PET radiopharmaceuticals, such as  $^{11}\text{C}$ -FE-CIT and  $^{18}\text{F}$ -fluorodopa, and of course the regular DaT SPECT (FP-CIT SPECT) highlight reduced uptake at the basal ganglia level.

### Vascular dementia

Cognitive impairment up to dementia can be found in a large family of cerebrovascular diseases, the most representative of which are subcortical ischaemic vascular disease, large brain infarctions and infarctions affecting 'strategic' areas. MRI is the cornerstone of the diagnosis, while  $^{18}\text{F}$ -FDG PET may highlight hypometabolism in the basal ganglia, in the thalami and, patchily, in several cortical areas, more often the temporal lobes.

### Pitfalls and limitations

Since most equipment is nowadays PET/CT and attenuation correction is based on CT scan, movement artefacts between CT and PET acquisitions should be carefully checked because they can generate false asymmetries. A fast of at least 4 h is essential because a standard dose of about 150–185 MBq of  $^{18}\text{F}$ -FDG (3D acquisition) without fasting may be insufficient to achieve a good image quality. Another limitation of  $^{18}\text{F}$ -FDG PET is that no standard analytical procedure has as yet been established. Scans are analysed in very different ways, ranging from simple visual evaluation to sophisticated computer-assisted comparisons with a normative database, either already available in working stations and supplied by the manufacturer or locally established. While simple visual analysis may be too sensitive even to trivial or physiological asymmetries and impairment in median structure hypometabolism can be missed, automatic analysis suffers from opposite issues because it is generally very specific but scarcely sensitive, although automatic analysis will help relative inexperienced Nuclear Medicine Physicians in better interpretation of the images.

## References Chapter 5.2

### References

1. Magistretti PJ. Cellular basis of functional brain imaging: insight from neural-glia metabolic coupling. *Brain Res* 2000;886:108-12.
2. Varrone A, Asenbaum S, Vander Borght T, et al. EANM procedure guidelines for PET brain imaging using [(18)F]FDG, version 2. *Eur J Nucl Med Mol Imaging* 2009;36:2103-10.
3. Ohnishi T, Hoshi H, Nagamachi S, Jinnouchi S, Flores LG 2nd, Futami S, Watanabe K. High-resolution SPECT to assess hippocampal perfusion in neuropsychiatric diseases. *J Nucl Med* 1995;36:1163-9.
4. Silverman DH, Small GW, Chang CY, et al. Positron emission tomography in evaluation of dementia: regional brain metabolism and long-term outcome. *JAMA* 2001;286:2120-7.
5. Patwardhan MB, McCrorg DC, Matchar DB, Samsa GP, Rutschmann OT. Alzheimer disease: operating characteristics of PET—a metaanalysis. *Radiology* 2004;231:73-80.
6. Dubois B, Feldman HH, Jacova C, et al., Research criteria for the diagnosis of Alzheimer's disease: revising the NINCDS-ADRDA criteria. *Lancet Neurol* 2007;6:734-6.
7. Gomperts SN, Rentz DM, Moran E, et al. Imaging amyloid deposition in Lewy body diseases. *Neurology* 2008;71:903-10.



# Chapter 5 – Clinical applications of PET/CT in neurology

## 5.3 Psychiatry

Marco Pagani

### Introduction

Neuroimaging in psychiatry has been used to assess functional, neurochemical and structural patterns related to specific disorders, to evaluate new molecules as therapeutic agents and to foresee individual response to treatment. In psychiatric studies, comorbidity is a critical issue since the co-occurrence of different pathological dimensions might impact on the neurobiological patterns, causing the neuroimaging findings to be unspecific. Furthermore, macroscopic changes have seldom been described since most psychiatric diseases show changes at the molecular level. All this results, for all forms of anxiety disorder, in a diagnostic accuracy far below that reported in neurodegenerative disorders. In this respect the diagnostic approach to the various mental disorders included in DSM-IV Axis I (major mental and learning disorders) needs specific knowledge in order to adopt the correct strategies for patient selection as well as advanced radiochemical and statistical methodologies. In most of the mental disorders included in DSM-IV Axis I, CBF, metabolism and transporter/receptor patterns have been investigated but only in some of them has a general consensus been reached.

### Major depression

Major depression (MD) is a common primary idiopathic condition characterised by one or more major depressive episodes of persistently low mood, dysregulated sleep, appetite and weight, anhedonia, cognitive impairment,

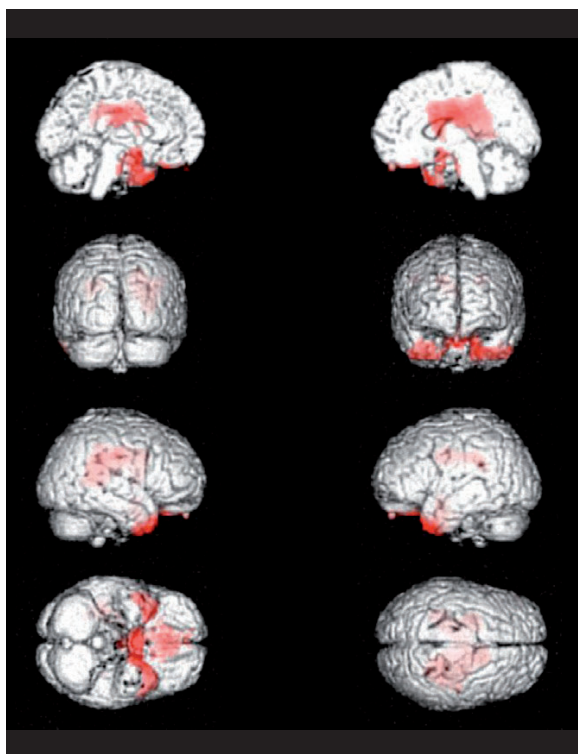
and suicidality not due to a medical condition, medication, abused substance or psychosis. MD is estimated to rival virtually every other known medical illness in burden of disease morbidity early in this millennium since it is estimated to affect, on a life-time basis, up to a quarter (26%) of the population. The neural networks modulating emotional expression seem to be implicated in the pathophysiology of MD, and this is in particular true of the medial prefrontal cortex, amygdala, hippocampus and basal ganglia, as reported by several PET studies. Serotonin 1A receptor (5-HT<sub>1A</sub>R) function appears to be abnormal in MD but disagreement still exists regarding the presence and direction of binding abnormalities [1]. An important use of PET in MD is the study and follow-up of antidepressant effects on monoamine receptor occupancy [2].

### Post-traumatic stress disorder

Post-traumatic stress disorder (PTSD) is an anxiety disorder following major psychological trauma reported to affect between 4% and 8% of the general population. It is defined by the coexistence of three clusters of trauma-related symptoms: re-experiencing, avoidance and hyperarousal. Neural correlates of PTSD have been investigated by means of different research paradigms such as symptom provocation, cognitive activation and functional connectivity. Functional studies by PET have consistently shown during emotional stimuli a concomitance of amygdala hyper-reactivity and a correspondingly reduced prefrontal



cortex and anterior cingulate cortex control over amygdalae. However, other structures have been consistently found to be involved in PTSD, i.e. anterior and posterior insular cortex, posterior cingulate cortex and certain portions of the temporal lobe and orbitofrontal cortex ([3]; for review see [4]). Figure 1 illustrates increased CBF in PTSD as demonstrated by  $^{99m}\text{Tc}$ -HMPAO SPECT imaging analysed by SPM2.



Courtesy of Department of Nuclear Medicine, Karolinska Hospital, Stockholm and of Nuclear Medicine Communication


Figure 1: Increased CBF in PTSD.  $^{99m}\text{Tc}$ -HMPAO SPECT images analysed by SPM2. Three-dimensional rendering of voxels reflecting higher tracer distribution in patients (n=15) as compared to controls (n=27). The significant statistical differences are highlighted

### Attention deficit hyperactivity disorder

Attention deficit hyperactivity disorder (ADHD) is a multifactorial and clinically heterogeneous neurobehavioural disorder characterised by symptoms of hyperactivity, inattention and impulsivity. It is suggested to be the most common chronic undiagnosed psychiatric disorder in adults and its prevalence in adults is estimated to be about 4%. Comorbidity with at least one other psychiatric disorder occurs in 87% of adult ADHD subjects. Neuroanatomical and neurobiological data underscore alterations in dopamine/noradrenaline-modulated fronto-striatal-cerebellar circuits. Owing to the high catecholamine concentration in these sensitive regions, both dopamine transporters and receptor ligands have often been used in ADHD studies [5] and the effect of stimulants, mostly methylphenidate, investigated. Moreover deficits in CBF and metabolism have been reported in both adolescents and adults with ADHD (for review see [6]).

### Autism spectrum disorders

Autism spectrum disorders (ASDs) are defined on the clinical basis by impairment in social interaction, impairment in verbal and non-verbal communication and repetitive or stereotypical behaviours. They affect almost 1% of the general population and have shown an impressive increase in prevalence since the early 1990s, probably attributable to the better awareness of the disease. Structural findings support the hypothesis of anomalous perinatal processes of neurogenesis and neuronal



---

maturation [7]. Regional CBF or metabolism abnormalities have been found in the cerebellum, limbic system, frontal and temporal cortices, corpus callosum and basal ganglia even though specific patterns for ASD have not yet been identified [8]. Furthermore, a growing body of evidence suggests weaker functional connectivity, especially in the default network, often associated with symptom severity.

### Conclusion

Neuroimaging in psychiatric disorders will help to provide a better understanding of the underlying pathophysiology, to assess the neurobiology of treatment outcome and to demonstrate the neuroanatomical, functional and chemical profiles associated with specific endophenotypes. It will also contribute in disclosing the neurobiology of the specific symptoms underlying psychiatric disorders and in progressing towards a more suitable dimensional approach.

## References Chapter 5.3

### References

1. Drevets WC, Thase ME, Moses-Kolko EL, Price J, Frank E, Kupfer DJ, et al. Serotonin-1A receptor imaging in recurrent depression: replication and literature review. *Nucl Med Biol* 2007;34:865-77.
2. Meyer JH, Wilson AA, Ginovart N, Goulding V, Hussey D, Hood K, et al. Occupancy of serotonin transporters by paroxetine and citalopram during treatment of depression: a [(11)C]DASB PET imaging study. *Am J Psychiatry* 2001;158:1843-9.
3. Pagani M, Högberg G, Salmaso D, Nardo D, Sundin O, Jonsson C, et al. Effects of EMDR psychotherapy on 99mTc-HMPAO distribution in occupation-related post-traumatic stress disorder. *Nucl Med Commun* 2007;28:757-65.
4. Francati V, Vermetten E, Bremner JD. Functional neuroimaging studies in posttraumatic stress disorder: review of current methods and findings. *Depress Anxiety* 2007;24:202-18.
5. Jucaite A, Fernell E, Halldin C, Forsberg H, Farde L. Reduced midbrain dopamine transporter binding in male adolescents with attention-deficit/hyperactivity disorder: association between striatal dopamine markers and motor hyperactivity. *Biol Psychiatry* 2005;57:229-38.
6. Zimmer L. Positron emission tomography neuroimaging for a better understanding of the biology of ADHD. *Neuropharmacology* 2009;57:601-7.
7. Amaral DG, Schumann CM, Nordahl CW. Neuroanatomy of autism. *Trends Neurosci* 2008;31:137-45.
8. Rumsey JM, Ernst M. Functional neuroimaging of autistic disorders. *Ment Retard Dev Disabil Res Rev* 2000;6:171-9.



# Chapter 5 – Clinical applications of PET/CT in neurology

## 5.4 Movement disorders

Jan Booij

The movement disorder Parkinson's disease (PD) is a clinical syndrome characterised by parkinsonism: bradykinesia, hypokinesia/akinesia, rigidity, tremor and postural instability. This syndrome is characterised neuropathologically by a severe loss of dopaminergic nigrostriatal neurons. The integrity of these dopaminergic neurons can be measured using radiopharmaceuticals for the dopamine transporter (located exclusively in the membrane of dopaminergic neurons) or the vesicular monoamine transporter (located in the membrane of vesicles in dopaminergic terminals) (Fig. 1).

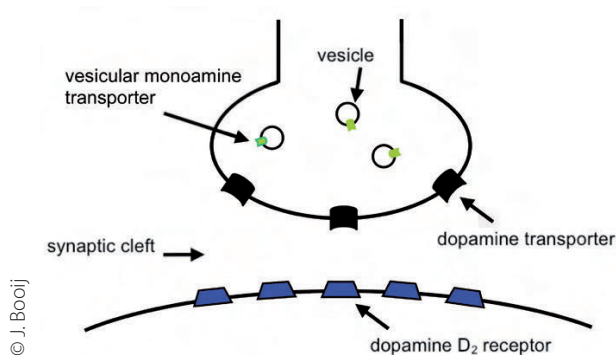


Figure 1: Schematic representation of a terminal of a dopaminergic neuron at the level of the striatum

Another method to measure the integrity of nigrostriatal neurons is PET imaging following injection of  $^{18}\text{F}$ -DOPA. The uptake rate constant of DOPA is determined by its transfer across the blood–brain barrier, its decarboxylation to dopamine and the retention in nerve terminals (for a review see Booij et al. [1]).

Radiopharmaceuticals to assess central dopamine transporters in vivo have been developed and validated for both SPECT and PET imaging in humans. Loss of striatal dopamine transporters in PD patients has been reported consistently, even in preclinical (premotor) phases of the disease (for a review see Booij and Knol [2]). Radiotracers for the vesicular monoamine transporter are available only for PET [1]. Use of such tracers also permits the accurate detection of loss of nigrostriatal neurons. Although in Europe the majority of centres use dopamine transporter radioligands and SPECT to assess the integrity of nigrostriatal neurons in clinical routine studies, some centres use  $^{18}\text{F}$ -DOPA PET [3].

In the majority of PD patients, the dopamine transporter binding or DOPA uptake in the striatum is asymmetrical. In addition, the reduced uptake/binding is more pronounced in the putamen than in the caudate nucleus (Fig. 2). In hemiparkinsonian patients (in the vast majority of PD patients, motor signs start on one side of the body) even bilateral loss of striatal DOPA uptake or dopamine transporter binding has been documented. Moreover, there is a correlation between striatal uptake/binding and disease severity [1].

Loss of dopamine neurons is not specific for PD. Also in certain other movement disorders, such as multiple system atrophy (MSA) or progressive supranuclear palsy (PSP), there is a severe loss of nigrostriatal neurons. MSA is a

movement disorder characterised by a variable combination of parkinsonism, cerebellar dysfunction, autonomic failure and involvement of the pyramidal tract. PSP is characterised by parkinsonism (frequently symmetrical and with an axial rigidity), vertical supranuclear gaze palsy, dysphagia, dysarthria and cognitive decline. Generally speaking, in both MSA and PSP the response to dopaminergic drugs is poor. On the other hand, drug-induced parkinsonism, essential tremor and psychogenic parkinsonism may sometimes be hard to differentiate clinically from PD; however, these disorders are not characterised by loss of dopaminergic neurons (Fig. 2). Therefore, imaging of the nigrostriatal dopaminergic neurons may be helpful in confirming or excluding an underlying dopaminergic deficit in uncertain cases.

Additionally, MSA and PSP are characterised by loss of postsynaptic striatal neurons bearing dopamine D2 receptors. Particularly in the earlier clinical phases, it may be hard to differentiate these syndromes from PD clinically. To help differentiate these syndromes from PD, some centres use PET and radiotracers for dopamine D2 receptors (such as  $^{11}\text{C}$ -raclopride) [1]. However, since several studies have observed a certain degree of overlap between data obtained in PD patients and in MSA/PSP patients, centres are starting to use  $^{18}\text{F}$ -FDG PET to differentiate MSA/PSP from PD.  $^{18}\text{F}$ -FDG PET studies have demonstrated loss of  $^{18}\text{F}$ -FDG uptake in the striatum of MSA patients but not in PD (Fig. 2).

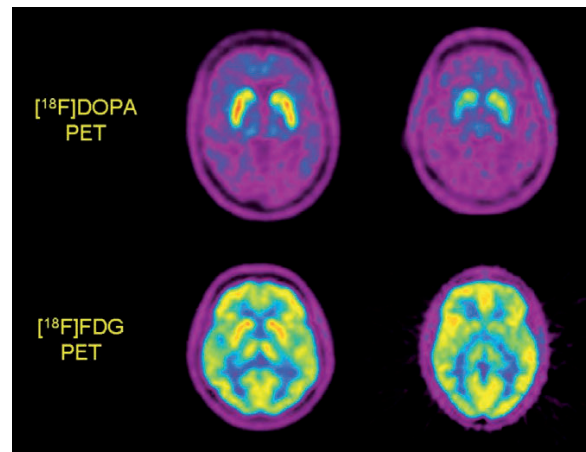


Figure 2: Transverse PET slices at the level of the striatum. Upper panel: left: normal  $^{18}\text{F}$ -DOPA uptake in the striatum in a patient suffering from essential tremor; right: reduced striatal uptake (particularly in posterior putamen) in a hemiparkinsonian PD patient (with motor signs on left side of body). Lower panel: note the lower striatal  $^{18}\text{F}$ -FDG uptake in the striatum of an MSA patient (right side) than in a patient suffering from PD (left). Images courtesy of L.K. Teune and K.L. Leenders, Department of Neurology, University Medical Center Groningen, Groningen, The Netherlands

Additional reduced uptake may be detected in MSA in the cerebellar hemispheres [4]. In PSP, reduced  $^{18}\text{F}$ -FDG uptake may not be restricted to the striatum, but may also involve the prefrontal lobe, thalamus and mesencephalon [4].

Courtesy: L.K. Teune and K.L. Leenders,  
Department of Neurology, University Medical Center  
Groningen, Groningen, The Netherlands



## References Chapter 5.4

---

### References

1. Booij J, Tissingh G, Winogrodzka A, van Royen EA. Imaging of the dopaminergic neurotransmission system using single-photon emission tomography and positron emission tomography in patients with parkinsonism. *Eur J Nucl Med* 1999;26:171-82.
2. Booij J, Knol RJJ. SPECT imaging of the dopaminergic system in (premotor) Parkinson's disease. *Parkinsonism Related Disord* 2007;13:S425-8.
3. Eshuis SA, Jager PL, Maguire RP, Jonkman S, Dierckx RA, Leenders KL. Direct comparison of FP-CIT SPECT and F-DOPA PET in patients with Parkinson's disease and healthy controls. *Eur J Nucl Med Mol Imag* 2009;36:454-62.
4. Teune LK, Bartels AL, de Jong BM, Willemsen AT, Eshuis SA, de Vries JJ, et al. Typical cerebral metabolic patterns in neurodegenerative brain diseases. *Mov Disord* 2010;25:2395-404.



# Chapter 5 – Clinical applications of PET/CT in neurology

## 5.5 Brain tumours

Klaus Tatsch and Gabriele Poepperl

### Introduction

In the diagnostic work-up of brain tumours, PET plays an important role by addressing several metabolic features of glioma which are helpful for diagnosis, classification, characterisation, preoperative evaluation and, especially, post-therapeutic monitoring. The two main functions extensively studied so far are glucose metabolism using 2-[ $^{18}\text{F}$ ]fluoro-2-deoxy-D-glucose ( $^{18}\text{F}$ -FDG) and amino acid transport/(incorporation) using amino acid tracers such as [methyl- $^{11}\text{C}$ ]-L-methionine ( $^{11}\text{C}$ -MET), O-(2-[ $^{18}\text{F}$ ]fluoroethyl)-L-tyrosine ( $^{18}\text{F}$ -FET) or [ $^{18}\text{F}$ ]fluorodopa. Major clinical applications of these techniques will be briefly covered.

### Differential diagnosis between brain tumours and benign lesions

Regarding this question,  $^{18}\text{F}$ -FDG PET may play a minor role. Owing to the high glucose consumption of normal grey matter, high-grade tumours may be masked and low-grade tumours, which usually present with  $^{18}\text{F}$ -FDG uptake close to that of normal white matter, may be missed when located there. In addition,  $^{18}\text{F}$ -FDG lacks specificity for malignancy since elevated glucose metabolism may also be observed in active inflammatory lesions, in recent ischaemic infarcts, in some benign

tumours or during epileptic seizures. In contrast, increased amino acid uptake is present in almost all patients with gliomas, even in those with low-grade types. In addition, non-tumoral lesions such as chronic or subacute ischaemic or inflammatory demyelinating lesions, reactive gliosis, dysplasia, haematoma, cavernoma or post-traumatic scar generally do not exhibit increased amino acid transport.

### Definition of tumour borders

Since surgical resection of brain tumours should be as complete as possible but at the same time largely spare functionally intact normal brain tissue, exact tumour delineation is needed for treatment planning. Precise determination of tumour borders is also mandatory to define the optimal volume for radiation therapy. In this context, radiolabelled amino acid tracers seem superior to  $^{18}\text{F}$ -FDG (Fig. 1).

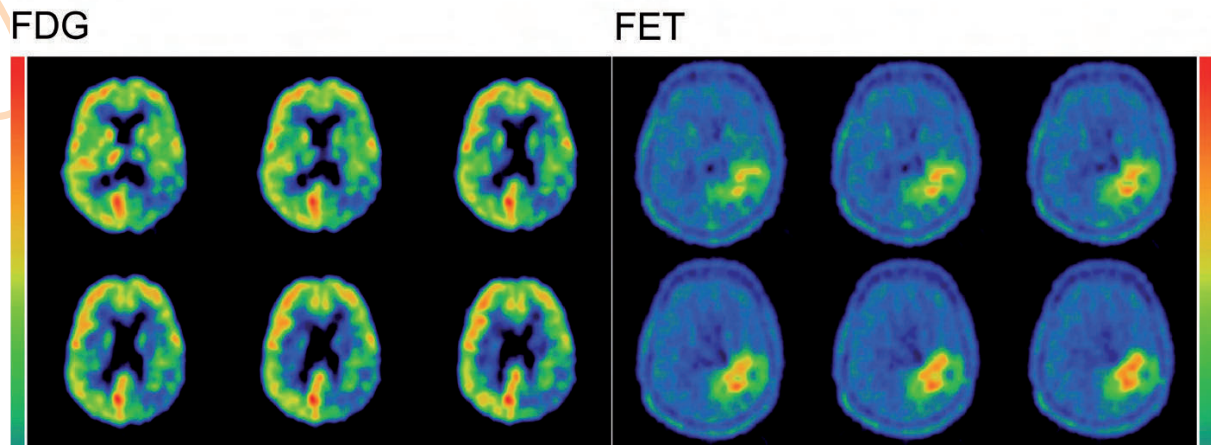


Figure 1: Glioblastoma: Major parts of the tumour in the left parietal lobe show  $^{18}\text{F}$ -FDG metabolism similar to or even below that of the normal cortex. There is reduced  $^{18}\text{F}$ -FDG metabolism in the surrounding oedema zone. Better delineation of the tumour borders and extent is achieved with the amino acid tracer  $^{18}\text{F}$ -FET. This may favour this type of tracer for biopsy and therapy planning

Especially brain tumours which appear hypo- or isometabolic compared with cortical uptake and which are located in or near to the grey matter may hardly be identified with  $^{18}\text{F}$ -FDG, thus hampering clear definition of tumour boundaries. On the other hand, results regarding tumour delineation by means of amino acid tracers are encouraging. As documented by stereotactic serial biopsies, these tracers may even better reflect the real tumour size than morphological imaging with CT or MRI.

### Grading/malignant progression

According to the World Health Organisation (WHO) system, tumour grading is based on histological criteria. Accurate pathological grading is essential because it determines treatment and prognosis. Since  $^{18}\text{F}$ -FDG up-

take correlates well with the histological grade of gliomas,  $^{18}\text{F}$ -FDG PET has been considered as a valuable diagnostic tool for this purpose. Cut-off levels of 1.5 and 0.6, respectively, for tumour-to-white matter and tumour-to-cortex uptake ratios have been proven to differentiate accurately between low- and high-grade tumours [1]. The role of radiolabelled amino acids or analogues for tumour grading is currently changing. Earlier studies using standard ratio methods taking into account the late uptake phase (>30 min) showed a slight but statistically not significant increase from low- to high-grade tumours [2,3]. The clinically most important differentiation between low- and high-grade, and especially between WHO grade II and III, tumours was not reliably achieved. More recently, however, assessment of uptake kinetics with a simple dynamic ac-

quisition protocol has been reported to have an excellent capability to discriminate between low- and high-grade gliomas [4]. Characteristically, steadily increasing uptake until the end of the acquisition period suggests reactive (benign) post-therapeutic changes or low-grade tumours, whereas decreasing curves following an early peak indicate recurrent glioblastoma or dedifferentiation of initially low-grade tumours.

### Prognosis

$^{18}\text{F}$ -FDG PET results are a valuable prognostic factor in gliomas, showing that  $^{18}\text{F}$ -FDG uptake correlates well with survival [5]. It has even been claimed that  $^{18}\text{F}$ -FDG PET might be better than pathological grading for determination of prognosis in gliomas. Although the prognosis depends on the histological tumour grade and the correlation between the tumour grade and the degree of amino acid tracer uptake in the late uptake phase seems poor (see above), a recent comparison of  $^{18}\text{F}$ -FDG PET and  $^{11}\text{C}$ -MET PET in gliomas has shown that  $^{11}\text{C}$ -MET PET results are a significant prognostic factor independent of tumour grading [6]. Meanwhile there is increasing evidence that amino acid uptake is an important prognostic indicator for patients with low-grade, high-grade and also pretreated recurrent tumours, and that high uptake is statistically associated with a poor survival time.

### Biopsy planning

Brain tumours are histologically often heterogeneous; therefore, stereotactic biopsies should be guided, taking into account the metabolic PET information. Nowadays PET imaging routines have been successfully implemented in planning systems of stereotactic brain biopsies.  $^{18}\text{F}$ -FDG PET-guided biopsies have previously shown an improvement in the diagnostic yield by obtaining samples from areas with the highest  $^{18}\text{F}$ -FDG uptake. However,  $^{18}\text{F}$ -FDG PET also has limitations: Targeting may be difficult in lesions with hypo- or isometabolic glucose metabolism, such as low-grade tumours. Problems can also arise in defining the borderline between tumoral and cortical  $^{18}\text{F}$ -FDG uptake when the hypermetabolic lesion is located near or within the grey matter. Amino acid tracers have likewise been tested and reported to be helpful for determination of the optimal biopsy site (Fig. 2).



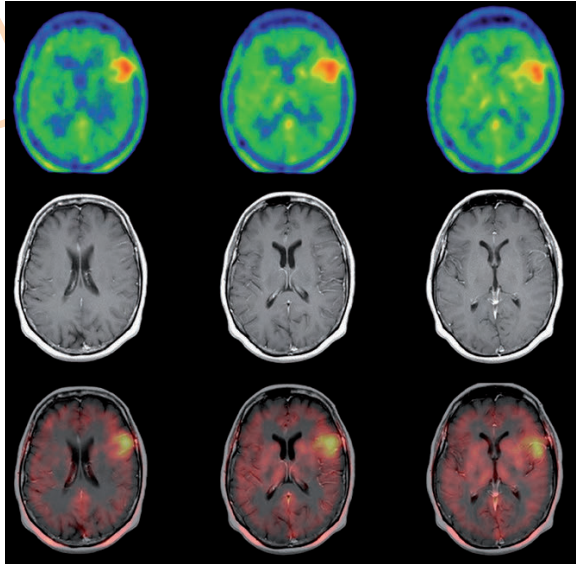


Figure 2: Amino acid PET (in this example with  $^{18}\text{F}$ -FET) also reliably depicts low-grade tumours in the majority of cases based on increased amino acid transport. Thus, it helps to define the metabolically most active area for biopsy planning even in cases where standard MRI shows only minor changes

Several studies have reported that PET-guided stereotactic biopsy provides accurate histological diagnoses in most individuals and allows a reduction in the number of trajectories in lesions located in high-risk/functional areas [2,7].

### Monitoring of therapy

Immediately after therapy, the critical question is whether treatment has been effective or not. Whereas high  $^{18}\text{F}$ -FDG uptake preceding therapy is a strong indicator of more aggressive tumours and shorter survival, results of immediate (within 2 weeks) post-radiation

$^{18}\text{F}$ -FDG PET scans alone have been found not to be related to survival. Thus,  $^{18}\text{F}$ -FDG PET seems of little use in assessing response immediately after (radiation) therapy. However, looking at longer time intervals after therapy, serial evaluation of metabolic activity with PET has provided more accurate prognostic information than a single scan [8]. Data on monitoring therapy with amino acid tracers are still limited, but promising. Both  $^{11}\text{C}$ -MET PET, used to monitor the effects of radiation therapy, systemic chemotherapy, or brachytherapy with  $^{125}\text{I}$ -seeds, and  $^{18}\text{F}$ -FET PET, used to monitor therapeutic effects of locoregional approaches such as intralesional radioimmunotherapy or convection-enhanced delivery of paclitaxel, have been shown to address therapeutic efficacy during and after these modalities.

### Tumour recurrence versus therapy-induced reactive changes

During long-term follow-up, the earliest possible reliable differentiation of therapy-induced reactive changes (e.g. radiation necrosis) from tumour recurrence is necessary in order to determine the most appropriate further treatment. For years,  $^{18}\text{F}$ -FDG PET was considered the gold standard for this differential diagnosis. However, more recent studies have questioned the efficacy and usefulness of  $^{18}\text{F}$ -FDG PET for this purpose and have reported low specificities especially in WHO grade II or III tumours [9]. Increased glucose uptake in inflammatory tissue is considered the main

source of false-positive  $^{18}\text{F}$ -FDG PET findings, and might occur especially after high-dose radiation beam therapy, radiosurgery or other locoregional approaches. Amino acid tracers like  $^{11}\text{C}$ -MET and  $^{18}\text{F}$ -FET are also well suited (or even better) for distinguishing reliably between tumour recurrence and therapy-induced benign changes, and this holds true even in multimodally pretreated glioma patients [3]. Some authors have suggested the combined use of  $^{18}\text{F}$ -FDG and amino acids to further enhance diagnostic accuracy by combining the independent and synergistic prognostic information of both approaches. Generally, amino acids have been postulated as the agent of choice for the diagnosis of recurrence by many studies.

### Conclusion and future perspectives

At present, the routinely used PET tracers add indispensable information for the differential diagnosis of brain tumours, tumour delineation and grading, estimation of prognosis, biopsy planning, therapy monitoring and post-therapeutic follow-up. While  $^{18}\text{F}$ -FDG is currently still considered the tracer of first choice for tumour grading or estimation of malignant transformation of initially low-grade tumours, there is rapidly increasing evidence that radiolabelled amino acids may have superior properties in delineation of tumour borders, biopsy planning, evaluation of treatment effects and differentiation of recurrent tumour and reactive post-therapeutic changes after conventional treatment. Apart from these

routine applications, new molecular treatment strategies may also call for new imaging tools to follow their effects. Currently many approaches are under evaluation, such as imaging gene expression following gene therapy in glioma patients, imaging tumour hypoxia with misonidazole derivatives, imaging proliferation of brain tumour using thymidine analogues, imaging of membrane biosynthesis with radiolabelled choline derivatives and imaging of  $\alpha(v)\beta(3)$  integrin expression as a marker of angiogenesis.





## References Chapter 5.5

---

### References

1. Delbeke D, Meyerowitz C, et al. Optimal cutoff levels of F-18 fluorodeoxyglucose uptake in the differentiation of low-grade from high-grade brain tumors with PET. *Radiology* 1995;195: 47-52.
2. Pauleit D, Floeth F, et al. O-(2-[18F]fluoroethyl)-L-tyrosine PET combined with MRI improves the diagnostic assessment of cerebral gliomas. *Brain* 2005; 128:678-87.
3. Popperl G, Gotz C, et al. Value of O-(2-[18F]fluoroethyl)-L-tyrosine PET for the diagnosis of recurrent glioma. *Eur J Nucl Med Mol Imaging* 2004; 31:1464-70.
4. Popperl G, Kreth FW, et al. Analysis of 18F-FET PET for Grading of Recurrent Gliomas: Is Evaluation of Uptake Kinetics Superior to Standard Methods? *J Nucl Med* 2006;47: 393-403.
5. Patronas NJ, Di Chiro G, et al. Work in progress: [18F] fluorodeoxyglucose and positron emission tomography in the evaluation of radiation necrosis of the brain. *Radiology* 1982;144: 885-9.
6. Kim S, Chung JK, et al. 11C-methionine PET as a prognostic marker in patients with glioma: comparison with 18F-FDG PET. *Eur J Nucl Med Mol Imaging* 2005;32: 52-9.
7. Pirotte B, Goldman S, et al. Combined use of 18F-fluorodeoxyglucose and 11C-methionine in 45 positron emission tomography-guided stereotactic brain biopsies. *J Neurosurg* 2004;101: 476-83.
8. Schifter T, Hoffman JM, et al. Serial FDG-PET studies in the prediction of survival in patients with primary brain tumors. *J Comput Assist Tomogr* 1993;17: 509-61.
9. Ricci PE, Karis JP, Heiserman JE, et al. Differentiating recurrent tumor from radiation necrosis: time for re-evaluation of positron emission tomography? *AJNR Am J Neuroradiol* 1998;19:407-13.



# Chapter 5 – Clinical applications of PET/CT in neurology

## 5.6 Epilepsy

Franck Semah and Gregory Petyt

### Introduction

Epilepsy is a very common disease, with a prevalence of approximately 0.5–1%. Almost 20–30% of epileptic patients develop refractory seizures, i.e. seizures that do not respond to anti-epileptic drugs [1]. In these patients, partial epilepsy [2] is the most common type of epilepsy and is one of the major prognostic factors for difficult-to-control seizures [3]. In a small number of these patients with refractory partial epilepsy, surgical removal of the epileptogenic zone is the treatment of choice. Ictal SPECT and interictal  $^{18}\text{F}$ -FDG PET are the two techniques that are currently used in most specialised centres for the assessment of epileptic patients who are candidates for epilepsy surgery.

The role of  $^{18}\text{F}$ -FDG PET in the presurgical evaluation of patients with intractable epilepsy is (1) to lateralise and, if possible, localise the epileptic foci and (2) to find a small area of brain abnormality in MRI-negative patients (i.e. patients without any brain abnormality detected by high-resolution MRI). The overall sensitivity of  $^{18}\text{F}$ -FDG PET in the detection of the epileptic brain region is around 85–90% [4, 5] and PET can provide additional information about the epileptic foci, impacting surgical decision-making [6, 7].

### Localisation of the epileptogenic focus in patients with MRI abnormality

The most frequent epileptic zone is located within the temporal lobe. The sensitivity of interictal  $^{18}\text{F}$ -FDG PET is high in patients with refractory temporal lobe epilepsy (TLE). The area of hypometabolism in TLE patients is often very large and interictal hypometabolic regions sometimes extend beyond the presumed epileptogenic zone to the ipsilateral parietal and frontal cortex as well as the thalamus and even occasionally to the contralateral temporal lobe (Fig. 1) [8, 9].



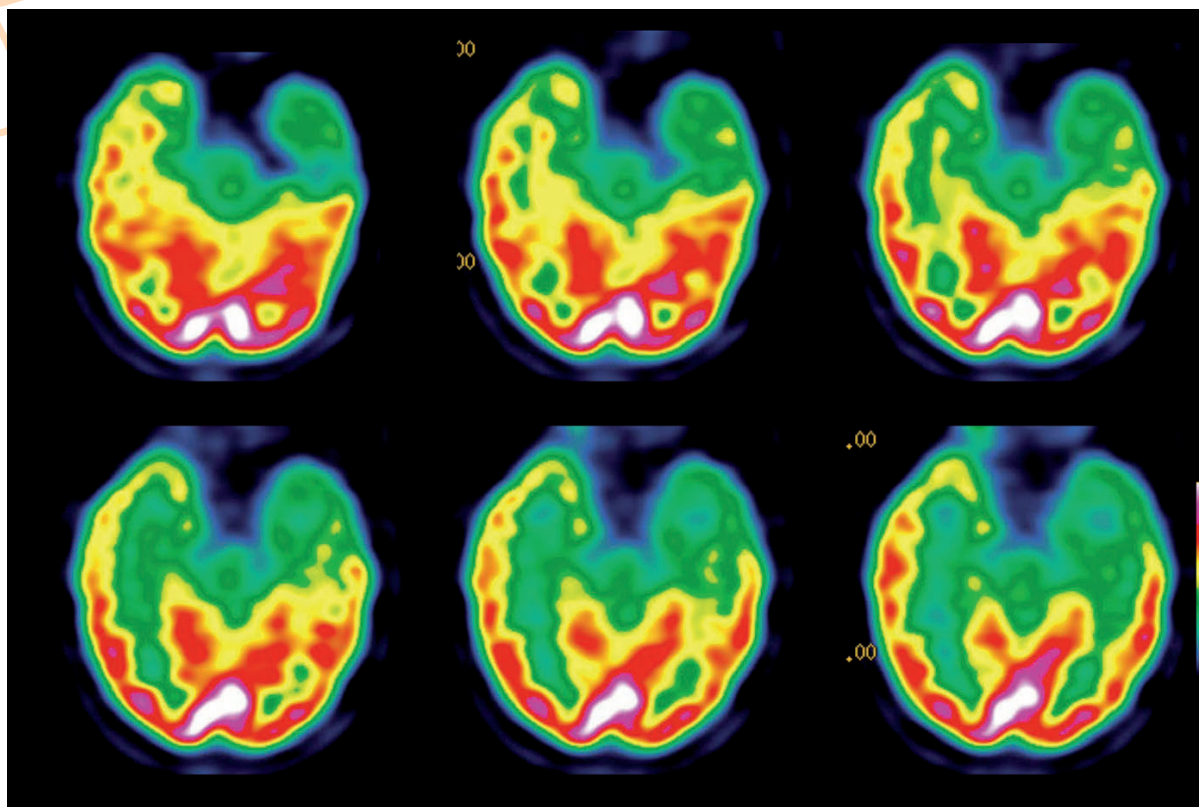


Figure 1: Interictal FDG PET scan in a patient with TLE, showing hypometabolism involving the left temporal lobe. The hypometabolism is more pronounced in the temporopolar region but involves the mesial part of the temporal lobe and extends to the lateral part (axial image in the hippocampal plane)

This may represent the epileptic network involved in seizure propagation [10].  $^{18}\text{F}$ -FDG PET may show occasional lateral or medial temporal lobe hypermetabolism, related to subclinical seizures or frequent interictal spiking. It seems that brain glucose hypometabolism shown by PET is a result of several effects and interactions, including underlying pathology, neuronal loss, seizure evolution and interictal changes [9].

PET can also be very helpful in the presurgical evaluation of extra-temporal lobe epilepsy (ETLE). Frontal lobe epilepsy (FLE) is the most frequent type of ETLE and may be associated with an MRI-detected cortical lesion. PET may show hypometabolism extending beyond the lesion or very restricted areas of hypometabolism. FLE is often associated with subtle structural changes, such as cortical dysplasia or heterotopias, which may not be apparent

on MRI but may show hypometabolism on  $^{18}\text{F}$ -FDG PET. In FLE, the sensitivity of  $^{18}\text{F}$ -FDG PET in localising the epileptogenic zone is lower than in TLE [11].

#### Localisation of the epileptogenic focus in patients with normal MRI

$^{18}\text{F}$ -FDG PET plays a very important role in the evaluation of refractory patients, particularly when MRI or other imaging modalities are negative. In these patients  $^{18}\text{F}$ -FDG PET is able to locate a small area of hypometabolism that is associated with the epileptogenic zone and reflects the presence of subtle structural changes, such as subtle cortical malformations which may not be apparent on MRI.  $^{18}\text{F}$ -FDG PET scan can help the clinician to localise these areas of cortical abnormality not detected on MRI.  $^{18}\text{F}$ -FDG PET has been found to be most useful in cases of negative MRI or when ictal EEG is discordant with MRI or videotaped seizure semiology; in these cases it improved the positive and negative predictive values of MRI and video EEG monitoring [7].

#### $^{18}\text{F}$ -FDG PET and surgical outcome

$^{18}\text{F}$ -FDG PET has been reported to be useful in predicting the outcome of epilepsy surgery. Ipsilateral PET hypometabolism appears to have a high predictive value for a favourable surgical outcome, even in cases of normal MRI or patients with non-localised ictal scalp EEG [12]. Patients with more severe temporal lobe hypometabolism appear to have better post-surgical seizure control [13]. The temporal pole seems to be a significant predictor of the postoperative outcome [14]. However, it remains difficult to predict who will not become seizure-free after surgery [15].



## References Chapter 5.6

### References

1. Kwan P, Brodie MJ. Early identification of refractory epilepsy. *N Engl J Med* 2000;342:314-9.
2. Proposal for revised classification of epilepsies and epileptic syndromes. Commission on Classification and Terminology of the International League Against Epilepsy. *Epilepsia* 1989;30:389-99.
3. Semah F, Picot MC, Adam C, Broglin D, Arzimanoglou A, Bazin B, et al. Is the underlying cause of epilepsy a major prognostic factor for recurrence? *Neurology* 1998;51:1256-62.
4. Ryvlin P, Bouvard S, Le Bars D, De Lamerie G, Gregoire MC, Kahane P, et al. Clinical utility of flumazenil-PET versus [18F]fluorodeoxyglucose-PET and MRI in refractory partial epilepsy. A prospective study in 100 patients. *Brain* 1998;121 (Pt 11):2067-81.
5. Gaillard WD, Bhatia S, Bookheimer SY, Fazilat S, Sato S, Theodore WH. FDG-PET and volumetric MRI in the evaluation of patients with partial epilepsy. *Neurology* 1995;45:123-6.
6. Ollenberger GP, Byrne AJ, Berlangieri SU, Rowe CC, Pathmaraj K, Reutens DC, et al. Assessment of the role of FDG PET in the diagnosis and management of children with refractory epilepsy. *Eur J Nucl Med Mol Imaging* 2005;32:1311-6.
7. Uijl SG, Leijten FS, Arends JB, Parra J, van Huffelen AC, Moons KG. The added value of [18F]-fluoro-D-deoxyglucose positron emission tomography in screening for temporal lobe epilepsy surgery. *Epilepsia* 2007;48:2121-9.
8. Theodore WH, Newmark ME, Sato S, Brooks R, Patronas N, De La Paz R, et al. [18F]fluorodeoxyglucose positron emission tomography in refractory complex partial seizures. *Ann Neurol* 1983;14:429-37.
9. Semah F, Baulac M, Hasboun D, Frouin V, Mangin JF, Papanicolaou S, et al. Is interictal temporal hypometabolism related to mesial temporal sclerosis? A positron emission tomography/magnetic resonance imaging confrontation. *Epilepsia* 1995;36:447-56.
10. Chassoux F, Semah F, Bouilleret V, Landre E, Devaux B, Turak B, et al. Metabolic changes and electro-clinical patterns in mesio-temporal lobe epilepsy: a correlative study. *Brain* 2004;127 (Pt 1):164-74.
11. Lee JJ, Lee SK, Lee SY, Park KI, Kim DW, Lee DS, et al. Frontal lobe epilepsy: clinical characteristics, surgical outcomes and diagnostic modalities. *Seizure* 2008;17:514-23.
12. Willmann O, Wennberg R, May T, Woermann FG, Pohlmann-Eden B. The contribution of 18F-FDG PET in preoperative epilepsy surgery evaluation for patients with temporal lobe epilepsy: a meta-analysis. *Seizure* 2007;16:509-20.
13. Theodore WH, Sato S, Kufta C, Balish MB, Bromfield EB, Leiderman DB. Temporal lobectomy for uncontrolled seizures: the role of positron emission tomography. *Ann Neurol* 1992;32:789-94.
14. Dupont S, Semah F, Clemenceau S, Adam C, Baulac M, Samson Y. Accurate prediction of postoperative outcome in mesial temporal lobe epilepsy: a study using positron emission tomography with 18fluorodeoxyglucose. *Arch Neurol* 2000;57:1331-6.
15. Uijl SG, Leijten FS, Arends JB, Parra J, van Huffelen AC, Moons KG. Prognosis after temporal lobe epilepsy surgery: the value of combining predictors. *Epilepsia* 2008;49:1317-23.

# Imprint

**DOI :** <https://doi.org/10.52717/NBXJ4555>

ISBN: 978-3-902785-02-2

ISSN: 2079-3138

**Publisher:**

European Association of Nuclear Medicine

EANM Technologist Committee

Hollandstrasse 14, 1020 Vienna, Austria

Tel: +43-(0)1-212 80 30, Fax: +43-(0)1-212 80 309

E-mail: [info@eanm.org](mailto:info@eanm.org)

URL: [www.eanm.org](http://www.eanm.org)

**Content:**

No responsibility is taken for the correctness of this information.

Information as per date of preparation: August 2011

**Layout and Design:**

kreativ · Mag. Evelyne Sacher

Linzer Straße 358a/1/7, 1140 Vienna, Austria

Tel: +43-(0)1/416 52 27, Fax: +43-(0)1/416 85 26

E-mail: [office@kreativ-sacher.at](mailto:office@kreativ-sacher.at)

URL: [www.kreativ-sacher.at](http://www.kreativ-sacher.at)

**Printing:**

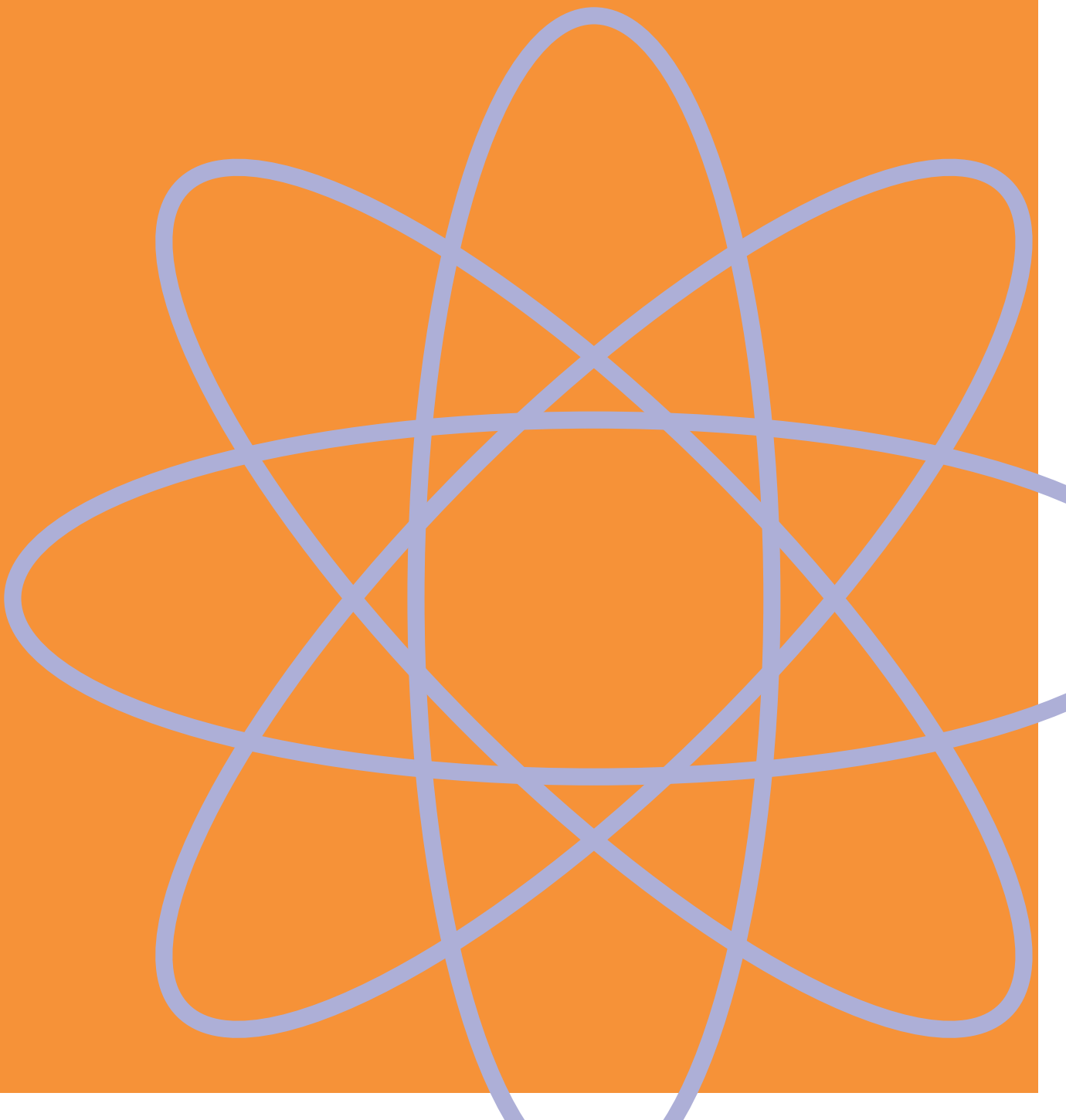
Laber-Druck Ges.m.b.H.

Michael-Rottmayr-Straße 46, 5110 Oberndorf, Austria

Tel: +43-(0)62 72-71 35-426, Fax +43-(0)6272-7135-499

E-mail: [hubert.jaud@laberdruck.at](mailto:hubert.jaud@laberdruck.at)

URL: [www.laberdruck.at](http://www.laberdruck.at)







**Principles and Practice of PET/CT Part 2 A Technologist's Guide**